Study of Pax3 and Pax7 functions during the development of the mouse embryo

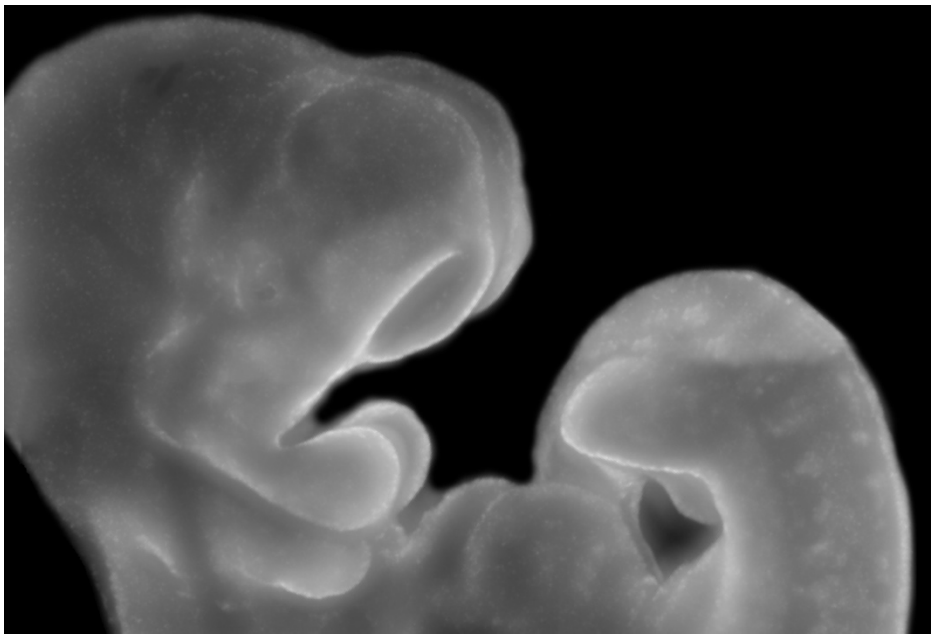

Antoine Zalc

Université Pierre et Marie Curie
&
Freie Universität Berlin

Ecole doctorale Complexité du Vivant et Myograd

Laboratoire UMR-S 974

Study of Pax3 and Pax7 functions during the development of the mouse embryo

By Antoine Zalc

Directed by Pr. Frédéric Relaix and Pr. Carmen Birchmeier

Thesis defence: the 26th of September 2014

In front of an international jury composed of:

Claire Fournier-Thibault, Professor, President
Simone Spuler, Professor, First Examiner
Chaya Kalcheim, Professor, Reviewer
Paul Trainor, Professor, Reviewer
Sigmar Stricker, Professor, Second Examiner
Christian Hiepen, Postdoctoral fellow

Table of contents

Acknowledgement

This thesis was defended on the 26th of September 2014, in front of an international jury composed of distinguished scientists whom I would like to acknowledge.

I thank them for accepting to examine my work. These people are important players in their field of research and will inspire me in my future career.

I would like first to thank **Pr. Claire Fournier-Thibault**, for accepting to be President of my thesis jury. I really like her work and input in the field of developmental biology.

I would like to thank my examiner **Pr. Sigmar Stricker**. I always liked his calm in and his scientific rigor. I would also like to thank **Dr. Christian Hiepen** for attending my defence.

Finally, I would like to thank my reviewers: **Pr. Chaya Kalcheim, Pr. Simone Spuler** and **Pr. Paul Trainor** for the time they spent reading my manuscript and writing their reports, as well as attending the defence, which implied travelling across the Rhine, the Mediterranean Sea and the Atlantic Ocean.

I heard so much about Pr. Chaya Kalcheim's work and about her scientific rigor and brightness both on the field of neural crest and muscle biology that she was the obvious person to evaluate my work.

Pr. Simone Spuler is the director of the Myograd Ph.D. program; during the time of my Ph.D. she displayed an incredible amount of effort and energy to get Myograd started and to create a scientific emulation for the students.

Pr. Paul Trainor is a pillar in the field of neural crest biology. When I met him in Italy in 2011 during the Craniofacial Gordon conference that he was chairing he was always available and invited me to have a drink with his friends several times during the conference.

Thank you very much for the discussions, comments and advice about my work. I was lucky to have you all in my thesis jury.

In the second part of the acknowledgement I will thank all the people who helped me during these years.

First I would like to thank **Fred**, who decided to recruit me in his lab for my master. Despite my willingness to work on muscles, I'm glad Fred offered me to work on neural crest cells, which I never heard about before. Agronomic studies are great, I learnt many things including how to recognise different races of cows, sheep and goats but the developmental biology was kind of absent from the programs. I would like to thank Fred for his support and his trust during the development of my project and for teaching me how to be rigorous and to always start by doing the proper controls first. I would also like to thank him for sending me around the world, from Il Ciocco, Italy to Cancun, Mexico, to present my work, which was a great opportunity to meet brilliant people from everywhere. I will also try to remember his lessons about scientific politics and how not saying too much can be more efficient than the opposite.

Then I would like to thank **Carmen** for the great inspiring scientific discussions we had over the years. She also was a great help for teaching me how to be precise in my descriptions with the use of the correct terms. I will always remember my first meeting with her in Berlin for the Ph.D. interviews. At the end of my talk, after presenting the work I wanted to do with her help, she simply said she disagreed with the whole project. First of all, she was right, the mutant I wanted to generate would not have lived after E8.5 but more importantly it was an excellent lesson: always be rock-solid about the work you present.

When I arrived in the lab, I had the chance to start working with **Revital**. She was the post-doc leading the project at the time and was tremendous in showing me how to work, how to ask the correct questions and in teaching me to be creative. She was essential in my development in the lab, especially by telling me to always ask people around for help instead of staying blocked. But more importantly, she told me which people to ask in order to learn from the best! For all this I would like to thank her.

Among these people was **Frédéric (MC Scouser)** whom I'd like to thank for teaching me everything I know about molecular biology (which is still not much compare to him). He also tried for several years to make me appreciate Vincent Delerm's "music" but was much more efficient in teaching me how to clone!

Of course I would like to thank **Vanessa (Vavavoum)** who was a tremendous help after Revital left the lab. It seems Vanessa knows everything and is always ready to help anytime, any day. She was essential in teaching me to organise my thinking, which allowed me to write my papers and this thesis! It was also pretty fun to realise we did the same study eight years apart, being

both slightly damaged by our stay in Lycée Saint-Louis. Her love for monkeys and for my stupid jokes was a great relief in the last month in the lab!

John (Monkey), who now moved to India, also shared the love of monkeys and stupid jokes. Back in the lab, he was always excited about everything including monkey stuff but especially photography, one of my favourite hobbies! I have to say he's much better than me concerning the stupid jokes. I'm glad to have John as my bestman for my wedding even if I was not excellent in translating his wedding back in 2012.

Speaking about wedding, I'm glad to be **Andrew (The Ho)**'s bestman for his future wedding! And I would like to thank Andrew who taught me the entire secret about immunostaining and Photoshop. I really miss having a beer with John and Andrew after a hard day of work in the lab but we still find way to see each other from time to time. When you speak about Andrew, **Piera (La Petite)**, future Mrs Ho is never far away! Piera was always in a good mood even when nothing was working in the lab! I'm looking forward to see these two when I go in Stanford for my post-doc!

I would also like to thank **Shin** who taught me how to ChIP like a professional and was a great critic concerning photography. However, I think I totally failed in making him pass an order…

I want to thank **Sonia (nita)** and **Maria-Grazia (Maraia)** for staying late in the lab so I would not feel alone and always being there to listen to whatever I wanted to talk about. I'm not sure this a good place to talk about the Maison Basque but thank you for that too!

I would like to thank **Bernie** who is taking care of all our mouse business in addition to the cell culture. She taught me how to deal with these two things and I'm grateful for this incredible knowledge. Not so sure if I should be thankful for teaching me the "Corde à Sauter" choreography but it was fun anyway!

I would also like to thank the other members (past and present) of the Relaix' lab, **Phillipos**, **Despoina**, **Anne, Muriel** and a special thank to **Ted** for his love of "Minitel" and for trying to invite me in the Catacombs.

When I joined the lab five years ago, it was an incredible place to be with many different people from different background working together! I would like first to thank **Edgar (Evil Gomes)** for always being available for a little chat about Science inside and outside the lab. Then I would like to thank his former lab with **Bruno**, **Vincent**, **Daniel (Les Poulets)** and **Sestina**.

Thank you Bruno for sharing your thought about weird movies you saw and for always being ready to take some nice pictures for a potential Nature cover… Thank you Vincent for constantly being in a good mood in the lab and for the "Caribou". Thank you Daniel for not

talking while you were working and for not stopping to talk about everything around a beer! Thank you also to Sestina who had to deal with those guys and for always being ready to discuss with me.

I would also like to thank **Aurore**, **Stéphanie**, **Mathilde**, **Benoit (Tournetoi)**, **Thibaut** and **Yannick (Manitas)** whom I discovered over the years who all shared the same floor. They are great people to work next to. I still hope to get my Pirate Cake one day!

I also want to thank **Izolina**, who is always ready to dance in the lab in addition of taking care of me when I hurt myself which didn't happen that often thankfully…

Now, I would like to thank some Myograd students. In particular **Elija (Goldie Locks)** and **Laurianne (Lolo)** who always were ready to grab a beer. A special thank to **Susanne (Susi)** for sending me numerous email to know how to organise the thesis defence but mainly for always sending news and finally for translating my abstract in "the finest German".

I would also like to thank **Alicia** from Margaret Buckingham's lab. We tried to set up a potentially exciting project together however we didn't have enough time to work it through.

Of course I want to thank **Catherine (La mère Bodin)** for spending so many hours at the cryostat cutting embryos for me and for keeping me aware of all the evolution inside the Pasteur Institute both professional and personal.

I want to thank the people from the FACS facility, **Bénédicte**, **Aurélien** and especially **Catherine** who is always ready to come to the lab on the 26th of December for one of my crazy experiment. I really hope I will have the chance to test this fantastic CyTOF machine.

I also want to thank people from the animal house facility in La Pitié-Salpétrière. **Serban** who always made sure I could rapidly treat my mice with products as dangerous as Dioxin without intoxicating myself. **Olivier** and **Bocar** for always making sure everything runs smoothly and for giving me a 24/7 access to the animal house. And a special thank to **Kim** for taking care of my mice for now five years and for teaching me how to manipulate them. Then I would like to thank people from the CDTA in Orléans, especially **Alexandre** and **Jérome** who are dealing with all our requests in a remarkable short time.

Now I would like to thank my family for always being with me during all these years.
First I would like to thank my future wife **Amandine**, who put off with many weekends where I was spending more time with my mice than with her and for always being supportive even when I was relatively bearable. I love her from all my heart.
Then I would like to thank my parents **Catherine** and **Boris** for always being of good advice and for suggesting me to do my master in Fred's lab in the first place.
I'd like to thank my brothers and sisters plus their kids, **Claire**, **Julien**, **Marianne**, **Jorg**, **Thomas**, **Maxime**, **Pierre**, **Elie**, **Joseph**, **Esther** and **Ezra**. Especially for my nephews and my niece, I'm sorry I forgot almost all of your birthdays; I'll try to work on that in the future.
I would like to thank my aunt and uncle **Cécile** and **Daniel**. Cécile is always interested in the latest development of my projects and Daniel simply is a walking encyclopaedia.
I would also like to thank my other aunts and uncles, **Isabelle** and **Marcel** and **Jacques** and **Nicole** for always being so welcoming when we were at their place either in Mevaseret or Paris 14. Then I would like to thank my numerous cousins, **Hélène**, **Barbara**, **Daniel**, **Eytan**, **Tali**, **Marius**, **Jules** and **Johanna** plus their wifes and husband and kids but it starts to be a bit too much.
Finally, I would like to thank my grand parents **Denise** and **Jean** for always believing in me even if I didn't learn Hebrew or become a (medical) doctor.

Two people were essential in my decision to do research, my two professors of Biology from the Lycée Claude Monet, **M. Delbet** and **Mme Dallot**. The passion the showed when they were teaching convinced me to ask my dad to do a first internship in a lab where I got infected but the virus of Science and I've never looked for cure since then!
During my training I had the chance to work with amazing people that I would like to thank, especially **Peter Brophy**, **Jeremy Brockes**, **Frédy Barneche** and **Chris Bowler**.
Then I would like to thank my friends who understood more or less what I was been doing during these four years: **Lyzah**, **Alicia**, **Célia**, **Thibaut**, **Agathe**, **Yannick**, **Franck**, **Sophie**, **Gaëtan**, **Arnaud**, **Caro**, **Lucie**, **Clémence**, **Aurore**, **Maud, Emilie** and **Matt** and **Rob** (my London partners in crimes).

Last, I would like to thank all the members of the Rock&Roll, Rythmes&Blues and Jazz for accompanying my days during my whole Ph.D., especially **Paul McCartney**, **Bob Dylan**, **David Bowie**, **Bruce Springsteen**, **Jim Morrisson, Renaud**, **Joe Strummer**, **The Black Keys**, **Ray Charles**, **Stevie Wonder, Otis Redding** and **Herbie Hancock**.

And to whom I forgot, let me buy you the first beer next time I see you!

List of figures

INTRODUCTION

RESULTS - PART I

Figure 1: Cell cycle exit occurs at the determination stage

Figure 2: Cell cycle exit can be uncoupled from cell differentiation

Figure 3: Myoblasts control muscle progenitor cells proliferation by preventing cell cycle exit

Figure 4: Close proximity of $Pax7^{+}$ and $Myod1^{+}$ cells, with decreased Pax7 and Hes1/Hey1 expression in muscle progenitor cells of *Myod1: Myf5* double mutant

Figure 5: The Notch pathway prevents activation of p57 in progenitor cells

Figure 6: Conditional ablation of *RBPJ* leads to upregulation of p57 and p21 and cell cycle arrest in muscle progenitor cells

Figure 7: Expression of a p57 muscle regulatory enhancer (MRE) in transgenic mice

Figure 8: Direct regulation of the p57 Muscle Regulatory Element (MRE) by Myod1 and Hes1/Hey1

Supplementary Figure 1: Stages of myogenic differentiation impairment using the different *Myod1: Myf5* mutant compounds

Supplementary Figure 2: Genomic sequence of p57MRE enhancer cloned in p57MRE-tk-nlacZ reporter

RESULTS - PART II

Figure 1: Pax3 and Pax7 are essential for facial development

Figure 2: Impaired Pax3/7 function leads to up-regulation of AhR signalling

Figure 3: Impairing Pax3/7 function induces cell cycle exit of CNCC

Figure 4: Interaction between Pax3 and AhR signaling is essential for normal craniofacial development

Figure S1: *Pax3* and *Pax7* dynamic expression and phenotypes of *Pax3/7* compound mutants

Figure S2: Analysis of $Pax3^{Pax3\text{-}ERD/GFP}$ embryos

Figure S3: Quantification of CNCC in facial prominences of $Pax3^{GFP/+}$ and $Pax3^{Pax3\text{-}ERD/GFP}$ embryos

Figure S4: Up-regulation of *p21* expression upon TCDD exposure

Table S1: Gene expression comparison between $Pax3^{Pax3\text{-}ERD/GFP}$ and $Pax3^{GFP/+}$ embryos (up-regulated genes).

Table S2: Gene expression comparison between $Pax3^{Pax3\text{-}ERD/GFP}$ and $Pax3^{GFP/+}$ embryos (down-regulated genes).

List of abbreviations

AhR: Aryl hydrocarbon receptor

Aldh1a3: Aldehyde dehydrogenase 1 family, member A3

AP-2α: Activator Protein 2 alpha

ARNT: Aryl hydrocarbon receptor nuclear translocator

BA: Branchial arch

bHLH: basic helix loop helix

bHLH/PAS: basic helix loop helix /Per-ARNT-Sim

BMP: Bone morphogenetic protein

CDK: Cyclin-dependent kinase

CDKI: Cyclin-dependent kinase inhibitor

ChIP-seq: Chromatin immunoprecipitation coupled to high-throughput sequencing

CLP: Cleft lip with or without palate

CNCC: Cranial neural crest cell

CNS: Central nervous system

Cxcr4: C-X-C chemokine receptor type 4

Cyp1a1: Cytochrome P450, family 1, subfamily A, polypeptide 1

Cyp1b1: Cytochrome P450, family 1, subfamily B polypeptide 1

Dll: Delta-like gene

Dlx: Distal-less gene

DNA: Deoxyribonucleic acid

DRE: Dioxin response element

E: Embryonic day

E-box: Enhancer box or Ephrussi box

Edn1: Endothelin gene

Ednra: Endothelin receptor A

EGF: Epidermal growth factor

EMT: Epithelial-to-mesenchymal transition

ERD: Engrailed repressor domain

Eya: Eyes-absent homolog genes

FACS: Fluorescence-activated cell sorting

FGF: Fibroblast growth factor

FgfR: FGF receptor

FNP: Fronto nasal prominence

FoxD: Forkhead related transcription factor D

GFP: Green fluorescent protein

GRN: Gene regulatory network

HAT: Histone acetyltransferase

Hes: Hairy and enhancer of split 1

Hey: Hairy and enhancer of split 1 related with YRPW motif protein

HMG-box: High Mobility Group box

Hox: Homeotic genes

Hsp90: Heat shock proteins

Lbx1: Ladybird homeobox 1

LNP: Lateral nasal processes

Mef2: Myocyte enhancer factor 2

Mesp2: Mesoderm posterior protein 2

Md: Mandibular processes

MNP: Medial nasal processes

MRF: Myogenic regulatory factors

Mrf4: Myogenic factor 6 also called herculin

mRNA: Messenger ribonucleic acid

Msx: Muscle segment-related homeobox gene

Mx: Maxillary processes

Myf5: Myogenic factor 5

MyoG: Myogenin also called myogenic factor 4

NCAM: Neural cell adhesion molecule

NCC: Neural crest cell

NF-κB: Nuclear factor kappa B

NICD: Notch intracellular domain

OFT: Outflow tract

p15: Cyclin-dependent kinase 4 inhibitor B, Cdkn2b

p16: Cyclin-dependent kinase inhibitor 2A, Cdkn2a

p18: Cyclin-dependent kinase 4 inhibitor C, Cdkn2c

p19: Cyclin-dependent kinase 4 inhibitor D, Cdkn2d

p21: Cyclin-dependent kinase inhibitor 1A, Cdkn1a

p23: Prostaglandin E synthase 3

p27: Cyclin-dependent kinase inhibitor 1B, Cdkn1b

p38: Mitogen-activated protein kinase 14, Mapk14

p57: Cyclin-dependent kinase inhibitor 1C, Cdkn1c

Pax: Paired box homeotic gene

PCAF: p300/CBP-associated

PCP: Planar cell polarity

PDGF: Platelet-derived growth factor

PNS: Peripheral nervous system

PSM: Presomitic mesoderm

pSmad3: Phosphorylated SMAD

PTA: Persistent truncus arteriosus

r: Rhombomere

RA: Retinoic acid

Rb: Retinoblastoma

RBPJ: Recombining binding protein suppressor of hairless

Sdf1: Stromal cell-derived factor 1

SF/HGF: Scatter factor/Hepatocyte growth factor

Shh: Sonic hedgehog

Six: Sine-oculis related homeobox gene

Sox: Sry-related HMG box gene

Swi/snf: Switch/Sucrose non fermentable

TCDD: 2,3,7,8-tetrachlorodibenzo-p-dioxine

Tg: Transgenic

TGFβ: Transforming growth factor beta

VEGF: Vascular endothelial growth factor

WNT: Wingless-type

XAP2: Immunophilin-like protein hepatitis B virus X-associated protein 2

XRE: Xenobiotic response element

+: Positive (ex: Pax3+ cell = Pax3 positive cell)

-: Negative (ex: $Myf5^-$ cell = Myf5 negative cell)

µm: Micrometer

Conventions:

Genes and transcripts are referred to in italics, contrary to proteins.

Human genes are in italics and in capital letters.

INTRODUCTION

In this introduction I summarize the scientific context relevant to my thesis work. My thesis being divided in two independent projects, I introduce both aspects. The first part analyses how limb muscles are generated and what are the mechanisms regulating their growth during development of the embryo. The second part examines how neural crest cells form the vertebrate face and how internal and external factors regulate their development and morphogenesis.

PART I DEVELOPMENTAL CONTROL OF LIMB MUSCLE PROGENITOR CELL GROWTH ARREST

"It is not birth, marriage, or death, but gastrulation which is truly the most important time in your life." Lewis Wolpert.

1. Origin of skeletal muscles

1.1. The somite

Development of multicellular organisms in most cases starts with a single cell, the zygote, which can be considered as the only truly totipotent cell. Upon fertilisation, the zygote divides mitotically to generate all the cells of the body and extra embryonic tissues. After a certain number of divisions, the embryo undergoes the process of gastrulation initiated by the formation of the primitive streak. During gastrulation, cells move towards the primitive streak and ingress through this structure to first generate the endoderm, then the mesoderm, the third embryonic layer, which will lie between the endoderm and the ectoderm (Figure 1A). Each embryonic layer then gives rise to different groups of specified cells. For example, cells

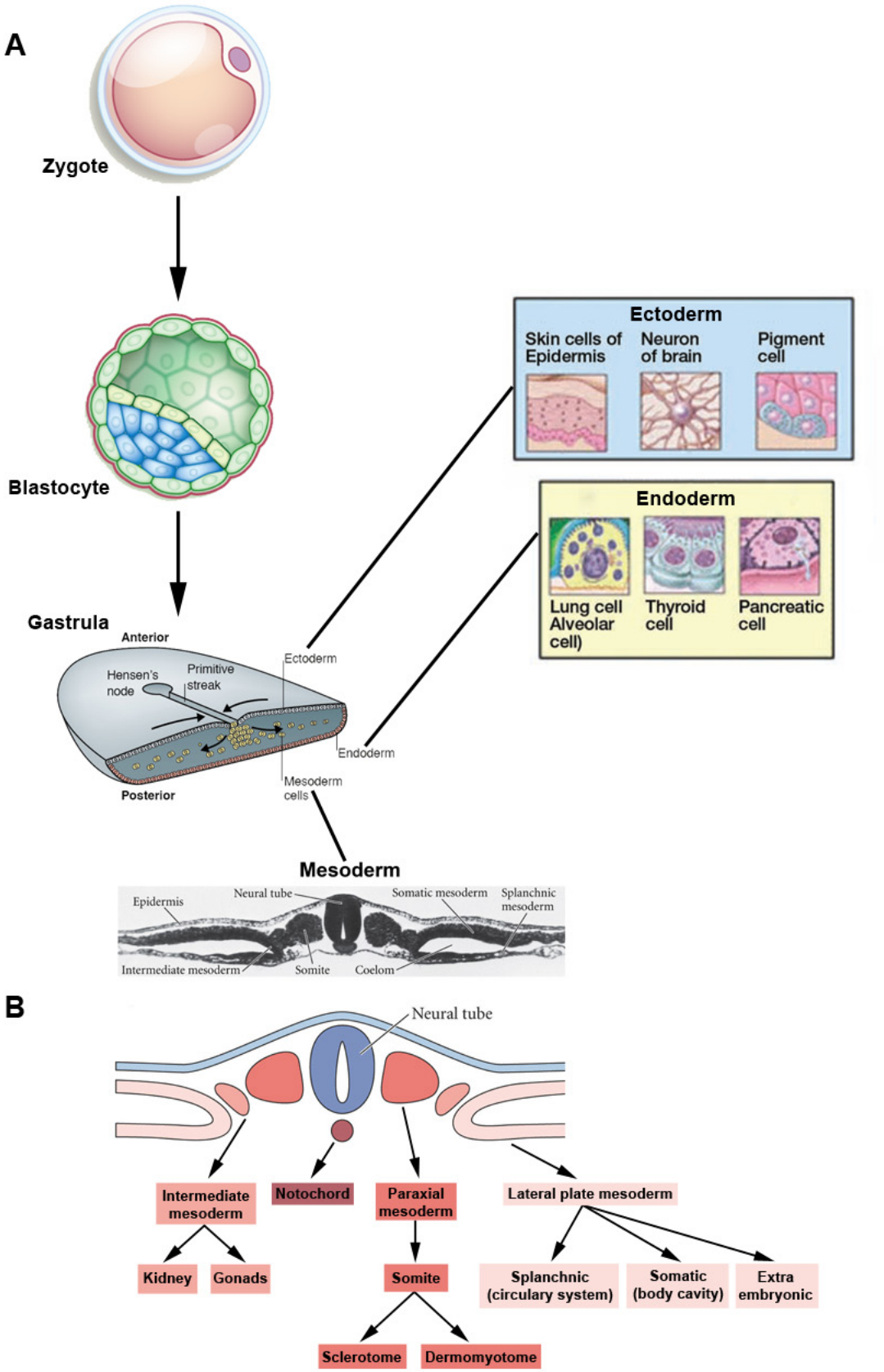
A
Zygote
Blastocyte
Gastrula
Anterior
Hensen's node
Primitive streak
Ectoderm
Endoderm
Mesoderm cells
Posterior
Ectoderm
Skin cells of Epidermis
Neuron of brain
Pigment cell
Endoderm
Lung cell Alveolar cell)
Thyroid cell
Pancreatic cell
Mesoderm
Epidermis
Neural tube
Somatic mesoderm
Splanchnic mesoderm
Intermediate mesoderm
Somite
Coelom
B
Neural tube
Intermediate mesoderm
Notochord
Paraxial mesoderm
Lateral plate mesoderm
Kidney
Gonads
Somite
Splanchnic (circulary system)
Somatic (body cavity)
Extra embryonic
Sclerotome
Dermomyotome

derived from the ectoderm give rise to the central and peripheral nervous systems (CNS and PNS), the sensory epithelia of the eye, ear, and nose, the epidermis, the mammary glands, the hypophysis, the subcutaneous glands and the amelobasts that deposit enamel of the teeth. Cells derived from the endoderm will generate most of the digestive and respiratory systems, the liver, the thymus, the thyroid, the pancreas, the bladder, the urethra and the epithelial lining of the tympanic cavity, tympanic antrum, and auditory tube (Figure 1A).

The mesoderm is anatomically divided into paraxial, intermediate and lateral mesoderm depending on the position from midline (Figure 1B). The paraxial or presomitic mesoderm (PSM) represents two bands of cells on each side of the neural tube. As the embryo elongates, the process of somitogenesis divides the PSM along the anterior-posterior axis and forms, on each side of the neural tube, repeated segments called somites (Figure 2A). As somites are generated at the anterior end of the PSM, it is replenished posteriorly by cells entering the PSM via the primitive streak (Figures 1A and 2A; Dequéant and Pourquié, 2008). The term somite was first introduced in 1881 by Balfour to insist on the segmental nature of this structure in the embryo, replacing the term “Protovertebra” previously introduced by Remak in 1850, which focused on the contribution of this structure to vertebral column development (Christ et al., 2007). Somites give rise to various tissues such as the vertebrae, the ribs, dermis of the back as well as all the skeletal muscles of the trunk and limbs (Christ et al., 2007).

Figure 1: Origin of the somite
(A) After a series of mitotic divisions the blastocyte undergoes the process of gastrulation. During the gastrula stage, cells ingress into the primitive streak to form a third embryonic layer called the mesoderm that lies between the endoderm and the ectoderm, the two other embryonic layers. Examples of endoderm derivatives are shown in the yellow box. Examples of ectoderm derivatives are shown in the blue box. Black and white picture represents a transversal section of an avian embryo after forty-five hours of incubation and shows the position of the mesoderm in the developing embryo (adapted from NCBI). (B) Schematic representation of the different mesoderm compartments with their derivatives. The somite derives from the paraxial mesoderm (adapted from Gilbert, 2013).

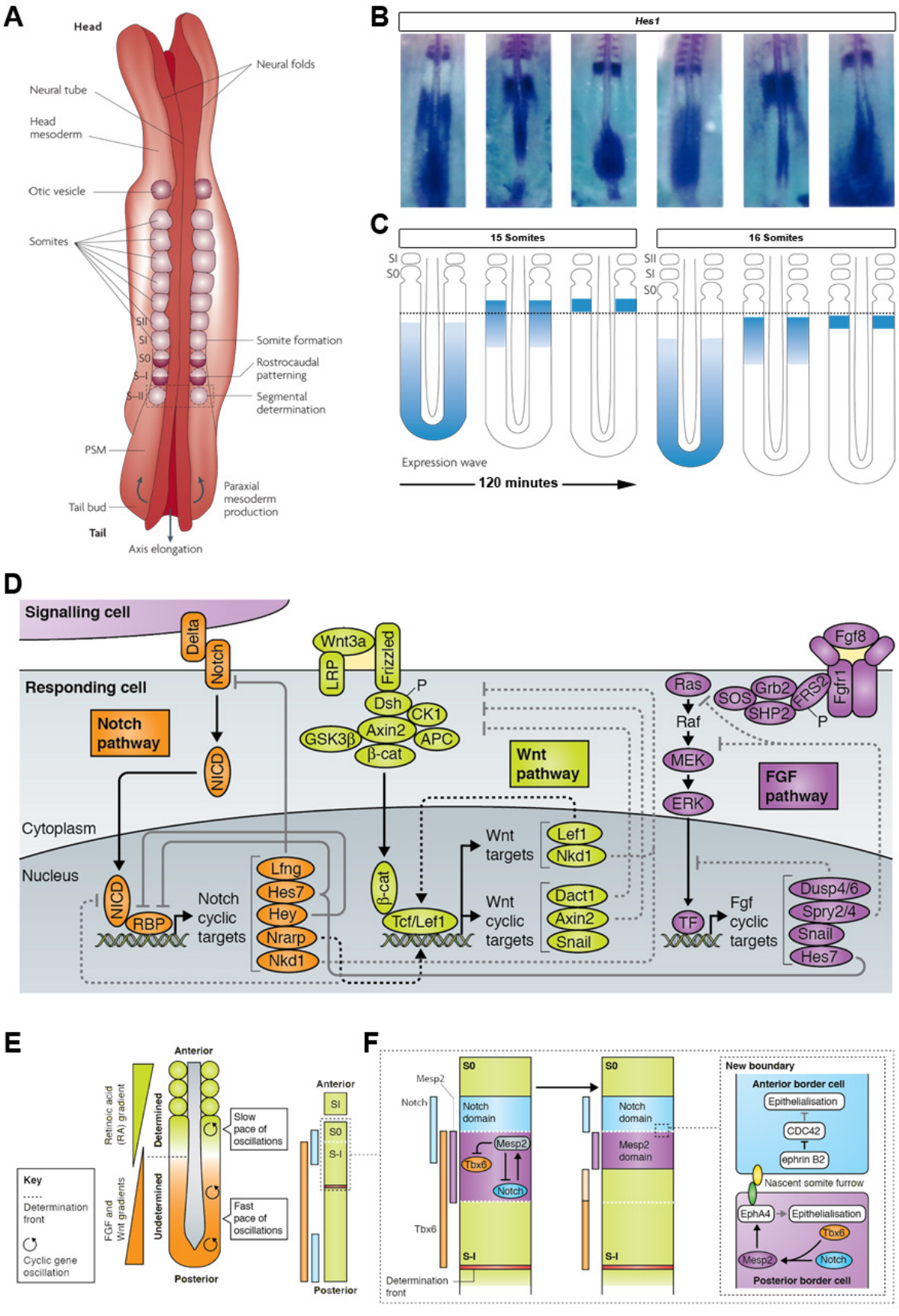
A
Head
Neural folds
Neural tube
Head mesoderm
Otic vesicle
Somites
SII
SI
S0
S-I
S-II
Somite formation
Rostrocaudal patterning
Segmental determination
PSM
Tail bud
Tail
Paraxial mesoderm production
Axis elongation
B
Hes1
C
15 Somites
16 Somites
SII
SI
S0
Expression wave
120 minutes
D
Signalling cell
Delta
Notch
Responding cell
Notch pathway
NICD
Wnt3a
LRP
Frizzled
P
Dsh
CK1
GSK3β
Axin2
APC
β-cat
Wnt pathway
Fgf8
Fgfr1
Ras
SOS
Grb2
FRS2
SHP2
P
Raf
MEK
ERK
FGF pathway
Cytoplasm
Nucleus
NICD
RBP
Notch cyclic targets
Lfng
Hes7
Hey
Nrarp
Nkd1
β-cat
Tcf/Lef1
Wnt targets
Lef1
Nkd1
Wnt cyclic targets
Dact1
Axin2
Snail
TF
Fgf cyclic targets
Dusp4/6
Spry2/4
Snail
Hes7
E
Anterior
Retinoic acid (RA) gradient
Determined
Undetermined
FGF and Wnt gradients
Slow pace of oscillations
Fast pace of oscillations
Posterior
Key
Determination front
Cyclic gene oscillation
Anterior
SI
S0
S-I
Posterior
F
Mesp2
Notch
S0
Notch domain
Mesp2
Tbx6
Notch
Tbx6
S-I
Determination front
S0
Notch domain
Mesp2 domain
S-I
New boundary
Anterior border cell
Epithelialisation
CDC42
ephrin B2
Nascent somite furrow
EphA4
Epithelialisation
Tbx6
Mesp2
Notch
Posterior border cell

1.2. The somitogenesis

In the vertebrate embryo, during axis formation, somitogenesis progressively segments the PSM into somites. The first somite is formed in the anterior part of the embryo, behind the otic placode (Figure 2A), then somitogenesis continues following an anterior-to-posterior direction as the embryo elongates, the last somite being formed in the tail of the embryo (Figure 2B; Bénazéraf and Pourquié, 2013).

Somitogenesis is a rhythmic process where somites are generated in a synchronous manner as pairs on each side of the neural tube by budding off the anterior tip of the PSM. This rhythm is conserved across vertebrates but presents with a species-specific period, for example about 90 min in chicken, 120 min in mouse, and 4 to 5 hours in humans (Figures 2B and C; Pourquié, 2011). Interestingly, this rhythm is deeply anchored within the PSM cells that will form the future somite. Even when isolated from the rest of the body, PSM segments in a synchronous manner (Dias et al., 2014; Palmeirim et al., 1998).

Somitogenesis is tightly orchestrated by a molecular oscillator controlling the synchronous formation of somites called the segmentation clock (Palmeirim et al., 1997). This segmentation clock generates dynamic and periodic pulses of mRNA expression travelling in a posterior-to-anterior fashion through the PSM each time a somite is being formed (Figures 2B and C).

Figure 2: The somitogenesis
(A) Schematic dorsal view of a 4 weeks old human embryo showing the generation of somites on each side of the neural tube. In the PSM, somites are numbered in a rostro-caudal series, somites S0 being the forming somite, S-I and S-II being the future somites to be formed. SI and SII represent the somites already formed. (B) Dynamic and periodic mRNA expression of *Hes1* across the PSM in a posterior-to-anterior fashion. (C) Schematic showing how the segmentation clock periodicity matches somite formation. (D) Model of interaction between Notch, WNT and FGF signalling pathways controlling the oscillatory expression of clock genes. (E) Scheme representing the anterior retinoic acid (RA) gradient opposing WNT and FGF gradients in the PSM. This combination of gradients forms the determination front that controls the somite segmentation together with the segmentation clock. (F) Schematic representing the signalling pathways and transcription factors involved in generating the somite boundaries prior to it segmentation from the PSM (adapted from Dequéant and Pourquié, 2008; Maroto et al., 2012; Pourquié, 2011).

These waves of expression are not due to cell movement but to cells switching cyclic gene expression on and off in an oscillatory manner (Pourquié, 2011). This oscillatory expression allows the synchronous formation of somites as a new somite buds off at the same time a wave of cyclic gene expression reaches the anterior end of the PSM (Figure 2C). Among the so-called cyclic genes, the *Hes* genes (targets of Notch signalling pathway) are essential in setting up the rhythm of the segmentation clock, nevertheless the mouse segmentation clock is composed of more genes than the *Hes* family alone (Figure 2D; Pourquié, 2011).

The segmentation clock is though to regulate somite formation, however a second mechanism is required to translate the action of the segmentation clock into the synchronous generation of somites together with the embryo axis elongation. This mechanism must maintain the cells from the posterior PSM in an undifferentiated state and spatiotemporally control when they can initiate differentiation to form the future somite (Figure 2E). This system consists of a complex combination of signalling gradients within the PSM between an anterior gradient of retinoic acid (RA) activity coming from the neural plate, which is opposing two parallel gradients of WNT and FGF signalling pathways coming from the posterior part of the PSM (Figure 2E; Aulehla et al., 2008; Del Corral et al., 2003; Dubrulle et al., 2001). These three gradients are generating a threshold of signalling in the PSM, called the determination front. In the PSM, posterior to the determination front, high levels of WNT and FGF signalling maintain the PSM cells in an undifferentiated state while the opposing gradient of RA signalling push them into differentiation when they pass the determination front (Figure 2E; Dequéant and Pourquié, 2008). It is though that the number of cells passing through the determination front is defining the size of the future somite. It is only after the PSM cells have passed through this determination front that they become competent to respond to the segmentation clock signal, corresponding to the controlled by activation of *Mesp2* (Figure 2F; Dequéant and Pourquié, 2008).

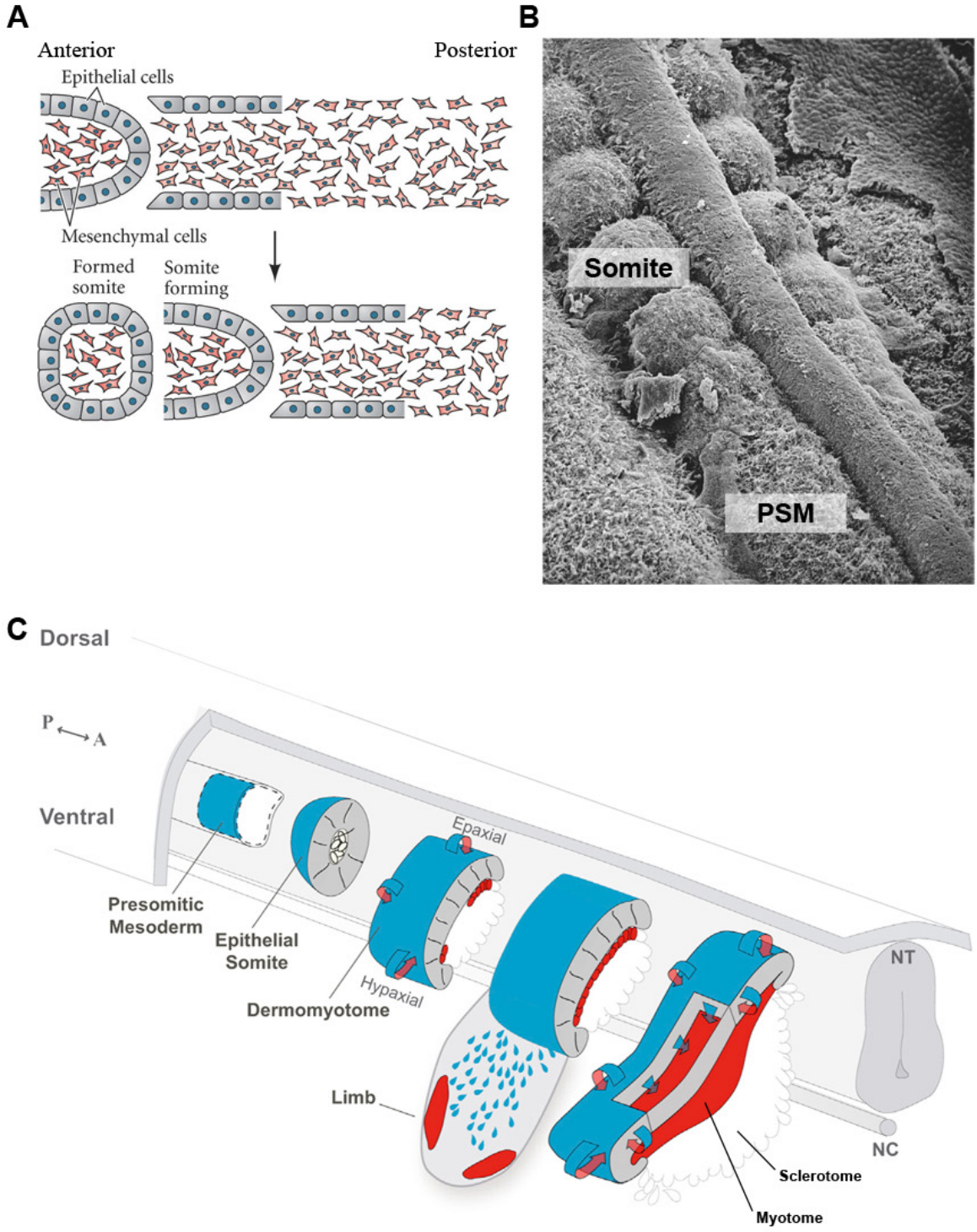

Figure 3: Somite maturation and muscle derivatives
(A) Schematic representing the epithelisation of the somite during it formation. (B) Dorsal view representing the differences between the mesenchymal structure of the PSM and the epithelial somites (adapted from Gilbert, 2013). (C) Schematic representation of somite maturation giving rise to three compartments, the dermomyotome, the myotome and the sclerotome. It highlights that cells from the dermomyotome migrate through the limb bud to establish the limb muscle masses. Curved arrows represent the delamination of cells from the lips of the dermomyotome to form the myotome. Flat arrows show the Pax3/7^{+} population giving rise to resident muscle

progenitor cells of the myotome. NT: Neural tube, NC: Notochord (adapted from Buckingham and Rigby, 2014).

Mesp2 expression is controlled by Notch signalling pathway (i.e. the segmentation clock) in the anterior PSM, while high levels of WNT and FGF signalling repress *Mesp2* activation in the cells located posteriorly to the determination front (Aulehla et al., 2008; Delfini et al., 2005; Dubrulle et al., 2001). *Mesp2* is essential to define the boundaries of the future somite by triggering the expression of Eph tyrosine kinase receptors and their ligands, the ephrins proteins, which are able to create a cell-cell repulsion effect (Figure 2F). Thus, separation of the somite from the anterior PSM occurs at the border between cells expressing the receptor EphA4 and those expressing its ligand EphrinB2 (Figure 2F; Barrios et al., 2003). In addition, cells forming the new somite acquired high levels of adhesion molecules such as N-cadherin and NCAM (Glazier et al., 2008).

Then the future somite presents a different morphology than the PSM (Figure 3A, B). While PSM cells are mesenchymal, cells from the future somite undergo and mesenchymal-to-epithelial transition. Thus the new somite consists of an epithelial layer of cells surrounding a mass of mesenchymal cells (Figure 3A, B).

1.3. Organisation of the mature somite

Upon stimulation of signalling pathways coming from the surrounding tissues, epithelial somites mature and differentiate. In the dorsal neural tube, WNT signalling, in combination with low level of Shh produced by the notochord and the floor plate, induces the differentiation of the myotome. In particular, *Wnt1* and *Wnt3* have been shown to be essential in this process as double mutant for these genes lacks part of the dermomyotome (Ikeya and Takada, 1998). Furthermore, when neural crest cells expressing Notch ligand *Delta-like1* (Dll1) pass next to the maturing somites, they provide a transient activation of Notch signalling pathway which is essential for the formation of the myotome (Rios et al., 2011).

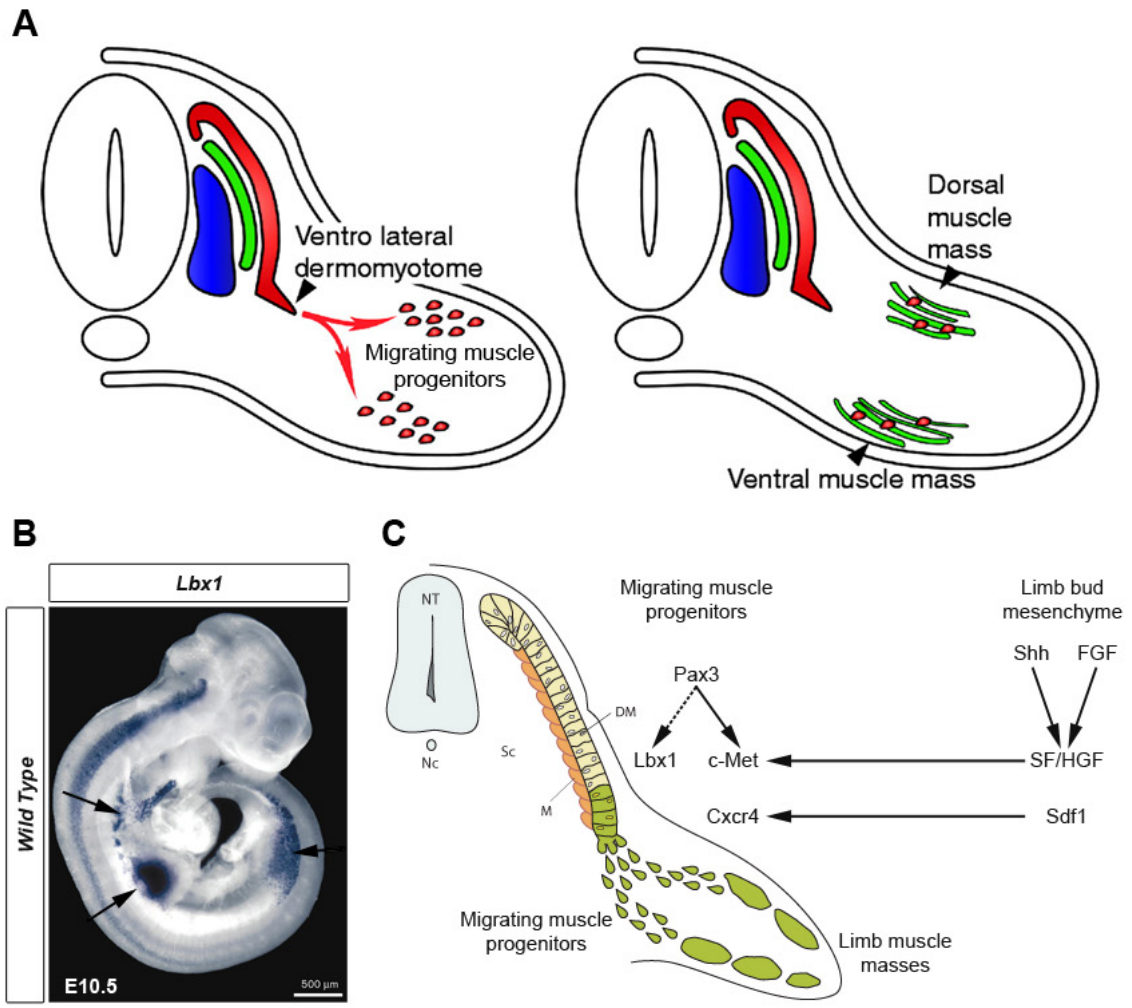

<u>Figure 4:</u> Establishment of the limb muscle masses

(A) Schematic representation of the migrating muscle progenitors from the hypaxial dermomyotome into the limb bud (from Mok and Sweetman, 2011). (B) *In situ* hybridization showing specific expression of Lbx1 in the migrating muscle progenitors (from Birchmeier and Brohmann, 2000). (C) Summary of the genes controlling the expressing of ligands and receptors involved in migration of muscle progenitors into the limb bud. Dotted arrow represents a supposed genetic interaction between *Pax3* and *Lbx1*.

In the ventral part of the somite, high concentrations of Shh induce the expression of *Pax1* that pushes the cells to generate the mesenchymal sclerotome (Chiang et al., 1996; Johnson et al., 1994), which will form bone and cartilage progenitor cells (Figure 3C). In the dorsal part of the somite, the dermomyotome is characterised by the conservation of an epithelial structure (Figure 3C). The brown fat, some endothelial and smooth muscles of the blood vessels and the entire trunk and limb skeletal muscles derived from the dermomyotome (Christ et al., 2007). Myogenesis starts in the somite where muscle progenitor cells delaminate from the dermomyotome and intercalate between the sclerotome and the dermomyotome to form the myotome (Ben-Yair and Kalcheim, 2005; Gros et al., 2005).

2. Migration to the limb bud and establishment of the muscle masses

In the dermomyotome, muscle progenitors also delaminate from its hypaxial lip and migrate to more distant locations such as the hypoglossal cord (that forms the pharyngeal and tongue muscles), the diaphragm and the limb buds where they establish the muscle masses (Figure 3C). From E9.25 to E11.0, at limb levels, cells from the dermomyotome form a pool of migrating muscle progenitors that will form distant muscles in the limbs (Figure 4A). In mouse embryos, forelimb muscles are derived from somites 9 to 14 while hindlimb muscles originate from somites 26 to 32 (Houzelstein et al., 1999). *Hox* genes are crucial in the specification of these pools of migrating muscle progenitors at specific axial level (Alvares et al., 2003), in addition to the action of BMP signalling (Bmp4; Dietrich et al., 1998; Pourquié et al., 1996). Once specified, this pool of migrating muscle progenitors, delaminate from the ventral part of the somite and migrate towards the limb buds where they establish both ventral and dorsal muscle masses (Figure 4A; Birchmeier and Brohmann, 2000).

Lbx1 is the only known gene specifically expressed in the migrating muscle progenitors (Figure 4B). This transcription factor is thought to play a critical role in the specification of migratory hypaxial progenitors however when absent, migration still occurs but some migrating progenitors are mis-routed (reviewed in Vasyutina and Birchmeier, 2006). *Pax3* is essential for the survival of the migratory progenitor pool in the hypaxial dermomyotome. In *Pax3* mutant mouse embryos, the hypaxial dermomytome is lost due to cell death (Borycki et al. 1999). Hence, migratory progenitors do not form nor delaminate, leading to a complete absence of limb muscles (Daston et al., 1996; Tremblay et al., 1998).

At limb levels, migrating muscle progenitors undergo an epithelial-to-mesenchymal transition (EMT) followed by a delamination. The receptor c-Met and its ligand SF/HGF are essential for delamination and migration of muscle progenitors as mouse mutants for both of them present a complete absence of skeletal muscle in the limbs (Bladt et al., 1995; Dietrich et al., 1999). The receptor c-Met is expressed in the hypaxial and epaxial lips of the dermomyotome at all axial levels whereas its ligand SF/HGF is not present in muscle progenitors but in the limb bud mesenchyme and along the routes used by the migrating cells (Dietrich et al., 1999). Its expression is controlled by Pax3 during the formation of limb muscles (Epstein et al., 1996; Relaix et al., 2003). The restricted expression of SF/HGF limits the activation of its receptor c-Met, thus allowing specific delamination of the migratory precursors at the limb buds level along the rostro-caudal axis. *SF/HGF* expression is maintained in the absence of migrating muscle progenitors demonstrating the paracrine action of this factor. Its expression is controlled by Shh and FGF signalling pathways generated from the apical ectodermal ridge in the limb bud (Figure 4C; Birchmeier and Brohmann, 2000; Scaal et al., 1999). In addition, the chemokine receptor *Cxcr4* genetically interacts with the c-Met downstream signalling pathway to control the guidance of migrating muscle progenitors with its ligand Sdf1 being expressed in a similar pattern to SF/HGF (Figure 4C; Vasyutina et al., 2005).

Interestingly, upon specification, delamination, migration and establishment in the limb bud, migratory muscle progenitor cells retain their proliferative capacity. It is only once they are established in the limb muscle masses that the muscle progenitors progressively enter the myogenic program, which is initiated when cells have reached their targets. The factors initiating myogenesis in the muscle masses are not known. However it has been suggested that muscle differentiation is triggered when inhibitory BMP signalling is down-regulated (Amthor et al., 1999). Nevertheless, a tight control of the balance between amplification of the muscle progenitors and entry into the myogenic program is needed to ensure the development of muscle masses of the correct shape and size (Cook and Tyers, 2007).

3. Muscle differentiation

3.1. The myogenic cascade

Cell differentiation depends on the activity of key transcription factors controlling the expression of sets of genes in order to give rise to specific cell types. Understanding this cascade of gene activation or repression is central in the generation of gene regulatory networks (GRN) capable of explaining the complex spatiotemporal process of differential gene expression patterns during development (Davidson, 2010).

Myogenesis has been one of the most studied systems during the past decades. Among the earliest markers of the epithelial somite stand the Paired-box transcription factors Pax3 and Pax7. The Pax family is composed of nine members (Figure 5A) characterised by the presence of a DNA binding Paired domain. The two paralogous genes *Pax3* and *Pax7* encode for proteins containing a Paired domain, an octapeptide and a homeodomain (Figure 5B; Chi and Epstein, 2002). They are expressed in the dermomyotome, where they mark the delaminating muscle progenitor cells that generate the myotome. In addition, they also form the future migrating muscle progenitors delaminating from the hypaxial lip of the somite and

A

Pax genes	Structural characteristics	Expression in developing tissues/organs	Examples of human diseases associated with *Pax* mutations
Pax3	PD OP HD1/HD2/3	CNS, craniofacial tissue, trunk neural crest, somites/skeletal muscle	Waardenburg syndrome, rhabdomyosarcoma
Pax7		CNS, craniofacial tissue, somites/skeletal muscle	Melanoma, neuroblastoma, rhabdomyosarcoma
Pax4		Pancreas, gut	Diabetes
Pax6		CNS, pancreas, gut, nose, eye	Aniridia, cataracts, G1 tumors
Pax2		CNS, kidney, ear	Kidney disease, e.g., Colomba syndrome, renal carcinomas
Pax8		CNS, kidney, thyroid	Congenital hypothyroidism, thyroid follicular carcinomas
Pax5		CNS, B-lymphocytes	Lymphomas
Pax1		Skeleton, thymus, parathyroid	Vertebral malformations, e.g., Klippell-Feil syndrome
Pax9		Skeleton, thymus, craniofacial tissue, teeth	Oligodentia

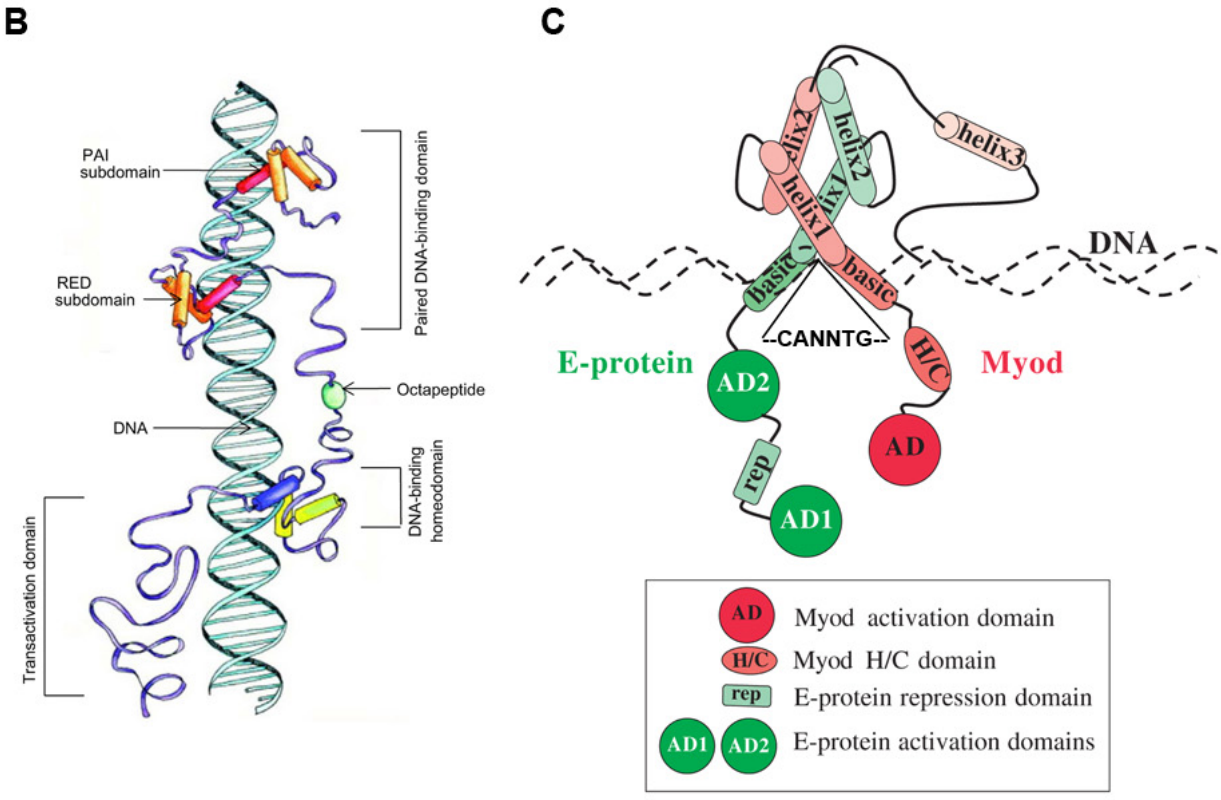

Figure 5: The Pax and MRFs families of transcription factors
(A) The Pax family of transcription factors (from Buckingham and Relaix, 2007). (B) Structure of the Pax3 protein highlighting the Paired domain, the octapeptide and the homeodomain (from Chi and Epstein, 2002). (C) Schematic representation of MyoD association with the E protein upon binding to DNA (from Tapscott, 2005).

migrating into the limb bud (Figure 3C and 4C). In the myotome and the limb muscle masses, $Pax3^{+}/Pax7^{+}$ cells form an amplifying proliferative population of muscle progenitors (Buckingham and Relaix, 2007).

Once established in the limb muscle masses, muscle progenitors enter the myogenic differentiation program by activating the Muscle Regulatory Factors (MRFs) expression. Among the MRFs, MyoD was the first to be identified based on its ability to convert fibroblasts into muscle cells (Tapscott et al., 1988). According to their homology to MyoD, three other MRFs have been isolated: Myf5 (Braun et al., 1989), Myogenin (MyoG) (Wright et al., 1989) and Mrf4 (Rhodes and Konieczny, 1989). These four proteins belong to the same super family of transcription factors characterised by the presence of a basic helix loop helix (bHLH) DNA binding domain that recognizes the E-box sequence (CANNTG; Figure 5C). In addition to all being able to induce myogenic conversion *in vitro* (Weintraub et al., 1989), they are essential for the induction of myogenic differentiation *in vivo* and their activation at the onset of myogenesis by upstream factors is tightly controlled (Moncaut et al., 2013).

Pax3 acts upstream of *Myf5* and *MyoD* (Bajard et al., 2006; Tajbakhsh et al., 1997), placing this factor a the top of the regulatory cascade that controls myogenesis (Figure 6A). Pax3 and its paralog Pax7 are the factors that specify skeletal muscle progenitor cells during development (Buckingham and Relaix, 2007). In *Pax3/Pax7* double mutants, the primary myotome is formed but subsequent myogenesis does not occur (Relaix et al., 2005). In these mutants, the pool of progenitor cells is in majority lost by apoptosis and in some cases mis-specified into alternative lineages such as bone. Pax3 directly activates the expression of *Myf5* (Bajard et al., 2006), by binding on an enhancer element 145bp upstream of the *Myf5* coding sequence. Pax3 binding of this element is responsible for *Myf5* activation in muscle progenitors, thus it places Pax3 upstream of *Myf5* in the myogenic cascade (Bajard et al., 2006).

Myf5 is considered as a determination factor and its expression marks the entry of muscle progenitors into the myogenic program. In *Myf5* mutants, muscle progenitors are still able to enter the myogenic program because of *MyoD* expression (Braun et al., 1994) demonstrating that *MyoD* compensates for *Myf5* absence to form skeletal muscles. Interestingly, while *Myf5* mutant displays normal limb muscles development, in *MyoD* mutants, limb muscle development is delayed by 2.5 days from E11.5 to E13.5 (Kablar et al., 1997). Neither limb muscle progenitor migration nor induction of *Myf5* expression are affected in the *MyoD* mutant demonstrating that *Myf5* alone is not sufficient for normal limb myogenesis. This suggests that *Myf5* and *MyoD* are involved in independent processes during the formation of limb muscles (Kablar et al., 1997). Consistent with this idea, lineage tracking experiments revealed that *Myf5* is only expressed in a subset of the myoblast population (Haldar et al., 2008). Thus that three populations are present in developing muscles, a $My5^{+}$; $MyoD^{-}$ and a $Myf5^{+}$; $MyoD^{+}$ belonging to the so-called Myf5-dependent lineage and a $Myf5^{-}$; $MyoD^{+}$ forming the Myf5-independent lineage (Haldar et al., 2008). Furthermore, genetic ablation of $Myf5^{+}$ cells in mouse embryo confirmed the existence of two parallel myogenic lineages and demonstrated that the loss of the Myf5 lineage is compatible with myogenesis. The MyoD lineage compensates for the loss of $Myf5^{+}$ cells by expanding its myoblast population (Gensch et al., 2008; Haldar et al., 2008), which also suggests the nature of compensation between *Myf5* and *MyoD* in the single mutants. In *Pax3/Myf5* mutants, skeletal muscles in the body are not formed, *MyoD* is not activated, thus demonstrating that *MyoD* is genetically downstream of these genes and that *MyoD* expression depends on both Myf5 and Pax3 (Tajbakhsh et al., 1997).

In the absence of *Myf5* and *MyoD*, the embryo fails to develop any skeletal muscles. $Pax3^{+}$/$Pax7^{+}$ progenitor cells are formed but either die or adopt alternative non-myogenic fates such as cartilage or bone (Kassar-Duchossoy et al., 2004; Tajbakhsh et al., 1996).

Mrf4 is also able to induce myogenesis, as its expression, from E13.5, rescues limb myogenesis that is paused in *MyoD* mutants (Kablar et al., 1997). However in *Myf5* mutants, its expression is compromised in *cis*, therefore making it linked to *Myf5* expression (Floss et al., 1996; Kassar-Duchossoy et al., 2004). Genetic ablation of $Mrf4^{+}$ cells abrogates the formation of myofibres, demonstrating its essential role for late myogenesis (Haldar et al., 2008). When both *Myf5* and *Mrf4* are absent, myotome formation is delayed which is associated with a delay in *MyoD* expression. This demonstrates that Mrf4 is also involved in the control of *MyoD* expression (Tajbakhsh et al., 1997).

MyoG only regulates the late stages of myogenesis as myoblasts are normally formed in *MyoG* mutants (Hasty et al., 1993; Nabeshima et al., 1993), which exhibit perinatal death due to severe muscle deficiency. In *MyoG* mutants, limb muscle masses are only populated with mononucleated cells demonstrating its implications in the control of myoblasts fusion during the formation of the muscle fibres. Furthermore, the generation of double mutants of *Myf5* and *MyoG* or *MyoD* and *MyoG* revealed that the muscle lineage is correctly specified, however the mice do not form any myofibres, a phenotype similar to the *MyoG* single mutant (Rawls et al., 1995). Furthermore, genetic ablation of $MyoG^{+}$ cells is incompatible with generation of myofibres, while early aspects of myogenesis are not affected confirming previous results (Gensch et al., 2008). This also suggests that the late myogenic program is shared between the Myf5 dependant and the Myf5 independent lineages. These models demonstrate that *MyoG* function is distinct from *Myf5* and *MyoD*, illustrating that *MyoG* acts downstream of these factors during muscle development (Figure 6A) as evidenced by its severe down regulation in *Myf5* mutants (Kassar-Duchossoy et al., 2004). In addition, analysis of the *MyoG* promoter suggests its expression is directly controlled by Myf5 (Yee and Rigby, 1993) and MyoD (Armand et al., 2008; de la Serna et al., 2005).

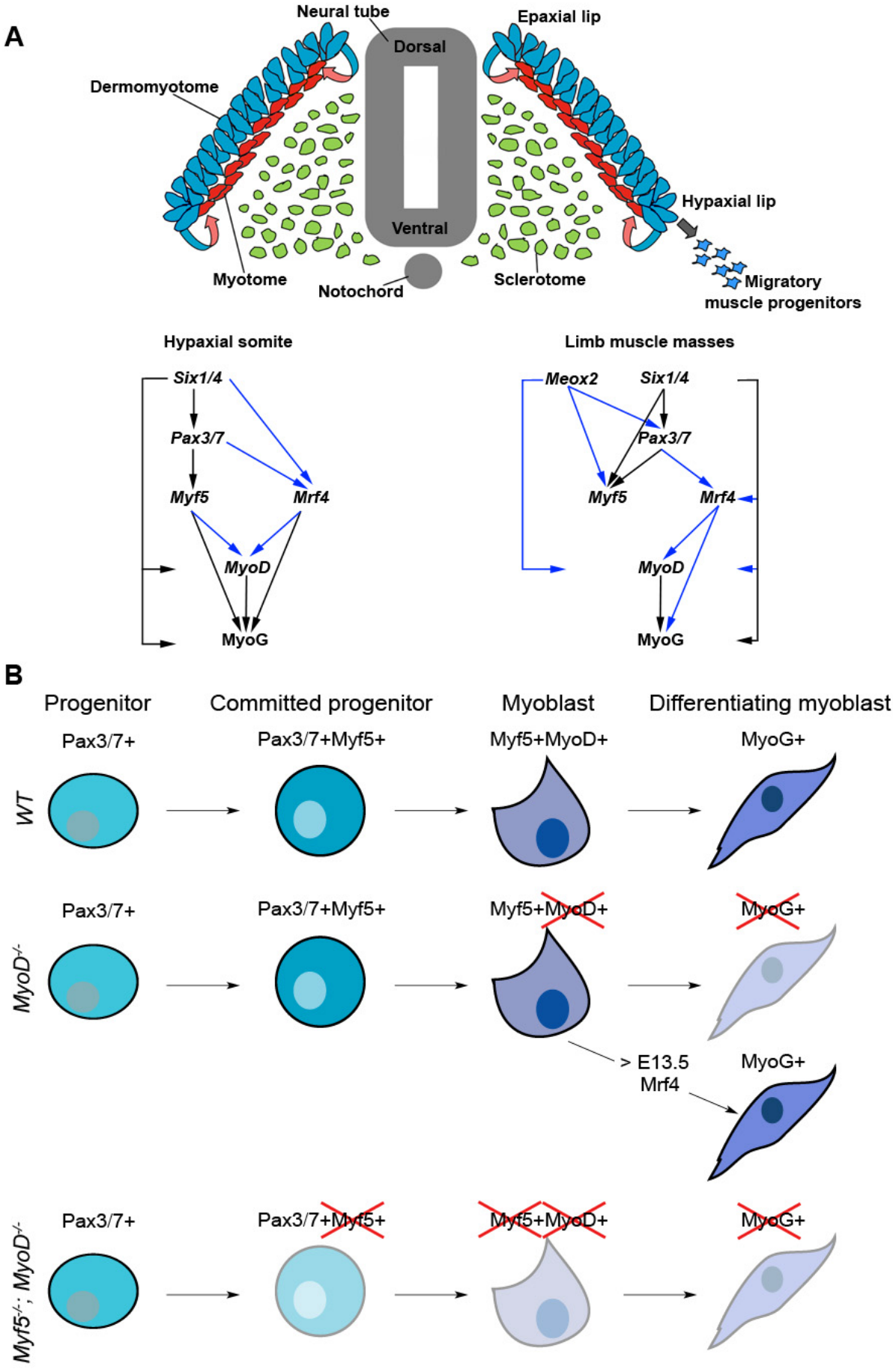
A
Neural tube
Dorsal
Epaxial lip
Dermomyotome
Hypaxial lip
Ventral
Myotome
Notochord
Sclerotome
Migratory
muscle progenitors
Hypaxial somite
Six1/4
Pax3/7
Myf5
Mrf4
MyoD
MyoG
Limb muscle masses
Meox2
Six1/4
Pax3/7
Myf5
Mrf4
MyoD
MyoG
B
Progenitor
Committed progenitor
Myoblast
Differentiating myoblast
Pax3/7+
Pax3/7+Myf5+
Myf5+MyoD+
MyoG+
WT
Pax3/7+
Pax3/7+Myf5+
Myf5+MyoD+
MyoG+
MyoD-/-
> E13.5
Mrf4
MyoG+
Pax3/7+
Pax3/7+Myf5+
Myf5+MyoD+
MyoG+
Myf5-/-; MyoD-/-

The sine-oculis related homeobox (Six) family, in particular *Six1* and *Six4*, is considered to be capping the myogenic cascade during muscle development. Six proteins are transcription factors that bind to eyes-absent homologs Eya1 and Eya2 in the nucleus (Grifone et al., 2007), where they activate the expression of *Pax3*, *MyoD*, *Mrf4* and *MyoG* (Figure 6A; Grifone et al., 2005, 2007; Relaix et al., 2013). Interestingly, in the limb, Six1 and Six4 also directly regulate the expression of *Myf5* (Figure 6A) by binding the same 145bp upstream enhancer element bound by Pax3 in the hypaxial somite (Giordani et al., 2007).

The homeobox gene *Meox2* encodes another transcription factor involved in the regulation of limb muscle development, which is expressed in migrating muscle progenitors. Analysis of *Meox2* mutants revealed that specific subsets of limb muscles are missing (Mankoo et al., 1999). Moreover, in *Meox2* mutants, expression of *Pax3* and *Myf5* is down-regulated while *MyoD* expression is not affected, which suggests that in the limb, *MyoD* expression is not regulated by these factors (Figure 6A; Mankoo et al., 1999).

During muscle development, activation of the MRFs is relatively linear. However, regulatory feedback loops do exist, in particular through the action of Mef2. While it was shown that MRFs activate their own expression in the myogenic cascade, they also induce the expression of *Mef2* (Potthoff and Olson, 2007).

Figure 6: The Myogenic Regulatory Factors drive cell toward muscle differentiation
(A) The myogenic cascades in the myotome and the limb muscle masses. Black arrows represent direct interactions at the transcriptional level, while blue arrows mark genetic interactions (adapted from Bismuth and Relaix, 2010; Blake and Ziman, 2014). (B) Top line represents a schematic representation of the different steps involved in muscle differentiation. Middle line represents the development of myoblasts in *MyoD* mutants. In the absence of *MyoD*, myoblasts do not activate *MyoG* expression leading to a defect in myoblast fusion and an absence of muscle fibres. However, in the limb, from E13.5, *Mrf4* is induces and activates *MyoG* expression, rescuing the phenotype of *MyoD* mutants after a paused of 2.5 embryonic days in their limb muscles development. Bottom line shows the development of muscle progenitors in *Myf5; MyoD* double mutant. In the absence of these two MRFs, muscle progenitors do not differentiate into myoblasts and either die by apoptosis or adopt an alternative cell fate.

Mef2 does not exhibit a myogenic activity *per se* but acts to potentiate the function of MRFs via transcriptional cooperation (Molkentin et al., 1995).

In conclusion, once $Pax3^{+}/Pax7^{+}$ progenitor cells are established in the muscle masses they enter myogenesis by activating *Myf5* expression and form the committed progenitors population (Figure 6B). Following *Myf5* activation, committed progenitors activate *MyoD* and form a transitory myoblasts population. Expression of both *Myf5* and *MyoD* manifests the differentiation from muscle progenitors to myoblasts. The final step in the myogenic cascade is the expression of *MyoG* (Figure 6B). $MyoG^{+}$ cells form the determined myoblasts population that fuse together to establish the first multinucleated muscle fibres called myotubes or myofibres that will later generate the muscle fibres of the limb muscles.

3.2. MRFs binding and control of muscle differentiation

Another step in understanding the fundamental basis of GRNs orchestrating developmental processes is to uncover how transcription factors specifically bind DNA sequences to control gene expression of their downstream targets.

The availability of the C2C12 cell line to recapitulate muscle differentiation has been a tremendous help to understand the MRFs transcriptional regulation during muscle differentiation. Chromatin immunoprecipitation coupled to high-throughput sequencing (ChIP-seq) has allowed the precise analysis of genome wide distribution of transcription factors binding sites. ChIP-seq analysis to investigate the dynamics binding of MyoD during muscle differentiation at the genome wide level (Cao et al., 2010) characterised the relationship between the binding of this transcription factor to DNA and the regulation of its target genes across the entire genome. This study revealed that MyoD is binding between 30000 to 60000 sites. Of note, there are about 14 million predicted E-boxes across the genome (Todeschini et al., 2014).

Hence, this study revealed that MyoD only binds a small fraction of these and does so during muscle differentiation. However, they discovered that MyoD also binds up to 75% of all genes despite no direct influence on their expression. This suggests that on a genome wide scale, most MyoD binding events are not associated with transcriptional regulation.

Although, this study did not elucidate the core transcriptional function of MyoD it revealed an unexpected function for this factor; most of its binding events being is associated with chromatin remodelling. The ability of MyoD to convert a wide variety of cells into skeletal muscles suggests that it could act as a pioneer transcription factor, which is consistent with the numerous MyoD binding events identified in the genome. A pioneer transcription factor is characterised as a factor that can access and activate genes located in a repressive chromatin context and remodel the chromatin landscape at different loci to allow gene transcription independently of the prior cell lineage.

Nuclease access studies revealed that prior to the presence of MyoD in the cell, *MyoG* which is regulated by MyoD, exists in a repressive chromatin state. However, when MyoD is present in the cell, *MyoG* gets expressed, suggesting that MyoD can remodel the chromatin landscape around the *MyoG* locus to make it accessible (Gerber et al., 1997). Furthermore, it was shown that MyoD directly binds the histone acetyltransferase (HAT) p300, which acetylates histones and recruits another HAT, the p300/CBP-associated factor (PCAF) that acetylates MyoD near its DNA-binding domain, in addition to recruiting the Swi/Snf chromatin-remodelling complex (Albini and Puri, 2010; Dilworth et al., 2004; Puri et al., 1997a, 1997b; Sartorelli et al., 1997, 1999). Inhibition of HAT or Swi/Snf activities prevents the ability of MyoD to initiate transcription and chromatin remodelling (de la Serna et al., 2001; Puri et al., 1997b). Altogether, theses results strongly suggest that MyoD can be considered as a pioneer transcription factor, being able to access loci located in a repressive chromatin context and to induce chromatin remodelling.

Currently, it is believed that most tissue-specific transcription factors are involved in remodelling the chromatin structure in order to make it accessible to the transcriptional machinery at precise gene loci characterising a defined cell type (Spitz and Furlong, 2012). However, these genomic studies only provide a snapshot of the transcription factors mechanistic action. They do not provide a complete understanding of the transcription factors binding dynamic in the context of transcriptional regulation (Todeschini et al., 2014). In other words, they do not elucidate how at a single locus MyoD regulates the transcription of its target gene. In addition they miss, if any, the relationships established with other transcription factors to determine the activation or repression of the given locus according of the spatiotemporal status of the cell.

3.3. Muscle growth and regeneration

After the formation of differentiated myoblasts, the next step in muscle development is the generation of the primary muscle fibres between E11.5 and E14.5 in the mouse limbs. Once embryonic myoblasts are formed and differentiated, they fuse together and give rise to the first multinucleated muscle fibres around E11.0 and establish the pattern of future muscles. From E14.5, foetal myoblasts are generated and form secondary fibres around the primary fibres (Ontell and Kozeka, 1984), while inhibition of Tgfβ and β-catenin signalling pathways regulate foetal myoblasts differentiation (Cusella-De Angelis et al., 1994; Hutcheson et al., 2009). Next, extensive growth of the muscle masses occurs during the foetal and perinatal stages. After birth, myogenesis only occurs during postnatal growth and regeneration of the mature adult muscles following muscle injuries. Both postnatal growth and muscle regeneration rely on the recruitment of stem cells to the sites of injuries. In mature muscles, these stem cells, called satellite cells, lie next to the muscle fibres under the basal lamina in a location called the satellite cell “niche” (Figure 7A; Mauro, 1961).

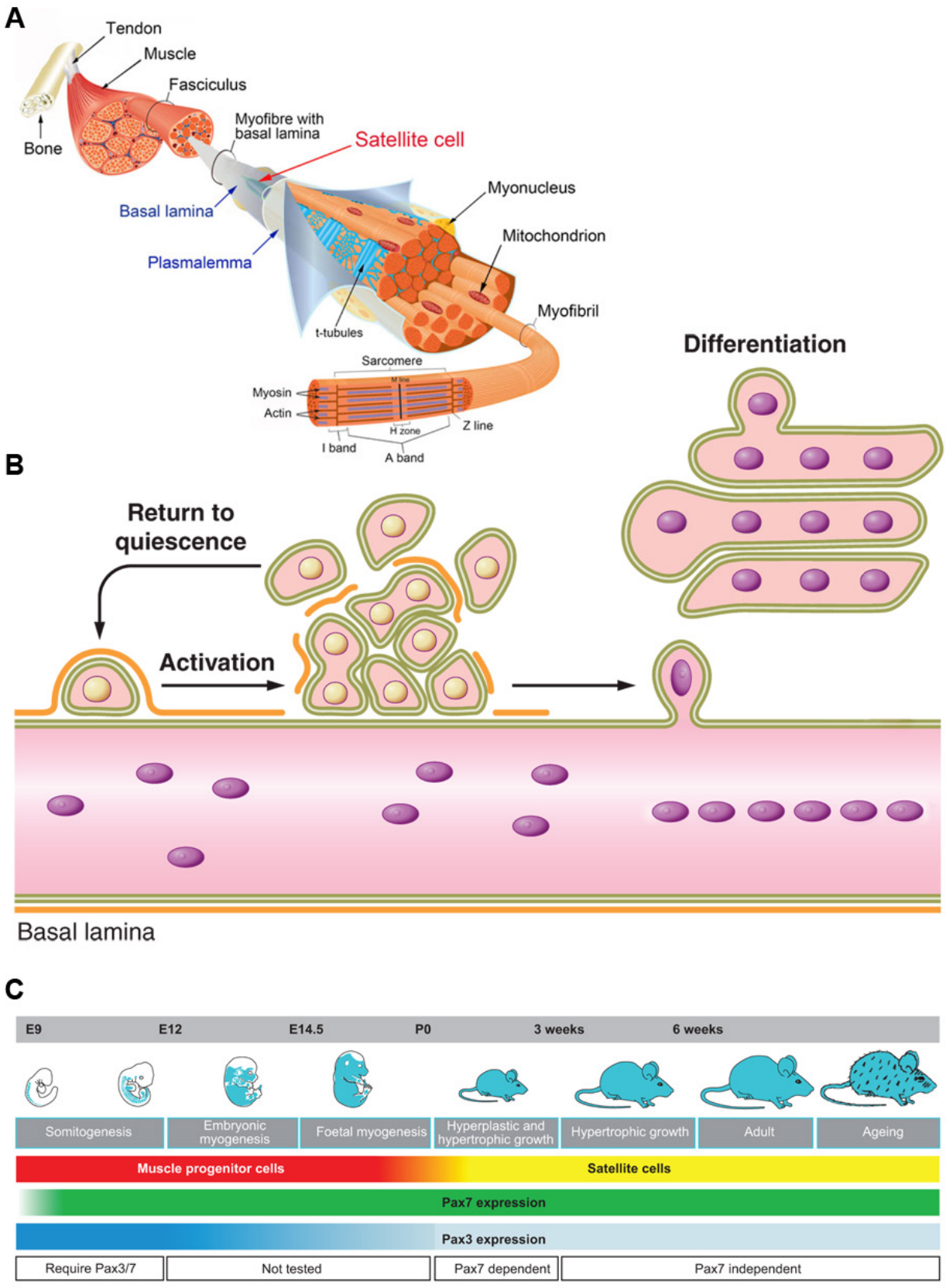

Figure 7: Adult myogenesis

(A) Schematic representing the formation of the muscle and the position of the satellite cells (from Relaix and Zammit, 2012). (B) Schematic representing satellite cells activation, differentiation, and fusion during muscle regeneration (adapted from Yin et al., 2013). (C)

Development of the myogenic lineage and dependence of muscle progenitor cells and satellite cells on *Pax3* and *Pax7* during embryonic and adult myogenesis (from Relaix and Zammit, 2012).

Satellite cells are histologically observed from E16.5 and are believed to resist differentiation in order to provide undifferentiated muscle progenitor cells to sustain the distinct waves of myogenesis (Gros et al., 2005; Kassar-Duchossoy et al., 2005; Murphy and Kardon, 2011; Relaix et al., 2005). The satellite cell "niche" corresponds to a location presenting a specific microenvironment, which promotes self-renewal and inhibits differentiation. During homeostasis, satellite cells remain quiescent in their "niche" where they display minimal metabolic activity (Figure 7B).

Identification of the satellite cell's developmental origin was demonstrated by both grafting quail somites into chick embryos (Armand et al., 1983) and cell lineage tracking using dye injection (Gros et al., 2005; Schienda et al., 2006). These studies demonstrated that in the somite, myogenic progenitors give rise to satellite cells. More specifically, mouse genetic lineage tracking experiments revealed that in addition to contributing to trunk and limb muscles, $Pax3^{+}$ and $Pax7^{+}$ cells also generate the satellite cell population (Figure 7C; Engleka et al., 2005; Lepper and Fan, 2010; Schienda et al., 2006).

Upon muscle injury, satellite cells are activated and start proliferating in order to provide muscle progenitors to allow muscle regeneration (Figure 7B). Several teams have genetically ablated the satellite cell population to assess the regenerative capacities of muscle, and in doing so were able to demonstrate that satellite cells are essential for muscle regeneration (for review see Relaix and Zammit, 2012). Skeletal muscles exhibit an important regenerative capacity; they are able to undergo several rounds of regeneration after multiple serial injuries. This implies that while satellite cells produce new cells for regenerating injured muscle, they also replenish their "niche" to avoid exhaustion of the satellite cell pool (Figure 7B). Interestingly, during this process, satellite cells use the same GRNs as those used during embryonic myogenesis (for review see Relaix and Zammit, 2012).

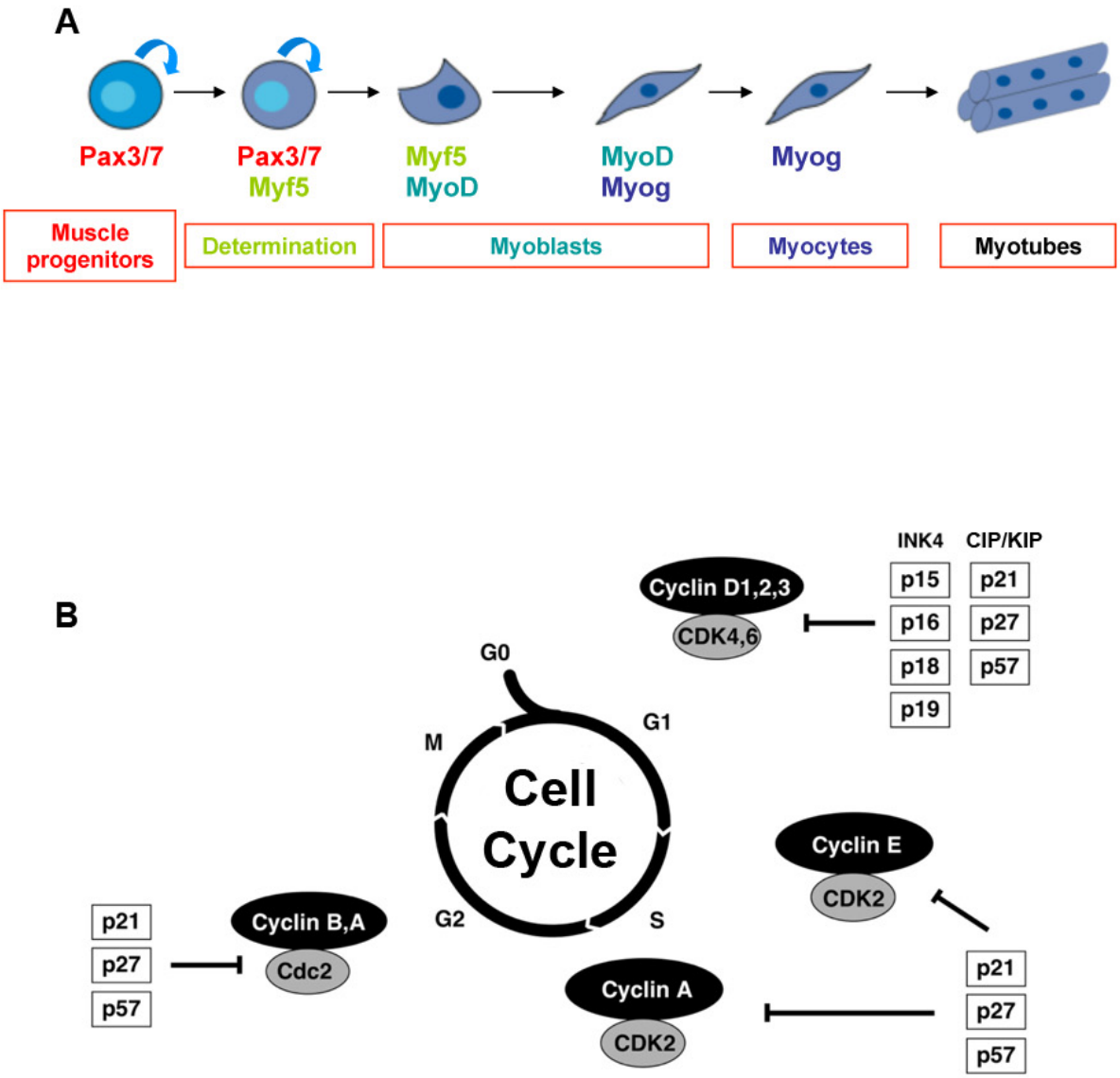

Figure 8: Muscle differentiation and regulation of the cell cycle
(A) Schematic representation of myogenesis highlighting the cell cycle exit occurring during the differentiation of muscle progenitors into myoblasts. Curved blue arrows indicate the cycling cell population. (B) CDKs and Cyclins dynamic association regulated the cell cycle progression through the different phases while members of the INK4 and CIP/KIP families are essential effectors of cell cycle arrest.

4. Control of cell cycle exit

Once muscle progenitors are established in the limb bud, equilibrium between cell proliferation and differentiation must be defined both temporally and spatially in order to generate muscles of the appropriate size. On the one hand, muscle progenitors must proliferate enough to create an adequate number of cells for the formation of the future muscle fibres while, on the other hand they must undergo muscle differentiation and turn into myoblasts in order to give rise to these muscle fibres. Thus, generation of muscles of the correct size requires these two mechanisms to work in a synchronous manner. This suggests the existence of a system avoiding precocious differentiation associated with depletion of the progenitors pool and belated differentiation correlated with excessive expansion of the progenitors pool. This regulation mechanism is therefore involved in coordinating cell growth arrest with muscle differentiation. During myogenesis, in addition to the activation of *Myf5* and *MyoD* expression that marks the start of myogenic differentiation, cell growth arrest is another phenomenon characterising the differentiation of muscle progenitors into myoblasts. While muscle progenitors form a proliferative population, myoblasts do not proliferate (Figure 8A; Picard and Marcelle, 2013). However, despite the identification of a GRN controlling myogenic differentiation, it remains unclear how cell cycle exit is synchronized with skeletal muscle differentiation.

The cell cycle can be divided in four main phases: G1 (for gap, where the cell increases in size and ensures that everything is ready for DNA synthesis), S (for synthesis, where DNA replication occurs), G2 (where the cell continues to grow and controls that everything is ready to divide) and M (for mitosis, where cell growth stops and cellular energy is focused on the orderly division into two daughter cells). G1 and G2 are intermediate phases between DNA synthesis and mitosis where in addition to growing; the cell inspects its internal and external environments to insure that all the conditions are favourable to enter the next phase of DNA

synthesis or mitosis (Figure 8B). The phase called G0 corresponds to a period where the cell exits the cell cycle and stops proliferating. This is also called cell growth arrest, and is usually linked with terminal differentiation.

The core regulation of the cell cycle is based on two families of molecules called the Cyclins (Cyclin A, Cyclin B, Cyclin D1, D2, D3 and Cyclin E) and the CDKs (cyclin dependant kinase; Cdc2, Cdk2, Cdk4 and Cdk6). These molecules exhibit a cyclic activity during cell cycle progression triggering cyclic phosphorylation of proteins involved in the major steps of the cell cycle such as DNA replication or mitosis. For instance, increased CDKs activity before mitosis drives increased phosphorylation of proteins involved in chromosome condensation. The cyclic activity of the CDKs is controlled by the Cyclins that associate with them (Figure 8B). While CDK concentration remains constant, Cyclins undergo cycles of production and degradation during each cell cycle. These cyclic variations in Cyclins concentration allow the periodic assembly of the Cyclin-CDK complexes that control cell cycle progression, which in turn regulate the cellular events (for review see Sherr and Roberts, 2004).

Each Cyclin is expressed during a specific phase of the cell cycle. The Cyclin D is the first produced during the phase G1 of the cell cycle where it binds to Cdk4 and Cdk6. These Cyclin-CDK complexes trigger the expression of the Cyclin A and Cyclin E, which bind to Cdk2. These complexes push the cell from G1 to S phase and initiate DNA replication. The Cyclin A is also expressed during the phase G2 together with the Cyclin B where they associate with Cdc2 (Figure 8B). These complexes cause the breakdown of the nuclear envelope and initiation of mitosis.

Cell growth arrest, also called cell cycle exit, relies on the CDKI (Cyclin Dependent Kinase Inhibitor) families. CDKIs bind to the Cyclin-CDK complexes to inhibit their cyclic variations and provide the main mechanism triggering cell cycle exit and cell growth arrest.

These CDKIs are divided in two families based on their evolutionary origins. The INK4 family encodes *p16*^{INK4a}, *p15*^{INK4b}, *p18*^{INK4c} and *p19*^{INK4d} all of which bind to Cdk4 and Cdk6, and interfere with their association with Cyclin D. The second family called CIP/KIP is composed of three members, *p21*$^{cip1/Waf1}$ (*Cdkn1a*), *p27*^{kip1} (*Cdkn1b*) and *p57*^{kip2} (*Cdkn1c*) abbreviated *p21*, *p27* and *p57* (for review see Besson et al., 2008), which bind to both Cyclins (A, D and E) and CDKs (Cdc2). Hence, expression of members of both INK4 and CIP/KIP family members is associated with proliferation blockade and cell cycle exit (Figure 8B; Cheng et al., 1999; Sherr and Roberts, 1999).

In particular, members of the CIP/KIP have been shown to be essential during embryonic development (Besson et al., 2008). Most notably, in the absence of both *p21* and *p57*, skeletal muscle development is severely affected and fibre formation is impaired, with myogenic cells undergoing apoptosis. This points towards an essential function of *p21* and *p57* in cell cycle arrest during myogenesis (Zhang et al., 1999); raising the possibility that p21 and p57 may also be involved in the regulation of *MyoG* expression and terminal differentiation in murine myogenesis during development. *In vitro*, MyoD has been suggested to be a direct regulator of *p21*, thus controlling cell cycle exit during adult muscle differentiation (Halevy et al., 1995). In addition, it was shown that in *MyoD* mutant mice, myoblasts fail to exit the cell cycle as the transcriptional regulator nuclear factor-κB (NF-κB) stays in the nucleus where it maintains the expression of essential cell cycle regulators (Parker et al., 2012). It has also been shown in mammalian cells (Reynaud et al., 2000) and zebrafish (Osborn et al., 2011), that p57 interacts and stabilizes MyoD to promote muscle differentiation, demonstrating a role for CDKIs beyond cell growth arrest. Analysis of *p21; p57* double mouse mutant embryos suggests that cell cycle exit occurs in parallel but independently of MyoG-dependent terminal differentiation (Zhang et al., 1999).

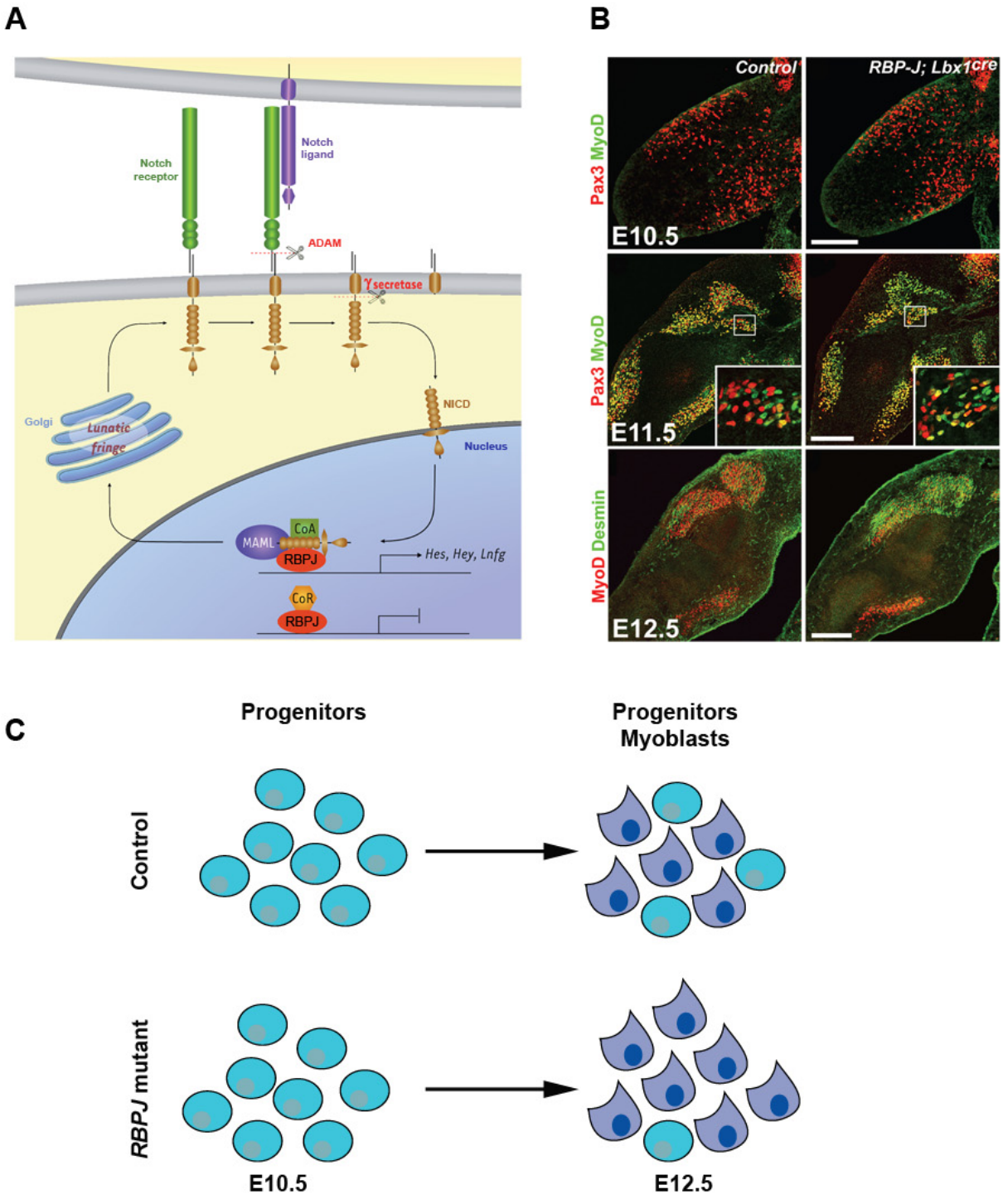

Figure 9: Notch signalling pathway and myogenesis
(A) Schematic representation of the Notch signalling pathway (adapted from Mayeuf and Relaix, 2011). (B) Precocious muscle differentiation when Notch signalling is impaired in limb muscle progenitor cells leads to exhaustion of the progenitor pool and small muscle masses (adapted from Vasyutina et al., 2007). (C) Schematic representation of the progenitor pool

exhaustion when Notch signalling is inhibited. Blue cells represent de progenitors and purple cells the myoblasts.

5. Notch signalling: a crucial regulator of cell fate decision

Previous studies have implicated the Notch signalling pathway as a key regulator of proliferation and differentiation of muscle progenitor cells (Buas and Kadesch, 2010). This pathway is highly conserved among species and plays key roles during development, including the regulation of cell fate decision, differentiation and homeostasis of progenitor cells in a large variety of tissues (for review see Artavanis-Tsakonas and Muskavitch, 2010). Notch signalling requires the direct interaction between a cell expressing at least one of the five ligands (Dll1, 3 and 4, and Jagged 1 and 2 in mammals) with a cell expressing one of the four receptors (Notch 1-4 in mammals). This interaction leads to a proteolytic cleavage of the Notch receptor that releases the Notch intracellular domain (NICD), which translocates into the nucleus and interacts with the transcription factor Rbpj that binds to regulatory elements of Notch target genes. Without NICD, Rbpj is though to interact with co-repressors. Upon activation of Notch signalling, NICD binding to Rbpj results in the recruitment of co-activators such as Mastermind-like and p300 and induces the expression of Notch downstream target genes, such as the *Hes/Hey* family of bHLH transcriptional repressors (Figure 9A; for review see Borggrefe and Liefke, 2012). The expression of Notch ligands and receptors in the limb bud and myotome suggests a role for this signalling pathway during muscle development (Beckers et al., 1999). Notch signalling function in skeletal muscle development was assessed in different studies. It was shown *in vitro* that overexpressing NICD blocks myoblasts differentiation (Jarriault et al., 1998; Kopan et al., 1994).Using chick embryos, *in vitro* and *in vivo* gain-of-function experiments suggest that Notch signalling is required for muscle differentiation. For instance, overexpressing *Dll1* in the limb bud leads to incorrect differentiation of muscle progenitors (Delfini et al., 2000).

This was correlated with a down-regulation of *MyoD* expression in myoblasts but interestingly *Myf5* and *Pax3* expression was unchanged (Delfini et al., 2000; Hirsinger et al., 2001). In addition, different mouse models demonstrated that canonical Notch signalling is required for the maintenance of muscle progenitors (Schuster-Gossler et al., 2007; Vasyutina et al., 2007). Using either a hypomorphic *Dll1* mutant (Schuster-Gossler et al., 2007) or a conditional mutant for *Rbpj* that abrogates its expression in migratory muscle progenitors ($Lbx1^{Cre}$) (Vasyutina et al., 2007), it was demonstrated that impairing Notch signalling leads to a precocious muscle differentiation (Figure 9B). This was associated with an enlarged population of myoblasts and a rapid exhaustion of the muscle progenitors pool leading to a near complete absence of skeletal muscles at the foetal stage (Figure 9C; Schuster-Gossler et al., 2007; Vasyutina et al., 2007). Notch signalling was also shown to play a key role in maintaining homeostasis of muscle stem cells in the adult (Bjornson et al., 2012; Carlson et al., 2008; Fukada et al., 2011; Kitamoto and Hanaoka, 2010; Mourikis et al., 2012a) and in colonization of the satellite cell "niche" (Brohl et al., 2012). In particular, Notch controls the quiescence of muscle satellite cells (Bjornson et al., 2012; Mourikis et al., 2012a). Conditional deletion of *Rbpj* in $Pax7^{+}$ satellite cells led to spontaneous differentiation without activation nor division of the cells (Bjornson et al., 2012; Mourikis et al., 2012a). Strikingly, *Rbpj* ablation does not lead to an immediate and complete differentiation or growth arrest in the $Pax3^{+}$ population during embryonic development, leaving open the possibility that other pathways may be involved. For instance, Notch activity in adult muscle stem cells is counteracted by Tgfβ signalling (Carlson and Conboy, 2007). This is mediated through the activation of pSmad3, which can directly bind and activate *p15*, *p16*, *p21* and *p27* promoters (Carlson and Conboy, 2007) to favour muscle stem cell differentiation.

Interestingly, during chicken myogenesis, Myostatin, a member of the Tgfβ family, has also been implicated in the control of terminal differentiation through the indirect activation of *p21* (Manceau et al., 2008). Of note, the role of Notch can be context-dependent, since during early initiation of myogenesis in the young somite of the chick embryo, $Dll1^{+}$ neural crest cells provide a transient stimulation of Notch activity that is important for the initiation of early myogenesis (Rios et al., 2011).

Thus, it appears that Notch signalling is involved in regulating the balance between amplifying the muscle progenitors pool and letting these cells undergo muscle differentiation during limb muscle development. Interestingly, when Notch signalling is impaired in muscle progenitors, the number of $Pax3^{+}/MyoD^{+}$ myoblasts is decreased while the proportion of $Pax3^{+}/Myf5^{+}$ myoblasts is unchanged (Vasyutina et al., 2007) which is consistent with previous studies performed in chick embryos. This suggests Notch signalling pathway is regulating the maintenance of the progenitor pool through the control of *MyoD* expression but not of *Myf5*.

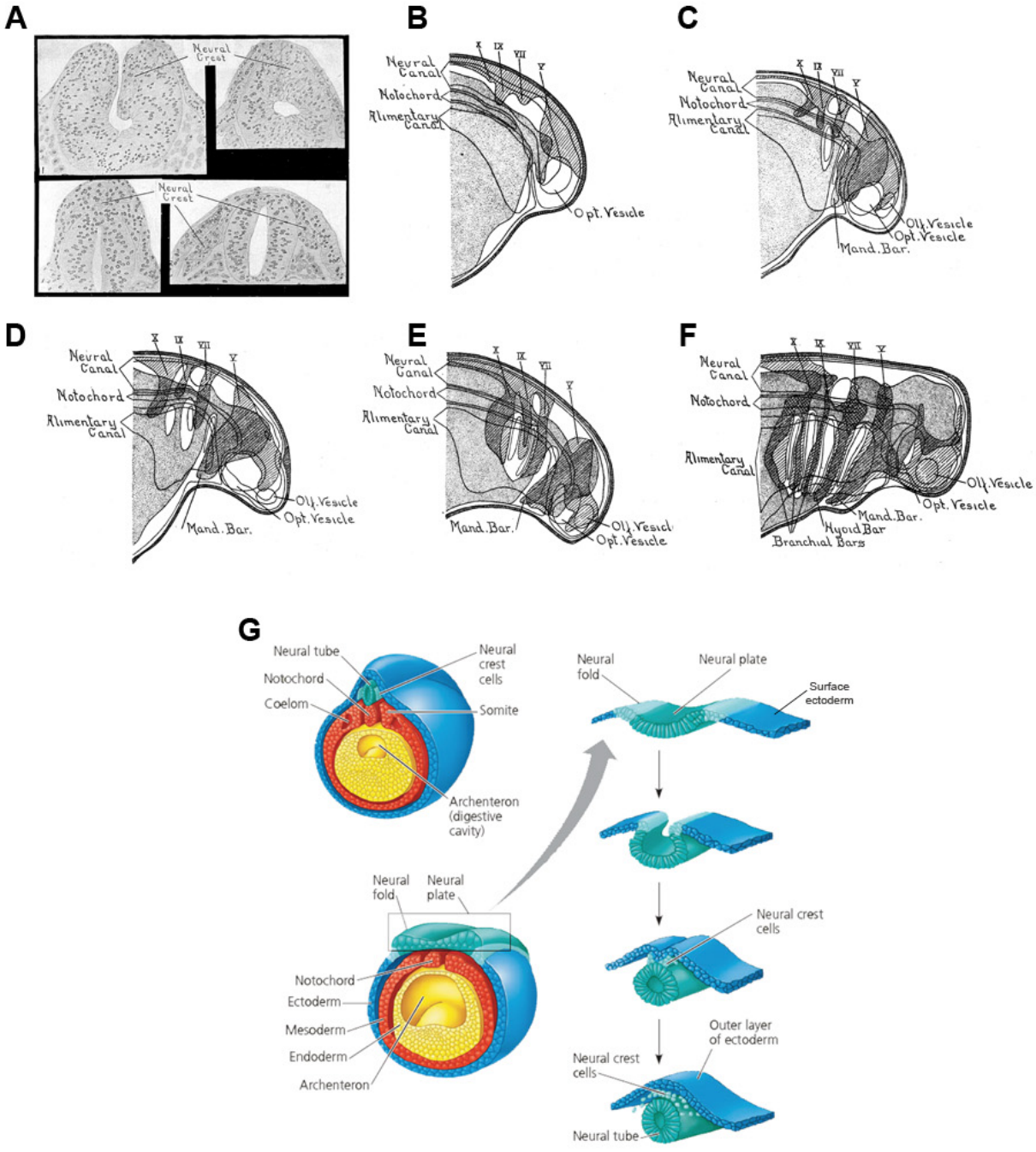

<u>Figure 10:</u> Description of the neural crest
(A-F) Early description of the ectodermal origin of the craniofacial skeleton in Urodeles (adapted from Landacre, 1921). (G) Formation of the neural crest occurs at the border between

the neural ectoderm and the surface ectoderm (adapted from http://www.devbio.biology.gatech.edu).

PART II GROWTH AND MAINTENANCE OF CRANIAL NEURAL CREST CELLS

"It is with our faces that we face the world, from the moment of birth to the moment of death. Our age and our gender are printed on our faces. Our emotions, the open and instinctive emotions that Darwin wrote about, as well as the hidden or repressed ones that Freud wrote about, are displayed on our faces, along with our thoughts and intentions. Though we may admire arms and legs, breast and buttocks, it is the face, first and last, that is judged "beautiful" in an aesthetic sense, "fine" or "distinguished" in a moral or intellectual sense. And, crucially, it is by our faces that we can be recognized as individuals." (Sacks, 2010)

1. Neural crest biology

The neural crest was first described in avian embryos by Wilhelm His in 1868 who called it "the chord in between" (Zwischenstrang in German) to describe a transient population of moving cells between the neural plate and the surface ectoderm of the embryo (Hall, 2008). In the 1890's, Julia Platt showed that craniofacial cartilages originated from the ectoderm adjacent to the neural tube (Platt, 1893), however as this concept was running against the germ-layer theory according to which skeletal tissues are generated by the mesoderm and not the ectoderm, it took more than five decades for her work to be recognized by her contemporary researchers (Hall, 2008). In the beginning of the 20th century, work performed in Urodeles (Landacre, 1921) confirmed Platt's observations that the neural crest was at the origin of different skeletal structures of the vertebrate head (Figure 10A-F). Later, by discovering and exploiting the quail nuclear marker, Nicole Le Douarin developed an instrumental technique to investigate the lineage of neural crest cells (NCC; Le Douarin, 1973). The generation of quail-chick chimeras by transplantation allowed a precise tracking

of the cells derived from neural crest and to rigorously demonstrate the neural crest origin of the vertebrate face (Le Douarin, 2004).

1.1. Neural crest induction

During embryonic development, once the three germ layers are established, the ectoderm is divided into two territories, the neural ectoderm, also called the neural plate, and the surface ectoderm (Figure 10G). The neural ectoderm generates the CNS while the surface ectoderm gives rise to the skin, placodes and dermis. It is at the interface between these two domains, also refered to as the neural plate border, that the neural crest, a new structure evolutionary key for the development of the vertebrate embryo, is formed (Sauka-Spengler and Bronner-Fraser, 2008). The neural crest corresponds to a transient population of multipotent migratory cells, determined before the elevation of the neural folds by several signalling pathways coming from the neural plate, the surface ectoderm and the underlying mesoderm (Figure 11A). A precise combination of extrinsic signalling, including BMP, WNT, FGF, RA and Notch signalling pathways has been shown to be essential in the induction of neural crest. Intermediate levels of BMPs received by the ectoderm are required but not sufficient for neural crest induction (García-Castro et al., 2002). BMP antagonists such as chordin, noggin or follistatin secreted by the underlying mesoderm are involved in generating these intermediate levels of BMPs (Marchant et al., 1998). In combination with BMPs, Ffg2 and Fgf8, also secreted by the mesoderm, have been shown to be able to induce the neural crest territory (Mayor et al., 1997; Monsoro-Burq et al., 2003). Moreover, studies in birds and frogs have shown that Notch signalling is acting upstream of BMPs to induce the neural crest and restricts its territory to the neural plate border (Endo et al., 2002). In addition to BMP, FGF and Notch, both gain-of-function and loss-of-function experiments demonstrated that

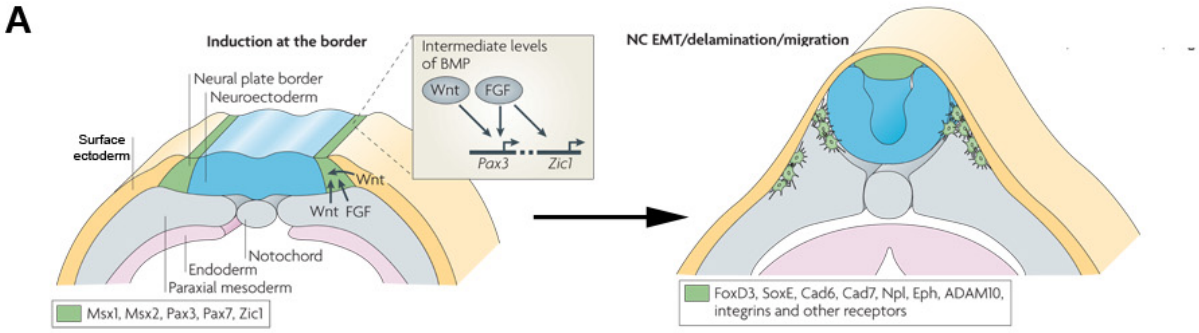
A
Induction at the border
Intermediate levels of BMP
Wnt
FGF
Pax3
Zic1
Neural plate border
Neuroectoderm
Surface ectoderm
Wnt
Wnt FGF
Notochord
Endoderm
Paraxial mesoderm
Msx1, Msx2, Pax3, Pax7, Zic1
NC EMT/delamination/migration
FoxD3, SoxE, Cad6, Cad7, Npl, Eph, ADAM10, integrins and other receptors

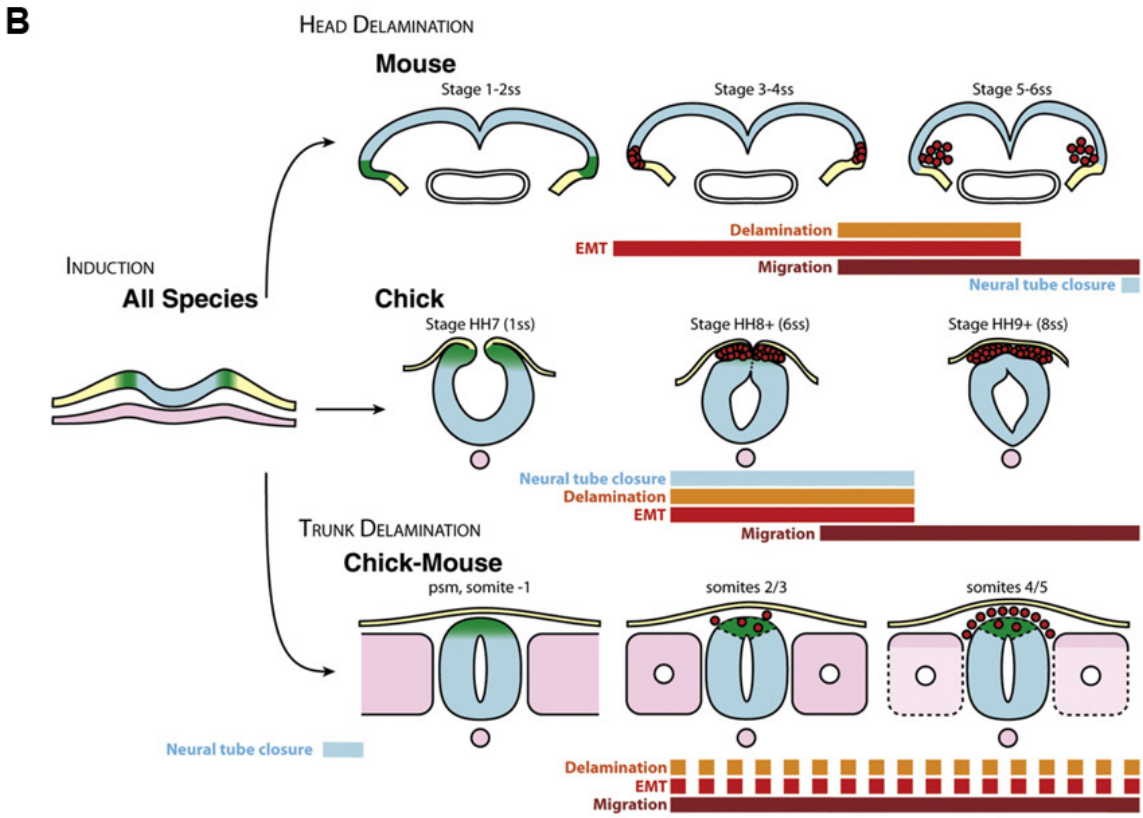
B
Head Delamination
Mouse
Stage 1-2ss
Stage 3-4ss
Stage 5-6ss
Delamination
EMT
Migration
Neural tube closure
Induction
All Species
Chick
Stage HH7 (1ss)
Stage HH8+ (6ss)
Stage HH9+ (8ss)
Neural tube closure
Delamination
EMT
Migration
Trunk Delamination
Chick-Mouse
psm, somite -1
somites 2/3
somites 4/5
Neural tube closure
Delamination
EMT
Migration

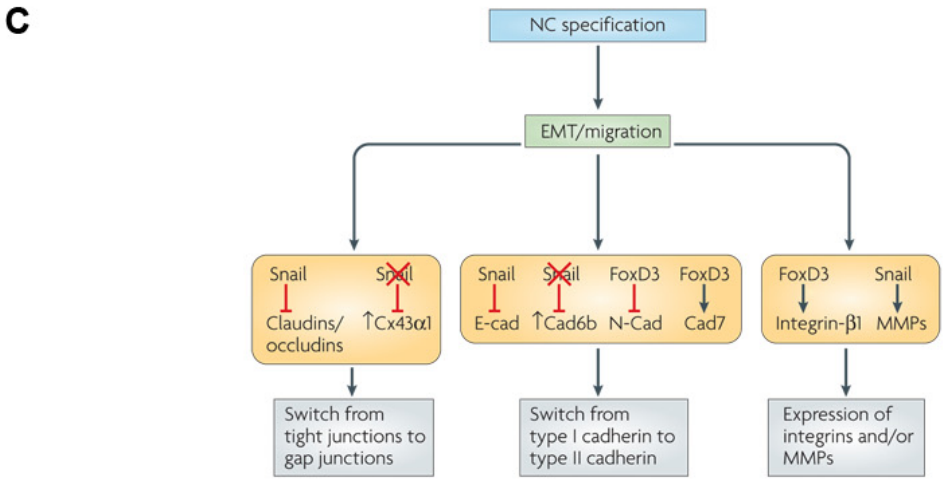
C
NC specification
EMT/migration
Snail
Snail
Claudins/ occludins
↑Cx43α1
Switch from tight junctions to gap junctions
Snail
Snail
FoxD3
FoxD3
E-cad
↑Cad6b
N-Cad
Cad7
Switch from type I cadherin to type II cadherin
FoxD3
Snail
Integrin-β1
MMPs
Expression of integrins and/or MMPs

WNT signalling pathway, provided by both mesoderm and surface ectoderm, is essential for neural crest induction (LaBonne and Bronner-Fraser, 1998). Finally, RA was also involved together with FGF and WNT signalling in being required for neural crest induction (Villanueva et al., 2002).

Although these studies were instrumental in the understanding of the orchestration of neural crest induction, most of them were performed in avian, amphibians or fish embryos. Evidences showing the implication of the same signalling pathways are still missing in the context of the mammalian neural crest induction (Crane and Trainor, 2006).

This complex combination of extrinsic signalling pathways activates the intrinsic expression of neural plate border specifiers such as *Pax3*, *Pax7*, *Zic1*, *Msx1*, *Msx2* and *Dlx5* that define the neural crest territory and neural crest specifier genes that include *Snail1/2*, *FoxD3*, *AP-2α*, genes of the *SoxE* family and *Twist* which are involved in the specification of the NCC and distinctive sublineages (Figure 11A; Sauka-Spengler and Bronner-Fraser, 2008). At the neurulation stage, a process during which cells from the neural plate and the surrounding epidermis undergo changes in shape that result in the formation of the neural tube, the neural crest is induced and NCC formed. *Pax3* and *Pax7* have been suggested to be involved in neural crest formation. In Xenopus, *Pax3* has been shown to cooperate with *Msx1* to regulate FGF and WNT signalling during induction of the neural crest (Monsoro-Burq et al., 2005).

Figure 11: Neural crest induction and formation of the neural crest cells
(A) The left schematic represents the neural crest induction at the border between the neural and the surface ectoderm showing the mesodermal and ectodermal origins of the inductive signals, WNT and FGF signalling being essential in the activation of neural crest specifier genes. The right schematic highlights the genes involved in EMT and delamination of the NCC (adapted from Sauka-Spengler and Bronner-Fraser, 2008). (B) Schematic representation of NCC delamination pointing out the spatiotemporal differences between chick and mouse cranial neural crest cells delamination. In both species, trunk NCC delaminate after closure of the neural tube (adapted from Theveneau and Mayor, 2012). (C) Representation of the action of *Snail* and *FoxD3* in controlling the molecular switches during the EMT.

Furthermore, it was shown that *Pax3* functions cooperatively with *Zic1* to regulate NCC formation. Mis-expression of these two factors are able to induce neural crest formation in ventral ectoderm while knockdown of *Pax3* expression using antisense morpholinos results in defects in the initiation of neural crest induction (Milet et al., 2013; Sato et al., 2005). In chick, *Pax7* is expressed prior to neural crest induction and has been shown to regulate NCC formation as treatment of chick embryos with *Pax7* morpholinos induced a decrease in the expression of the NCC markers *Snail1/2* and *Sox9* (Basch et al., 2006).

1.2. Neural crest cells formation

Once specified, NCC undergo an EMT and delaminate from the neural tube. The function of EMT is to switch from a polarized epithelial layer of cells linked with tight junctions and strong adhesion molecules to an individual mesenchymal cell population. EMT involves major cytoskeleton rearrangements, changes in cell junctions and adhesion molecules which are orchestrated by the activity of transcription factors and signalling pathways (reviewed in Thiery and Sleeman, 2006).

In the cranial regions of the embryo, cranial NCC (CNCC) delamination presents with some species-specific divergences in timing. In mouse, CNCC delamination occurs when the neural plate is still open, before the fusion of the neural folds while in chick, CNCC delamination occurs while the neural tube is closing (Figure 11B). Of note, in all species, trunk NCC delaminate after neural tube closure (Figure 11B; reviewed in Theveneau and Mayor, 2012).

In the trunk, NCC delamination is mainly promoted by BMP (*Bmp4*) and WNT (*Wnt1*) signalling pathways, which activate the expression of *Snail1/2*, *FoxD3*, *Sox9* and *Sox10* (Burstyn-Cohen et al., 2004; Cheung and Briscoe, 2003; Cheung et al., 2005; Sela-Donenfeld and Kalcheim, 2002).

However, CNCC express BMP and WNT inhibitors, which suggests that additional factors such as *Ets-1*, *Id2* and *LSox5* are involved in controlling CNCC EMT and delamination. It was shown that overexpression of both *Snail1/2* and *Ets-1* induces CNCC delamination from ectopic regions of the neural tube (Martinsen and Bronner-Fraser, 1998; Perez-Alcala et al., 2004; Théveneau et al., 2007).

Trunk and cranial neural crest specifiers orchestrate the EMT by controlling a cadherin molecular switch to allow the transition from a cadherin-based strong cell-cell adhesion (N-cadherin) required to maintain the epithelial integrity to a weak cell-cell adhesion involving Cadherin6, 6B, 7 and 11, allowing the formation of a mesenchymal cell population. For instance, *Snail1/2* and *FoxD3* have been shown to induce NCC EMT by directly regulating this transition (Figure 11C; del Barrio and Nieto, 2002; Batlle et al., 2000; Cano et al., 2000; Taneyhill et al., 2007). Finally, to be able to migrate through the extra cellular matrix, NCC require proteolytic activities that they obtain by up-regulating the expression of metalloproteases during the EMT process (Cai et al., 2000).

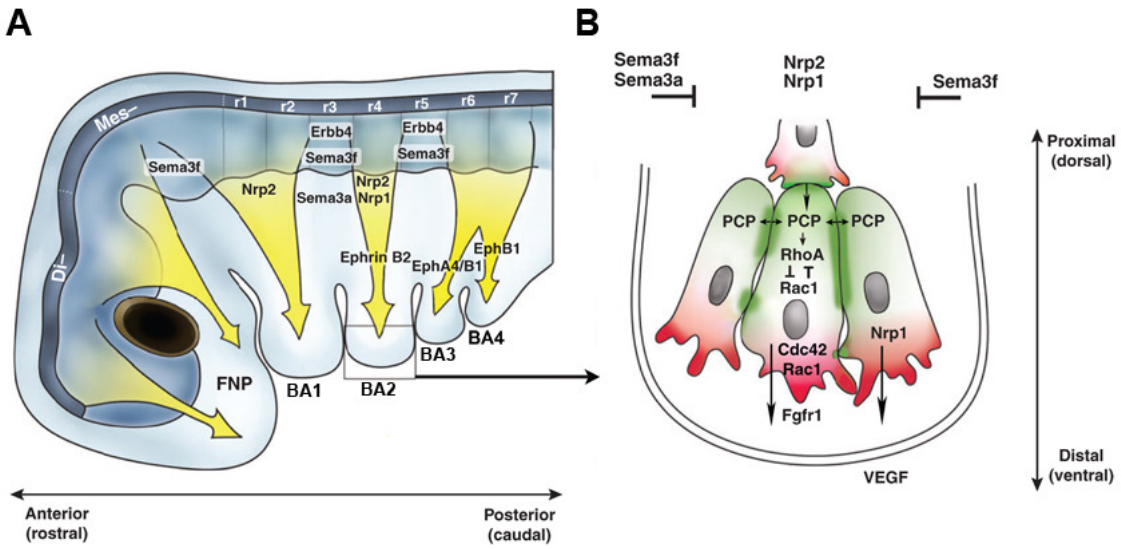
A
B
Mes
r1
r2
r3
r4
r5
r6
r7
Di
Sema3f
Nrp2
Sema3a
Erbb4
Sema3f
Nrp2
Nrp1
Erbb4
Sema3f
Ephrin B2
EphA4/B1
EphB1
FNP
BA1
BA2
BA3
BA4
Anterior
(rostral)
Posterior
(caudal)
Sema3f
Sema3a
Nrp2
Nrp1
Sema3f
Proximal
(dorsal)
PCP
PCP
PCP
RhoA
⊥ T
Rac1
Cdc42
Rac1
Nrp1
Fgfr1
VEGF
Distal
(ventral)

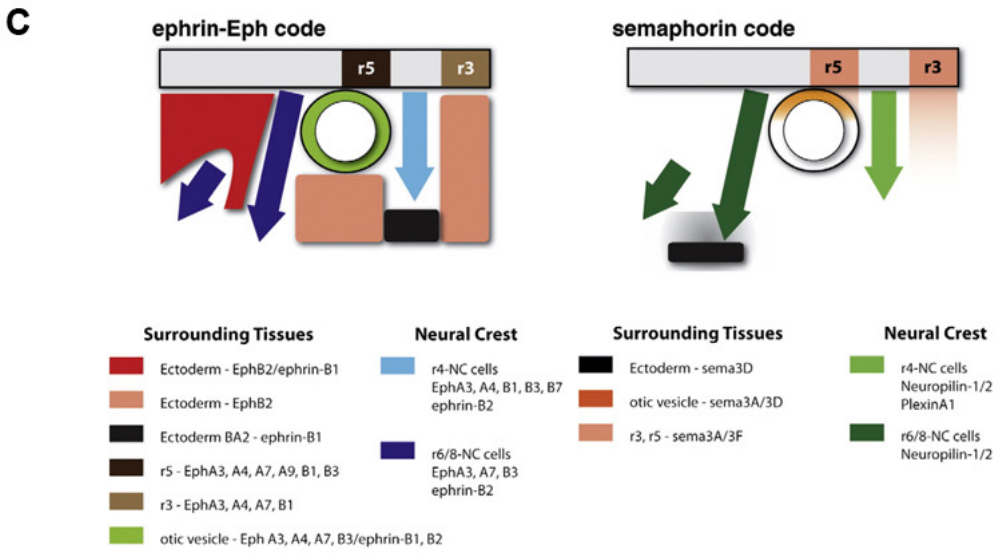
C
ephrin-Eph code
r5
r3
semaphorin code
r5
r3
Surrounding Tissues
Ectoderm - EphB2/ephrin-B1
Ectoderm - EphB2
Ectoderm BA2 - ephrin-B1
r5 - EphA3, A4, A7, A9, B1, B3
r3 - EphA3, A4, A7, B1
otic vesicle - Eph A3, A4, A7, B3/ephrin-B1, B2
Neural Crest
r4-NC cells
EphA3, A4, B1, B3, B7
ephrin-B2
r6/8-NC cells
EphA3, A7, B3
ephrin-B2
Surrounding Tissues
Ectoderm - sema3D
otic vesicle - sema3A/3D
r3, r5 - sema3A/3F
Neural Crest
r4-NC cells
Neuropilin-1/2
PlexinA1
r6/8-NC cells
Neuropilin-1/2

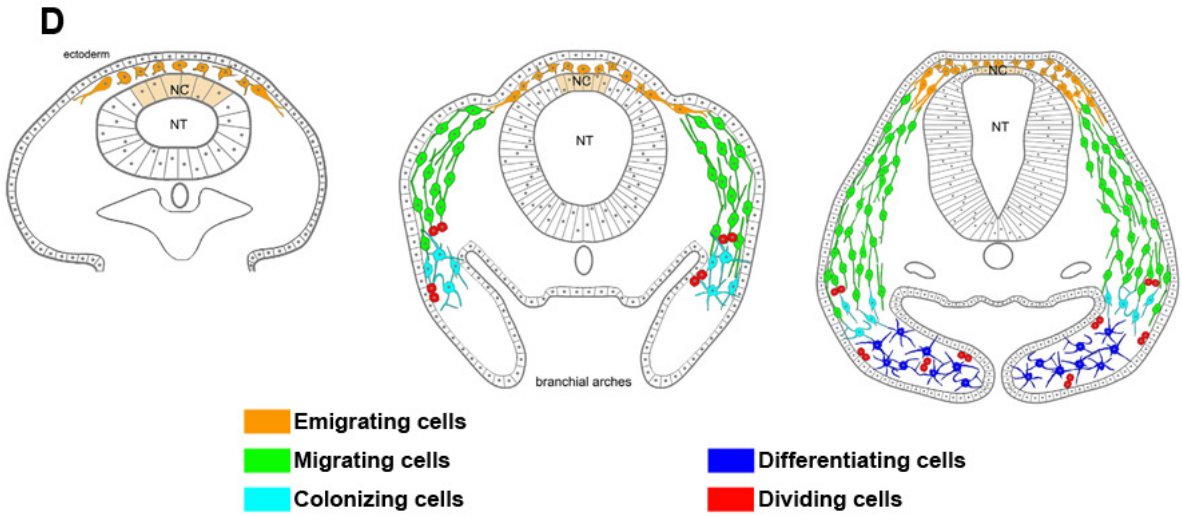
D
ectoderm
NC
NT
NC
NT
NC
NT
branchial arches
Emigrating cells
Migrating cells
Colonizing cells
Differentiating cells
Dividing cells

1.3. Neural crest migration

Depending on their rostro-caudal origin, NCC are divided into four major domains: the cranial, cardiac, trunk and vagal populations (Sauka-Spengler and Bronner, 2010). Elegant studies in chick embryos have facilitated the precise fate mapping and identification of specific derivatives that arise from each NCC population (Le Douarin, 2004; Le Douarin and Kalcheim, 1999).

CNCC migrate as a continuous wave of cells that rapidly split into different streams (Theveneau and Mayor, 2012). CNCC migrate ventro-laterally within the embryo to populate different locations (Figure 12A). A sub-population of CNCC migrates to the cranial ganglia while the others continue their migration into the branchial arches to populate the facial prominences. Diencephalon and anterior mesencephalon-derived CNCC migrate into the fronto-nasal prominence (FNP) while CNCC that originate from more caudal regions, the posterior mesencephalon and hindbrain {transiently subdivide into neuroepithelial segment called rhombomere (r)} migrate into the branchial arches (Figure 12A; reviewed in Minoux and Rijli, 2010). It is generally accepted that CNCC arise from the mid-diencephalon until r7 of the hindbrain and stereotypically migrate in highly conserved migratory streams (Figure 12A; Kulesa et al., 2010). Once they have delaminated, CNCC display directed motility. It has been suggested that the process of contact inhibition of movement is a major mechanism providing guidance for this directed motility (Figure 12B).

Figure 12: Migration of the cranial neural crest cells
(A) Schematic representation of a mouse embryo at E9.5 showing the migration streams of cranial neural crest cells and the signalling molecules involved in shaping the migration streams. FNP: Fronto-nasal prominence, BA: Branchial arch, Di-: Diencephalon, Mes-: Mesencephalon, r1-r7: Rhombomeres 1 to 7. (B) Schematic representing how contact inhibition of movement induces directional motility in cranial neural crest cells (adapted from Minoux and Rijli, 2010). (C) Schematic representing how Ephrin/Eph and Semaphorin inhibitory signalling pathways shape the migratory streams (from Theveneau and Mayor, 2012). (D) Schematic representation of cranial neural crest cells delamination, migration and establishment in the branchial arches (adapted from Kulesa et al., 2010).

Studies demonstrated that cell-cell contact induces local activation of Planar Cell Polarity (PCP), which coordinates the orientation of cell protrusions and thus the direction of the cell migration (reviewed in Theveneau and Mayor, 2012). Briefly, Syndecan4 inhibits *Rac1* expression at the back of the cell leading to the formation of cell protrusions at the front only, while cell-cell contact induces local activation of RhoA, which inhibits formation of protrusions in the region (Figure 12B). Therefore the only place where protrusions can form is at the front of the cell providing a directional motility to the NCC (Carmona-Fontaine et al., 2008; Mayor and Carmona-Fontaine, 2010). However, the process of contact inhibition of movement implies that CNCC would disperse into less populated regions. In order for contact inhibition of movement to propagate stereotypical CNCC migratory streams, other mechanisms must be involved in maintaining distinct migratory streams that are essential for the future patterning of the craniofacial complex (Figure 12A). Segregation of the different streams of migratory CNCC depends on both repulsive and positive signalling. Two classes of signalling molecules control the splitting of the continuous wave of migratory CNCC: the Ephrin and their Eph receptors together with Semaphorin3 and their receptors, Neuropilin1/2 (Figure 12C). These two types of molecules generate CNCC-free zones in the embryo by inducing the collapse of cell protrusions therefore inhibiting cell migration in this territory (Gammill et al., 2007; Kulesa et al., 2010; Smith et al., 1997; Theveneau and Mayor, 2012). It was shown that inhibiting Ephrin/Eph or Semaphorin3 signalling pathways induce CNCC migration into the CNCC-free zones demonstrating their role in establishing these territories (Smith et al., 1997). In addition, the EGF-like receptor ErbB4 is expressed in the mesenchyme adjacent to r3 and r5, which are CNCC-free regions (Figure 12A). In *ErbB4* mouse mutant embryos, CNCC originating from r4 migrate into the mesenchyme lateral to r3 suggesting that ErbB4 is involved in generating repulsive cues to segregate migratory CNCC streams coming from r2 and r4 (Golding et al., 2000, 2004).

Another way to shape distinct stream of migratory CNCC is the presence of physical obstacle on their route. Thus, laterally to r5, the otic vesicle has been suggested to be an important physical barrier on the route the migratory CNCC (Figure 12C; reviewed in Theveneau and Mayor, 2012). This physical opposition is thought to be playing a role in segregating the migratory CNCC streams, as CNCC facing the otic vesicle have to migrate either more rostrally or caudally right after they have delaminated from the neural plate (Figure 12C). The optic vesicle is also most likely to be playing a similar role in sculpting the migratory streams in the most rostral part of the embryo.

In addition to negative cues segregating the migratory streams, FGF, VEFG and PDGF signalling pathways have been implicated in being positive regulators of migratory CNCC streams by creating a permissive environment in the branchial arches to enhance cell motility (Le Douarin and Kalcheim, 1999; McLennan et al., 2010; Trokovic et al., 2005).

Finally, together with these signalling pathways, the chemo-attractant Sdf1 is expressed in the head mesenchyme, along the migratory routes of the CNCC and its receptor Cxcr4 is expressed in CNCC. In chick and Xenopus, it was demonstrated that the Sdf1/Cxcr4 signalling pathway is involved in correct migration of the cardiac and CNCC, as inhibiting this signalling impairs their migration (Escot et al., 2013; Theveneau et al., 2010).

The final destinations of the CNCC are the facial prominences and the branchial arches where they establish at the end of the migration phase to participate in the development of the craniofacial complex (Figure 12D).

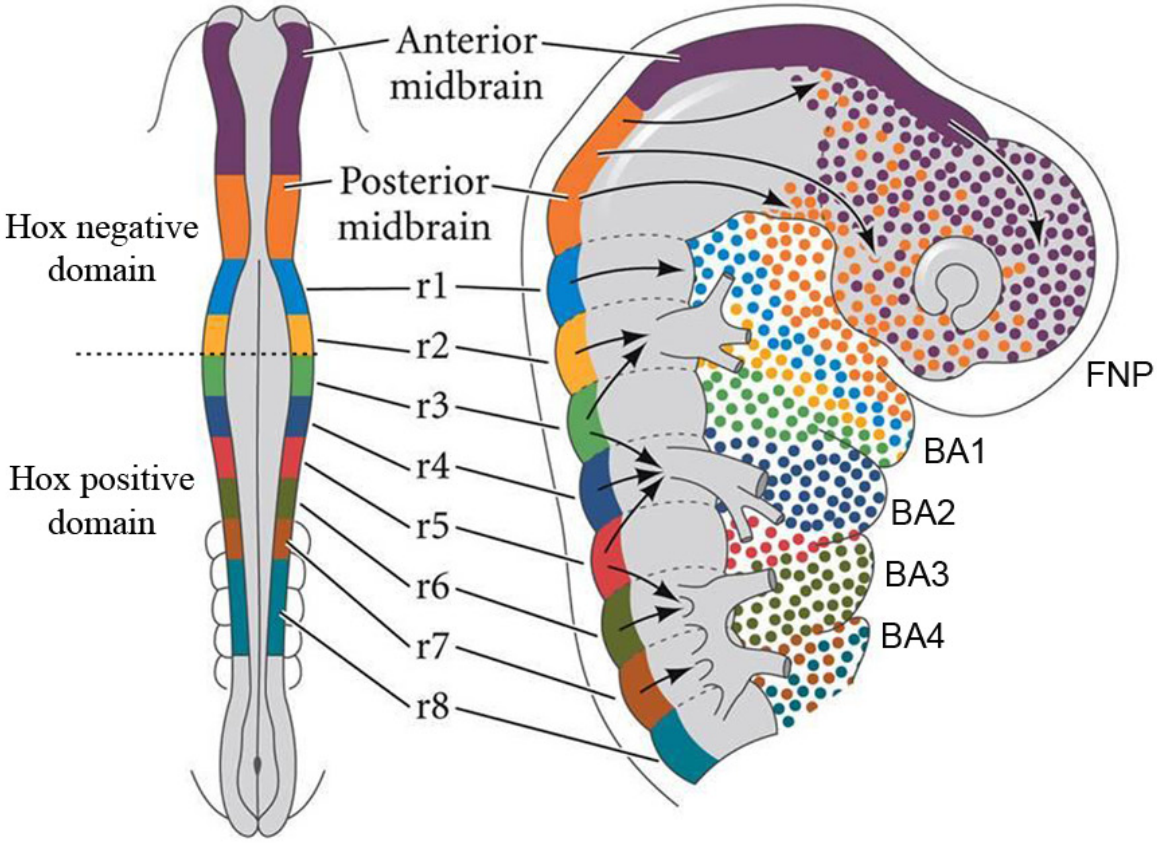

<u>Figure 13:</u> Origin of the cranial neural crest cells populating facial prominences and branchial arches
(from Gilbert, 2013)

2. Development of the craniofacial complex

2.1. Cranial neural crest cells contribution to the developing face

CNCC contribution to a branchial arch is highly conserved across multiple vertebrate species (Figure 13; Kiecker and Lumsden, 2005). Branchial arches are metameric structures composed of an ectodermal outer layer and an endodermal inner layer. Between these two layers stand a mesodermal core, which is surrounded by CNCC-derived mesenchyme (Szabo-Rogers et al., 2010). The FNP is populated by CNCC arising from the developing diencephalon and mesencephalon. CNCC that migrate into the first branchial arch (BA1) are originated from the posterior mesencephalon, r1 and r2. The second branchial arch (BA2) is populated by CNCC arising from r3 and r4 with a contribution from r5. This second stream receives cells migrating from r4 as well as caudal and rostral migrating CNCC from r3 and r5, respectively. Finally, cells from r6 and r7 populate the third branchial arch (BA3; Figure 13; Creuzet et al., 2005; Lumsden and Guthrie, 1991; Trainor and Krumlauf, 2000).

Once established in the branchial arches, CNCC proliferate to form the different facial prominences. By E9.5, the mouse embryo face consists of five swellings called facial prominences surrounding the stomodeum, the future mouth. During their development these prominences fuse together to shape the future face. These prominences are the FNP that give rise to two lateral nasal processes (LNP) and two medial nasal processes (MNP) by E10.5, two maxillary processes (Mx) and two mandibular processes (Md) (Figure 14; Helms et al., 2005; Szabo-Rogers et al., 2010). The FNP and MNP will develop into the forehead, ridge of the nose, part of the nasal pits, and primary palate, including the premaxillary segment of the upper jaw. The LNP and Mx contribute to the nasal pits, the sides of the nose and upper jaws. Finally, the Md form the lower jaw (Figure14; reviewed in Szabo-Rogers et al., 2010).

The formation of the upper face can be divided in two phases. A first phase where at E11.5,

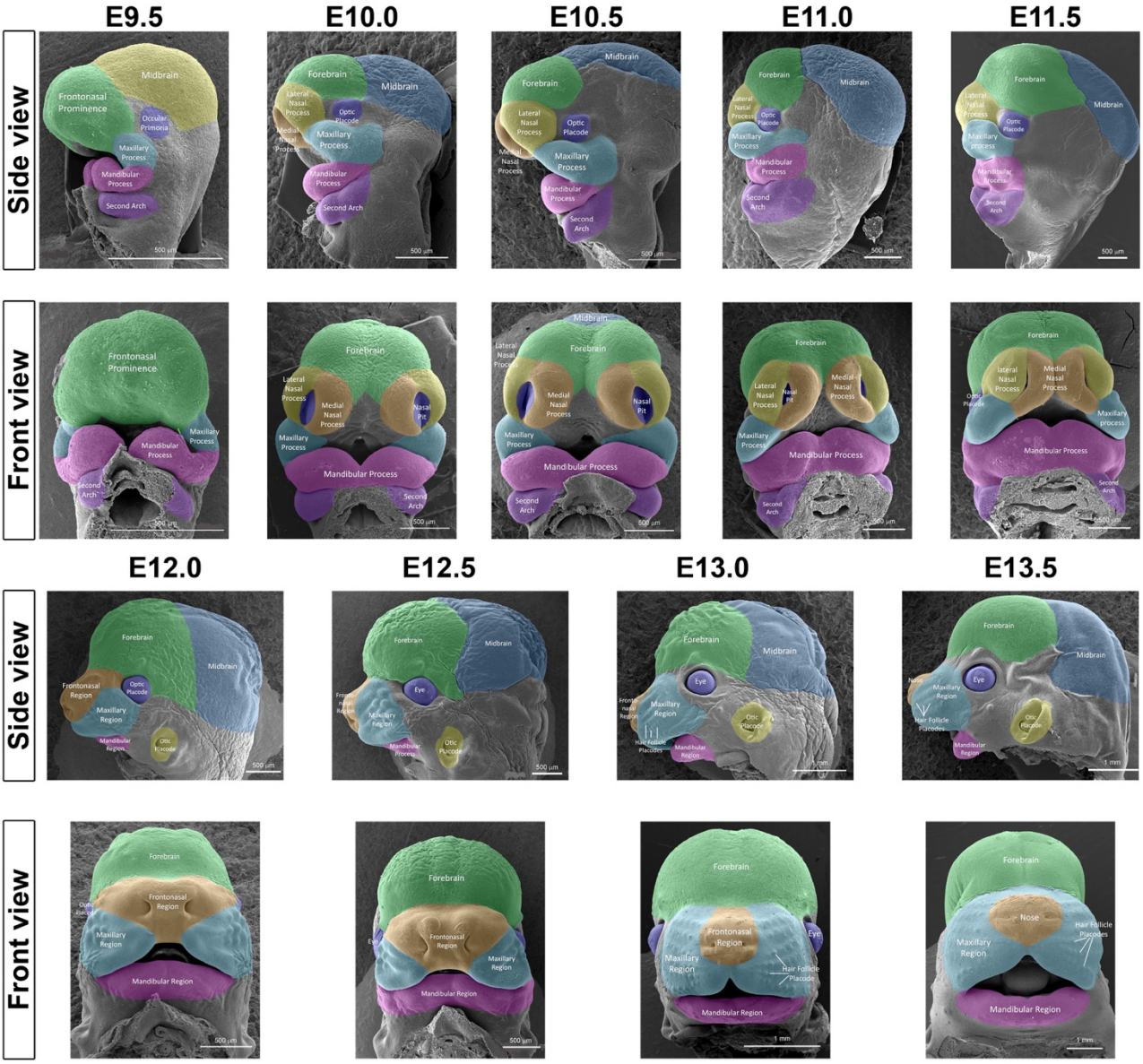

Figure 14: Development of the facial prominences from E9.5 to E13.5
(from FaceBase consortium, images provided by Iwata, J., Bringas, P., and Chai, Y.)

the MNP, LNP and Mx fuse together to generate the upper lip with the primary palate. Next the two MNP merge together to form the nasal septum, which later forms the nasal cartilages and bones (Figure 14). The second phase is called the secondary palatogenesis. It corresponds to the vertical growth of the palatal shelves that originate from the Mx and Md that surround the tongue. Next, these shelves grow horizontally resulting in the fusion of the palatal shelves in the midline (reviewed in Bush and Jiang, 2012). By E15.5, this results in the formation of both the nasal and oral cavities. The upper and lower jaw growth being synchronized by mechanisms which are still unclear.

The skull vault has been demonstrated to be of mixed origin (Couly et al., 1993; Jiang et al., 2002; Yoshida et al., 2008). CNCC form the entire viscerocranium, which includes the bones of the face, the palatal, temporal and auditory bones. Together with the mesoderm, CNCC form part of the neurocranium, which surrounds and protects the brain and sense organs, and is composed of the frontal, the parietal, the occipital, the sphenoid and temporal bones (Figure 15; Noden, 1983; Santagati and Rijli, 2003; Wilkie and Morriss-Kay, 2001). In addition, CNCC give rise to a wide variety of derivatives including the entire PNS (with a contribution of the ectodermic placodes) and enteric nervous system of the head, including cranial and parasympathetic ganglia. They also generate non-neuronal derivatives such as Schwann cells that wrap around axons to form the myelin sheath, melanocytes and endocrine cells such as calcitonin-producing cells and parafollicular cells of thyroid. Finally, they give rise to connective tissues including the dermis as well as the fat and smooth muscles associated with the skin, the ciliary muscles that control the accommodation for viewing objects at varying distances, the cornea, stroma of the head and neck glands, dental papilla, walls of aortic and branchial arch-derived arteries, meninges of the prosencephalon and part of the mesencephalon (Le Douarin and Kalcheim, 1999; Santagati and Rijli, 2003).

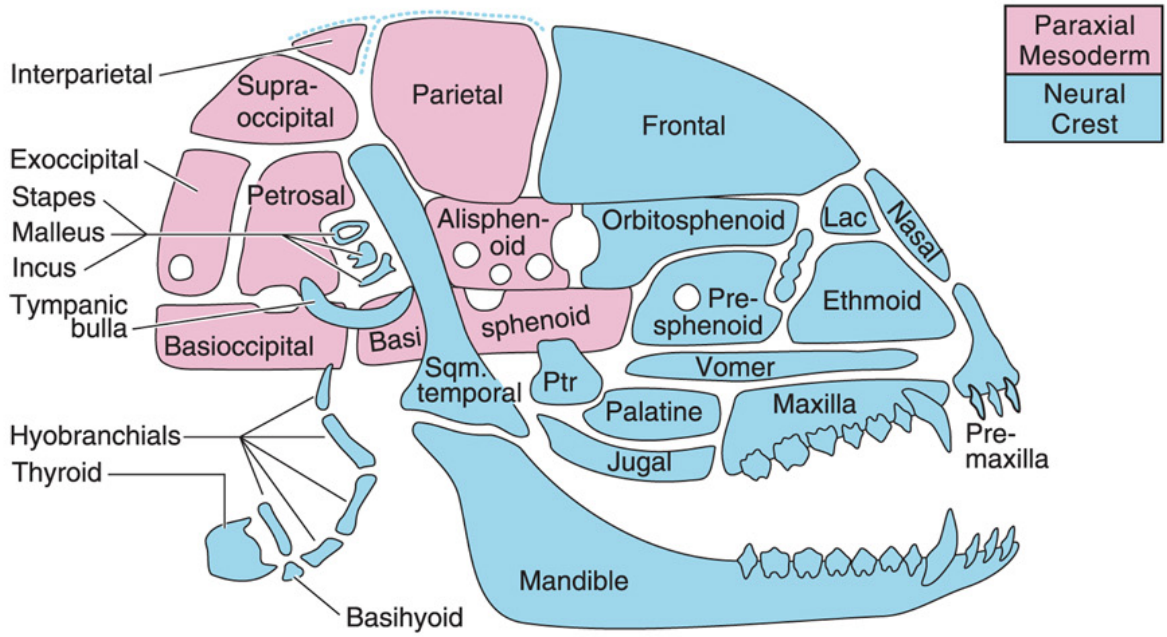

Figure 15: Mixed origin of the craniofacial skeleton
Schematic representation of an adult mouse skull. Neural crest-derived bones are indicated in blue, mesoderm-derived bones are in pink. Lac: lacrimal, Ptr: pterygoid, Sqm: squamosal (adapted from Noden and Trainor, 2005).

2.2. Gene regulatory networks regulating neural crest cells development and differentiation

As previously described, formation of the face is based on the correct development of the neural crest and its derivatives, which form in a series of events including induction of the neural crest territory at the neural plate border, CNCC formation, migration and differentiation into various derivatives. These processes depend on the correct transcriptional regulation of neural crest genes, this regulation being highly conserved among different vertebrate species. Therefore, craniofacial development relies on many signalling molecules and transcription factors (Figure 16), that can be organised in different GRNs controlling the different phases of neural crest development (Figure 17; Betancur et al., 2010). Hence, assembling these GRNs controlling developmental process is essential to understand gene function and predict cellular behaviour (Davidson, 2010).

In the following part, I describe the function of the different signalling pathways and transcription factors essential for understanding my studies.

2.2.1. *Hox* genes pattern the neural crest

Depending on their origin along the rostro-caudal axis, CNCC have specific transcriptional signatures. Interestingly, it is possible to sub-divide the cranial neural crest into two parts, a *Hox* negative population (rostral to r2) that populate the FNP and BA1, and a *Hox* positive (caudal) that populate the caudal branchial arches. Of note, *Hoxa2* is the most rostral *Hox* paralog and is expressed in r2 but CNCC arising from it are devoid of *Hox* expression (Figure 13; Couly et al., 1998). *Hox* genes have been shown to be essential in patterning the whole body. However, the most rostral part of the embryo (anterior to BA1) is devoid of *Hox* expression (Trainor and Krumlauf, 2001). Both endochondral and intramembranous ossification occurs in this rostral part of the head. Unlike intramembranous ossification, cartilage is present during endochondral ossification. In BA2 and more caudally, *Hoxa2* is expressed and these structures primarily undergo endochondral ossification. Upon *Hoxa2* inactivation, in addition to birth lethality, mouse embryos present with homeotic transformation of the neural crest derivatives from BA2 into more rostral derivatives of BA1 (Rijli et al., 1993). Interestingly, structures generated through intramembranous ossification were then present in BA2. This demonstrates that *Hoxa2* is essential in patterning neural crest derivatives and in controlling downstream factors regulating intramembranous and endochondral ossification (Rijli et al., 1993). Consistent with this idea, studies performed in chick, frog and fish embryos, confirmed that mis-expression of *Hoxa2* impairs jaw formation (Grammatopoulos et al., 2000; Hunter and Prince, 2002; Pasqualetti et al., 2000). Hox expression is considered to inhibit ossification in the facial prominences (Creuzet et al., 2002) therefore, in the most rostral CNCC the absence of *Hox* genes expression is essential for development of the craniofacial skeleton. Hence, *Hox* gene function highlights the variety in multipotence of the neural crest depending on it position along the axis of the embryo (discussed below).

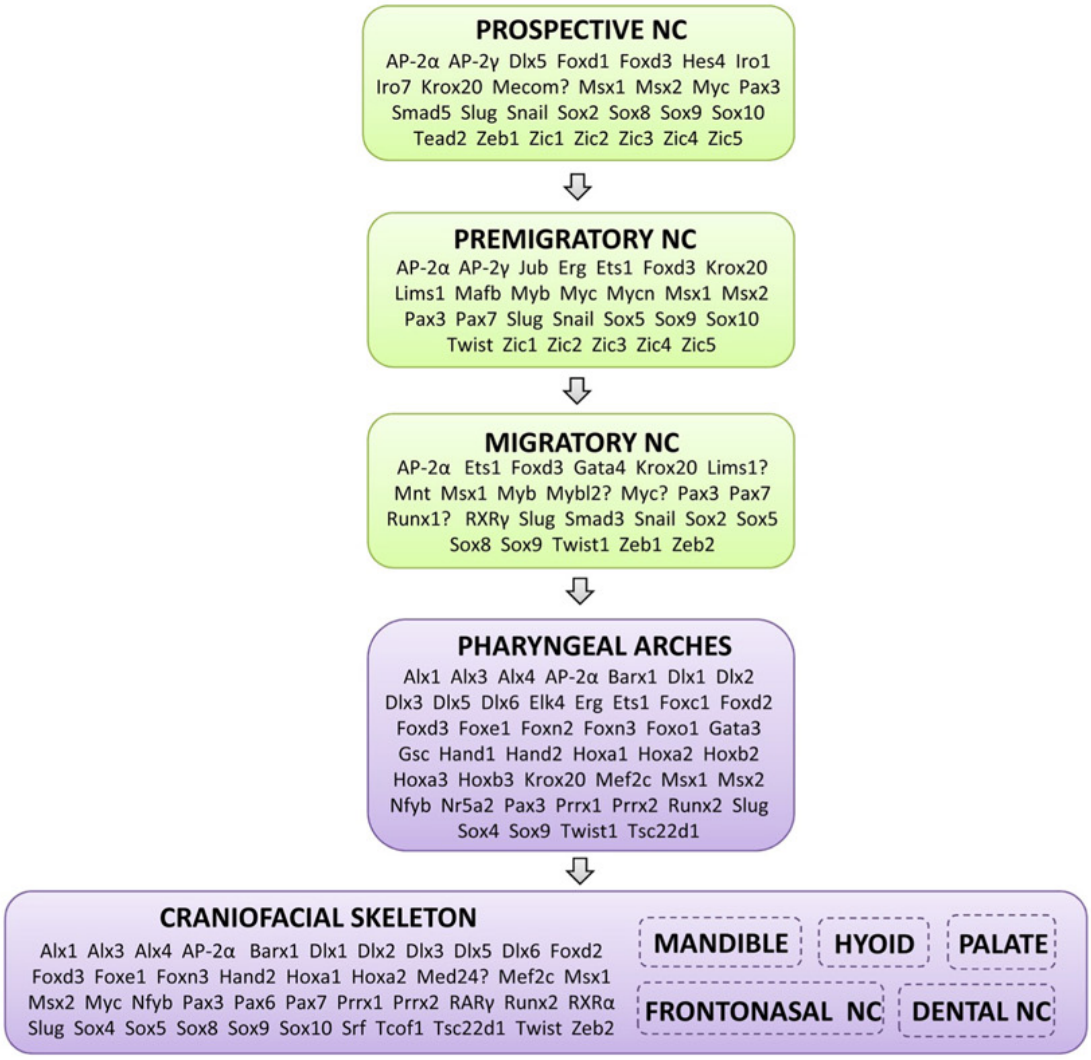

Figure 16: List of transcription factors regulating different steps of neural crest development (adapted from Nelms and Labosky, 2011)

2.2.2. Signalling pathways patterning the branchial arches

While *Hox* genes are essential in patterning the caudal part of the cranial neural crest (from r2 to r7) the most rostral CNCC are coming from the *Hox* negative domain. Nevertheless, they are able give rise to distinct skeleton structures such as the upper and the lower jaw.

Studies using mutant mice for *Endothelin* (*Edn1*) or its receptor (*Ednra*) suggested that the Endothelin signalling pathway is essential in patterning BA1. In these mutants, a homeotic transformation was observed, the lower jaw being transformed into a maxillary structure. Conversely, overexpression of *Edn1* was sufficient to transform the upper jaw into a lower jaw (Clouthier et al., 1998; Sato et al., 2008). Interestingly, in mouse, Endothelin signalling is required between E8.5 and E9.5 suggesting the identity of CNCC is defined early during development, more specially before they established into the branchial arches.

Once the branchial arches are correctly patterned, facial prominences undergo morphological changes mainly correlated with differential rates of proliferation of the CNCC.

However, whether the development of the cranial neural crest-derived mesenchymal cells is cell-autonomous or non-cell autonomous controlled remains controversial. Some studies have shown that CNCC are pre-patterned before establishing in the branchial arches and that they influence their surrounding environment when invading the branchial arches (Noden, 1983).This was demonstrated by transplantation experiments of pre-migratory CNCC from quail into duck embryos. This results in duck embryos exhibiting quail-like beak, suggesting that the CNCC from the donor and not the environment of the host was dictating the facial morphology (Helms and Schneider, 2003; Schneider and Helms, 2003) This suggests that most of the skeletal patterning is brought by the CNCC (Tucker and Lumsden, 2004).

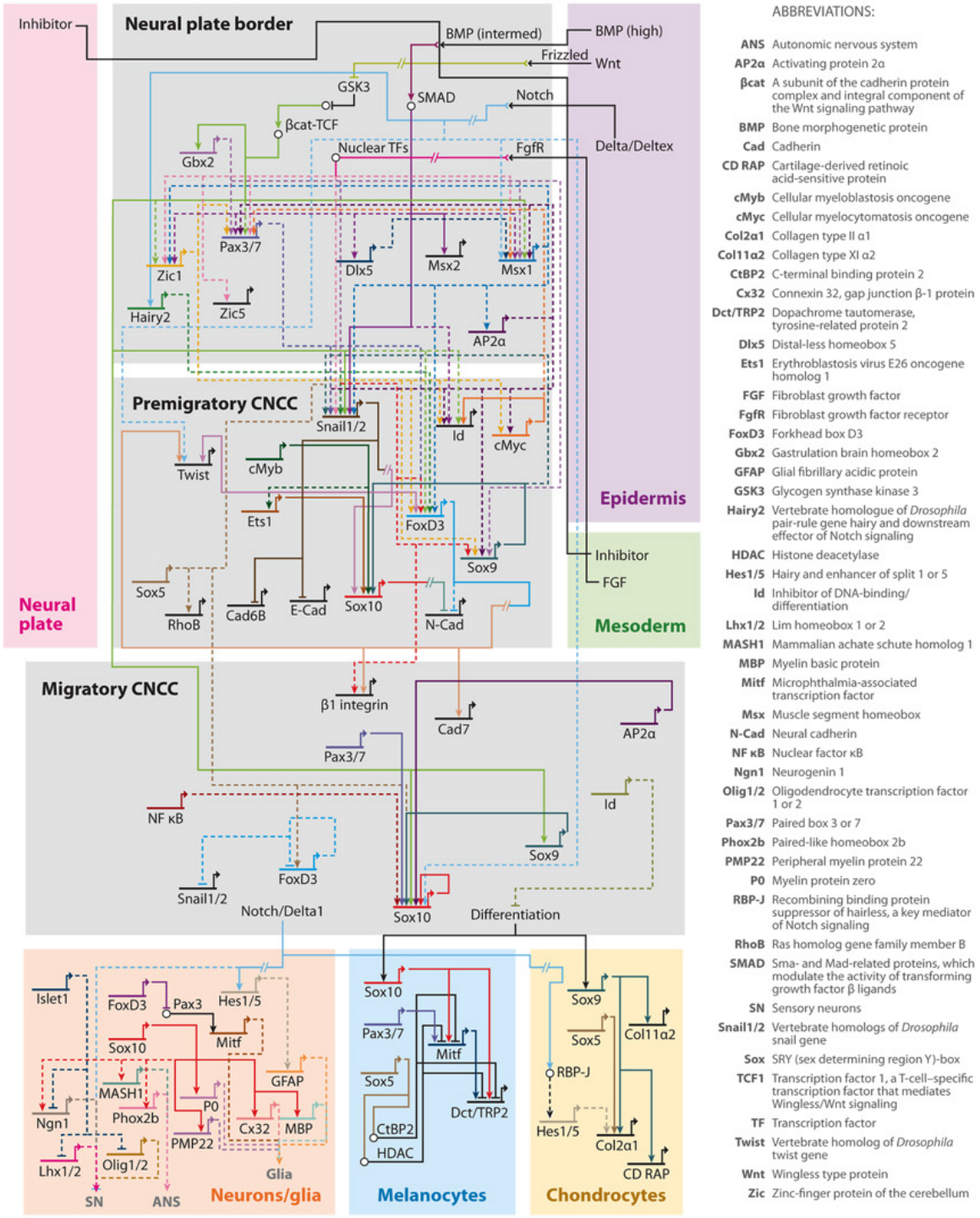

<u>Figure 17:</u> Model of a gene regulatory network representing the hierarchical genetic interactions during cranial neural crest cell development

Solid lines indicate direct interactions based on promoter and cis-regulatory analysis. Dashed lines show potential direct interactions based from gene perturbation studies. Broken lines represent potential indirect interactions. Bubble nodes indicate protein-protein interactions (from Betancur et al., 2010).

However, other studies demonstrated the existence of patterning centres that form independently of the neural crest in the ectoderm surrounding the facial prominences. This centres are involved in controlling the morphogenesis of the face through positive influences of growth factors such as Bmp4 acting on the proliferation of the underlying cranial neural crest-derived mesenchymal cells (Hu and Marcucio, 2012; Hu et al., 2003; Wu et al., 2006).

In addition FGF signalling, especially the ligand Fgf8 (its receptor FgfR1 is ubiquitously expressed in the facial prominences) has been shown to be an essential factor controlling facial morphogenesis through the regulation of mesenchymal CNCC proliferation. For instance, longer expression of *Fgf8* inducing a higher rate of proliferation in the FNP could be an explanation for the wider shape of the duck beak compare to chicken (Wu et al., 2006).

Therefore while CNCC bring most of the skeletal patterning information, they remain dependant on the ectoderm, which provides the growth factors (Fgf8 and Bmp4) influencing the proliferation of CNCC in order to regulate the morphogenesis of the face. Hence, the control of the developing face relies on complex interactions between the CNCC and their surrounding tissues and a precise control of CNCC cell cycle appears to be essential for insuring a correct craniofacial development.

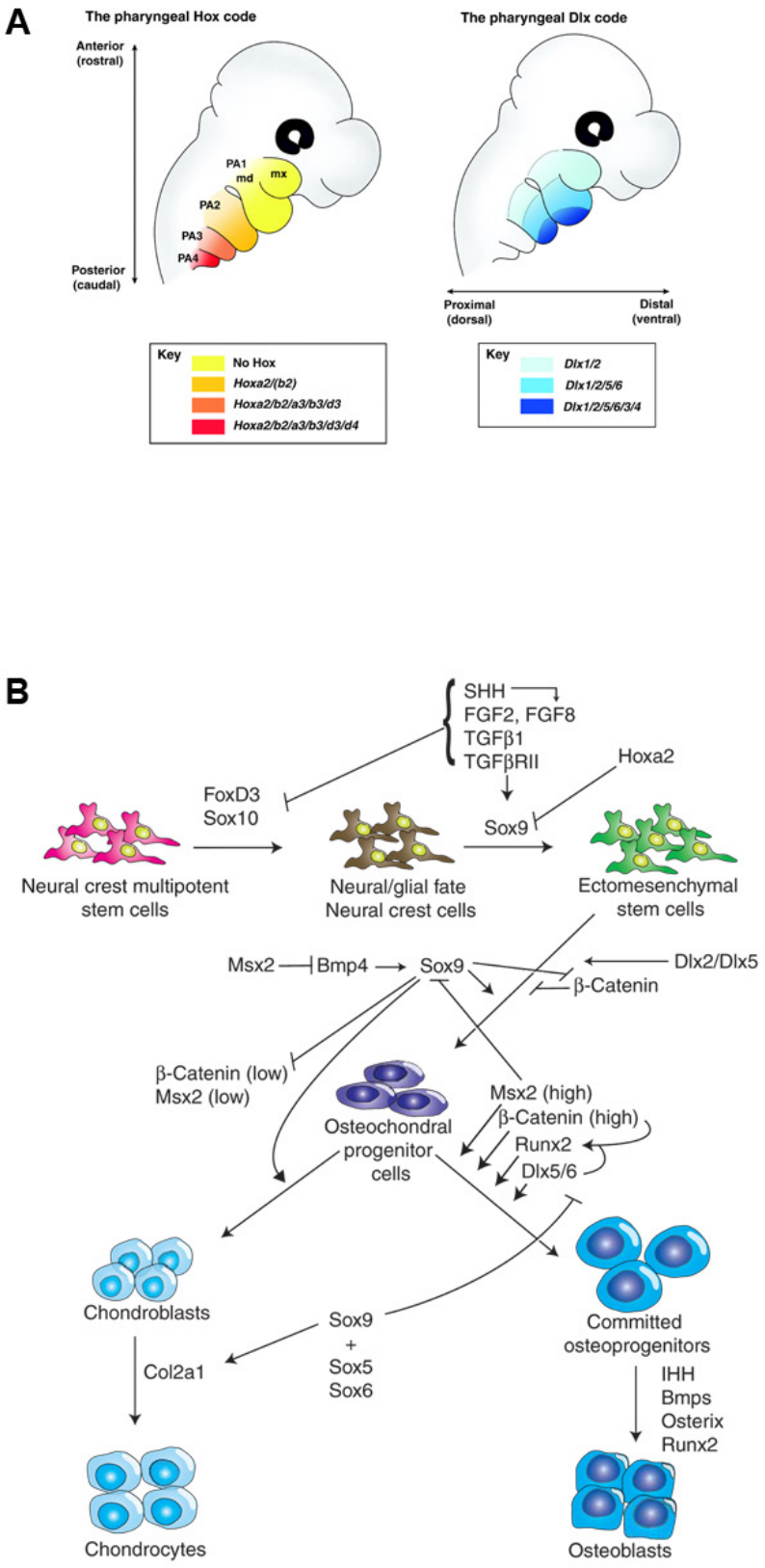

Figure 18: Examples transcription factors patterning the face and regulating CNCC differentiation

(A) Hox and Dlx genes expression in the first branchial arch (from Minoux and Rijli, 2010). (B) Schematic representation of the transcription factors regulating neural crest cell differentiation (from Bhatt et al., 2013).

2.2.3. *AP-2* genes

There are five identified *Activator Protein 2* (*AP-2*) genes (*Tcfap2α-ε*, also known as *AP-2α*, *β*, *γ*, *δ* and *ε*) that share a high degree of similarity, AP-2α being the predominant isoform. In mouse embryo, *AP-2α* is expressed in the ectoderm and CNCC from E8.5 to E12.5 (Figure 17; Mitchell et al., 1991; Morriss-Kay, 1996). The essential role of *AP-2α* during craniofacial development was demonstrated by the generation of null mutant mice that die perinatally with cranial closure failure and severe facial dysmorphogenesis (Schorle et al., 1996). In addition, knockdown of *AP-2α* in Xenopus results in a severe reduction of the neural crest territory (Luo et al., 2003), demonstrating its role during early neural crest development.

Although AP-2α acts as a transcriptional activator most of the time, there is evidence that it can also repress gene expression as precocious gene expression was observed *AP-2α* mutant mice (Pfisterer et al., 2002). Most of these genes are implicated in the inhibition of proliferation and induce differentiation suggesting a role for *AP-2α* in maintaining the progenitor state of CNCC (Pfisterer et al., 2002). Together, these observations suggest that AP-2α can be used as an early CNCC marker.

2.2.4. *Dlx* genes

The *Distalless homeobox* (*Dlx*) gene family consists of six homologs in mammals. The six *Dlx* genes are expressed in cranial neural crest derivatives where they are patterning the branchial arches (Figure 18A) as revealed by the generation of null alleles for *Dlx1*, *Dlx2*, (Qiu et al., 1995, 1997) and *Dlx5* and *Dlx6* in the mouse (Merlo et al., 2000).

Dlx1 and *Dlx2* single mutants present defects in the morphogenesis of proximal craniofacial bones, derived from BA1 and BA2, forming the base of the skull (Qui M. 1995, Qui M. et al 1997). Both mutants present with an abnormal ala temporalis, a cartilaginous component bridging the skull base to the temporal wall.

In addition, *Dlx2* mutants present extensive defects including reduction of the bones forming the temporal wall of skull, apparition of ectopic cartilage, together with a partially penetrant cleft of the secondary palate (Qiu et al., 1995). *Dlx1/2* double mutant presents more severe phenotype than the single *Dlx2* mutant; in particular it lacks maxillary molars and a fully penetrant cleft of the secondary palate (Qiu et al., 1997), suggesting a certain level of redundancy between *Dlx1* and *Dlx2* functions (Qiu et al., 1997).

Early during development, *Dlx5* expression is localised to the anterior neural ridge, defining the rostral boundary of the neural plate, then extends caudo-laterally, marking the prospective neural crest (Figure 17; Yang et al., 1998). Later *Dlx5* is expressed in a BMP-dependent manner in the developing skull and mandibular bones but not in the maxilla (Ferguson et al., 2000; Holleville et al., 2007). Like *Dlx2*, *Dlx5* mandibular expression is induced by signals coming from the mandibular and maxillary epithelia (Ferguson et al., 2000). *Dlx5* is also involved in chondrogenesis as it can induce *Runx2* expression and osteoblast differentiation *in vitro* (Figure 18B; Holleville et al., 2007).

Moreover, *Dlx* genes provide positional identity to the CNCC along the anterior-posterior axis of the embryo. For instance, deletion of both *Dlx5* and *Dlx6* resulted in an embryo with transformation of the lower jaw into an upper (Depew et al., 2002).

2.2.5. Sox genes

The Sry-related high mobility group box (HMG-box; Sox) family consists of transcription factors that contain a conserved HMG-box DNA binding domain *Sox* genes are often associated with lineage commitment and cellular differentiation during development and often function as transcriptional activators (Figure 17 and 18B; Sauka-Spengler and Bronner-Fraser, 2008).

Among the different family members, *Sox9* is active from the earliest steps of neural crest development in the neural plate border where it regulates neural crest formation and the EMT by directly activating *Snail1/2* expression (Sakai et al., 2006). *Sox9* expression persists in migrating CNCC as they populate the branchial arches (Spokony et al., 2002) however it does not seem to be required for their migration. In chicken embryos, *Sox9* overexpression in the neural tube induces a migratory neural crest-like phenotype and maintains these cells in an undifferentiated state (McKeown et al., 2005). Once CNCC are established in the facial prominences, *Sox9* is expressed in all cartilage progenitors and is an upstream regulator of the chondrogenic lineage (Sahar et al., 2005; Thomas et al., 1997). *Sox9* regulates the cartilage-specific gene *Col2a1* (which encodes type II collagen, the major collagenous component of cartilage extracellular matrix) and the bone-specific gene *Runx2* (Figure 17 and 18B; Akiyama et al., 2005). Homozygote *Sox9* mouse mutants die during gestation. In the heterozygotes, that die perinatally, cartilages are reduced in size and the animals exhibit cleft palate (Mori-Akiyama et al., 2003). When *Sox9* is specifically knocked-out in NCC using a *Wnt1-Cre* transgenic approach, embryos lack the entire cranial cartilages but intramembranous bones remain, as they do not form cartilage (Lee and Saint-Jeannet, 2011; Mori-Akiyama et al., 2003). Sox9 is therefore a marker of CNCC progenitors and a marker of cartilaginous lineage commitment later during development.

2.2.6. Msx genes

The muscle segment-related homeobox (Msx) family consists of *Msx1*, *Msx2*, and *Msx3* in mammals, but only expression of *Msx1* and *Msx2* has been described in the neural crest, Msx3 expression being strictly restricted to the dorsal neural tube but not the neural crest territory (Shimeld et al., 1996; Wang et al., 1996). In the mouse, *Msx1* and *Msx2* are expressed during critical stages of neural crest and craniofacial development. *Msx1* is

expressed in migrating NCC (Figure 17) and homozygous null mice die at birth with craniofacial defects including cleft of the secondary palate, abnormal mandible and maxillary, and failure of tooth development (Satokata and Maas, 1994). Of note, in the face of these mutants, *Msx2* is not expressed in the affected regions (Houzelstein et al., 1997), hence it cannot compensate for *Msx1* loss. *Msx2* mutants also present with an abnormal skull ossification linked to a defect in the proliferation of osteoprogenitors (Satokata et al., 2000). Generation of double mutants for *Msx1* and *Msx2* confirmed the role of these transcription factors during CNCC development. The double mutants died around E17.5 with no frontal bone (Han et al., 2007). While CNCC migration appears normal, ossification of the frontal mesenchyme is defective. Furthermore, it was suggested that Msx1 and Msx2 act on *Runx2* expression in the FNP indicating that *Msx1* and *Msx2* genes are necessary for CNCC differentiation (Han et al., 2007). Moreover, *Msx1*; *Msx2* double mutant embryos present an increased number of apoptotic cells in neural crest-derived cells contributing to BA1, which induces a hypoplasia of BA1 and demonstrate the essential role of *Msx1* and *Msx2* for the survival of CNCC (Ishii et al., 2005).

2.2.7. Pax genes

In mouse, *Pax3* is first detected at E8.5 in the dorsal neuroepithelium and is maintained in migratory CNCC. *Pax3* expression is detected throughout craniofacial development, in NCC of the developing PNS, the CNCC-derived craniofacial mesenchyme and in the migratory cardiac NCC (Figure 17; Goulding et al., 1991). Persistent *Pax3* expression in CNCC using the Rosa locus results in cleft palate and other craniofacial defects associated with impaired skeletal development (Wu et al., 2008). Persistent *Pax3* expression inhibits BMP-dependent chondrogenesis by inducing the overexpression of *Sostdc1*, a BMP inhibitor (Wu et al., 2008).

This suggests that *Pax3* can maintain CNCC in an undifferentiated state by blocking responsiveness to differentiation signals.

Pax3 mouse mutant embryos are characterised by the formation of spina bifida due to a failure of neural tube closure (Epstein et al., 1991) which is induced by increased apoptosis in the dorsal neural tube in the absence of *Pax3* (Borycki et al., 1999). However, NCC formation and migration in anterior regions appears normal (Franz, 1992). Yet, in the caudal regions, Pax3 mutants present with a reduction or loss of spinal and sympathetic ganglia and pigmentation defects (Conway et al., 1997a; Epstein et al., 2000; Franz and Kothary, 1993; Lang et al., 2000; Tremblay et al., 1995). In addition, they develop persistent truncus arteriosus (PTA), signs of cardiac failure (Conway et al., 1997a, 1997b, 1997c), with defects of the aortic arches, leading to a cardiac outflow tract (OFT) septation failure (Henderson et al., 1997) due to a decrease in the number of migrating cardiac NCC into the developing heart (Conway et al., 2000; Epstein et al., 2000). Together, these anomalies lead to heart failure and ultimately to the death of the embryo at E14.5.

The absence of Pax3, results in a severe reduction in the number of NCC delaminating from the neural tube at the vagal and rostral trunk levels and a complete loss of cells at the caudal, lumbar and sacral levels (Serbedzija and McMahon, 1997). However, in this mutant, craniofacial development is not affected suggesting a divergent function for this transcription factor in the cranial neural crest compared to the trunk neural crest. In Xenopus, *Msx1* can induce multiple early neural crest genes including *Pax3* and *Zic1* (Monsoro-Burq et al., 2005), which are among the first genes expressed in response to neural plate border-inducing signals (Sauka-Spengler and Bronner-Fraser, 2008). Multiple experiments demonstrate that *Pax3* and *Zic1* together are both necessary and sufficient to specify the neural crest. Where *Pax3* and *Zic1* expression overlap, they act together (before other early neural crest marker

genes like *FoxD3* and *Snail1/2* are expressed) to specify the neuroectoderm to adopt a neural crest fate (Hong and Saint-Jeannet, 2007; Sato et al., 2005) and activate *Snail1/2* expression in a WNT-dependent manner (Monsoro-Burq et al., 2005). In chicken embryos, *Pax3* is expressed in the dorsal neural tube and plays a role in specification of NCC. *Pax3* is up-regulated in the dorsal neural tube in response to WNT signalling but also depends on BMP signalling (Burstyn-Cohen et al., 2004; Taneyhill and Bronner-Fraser, 2005).

In chicken embryos *Pax7* is one of the earliest indicators of neural crest precursors (Basch et al., 2006), along with *Pax3*, *Snail1/2*, *FoxD3* and *Sox9*. *Pax7* expression begins in the dorsal neural tube and indicates a region of early neural crest induction (Basch et al., 2006). *Pax7* is broadly expressed in CNCC and is also expressed in the trunk neural crest including both premigratory and migratory NCC. In addition, *Pax7* is a marker of the xanthophore lineage in zebrafish and a reduction in *Pax7* expression is seen after morpholinos-mediated knockdown of *Pax3*, which causes defects in xanthophore fate specification (Minchin and Hughes, 2008) and suggests an influence of Pax3 on *Pax7* expression in this lineage.

Mouse mutants for *Pax7* survive until postnatal stages and only display discrete craniofacial defects related to the shape of the maxilla and nose (Mansouri et al., 1996). This points out that in mammals, *Pax7* function in neural crest induction must be compensated by other factors. Moreover, this suggests that mammalian GRNs involved in NCC formation are more complex and must rely and additional compensatory feedback loops in order to insure the correct development of the neural crest.

Mouse *Pax9* is expressed in the cranial neural crest, the midbrain, somites, limb mesenchyme, and in foregut endoderm derivatives (Kist et al., 2007; Peters et al., 1998). In the mandibular arch mesenchyme, *Pax9* marks the prospective sites of tooth development before morphological indicators appear (Peters et al., 1998).

Pax9 homozygous null mice die at birth, but neural crest-specific deletion of *Pax9* using a *Wnt1-Cre* transgenic approach results in mice with cleft in the secondary palate and lack of tooth development (Kist et al., 2007). Furthermore, Pax9 genetically associates with *Msx1* to control cell proliferation during tooth development, such that in *Pax9*; *Msx1* double heterozygote embryos, cell proliferation is significantly reduced in both the dental epithelium and mesenchyme (Nakatomi et al., 2010).

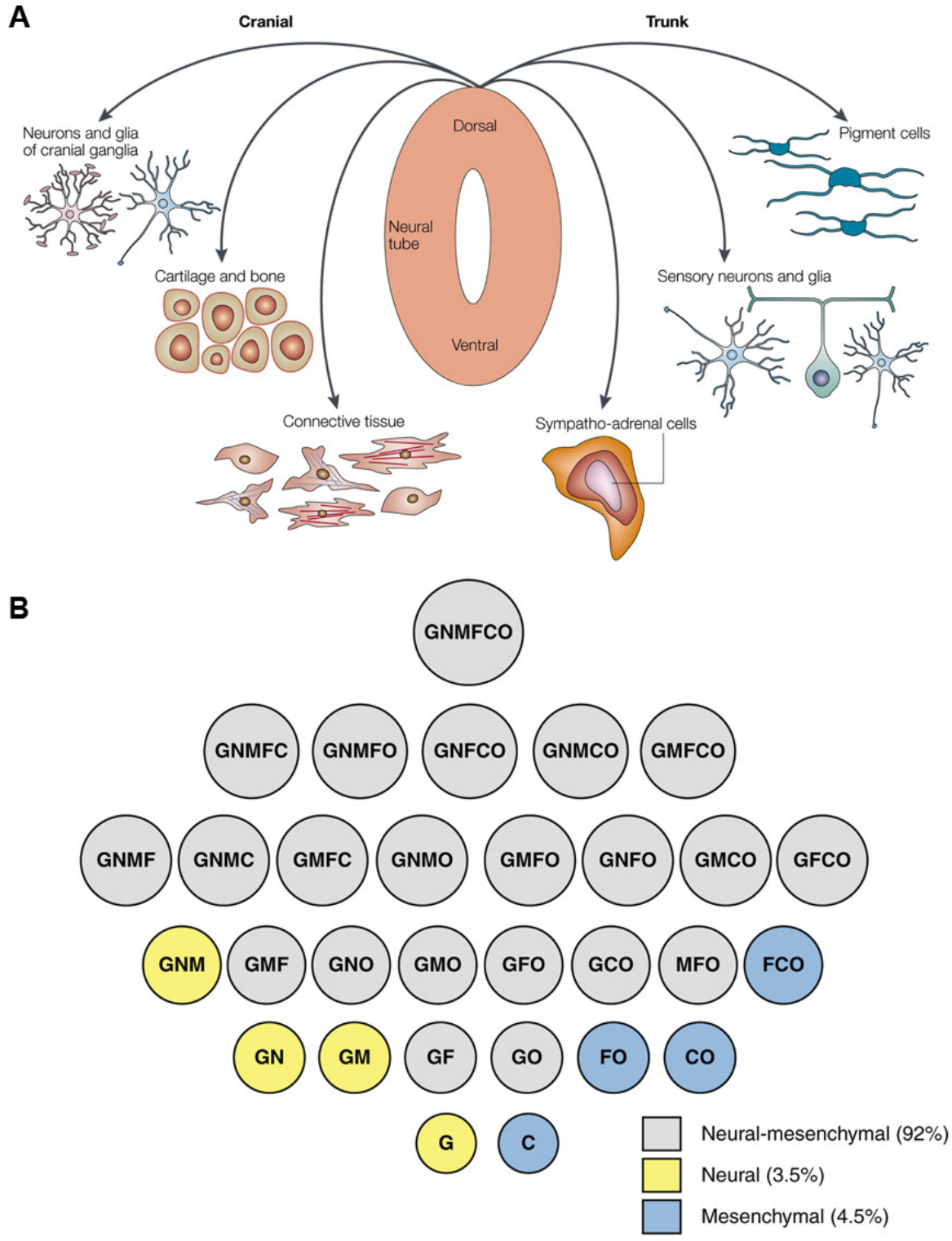

Figure 19: Multipotence of the neural crest
(A) Schematic representation of the neural crest derivatives. While the neural crest gives rise to the entire PNS, cranial neural crest also generates craniofacial bones and cartilages (from Knecht and Bronner-Fraser, 2002). (B) Classification of the different cranial neural crest progenitors based on their developmental potential assess by clonal analysis. G: glia, N: neurons, M: melanocytes, F: myofibroblasts, C: chondrocytes, O: osteoblasts. At the top of the progenitor hierarchy, GNMFCO indicates a highly multipotent CNCC (from Le Douarin and Dupin, 2012).

3. Multipotence of the neural crest cells

Once CNCC have reached the facial prominences, they give rise to a wide variety of cell types (Le Douarin and Kalcheim, 1999). In addition to giving rise to glial cells, melanocytes and, together with the ectodermal placodes, to the entire PNS, CNCC can also generate bones, cartilages and connective tissues (Figure 19A). The generation of quail/chick chimeras demonstrated that the cranial neural crest gives rise to most of the bones and cartilages of the face and skull, but also the facial dermis, adipose tissue, connective tissue and tendons associated with the head muscles and participates in the establishment of the blood vessels irrigating the forebrain and facial area. In addition, in mammals, CNCC give rise to the ondotoblasts of the teeth (Crane and Trainor, 2006). To demonstrate the importance of the neural crest in the development of vertebrates, there is not a single organ or tissue in the body that does not contain neural crest derived cells, even if the contribution is minor (Le Douarin et al., 2004). To explain the diversity of cell types generated by the neural crest, two mechanisms can be taken in account. The CNCC population could be composed of a pool of heterogenic progenitor cells, each of them giving rise to a specific cell type or CNCC could be highly multipotent. *In vitro* clonal analysis revealed that most individual CNCC are at least bi-potent, being able to generate both chondrogenic and neural cell types arguing for the idea of the neural crest as a highly mutipotent structure (Figure19B; Crane and Trainor, 2006; Dupin et al., 2010). Extensive transplantation experiments demonstrated that while trunk NCC possess an irreversible memory of their rostro-caudal origin, CNCC present the capacity to alter their fate according to local signals, giving them the ability to compensate and replace missing cells until late neurulation (Le Douarin et al., 2004).

In vivo studies in avian embryos demonstrated the pluripotence of trunk NCC that can generate different cell types such as glial cells, sensory and sympathetic neurones,

melanocytes and adrenomedullary glands (Bronner-Fraser and Fraser, 1988). Cell types such as bones and cartilages being generally derived form the mesoderm germ layer but not from the neural crest. This suggests that *in vivo* trunk neural crest does not have the capacity to form these cell types demonstrating a striking difference in the degree of multipotence of the neural crest along the rostro-caudal axis of the embryo, the ability of NCC to form mesenchymal derivatives being exclusive to the cranial neural crest (Figure 19A).

However, several evidences support that trunk NCC can be committed to the chondrogenic lineage *in vitro* (Ido and Ito, 2006). In addition, in turtles, trunk NCC are generating the osteogenic plastron and carapace (Cebra-Thomas et al., 2007, 2013).

Because of its multipotent nature and the numerous derivatives produced by the neural crest, both neuronal and mesenchymal, the neural crest has been described as the fourth embryonic layer (Hall, 2000). However, the mechanisms conferring this multipotence to CNCC and explaining the differential potential between trunk and cranial NCC remain to be elucidated.

4. Evolution of the neural crest

The neural crest is a synapomorphic structure characteristic of most vertebrates. It is believed its origin concurs with the evolution of a brain, a muscular pharynx and paired sensory organs and allowed the development of evolutionarily advantageous complex head structures. In 1983, Gans and Northcutt introduced a new theory called “The New Head Hypothesis” (Gans and Northcutt, 1983) that appearance of the neural crest was linked to a transition from passive filter feeding to active predation. In “The New Head Hypothesis”, Gans and Northcutt proposed that emergence of a CNS allowed an epidermal nerve plexus including primitive neural crest cells that was controlling cilliary function during movement and feeding to be freed to diversify and evolve new functions (Gans and Northcutt, 1983).

A striking difference between vertebrates and the rest of metazoans is the presence of complex head structures made of bones and cartilages derived from the neural crest. Among these structures, jaws brought a decisive advantage concerning rapid predation. It has been suggested that glial cells responsible for generating myelin evolved together with skeletal elements of the head (Zalc and Colman, 2000). In the PNS, neural crest-derived Schwann cells synthesize the myelin sheath, which wrap around axons allowing them to conduct action potentials a hundred times faster than an axon devoid of myelin. A myelinated axon with a diameter of 1 to 10μm propagates nerve impulses with a velocity of 50 to 100m/second, while a non-myelinated axon with a diameter of 10μm propagates action potential at 1m/second.

Among fishes, Placoderms were the first to acquire a hinged jaw, which required a rapid conduction of the nerve impulse in order to efficiently activate this structure (i.e., snapping their prey). This suggests the appearance of the jaw may have been coincident with myelin during the evolution of the neural crest (Zalc et al., 2008). Analysis of cranial nerves length and diameter in fossils revealed that in ostracoderms (species ancestral to the apparition of Placoderm), while the width remains unchanged, the length of the nerve was about ten times longer in Placoderm compare to ancestral species confirming that myelin was a novel feature of the Placoderm nervous system (Zalc et al., 2008). Interestingly, this increase in nerve length also corresponds to an increase in the size of the craniofacial complex (Zalc et al., 2008). Another way to increase the conduction of the nerve impulses is to increase the diameter of the nerve. However, the bony structure of the vertebrate head induces a physical constraint limiting any increase in the volume of axons (Zalc and Colman, 2000). It is estimated that for human non-myelinated axons to have the same velocity in the propagation of the action potentials, the spinal cord would need to be about 1 meter in diameter demonstrating the incredible advantage brought by myelinated axons (Zalc, personal communication).

While in jawless fish, feeding was closer to a passive filter feeding behaviour; Placoderm myelinisation was a necessary acquisition for rapid predation, together with the development of myelinated visual and locomotor systems. This result confirms the proposition of the "The New Head Hypothesis" which states that neural crest and its derivatives allowed the switch from passive to active feeding (Gans and Northcutt, 1983). Furthermore, it reinforces the idea that neural crest-derived glial and chondrogenic cells arose together during evolution, showing how apparition of the neural crest was a tremendous input in the success of vertebrates.

5. Environmental influence on craniofacial development

5.1. Environmental risk factors linked to craniofacial defects

Normal craniofacial development requires the correct interaction of dynamic processes involving growth, differentiation and exchange of signals between the ectoderm, the endoderm, the mesoderm and CNCC. Hence, slight spatiotemporal alterations in these interactions resulting in changes of the craniofacial morphology may have been a driving force during evolution. However, given the complexity of these interactions and of the GRNs involved in craniofacial development, these alterations can also be at the origin of congenital craniofacial malformations. Thus, craniofacial defects represent a third of all congenital malformations within human populations (Gilbert-Barness, 2010). Most of the craniofacial malformations originate from defects in the formation, migration or differentiation of CNCC. Regulation of the proliferation of CNCC derivatives is essential to control the growth of facial prominences and allow the correct craniofacial morphogenesis.

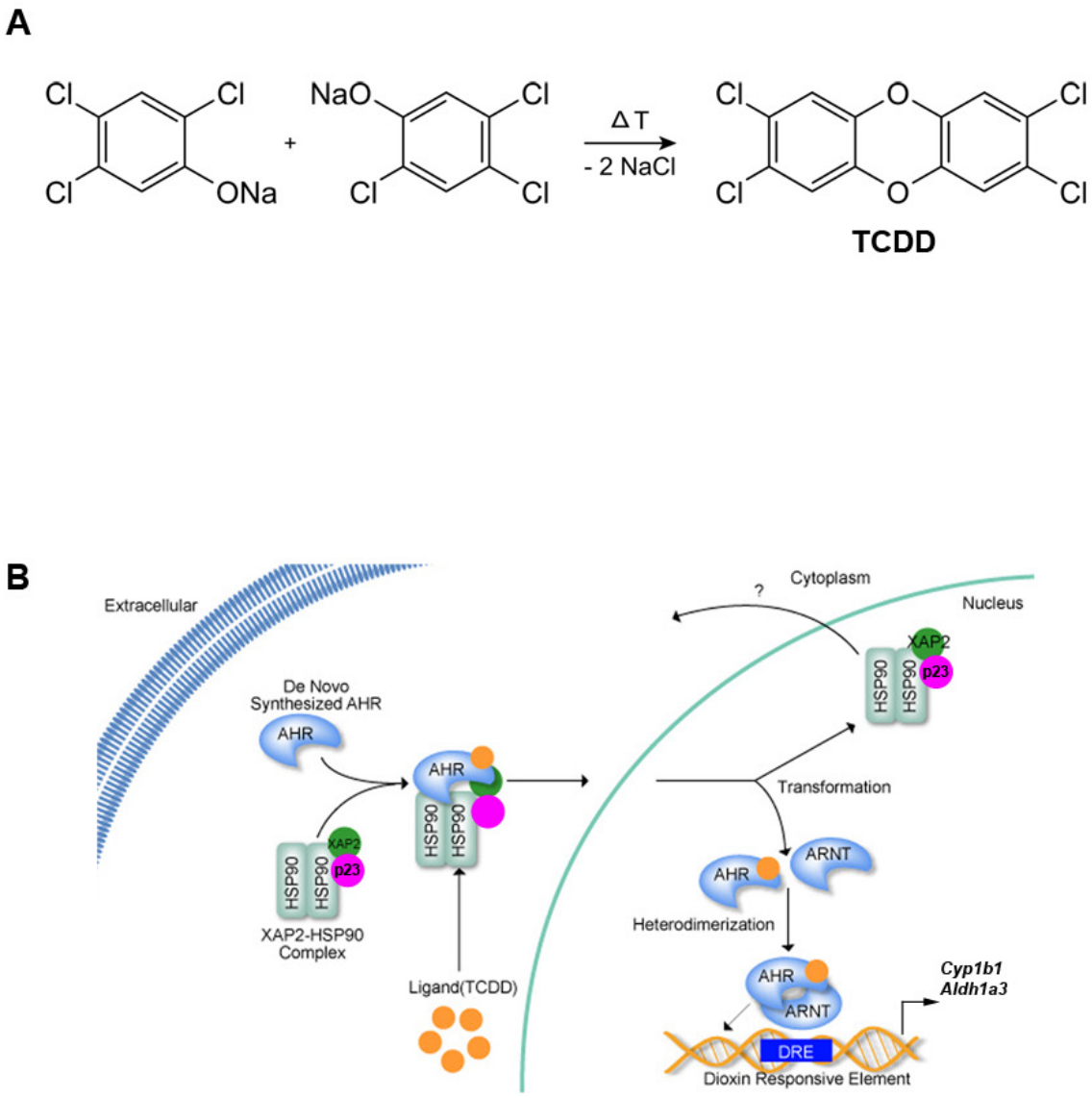

<u>Figure 20:</u> AhR signalling pathway mediates the response to dioxin exposition
(A) Chemical equation representing the formation of 2,3,7,8-tétrachlorodibenzo-p-dioxine (TCDD). (B) TCDD binding to AhR induces it translocation into the nucleus and the activation of AhR target genes.

Among craniofacial defects, cleft lip with or without palate (CLP) affect approximately 1 in 700 live births, however 70% of CLP are non-syndromic. Nevertheless, a large quantity of genes has been linked with non-syndromic CLP but few of them display a clear Mendelian inheritance. For instance, in humans, mutations in the genes *MSX1*, *FGFR1*, *FGF8* or *BMP4*, are strongly associated with CLP (Wilkie and Morriss-Kay, 2001). In addition, CLP is influenced by environmental risk factors. As a consequence, occurrence of CLP is considered as a multifactorial model of inheritance in which genetic risk factors are highly associated with environmental variables (Dixon et al., 2011).

Among the environmental variables, nutritional factors such as alcohol consumption or folate deficiency are associated with increased risk of CLP (Dixon et al., 2011). Maternal smoking is linked to an increased occurrence of CLP, suggesting that metabolic pathways may be involved in regulating craniofacial development. Finally, it is estimated that 10 to 15% of congenital malformations are linked to exposure of pregnant women to teratogens (Dixon et al., 2011). A teratogen defines an environmental factor that can generate permanent abnormalities in structure or function, growth retardation or even death of the embryo.

5.2. Dioxin exposure is linked with craniofacial malformations

Among environmental pollutants, 2,3,7,8-tetrachlorodibenzo-p-dioxine (TCDD), commonly known as dioxin is considered the most potent teratogen. Incomplete combustions such as forest fires and volcanic eruptions are natural sources of TCDD production (Figure 20A). However, increases in TCDD production only really started 200 years ago and still persist today due to anthropogenic causes. During the 20th century industrial activities were the largest source of TCDD production as it was used in various chemical processes or generated as a by-product of these processes (Beischlag et al., 2008). However, most of these processes have been regulated and today the major sources of TCDD production remain the

non-controlled combustions of industrial and municipal wastes (White and Birnbaum, 2009). TCDD is a highly toxic persistent chemical released into the environment as an unintentional by-product of incomplete combustion during the incineration of municipal and industrial wastes. In humans, most of the exposure occurs through food, mainly meat and dairy products, fish and shellfish. The developing foetus is especially sensitive to TCDD exposure, thus it is crucial to monitor the *in vivo* cellular response to TCDD during development in order to understand and prevent the molecular and cellular response following exposure to dioxins.

The violent effects of dioxins during pregnancy were revealed worldwide after the American Vietnam war. Between 1962 and 1970, in Vietnam, to reduce enemy ground cover, the American Army extensively used a defoliant called Agent Orange containing TCDD. The Vietnamese population as well as the American military were exposed to high doses of TCDD. It was estimated than the spreading of TCDD-containing Agent Orange led to the birth of more than 500 000 children with congenital defects (Beischlag et al., 2008; York and Hayley, 2008). In 1976, in Seveso, Italy, the explosion of a chemical plant producing an intermediate compound in the production of TCDD, lead to the release of critically high doses of TCDD in the environment. While the normal dose for TCDD contamination is around 1ppm, the levels of TCDD measured in the environment after the incident approached 100ppm (Beischlag et al., 2008). These expositions to TCDD were later linked to skin lesion consistent with chloracne as well as increased risk of diabetes and various cancers. Furthermore, it was demonstrated that TCDD is a teratogen as embryonic exposure was dramatic for the future development of the individuals, which display many defects such as altered psychomotor function, cognition as well as reproductive and developmental defects (White and Birnbaum, 2009).

In laboratories, mouse embryos exposed to TCDD present with cleft palate, hydronephrosis, thymic hypoplasia, reduced weight and even death at high doses. Interestingly, cleft palate is observed with TCDD concentrations that are non-toxic for the mother and are induced when the exposure occurs before E14.0, during the development of the CNCC and fusion of the facial prominences (Courtney and Moore, 1971; King-Heiden et al., 2012; Kransler et al., 2007; Moore et al., 1973; Pratt et al., 1984; Yonemoto, 2000). While the receptor to TCDD has been identified for several decades now, it remains unclear how TCDD exposition trigger the developmental defects observed in populations.

5.3. AhR signalling pathway mediates dioxin action

The cellular responses to TCDD are mediated via binding to a bHLH/PAS (basic Helix-Loop-Helix/Per-ARNT-Sim) transcription factor, named Aryl hydrocarbon Receptor (AhR). *AhR* is expressed in almost all mouse tissues (Abbott et al., 1995) however in the embryo, craniofacial expression does not start before E10.5 (Abbott et al., 1995; Jain et al., 1998). By E13.5, *AhR* is highly expressed in many tissues, in particular in the palatal shelves and nasal septum cartilage (Jain et al., 1998).

Null mice embryos for *AhR* are insensitive to TCDD exposure and are morphologically similar to untreated wild-type embryos (Fernandez-Salguero et al., 1995; Gonzalez and Fernandez-Salguero, 1998). Haplo-insufficiency for *AhR* is also sufficient to prevent the formation of cleft palate upon TCDD exposure, but not of hydronephrosis (Mimura et al., 1997). In addition, *in vitro* studies have shown that the binding of TCDD to this receptor up-regulates its target gene expression in an inappropriate and sustained manner (Hankinson, 1995; Mimura and Fujii-Kuriyama, 2003). The conventional model of AhR action proposes that the non-activated form of AhR is mainly found in the cytosol where it associates with two heat shock proteins (Hsp90), one molecule of prostaglandin E synthase 3 (p23) and one

molecule of immunophilin-like protein hepatitis B virus X-associated protein 2 (XAP2) (Furness et al., 2007). Upon ligand binding, AhR releases its chaperones and translocates into the nucleus, where it associates with the aryl hydrocarbon receptor nuclear translocator (ARNT). There, the AhR/ARNT complex binds to DNA through specific sequences called XRE (Xenobiotic Response Element, also called DRE for Dioxin Response Element) and drives gene expression (Figure 20B; Beischlag et al., 2008). Recent ChIP-seq analyses for AhR and ARNT in untreated and TCDD-treated cell lines have indicated that this model may only be partially true. Indeed AhR was found to be bound to genomic regions in the absence of its ligand, and only 40% of the AhR bound regions are also bound by ARNT upon ligand activation (Lo and Matthews, 2012). Further controversy surrounds the existence of other AhR ligands and their implication during teratogenesis (Kiss et al., 2011; Li et al., 2011). Derivatives of tryptophan and cytokines have also been suggested to be potential endogenous ligands (Opitz et al., 2011).

The TCDD bound AhR triggers physiological responses in target cells, including xenobiotic metabolism, vasculature development, immunosuppression, cell differentiation and cell cycle progression (Marlowe and Puga, 2005; Puga et al., 2009). In particular, it induces the transcription of an array of environmental stress response genes (Hankinson, 2005). The teratogenic effects of TCDD are also likely to be mediated by the activation of AhR. Yet, the mechanism by which AhR signalling interacts with developmental pathways remains unknown. Most of the identified AhR targets, such as *Cyp1a1*, *Cyp1b1* and *Aldh1a3*, encode for detoxifying proteins, and constitute a landmark of the environmental stress response (Beischlag et al., 2008). Importantly, their link (if they are implicated) with the congenital malformations upon TCDD exposure during development is not understood.

Finally, cross talks between the TCDD-AhR signalling and those regulating the cell cycle have been previously identified (Marlowe and Puga, 2005; Puga et al., 2009). Several studies point out a role for ligand-activated AhR in inhibition of proliferation and induction of cell cycle arrest in normal cycling cell population (Gierthy and Crane, 1984; Jin et al., 2004). For instance, it is suggested that direct interaction between ligand activated AhR and the retinoblastma (Rb) protein would block Rb phosphorylation and inhibit the transcription of specific S-phase genes leading to a G1 arrest (Barnes-Ellerbe et al., 2004). Other studies reported that ligand activated AhR activates the expression of CDKIs. For instance, induction of *p21* or *p27* expression is associated with the activation of AhR signalling (Barnes-Ellerbe et al., 2004; Pang et al., 2008). Furthermore, it was shown that AhR regulates *p21* and *p27* expression by directly binding their regulatory sequences (Pang et al., 2008).

Together, these observations suggest that when activated, AhR can inhibit cell cycle progression by either interacting directly with Rb and blocking the expression of genes required for entry into S-phase or by activating the expression of CDKIs and inducing cell cycle arrest (Puga et al., 2009).

RESULTS

PART I FIRST PAPER

Development

Antagonistic regulation of $p57^{kip2}$ by Hes/Hey downstream of Notch signaling and muscle regulatory factors regulates skeletal muscle growth arrest

2014

https://doi.org/10.1242/dev.110155

© 2014. Published by The Company of Biologists Ltd | Development (2014) 141, 2780-2790 doi:10.1242/dev.110155

RESEARCH ARTICLE

STEM CELLS AND REGENERATION

Antagonistic regulation of p57kip2 by Hes/Hey downstream of Notch signaling and muscle regulatory factors regulates skeletal muscle growth arrest

Antoine Zalc[1,2,3,*], Shinichiro Hayashi[1,2,3,*], Frédéric Auradé[1,2,3,‡], Dominique Bröhl[4,‡], Ted Chang[1,2,3,‡], Despoina Mademtzoglou[1,2,3], Philippos Mourikis[1,2,3], Zizhen Yao[5,§], Yi Cao[5,§], Carmen Birchmeier[4] and Frédéric Relaix[1,2,3,¶]

ABSTRACT

A central question in development is to define how the equilibrium between cell proliferation and differentiation is temporally and spatially regulated during tissue formation. Here, we address how interactions between cyclin-dependent kinase inhibitors essential for myogenic growth arrest (p21^{cip1} and p57^{kip2}), the Notch pathway and myogenic regulatory factors (MRFs) orchestrate the proliferation, specification and differentiation of muscle progenitor cells. We first show that cell cycle exit and myogenic differentiation can be uncoupled. In addition, we establish that skeletal muscle progenitor cells require Notch signaling to maintain their cycling status. Using several mouse models combined with *ex vivo* studies, we demonstrate that Notch signaling is required to repress p21^{cip1} and p57^{kip2} expression in muscle progenitor cells. Finally, we identify a muscle-specific regulatory element of *p57^{kip2}* directly activated by MRFs in myoblasts but repressed by the Notch targets Hes1/Hey1 in progenitor cells. We propose a molecular mechanism whereby information provided by Hes/Hey downstream of Notch as well as MRF activities are integrated at the level of the *p57^{kip2}* enhancer to regulate the decision between progenitor cell maintenance and muscle differentiation.

KEY WORDS: Myogenesis, Cell cycle regulation, p57^{kip2}, Cdkn1, Notch signaling, MRF

INTRODUCTION

The formation of functional organs of an appropriate size is highly controlled during development. Organ transplantation and regeneration studies have revealed that organ size relies on both intrinsic and extrinsic mechanisms (reviewed by Cook and Tyers, 2007). Systemic factors, such as growth hormones and nutritional status, have been known for many years to regulate organ size, while more recently the role of the Hippo and insulin/TOR pathways has emerged (Tumaneng et al., 2012). Of note, increasing evidence links these pathways with stem cell self-renewal and differentiation (Cherrett et al., 2012). Nevertheless, how cell fate decisions and differentiation programs are coordinated with cell cycle progression and arrest remains poorly understood.

[1]UPMC Paris 06, U 974, Paris, F-75013, France. [2]INSERM, Avenir Team, Pitié-Salpétrière, Paris, F-75013, France. [3]Institut de Myologie, Paris, F-75013, France. [4]Max-Delbrück-Center for Molecular Medicine, Berlin 13125, Germany. [5]Human Biology Division, Fred Hutchinson Cancer Research Center, Seattle, WA 98109, USA.
*These authors contributed equally to this work
‡These authors contributed equally to this work
§These authors contributed equally to this work

¶Author for correspondence (frelaix@gmail.com)

Received 14 March 2014; Accepted 13 May 2014

Skeletal muscle provides a suitable model for such studies because the molecular pathways regulating differentiation and growth arrest have been identified. Muscle formation relies on a proliferating population of progenitor cells that express and require the Paired homeobox transcription factors Pax3 and Pax7 (Buckingham and Relaix, 2007). These resident progenitors are maintained in the developing muscles, where they provide a source of cells for muscle growth during development and eventually generate the adult stem cells population, termed satellite cells (Gros et al., 2005; Kassar-Duchossoy et al., 2005; Lepper and Fan, 2010; Relaix et al., 2006). Initially, muscle progenitor cells are located in the somite where they give rise to the trunk musculature of the myotome (Ben-Yair and Kalcheim, 2005; Kassar-Duchossoy et al., 2005; Relaix et al., 2005) or migrate out of the somitic dermomyotome to form limb skeletal muscles (Birchmeier and Brohmann, 2000; Schienda et al., 2006). During limb embryonic myogenesis, Pax3/7^{+} progenitor cells undergo consecutive steps of differentiation via sequential expression of bHLH myogenic regulatory factors [MRFs; Myf5, Myod1 and myogenin (Myog)], and first form committed progenitor cells that express Pax3/7 and Myf5, which correspond to a transit amplifying population (Picard and Marcelle, 2013), followed by the generation of myoblasts that express Myf5 and Myod1, culminating in the appearance of differentiating myoblasts marked by Myog (Fig. 1) (Murphy and Kardon, 2011). The Myog^{+} cells then fuse to form multinucleated muscle fibers. In the absence of Myod1, despite upregulated Myf5 expression, myogenic differentiation is delayed during early limb development, resulting in a transient absence of differentiating (Myog^{+}) myoblasts and fibers prior to E14.5 (Kablar et al., 1998). When both Myf5 and Myod1 are impaired, Pax3/7^{+} cells do not enter the myogenic program and skeletal muscle formation is abolished at all sites of myogenesis (Rudnicki et al., 1993).

Building a tissue requires the coordination of cell cycle exit with differentiation. Despite the identification of key molecular regulators of myogenic specification and differentiation (Buckingham and Relaix, 2007), how cell cycle exit is synchronized with skeletal muscle differentiation is not well understood. Cell cycle exit in muscle cells is orchestrated by cyclin-dependent kinase inhibitors (CDKIs) belonging to the CIP/Kip family: p21^{cip1} (Cdkn1a, p21^{waf1}), p27^{kip1} (Cdkn1b) and p57^{kip2} (Cdkn1c), abbreviated here as p21, p27 and p57, respectively. These CDKIs can bind and inhibit all combinations of cyclin-CDK complexes (reviewed by Besson et al., 2008). Most notably, in the absence of both *p21* and *p57*, skeletal muscle development is severely affected and fiber formation is impaired, with myogenic cells undergoing apoptosis. This points to an essential function of p21 and p57 in cell cycle arrest during myogenesis (Zhang et al., 1999). *In vitro*, Myod1 has been suggested to be a direct regulator of *p21*, thus controlling cell cycle exit during

Development (2014) 141, 2780-2790 doi:10.1242/dev.110155

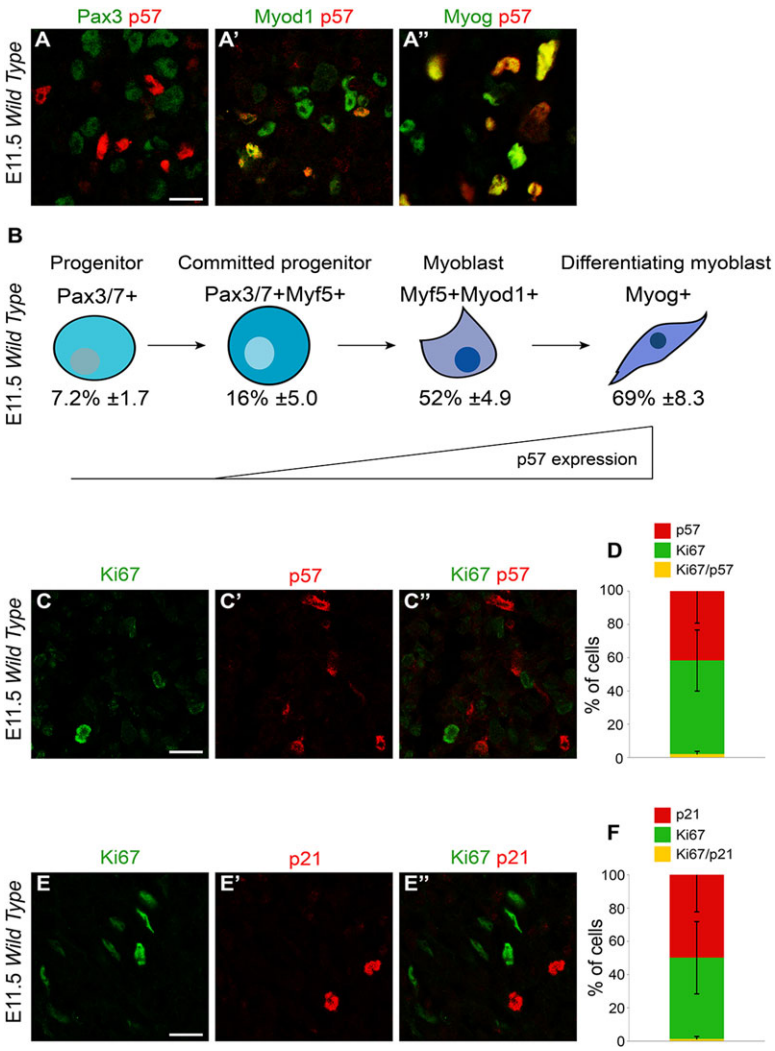

Fig. 1. Cell cycle exit occurs at the determination stage. (A-A″) Co-immunostaining for Pax3 (A), Myod1 (A′) and myogenin (Myog, A″) in green, and p57 (A′,A″) in red in E11.5 embryonic limb muscles. (B) Percentage of p57-expressing cells during forelimb myogenesis is given for each population. Progenitors and committed progenitors are mostly proliferating, whereas myoblasts and differentiating myoblasts are exiting the cell cycle. (C-C″) Co-immunostaining for Ki67 (C,C″, green) and p57 (C′,C″, red) in E11.5 embryonic limb muscles. (D) Quantification of C-C″. (E-E″) Co-immunostaining for Ki67 (E,E″, green) and p21 (E′,E″, red) in E11.5 embryonic limb muscles. (F) Quantification of E-E″. Ki67 is not expressed in cells expressing p21 or p57. For all experiments n=3 embryos; error bars indicate s.d. Scale bars: 10 μm.

adult muscle differentiation (Halevy et al., 1995). It has also been shown, both in mammalian cells (Reynaud et al., 2000) and in zebrafish (Osborn et al., 2010), that p57 interacts and stabilizes Myod1 to promote muscle differentiation, demonstrating a role for CDKIs beyond that in growth arrest. Analysis of *p21*; *p57* double-mutant mouse embryos suggested that cell cycle exit occurs in parallel to, but independently of, Myog-dependent terminal differentiation, while the lack of Mef2c expression in these mice suggested that late differentiation is defective (Zhang et al., 1999).

Previous studies have implicated the Notch signaling pathway as a key regulator of proliferation and differentiation of muscle progenitor cells (Buas and Kadesch, 2010; Mourikis and Tajbakhsh, 2014). This pathway is highly conserved during evolution and plays key roles during development, including the regulation of cell fate decisions, differentiation and homeostasis of progenitor cells in a wide variety of tissues (reviewed by Artavanis-Tsakonas and Muskavitch, 2010). Notch signaling requires direct interaction between a cell expressing at least one of the ligands [delta-like 1 (Dll1) and 4 and jagged 1 and 2 in mammals] with a cell expressing one of the receptors (notch 1-4 in mammals). This interaction leads to a proteolytic cleavage of the receptor that releases the Notch intracellular domain, which translocates into the nucleus and interacts with the Rbpj transcription factor to induce downstream effectors, such as the Hes/Hey family of bHLH transcriptional repressors (reviewed by Borggrefe and Liefke, 2012).

The role of Notch signaling in skeletal muscle development has been assessed in two mouse models: in a hypomorphic *Dll1* mutant (Schuster-Gossler et al., 2007) or in mice in which *Rbpj* expression was conditionally abrogated specifically in the myogenic lineage (Vasyutina et al., 2007). These *in vivo* models, along with studies performed in chick embryos, have demonstrated that Dll1-triggered canonical Notch signaling is required for the maintenance of muscle progenitor cells (Delfini et al., 2000; Hirsinger et al., 2001; Mourikis et al., 2012a; Schuster-Gossler et al., 2007; Vasyutina et al., 2007). Dll1 absence leads to early onset differentiation (Schuster-Gossler et al., 2007; Vasyutina et al., 2007), resulting in rapid exhaustion of the muscle progenitor cell pool and near complete absence of skeletal muscles at the fetal stage (Schuster-Gossler et al., 2007; Vasyutina et al., 2007). This is in part mediated by the repression of Myod1 target genes through direct binding of Hey1 to their promoters (Bröhl et al., 2012; Buas et al., 2010). Interestingly, the role of Notch can be context dependent, since in the young somite of the chick embryo, $Dll1^{+}$ neural crest cells provide a transient stimulation of Notch activity that is important for the initiation of early myogenesis (Rios et al., 2011).

Here, we evaluated the *in vivo* expression of p57 and its link with muscle cell differentiation. Although cell cycle exit is normally synchronous with cell differentiation, we show that these events can be uncoupled. In fact, we found that during embryonic myogenesis p57-mediated cell cycle arrest occurs earlier than

Development (2014) 141, 2780-2790 doi:10.1242/dev.110155

previously recognized, namely in determined muscle cells. Moreover, we demonstrate that in the absence of terminal differentiation muscle progenitor cells aberrantly induce p57 expression, leading to growth arrest. We further show that this growth arrest is associated with a loss of Notch signaling. This is confirmed by conditional genetic ablation of *Rbpj* that leads to upregulation of p21 and p57 in muscle progenitors associated with increased growth arrest. We finally identify a muscle-specific *p57* regulatory element and show that this enhancer is the target of both positive regulation by MRFs in myoblasts and negative regulation by Hes/Hey repressors downstream of Notch in progenitor cells. Our data therefore demonstrate that the regulation of cell cycle exit integrates both negative (via Hes/Hey downstream of Notch signaling) and positive (by MRFs) regulation at the same *p57* regulatory element during muscle differentiation, and that Notch signaling acts upstream, but independently, of both differentiation and cell growth arrest.

RESULTS

Cell cycle exit and differentiation can be uncoupled during skeletal muscle development

We first assessed whether myogenic progenitors leave the cell cycle at specific steps of the MRF-mediated differentiation program, by comparing p57 expression with that of MRFs in E11.5 mouse limbs by immunofluorescence (Fig. 1A-A″). As expected, p57 expression was very low in Pax3/7^{+} progenitors (7.2 ±1.7%). By contrast, a proportion of the Pax3/7^{+}/Myf5^{+} committed progenitor cells did express p57 (16±5%), and this proportion increased significantly in Myf5^{+}/Myod1^{+} (52±4.9%) and Myog^{+} (69±8.3%) populations (Fig. 1B). Similar results were obtained with p21 (data not shown). We verified that p21 and p57 are accurate markers of cell cycle exit of myogenic progenitors as their expression almost never co-localized with that of Ki67, a marker of cycling cells (Fig. 1C-F). Our data are consistent with the results of previous *in vivo* studies analyzing the proliferation of myogenic cells during development (Gros et al., 2005; Lagha et al., 2008; Relaix et al., 2005).

In order to test the existence of a link coupling cell cycle arrest with muscle differentiation, we first investigated whether muscle differentiation is affected when cell cycle exit is impaired. We examined whether the differentiation program proceeds normally in *p21: p57* double-null embryos, in which growth arrest is abolished (Zhang et al., 1999). In limb muscles of control mice, 4.7±1.4% of Myog-positive cells underwent proliferation as assessed by phospho-histone H3 (P-H3) (Fig. 2A-A″,C). By contrast, $p21^{-/-}$; $p57^{+/-m}$ double-mutant embryos displayed a marked increase in Myog^{+}/P-H3^{+} cells (25.2±3.2%; Fig. 2B-C). Taken together, we conclude that p21- and p57-mediated cell cycle exit and MRF-mediated myogenic differentiation can occur independently of each other.

We then examined whether the uncoupling of proliferation and differentiation that we observed in the $p21^{-/-}$; $p57^{+/-m}$ double-mutant embryos holds true in a complementary condition. Delayed myogenesis in *Myod1* mutant embryos provides a useful model for such analysis (Kablar et al., 1997). As expected, Myog and p57 co-localized in the forelimbs of control $Myod1^{+/-}$ mice at E12.5 (Fig. 2D-D″). By contrast, in the E12.5 $Myod1^{-/-}$ forelimbs, even

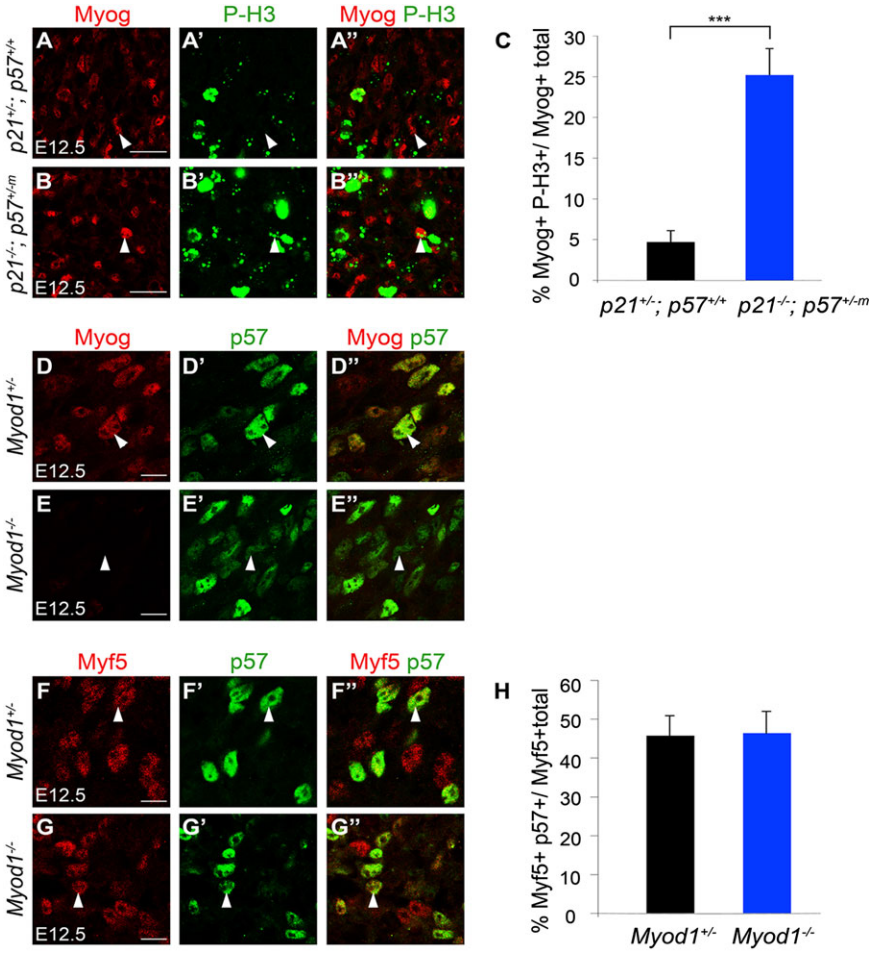

Fig. 2. Cell cycle exit can be uncoupled from cell differentiation. (A-B″) Co-immunostaining for Myog (A,A″,B,B″, red) and P-H3 (A′,A″,B′,B″, green) in $p21^{+/-}$; $p57^{+/+}$ (A-A″) or $p21^{-/-}$; $p57^{+/-m}$ (B-B″) forelimbs at E12.5. Myog^{+} cells (A) do not normally express P-H3 (A′,A″), whereas in $p21^{-/-}$; $p57^{+/-m}$ embryos Myog^{+} cells aberrantly proliferate (B-B″). (C) Quantification of A″,B″. (D-G″) Co-immunostaining for Myog (D,D″,E,E″, red), p57 (D′,D″,E′,E″,F′,F″,G′,G″, green) and Myf5 (F,F″, G,G″, red) in $Myod1^{+/-}$ (D-D″,F-F″) or $Myod1^{-/-}$ (E-E″, G-G″) embryonic limb muscles at E12.5. Myog^{+} cells express p57 in $Myod1^{+/-}$ embryos (D-D″, arrowheads). p57 is expressed in $Myod1^{-/-}$ embryos (E′) despite the absence of Myog (E). Myf5 is co-expressed with p57 in both $Myod1^{+/-}$ (F-F″, arrowheads) and $Myod1^{-/-}$ (G-G″) embryos. (H) Quantification of F″,G″. For all experiments n=3 embryos for each genotype; error bars indicate s.d.; ***P<0.001. Scale bars: 10 μm.

Development (2014) 141, 2780-2790 doi:10.1242/dev.110155

though Myog is not expressed, p57 is detected in the forming muscle masses (Fig. 2E-E″), where it labels nearly half of the Myf5^{+} cells in both *Myod1*$^{+/-}$ (Fig. 2F-F″,H) and *Myod1*$^{-/-}$ (Fig. 2G-H) forelimb (45.6±5.1% versus 46.3±5.5%). These data suggest that cell cycle exit coincides with Myf5 expression in myoblasts and is unaffected when Myod1/Myog-mediated differentiation is impaired.

In the absence of differentiated myoblasts, muscle progenitors precociously express p57 and exit the cell cycle

It has been previously shown that differentiating myoblasts are required for the survival of muscle progenitor cells throughout development (Kassar-Duchossoy et al., 2005). We examined in more detail the impact of differentiating myoblasts on the proliferation state of Pax3^{+} cells by analyzing different allelic combinations of *Myod1: Myf5* double-null embryos to allow key steps during myogenic commitment to be separated. In the absence of Myod1^{+} myoblasts but in the presence of Myf5^{+} myoblasts in *Myod1*$^{-/-}$; *Myf5*$^{+/nlacZ}$ mice (Rudnicki et al., 1993; Tajbakhsh et al., 1997) (supplementary material Fig. S1), the proliferation rate of Pax3^{+} cells was comparable to that observed in control mice at E12.5 (23.6±3.9% versus 25.6±4.6%; Fig. 3A-B″,D). By contrast, in the double-mutant *Myod1*$^{-/-}$; *Myf5*$^{nlacZ/nlacZ}$ forelimbs, which lack both committed progenitors and myoblasts (supplementary material Fig. S1), we observed a significant decrease in the proliferation of Pax3^{+} cells (12.8±3.6% versus 25.6±4.6%; Fig. 3C-D). These data suggest that committed progenitors are required to maintain the proliferation of muscle progenitor cells, whereas differentiated myoblasts are dispensable.

Consistent with the proliferation profile, the cell cycle inhibitor p57 was aberrantly expressed in Pax3^{+}/MRF^{-} progenitor cells of *Myod1*$^{-/-}$; *Myf5*$^{nlacZ/nlacZ}$ embryos compared with control embryos (28.4±2.7% versus 2.3±2.7%; Fig. 3E-G). These data suggested that myoblasts are required to maintain cycling muscle progenitor cells by preventing p57 expression and cell cycle arrest.

Impaired Notch signaling in *Myod1; Myf5* mutant embryos

Our analysis of *Myod1; Myf5* mutant embryos reinforced the notion that functional interactions are taking place between myoblasts and muscle progenitor cells. A strong candidate pathway to mediate these interactions is Notch signaling. It has been previously shown that differentiating myogenic cells express Dll1 and possibly signal to the upstream population that expresses higher levels of Notch receptors (mainly notch 1, 2 and 3) (Delfini et al., 2000; Hirsinger et al., 2001; Mourikis et al., 2012b; Schuster-Gossler et al., 2007). This feedback mechanism of receptor/ligand regulation is supported by many independent *in vivo* studies. However, it has not been formally shown that such cell-cell interactions occur during development, a prerequisite for Notch signaling.

To demonstrate an interaction between myoblasts and muscle progenitor cells, we analyzed the cellular organization on sections of embryonic forelimb muscle masses by co-immunostaining, and found that the majority of Pax7^{+} progenitor cells are in close proximity to Myod1^{+} myoblasts (Fig. 4A-B). Our analysis therefore suggests that direct cell-cell signaling via Notch can occur between progenitors and myoblasts.

To further assess the significance of differentiating muscle cells in Notch activation, we measured endogenous pathway activity in E12.5 *Myod1*; *Myf5* double-mutant embryos that lack differentiated muscle due to the MRF deficiency. It was previously shown that Pax7 expression is lost when Notch signaling is abrogated in myogenic progenitor cells (Vasyutina et al., 2007). Consistent with impaired Notch activity, Pax7 protein was undetectable by immunofluorescence at E12.5 in *Myod1*$^{-/-}$; *Myf5*$^{nlacZ/nlacZ}$ forelimbs (Fig. 4C-E), whereas it was expressed in *Myod1*$^{-/-}$; *Myf5*$^{+/nlacZ}$ embryos (Fig. 4C-E). In addition, we found downregulation of the Notch target genes *Hes1* and *Hey1* in the forelimbs of *Myod1*$^{-/-}$; *Myf5*$^{nlacZ/nlacZ}$ compared with *Myod1*$^{+/-}$; *Myf5*$^{+/nlacZ}$ or with *Myod1*$^{-/-}$; *Myf5*$^{+/nlacZ}$ at E12.5 (Fig. 4F,G).

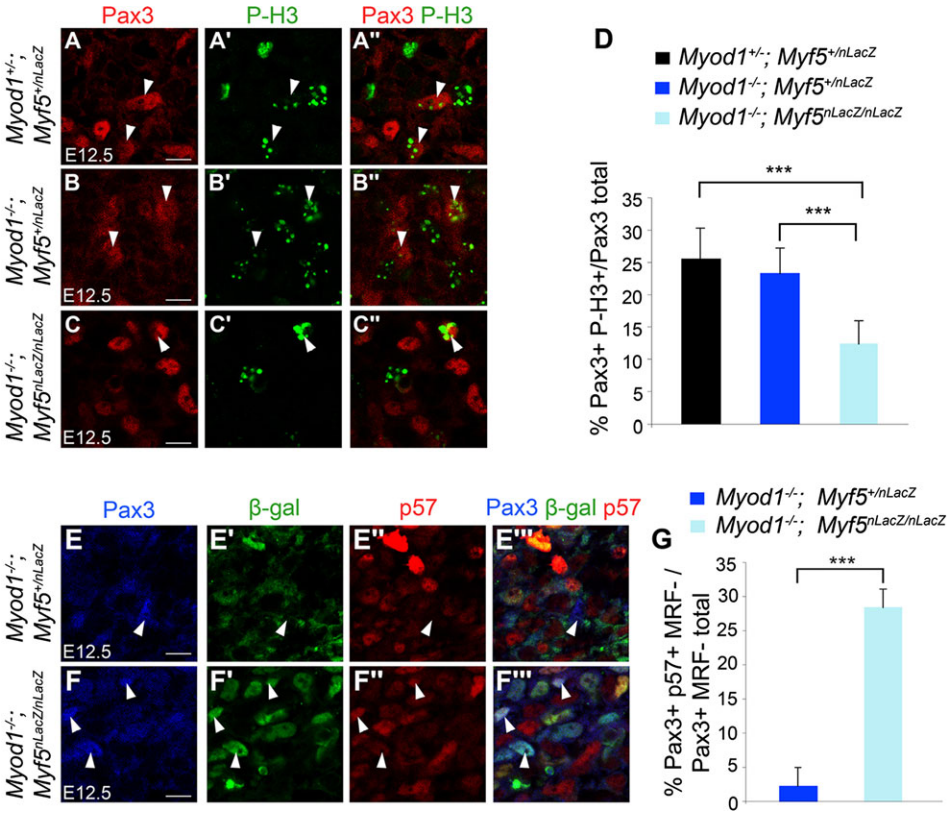

Fig. 3. Myoblasts control muscle progenitor cell proliferation by preventing cell cycle exit. (A-C″) Co-immunostaining for Pax3 (red) and P-H3 (green) in *Myod1*$^{+/-}$; *Myf5*$^{+/nlacZ}$ (A-A″), *Myod1*$^{-/-}$; *Myf5*$^{+/nlacZ}$ (B-B″) and *Myod1*$^{-/-}$; *Myf5*$^{nlacZ/nlacZ}$ (C-C″) embryos at E12.5. Arrowheads indicate Pax3^{+} cells undergoing mitosis. (D) Quantification of A″,B″,C″. (E-F‴) Co-immunostaining for Pax3 (blue), β-gal (green) and p57 (red) in *Myod1*$^{-/-}$; *Myf5*$^{+/nlacZ}$ (E-E‴) or *Myod1*$^{-/-}$; *Myf5*$^{nlacZ/nlacZ}$ (F-F‴) embryos at E12.5. Myf5^{-}/β-gal^{-} cells do not express p57 (arrowheads in E-E‴) in *Myod1*$^{-/-}$; *Myf5*$^{+/nlacZ}$ embryos, whereas in *Myod1*$^{-/-}$; *Myf5*$^{nlacZ/nlacZ}$ embryos Pax3^{+} cells are p57^{+} (arrowheads in F-F‴). (G) Quantification of E‴,F‴. For all experiments *n*=3 embryos for each genotype; error bars indicate s.d.; ***P<0.001. Scale bars: 10 μm.

Development (2014) 141, 2780-2790 doi:10.1242/dev.110155

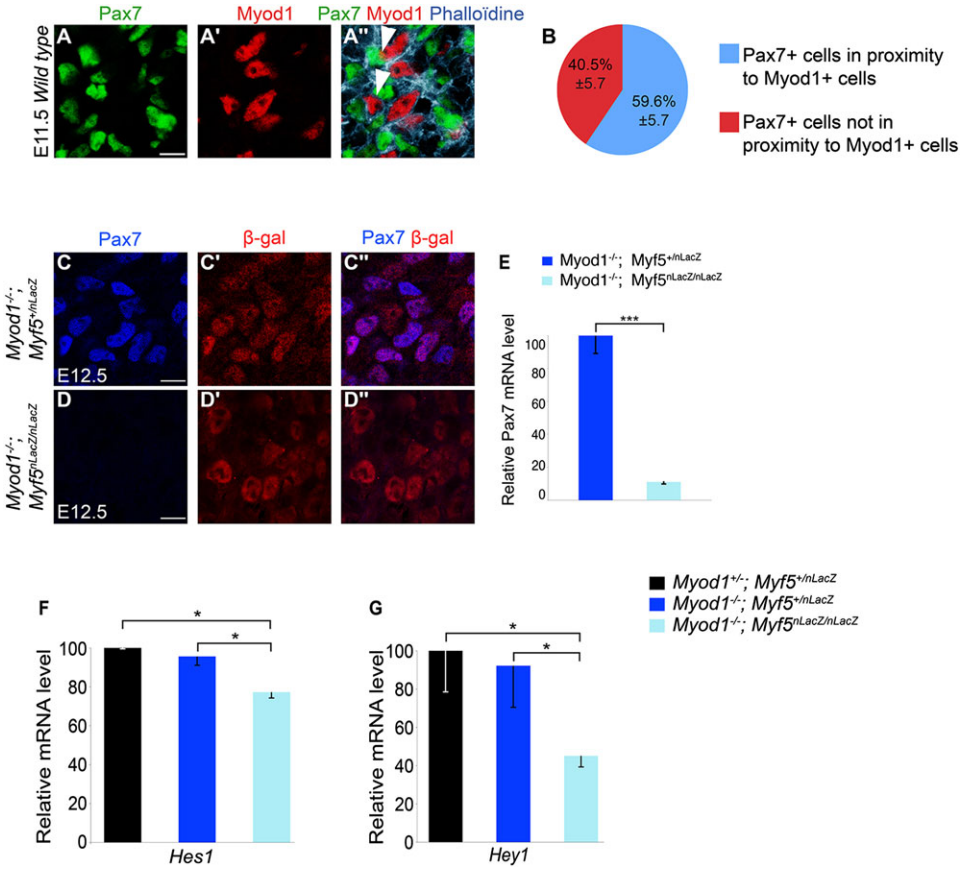

Fig. 4. Close proximity of Pax7$^+$ and Myod1$^+$ cells, with decreased Pax7 and Hes1/Hey1 expression in muscle progenitor cells of the *Myod1; Myf5* double mutant. (A-A″) Co-immunostaining for Pax7 (green) and Myod1 (red), with phalloidin (cyan) to label actin to visualize cell membranes, in wild-type limb muscles at E11.5. (B) Percentage of Pax7$^+$ cells in proximity to Myod1$^+$ cells in limb muscle masses. (C-D″) Co-immunostaining for Pax7 (blue) and β-gal (red) in *Myod1*$^{-/-}$; *Myf5*$^{+/nlacZ}$ (C-C″) and *Myod1*$^{-/-}$; *Myf5*$^{nlacZ/nlacZ}$ (D-D″) embryos at E12.5. (E-G) qRT-PCR for *Pax7* (E), *Hes1* (F) and *Hey1* (G) on E12.5 forelimbs of the genotypes indicated. For all experiments n=3 embryos for each genotype; error bars indicate s.e.m.; *P<0.05, **P<0.01, ***P<0.001. Scale bars: 10 μm.

Notch signaling prevents activation of p57 in muscle progenitor cells

Based on our results (Fig. 4) and previous reports (Georgia et al., 2006), we hypothesized that myoblasts control progenitor cell proliferation by activating the Notch/Hes1/Hey1 pathway, which would then repress p57 expression.

First, to establish whether Notch signaling participates directly in the coordinated control of cell cycle exit and differentiation, we used an *ex vivo* whole limb culture system (Zúñiga et al., 1999). We cultured E11.5 mouse forelimbs for 28 h, with or without 20 μM γ-secretase inhibitor DAPT, an inhibitor of Notch signaling. As expected, we saw decreased expression of the Notch target genes *Hes1* and *Hey1* after DAPT treatment (Fig. 5A). In addition, inhibition of Notch signaling led to reduced numbers of Pax7$^+$ cells (56.8±5.6% in control versus 27.7±7.0% in DAPT-treated limb explants; Fig. 5B′,C′,D), whereas the Myod1$^+$ cell population was increased (62.7±9.0% compared with 32.6±5.3% in control DMSO-treated explants; Fig. 5B″,C″,D), confirming previous reports (Schuster-Gossler et al., 2007; Vasyutina et al., 2007) and the robustness of our *ex vivo* model. Accordingly, we found decreased levels of *Pax7* mRNA and increased levels of *Myod1* mRNA in DAPT-treated samples (Fig. 5A). We next examined whether pharmacological inhibition of Notch signaling induces cell cycle arrest in cultured muscle progenitor cells. We found a 5-fold increase in p57 expression in Pax3$^+$/MRF$^-$ cells in DAPT-treated limb explants compared with controls (Fig. 5E-G).

To confirm these results *in vivo*, we genetically abrogated Notch signaling in progenitor cells by conditionally deleting *Rbpj*. RbpJ is a DNA-binding transcription factor and the major effector of all four Notch receptors (Fortini and Artavanis-Tsakonas, 1994; Jarriault et al., 1995; Kopan and Ilagan, 2009; Schweisguth and Posakony, 1992). We performed a conditional deletion of *Rbpj* in the Pax3 lineage by crossing *Rbpj*$^{flox/flox}$ mice (Han et al., 2002) with a *Pax3*$^{Cre/+}$ allele (Engleka et al., 2005). Ablation of *Rbpj* led to increased myogenic differentiation as previously reported (Vasyutina et al., 2007), with a severe loss of progenitor cells leading to tiny limb muscles at a fetal stage. Strikingly, both p57 and p21 were upregulated in the Pax3$^+$/Myf5$^-$ muscle progenitor cells in the forelimbs of *Rbpj*$^{flox/flox}$; *Pax3*$^{Cre/+}$ mice at E11.5, whereas Pax3 and these CDKIs were rarely co-expressed in such cells in control mice (Fig. 6A-D, see also Fig. 1). To demonstrate that expression of p21 and p57 is associated with growth arrest in these mutants, we analyzed the co-expression of Ki67 with either p57 or p21 in Pax3$^+$ muscle progenitors (Fig. 6E,F) in the forelimbs of *Rbpj*$^{flox/flox}$; *Pax3*$^{Cre/+}$ mice at E11.5. We found a small but significant increase of Pax3$^+$ cells co-expressing p21 or p57 with Ki67 in the mutant embryos; nevertheless, the large majority of the Pax3$^+$/p57$^+$ cells did not express Ki67, as predicted.

Altogether, these results demonstrate that in embryonic muscle progenitor cells Notch signaling antagonizes cell cycle exit by repressing p57 expression.

A *p57* muscle-specific enhancer is directly regulated by Notch signaling and MRFs

To gain insight into the molecular mechanisms of *p57* regulation, we used data generated by a Myod1 ChIP sequencing experiment (Cao et al., 2010) to identify Myod1 binding sites in the vicinity of the *p57* locus. A previous study had predicted that *p57* muscle-specific regulatory elements are located between +35 and +225 kb from the *p57* transcription start site (John et al., 2001). In keeping with this, a high density of Myod1 binding sites was found in a conserved region located +59 kb from *p57*. We isolated an evolutionarily conserved

Development (2014) 141, 2780-2790 doi:10.1242/dev.110155

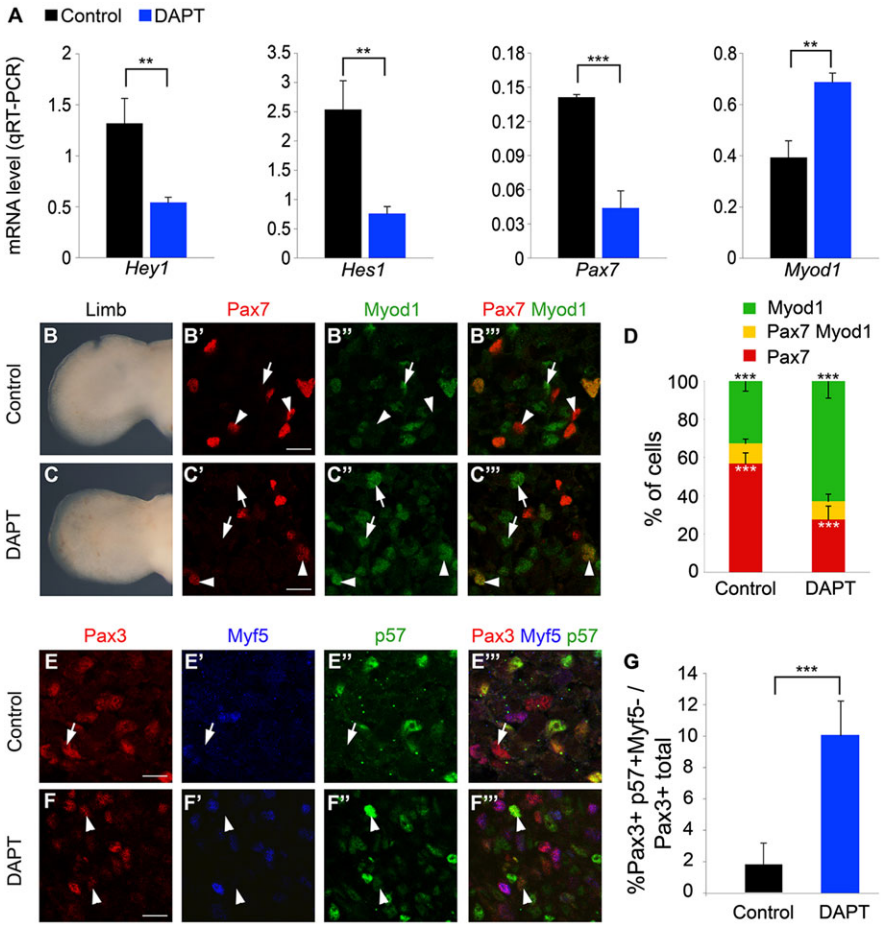

Fig. 5. The Notch pathway prevents activation of p57 in progenitor cells. (A) qRT-PCR for *Hey1*, *Hes1*, *Pax7* and *Myod1* mRNA in control (DMSO-treated) and DAPT-treated *ex vivo* whole limb culture. (B,C) An E11.5 forelimb kept in culture for 28 h treated with DMSO (B) or 20 μM DAPT (C). (B′-B‴,C′-C‴) Co-immunostaining for Pax7 (red) and Myod1 (green) in DMSO-treated (B′-B‴) or 20 μM DAPT-treated (C′-C‴) explants from E11.5 limb muscles. Arrowheads indicate Pax7^{+}/Myod1^{-} cells in B′-B‴ and Pax7^{+}/Myod1^{+} cells in C′-C‴; arrows indicate Myod1^{+}/Pax7^{-} cells. (D) Quantification of B‴,C‴. (E-F‴) Co-immunostaining for Pax3 (red), Myf5 (blue) and p57 (green) in DMSO-treated (E-E‴) or 20 μM DAPT-treated (F-F‴) explants from E11.5 limb muscles. Arrow in E-E‴ indicates a Pax3^{+}/Myf5^{-}/p57^{-} cell. Arrowheads in F-F‴ indicate Pax3^{+}/Myf5^{-}/p57^{+} cells. (G) Quantification of E‴,F‴. For all experiments n=3; error bars indicate s.d.; $^{**}P$<0.01, $^{***}P$<0.001. Scale bars: 10 μm.

686 bp fragment that contains 15 E-boxes, which are binding sites for MRFs, Hey1 and Hes1 (supplementary material Fig. S2).

We first validated this *p57* muscle regulatory element (*p57MRE*) as a functional enhancer *in vivo* by generating transgenic embryos carrying a *p57MRE-tk-nlacZ* construct. Following analysis of *lacZ* expression at E12, we detected robust reporter expression in all myogenic domains (Fig. 7A,A′), with an expression profile that matched that of Myod1. Interestingly, this element is skeletal muscle specific, since no other sites of p57 expression, such as parenchymal organs and intestine (Westbury et al., 2001), were observed. In order to characterize the myogenic cell type that expresses the p57 reporter, we performed immunohistochemical analyses on limb buds from these transgenic embryos. β-Gal^{+} cells co-expressed p57 (Fig. 7B-B″) and Myod1 (Fig. 7C-C″) but not Pax7 (Fig. 7D-D″), defining the cellular specificity of the *p57MRE*.

We next hypothesized that this regulatory element integrates negative regulation by Hes/Hey proteins and positive regulation via direct activation by the MRFs. We performed ChIP experiments on E12.5 wild-type forelimbs and found that both Myod1 and Hes1 were bound *in vivo* to the *p57MRE* fragment (Fig. 8A). To ensure that our assay was specific, and given the lack of known positive controls for Hes1 in the myogenic lineage, we performed ChIP experiments in HEK293 cells transfected with either Hes1 or Myod1 and either wild-type *p57MRE* or containing mutations in the MRF and Hes binding sites (*p57MREΔE-Boxes*). Robust binding was observed for Hes1 (Fig. 8B) and Myod1 (Fig. 8C) on the *p57MRE* and this binding was abrogated on *p57MREΔE-Boxes* (Fig. 8B,C).

Finally, to further establish this interplay between positive and negative regulation, we tested the transcriptional activity of Myod1, Hes1 and Hey1 on *p57MRE-tk-nlacZ* in transient transfection experiments in C2C12 muscle cells. Myod1 enhanced the activation of the *p57MRE* (Fig. 8D), but was not able to activate the *p57MREΔE-Boxes* element. Furthermore, Myod1 transcriptional activation was abolished when exposed to increasing concentrations of Hes1 or Hey1 (Fig. 8D), suggesting that both are able to repress the Myod1-dependent activation of *p57MRE*.

We propose a model in which the integration of Notch and MRF activities at the level of a muscle-specific enhancer of the key cell cycle arrest gene *p57* provides a means to control the equilibrium between progenitor pool amplification and the establishment of definitive functions of skeletal muscle (Fig. 8E).

DISCUSSION

The generation of organs of a defined size requires a balance between proliferation and differentiation. This balance is ensured by regulated cell growth, which prevents prolonged proliferation or premature differentiation, both of which are deleterious for normal development.

During skeletal muscle development and postnatal regeneration, Notch signaling activity is crucial for sustaining stem/progenitor cell self-renewal and its downregulation is required to allow myogenic differentiation. Cell cycle exit was previously thought to be controlled by the differentiation program (Halevy et al., 1995). In this report we show that growth arrest is also negatively regulated by Notch signaling and demonstrate that these two events, despite appearing synchronous, can be uncoupled. In *Myod1*$^{-/-}$ forelimbs, myogenesis is paused between E11.5 and E14.5 (Kablar et al., 1998). Although Myf5 is unable to drive myogenesis and activate *Myog* at these stages,

Development (2014) 141, 2780-2790 doi:10.1242/dev.110155

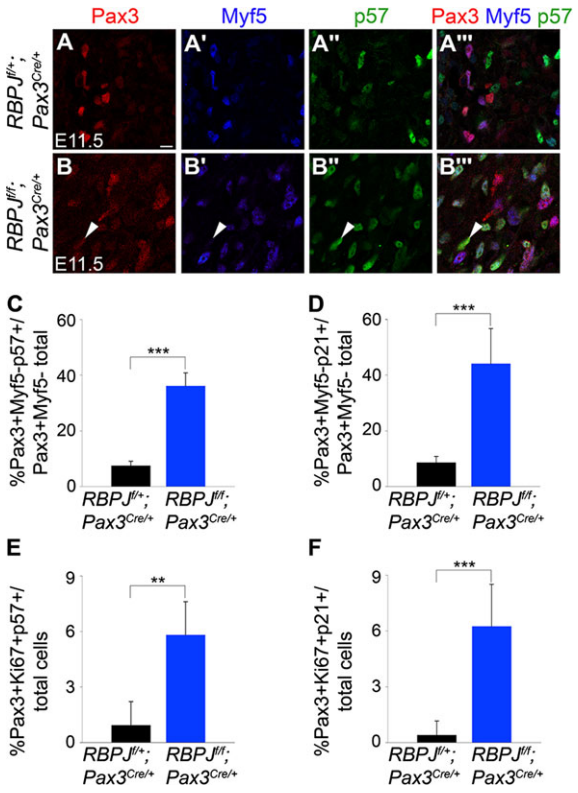

Fig. 6. Conditional ablation of *Rbpj* leads to upregulation of p57 and p21 and to cell cycle arrest in muscle progenitor cells. (A-B‴) Co-immunostaining for Pax3 (red), Myf5 (blue) or p57 (green) in $Rbpj^{flox/+}$; $Pax3^{Cre/+}$ (A-A‴) or $Rbpj^{flox/flox}$; $Pax3^{Cre/+}$ (B-B‴) forelimbs at E11.5. Arrowhead indicates a $Pax3^{+}/Myf5^{-}/p57^{+}$ cell. Scale bars: 10 μm. (C) Quantification of A‴,B‴. (D) Quantification of co-immunostaining for Pax3, Myf5 or p21 in $Rbpj^{flox/+}$; $Pax3^{Cre/+}$ or $Rbpj^{flox/flox}$; $Pax3^{Cre/+}$ forelimbs at E11.5. (E) Quantification of co-immunostaining for Pax3, Ki67 or p57 in $Rbpj^{flox/+}$; $Pax3^{Cre/+}$ or $Rbpj^{flox/flox}$; $Pax3^{Cre/+}$ forelimbs at E11.5. (F) Quantification of co-immunostaining for Pax3, Ki67 or p21 in $Rbpj^{flox/+}$; $Pax3^{Cre/+}$ or $Rbpj^{flox/flox}$; $Pax3^{Cre/+}$ forelimbs at E11.5. For all experiments n=3 embryos for each genotype; error bars indicate s.d.; $^{**}P<0.01$, $^{***}P<0.001$.

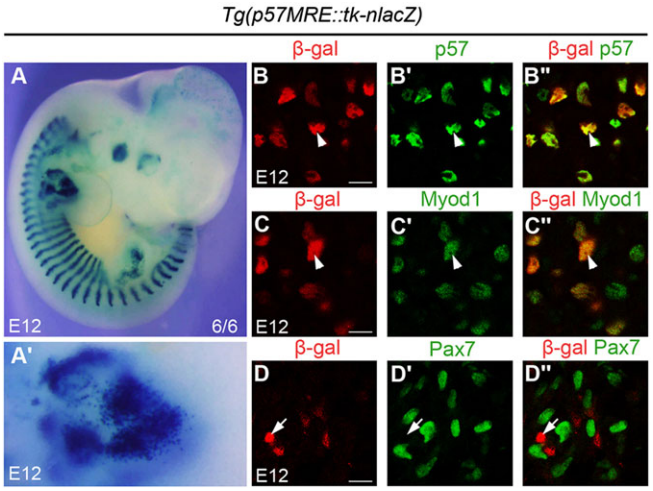

Fig. 7. Expression of a *p57* muscle regulatory enhancer (MRE) in transgenic mice. (A,A′) X-Gal staining on a transgenic *p57MRE-tk-nlacZ* embryo. A′ is a higher magnification of the forelimb region from A. (B-D″) Co-immunostaining for β-gal (B,C,D,B″,C″,D″, red), p57 (B′,B″, green), Myod1 (C′, C″, green) and Pax7 (D′,D″, green). Arrowheads indicate $\beta\text{-gal}^{+}/p57^{+}$ (B-B″) and $\beta\text{-gal}^{+}/Myod1^{+}$ cells (C-C″); arrows indicate $\beta\text{-gal}^{+}/Pax7^{-}$ cells. Scale bars: 10 μm.

we found that $Myf5^{+}/Pax3/7^{-}$ cells expressed p57 at E12.5 and this did not prevent them from resuming differentiation at E14.5 (presumably when Mrf4 is activated). Given our finding that Myod1 directly binds and activates *p57* via the *p57MRE* sequence, we believe that Myf5 operates in the same way, thereby providing a functional uncoupling between MRF myogenic activity and growth arrest. Moreover, our study and those of others indicate that cell cycle exit occurs at the transition from committed progenitors to determined myoblasts (Fig. 1A). Consistently, we found that committed progenitor cells express Pax3/7 and Myf5, but neither p21 nor p57. This finding is consistent with the robust repressive activity exerted by Hes/Hey on MRF-mediated transactivation (Fig. 8D). The cycling status of committed progenitor cells is therefore of interest. A recent study showed that whereas the undifferentiated resident progenitor cells that express Pax7 represent a slow-cycling pool, the $Pax3/7^{+}/Myf5^{+}$ committed progenitors correspond to a fast-cycling population (Picard and Marcelle, 2013). Our study did not address the subtle cell cycle regulation of these progenitor cell populations and future studies will be required to determine whether these changes in cell proliferation are linked to Myf5 or to other, as yet unidentified, factors.

The model of coordinated regulation that we propose, with a single *p57* element integrating positive (from the MRFs) and negative (from Hes/Hey) regulatory information suggests that the interplay between Notch repression of *p57MRE* in Pax3/7 progenitors and its activation by MRFs in myoblasts is crucial for growth arrest. The molecular mechanisms regulating Notch signaling components during myogenesis are not fully characterized. It was reported that during *Xenopus* development Dll1 expression is regulated by Myod1 (Wittenberger et al., 1999) and that Myod1 expression is repressed by Hairy-1 (Umbhauer et al., 2001). It is unclear if these regulatory mechanisms also exist in amniotes, but our data are compatible with such a sequence of events. Resolving the precise molecular interplay between Pax gene expression, cell growth arrest, MRF regulation and the switch in Notch signaling will require additional investigations.

Notch signaling plays a key role in maintaining the homeostasis of muscle stem cells in the adult (Bjornson et al., 2012; Carlson et al., 2008; Fukada et al., 2011; Kitamoto and Hanaoka, 2010; Mourikis et al., 2012b) and in colonization of the satellite cell niche (Bröhl et al., 2012). In particular, Notch controls quiescence of muscle satellite cells (Bjornson et al., 2012; Mourikis et al., 2012b). This activity might be mediated by Hey1 and HeyL, which are required in the adult lineage for satellite cell homeostasis and skeletal muscle regeneration (Fukada et al., 2011). Conditional deletion of *Rbpj* in $Pax7^{+}$ satellite cells led to spontaneous differentiation without activation or division of the cells (Bjornson et al., 2012; Mourikis et al., 2012b). Strikingly, *RbpJ* ablation does not lead to an immediate and complete differentiation or growth arrest in the $Pax3^{+}$ population during embryonic development, leaving open the possibility that other pathways are involved. For instance, Notch activity on adult muscle stem cells is counteracted by TGFβ signaling (Carlson and Conboy, 2007). This is mediated through the activation of phosphorylated Smad3, which can directly bind and activate the *p15* (*Cdkn2b*), *p16* (*Cdkn2a*), *p21* and *p27* promoters (Carlson and Conboy, 2007) to favor muscle stem cell differentiation. Interestingly, during chicken myogenesis myostatin, which is a member of the TGFβ family, has also been implicated in the control of terminal differentiation through indirect activation of p21 (Manceau et al., 2008).

In addition to driving cell cycle exit during adult myogenesis, p57 has also been implicated in stabilization of Myod1 through direct association in C2C12 cells, resulting in enhanced myogenesis

Development (2014) 141, 2780-2790 doi:10.1242/dev.110155

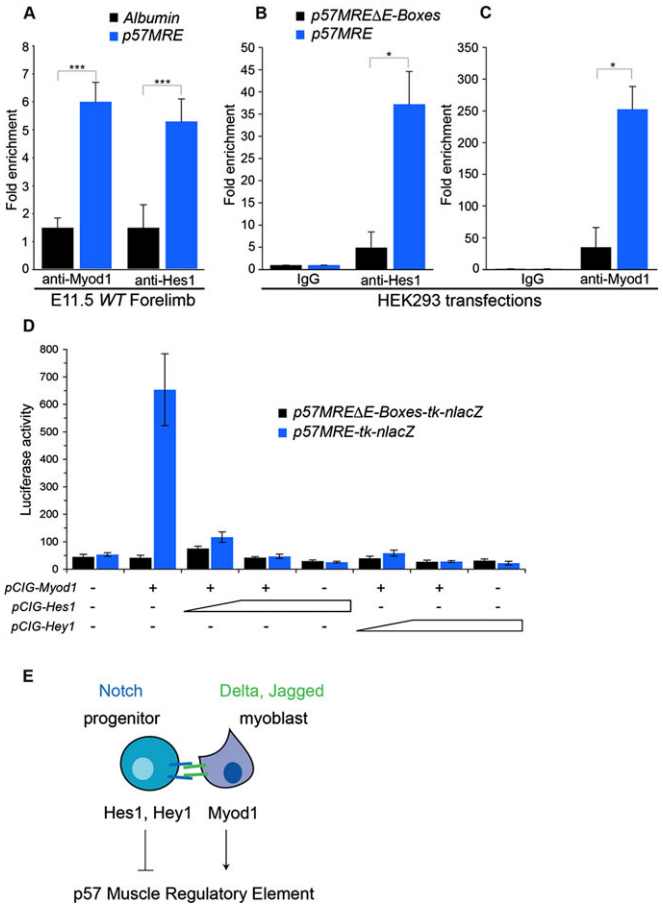

Fig. 8. Direct regulation of the *p57MRE* by Myod1 and Hes1/Hey1. (A) Chromatin immunoprecipitation followed by qPCR on wild-type forelimbs at E11.5. *p57MRE* is enriched when precipitated with anti-Myod1 or anti-Hes1 antibodies compared with an albumin gene control. (B,C) Validation of antibody ChIP capacities on transfected HEK293 cells: enrichment with anti-Hes1 (B) or anti-Myod1 (C) is obtained with the *p57MRE* compared with the construct in which all putative E-boxes have been mutated (*p57MREΔE-Boxes*). n=3; error bars indicate s.e.m.; *P<0.05, ***P<0.001. (D) Transactivation assay on C2C12 cells with the expression plasmids and reporters indicated (n≥3). (E) Schematic representation of the regulation of cell cycle exit during myogenesis. In muscle progenitors, Notch downstream effectors Hes1 and Hey1 repress the activation of p57 to allow the amplification of the pool, while in the neighboring myoblasts that express the Notch ligands, Myod1 directly activates p57 expression.

(Reynaud et al., 2000). A similar mechanism has also been identified in zebrafish, in which p57 cooperates with Myod1 to drive the differentiation of several early zebrafish muscle fiber types (Osborn et al., 2010). It is not known if this positive-feedback loop also operates during early murine skeletal muscle formation. One could propose that, although the initiation of myogenic differentiation and growth arrest are independent, these events may synergize subsequently, for instance to enhance Myod1 activity and reinforce terminal differentiation. In zebrafish, p57 cooperates with Myod1 to drive *myog* expression (Osborn et al., 2010); nevertheless, proliferating Myod1^{+} and Myog^{+} cells are detected in *p21*$^{-/-}$*; p57*$^{+/-}$ mice (see Fig. 2A-C; our unpublished observations). Interestingly, expression of Mef2c is impaired in these mutant mice (Zhang et al., 1999), raising the possibility that p57 may also be involved in terminal differentiation in murine myogenesis during development.

In our study, the expression of p57 is firmly linked to an absence of cell cycle progression, since we observe no overlap between p57 (or p21) expression and Ki67 (Fig. 1C-F) under normal conditions. Strikingly, a small but significant proportion of the Pax3^{+}/p21^{+} or Pax3^{+}/p57^{+} cells are Ki67^{+} in the *Pax3*$^{Cre/+}$*; Rbpj*$^{flox/flox}$ mutant context. Although this might correspond to a transitory state due to the differentiation phenotype of these mutant embryos, one cannot exclude the possibility that Notch might also be involved in both cell cycle progression and cell cycle arrest via a complex regulatory loop.

p57 expression has been reported previously in adult satellite cells (Fukada et al., 2007), but the precise timing of expression has yet to be characterized. The identification of *p57MRE* through a Myod1 ChIP-seq screen performed in C2C12 cells raises the possibility that this element is reused in adult muscle cells *in vivo*. Owing to the perinatal death of *p57* mutant mice, the role of p57 in postnatal myogenesis cannot be studied *in vivo*. *p21*-deficient mice display normal muscle development but impaired skeletal muscle regeneration (Hawke et al., 2003). Given the functional overlap between p21 and p57 during development, it would be interesting to evaluate the combined role of these two proteins in postnatal satellite cell homeostasis and skeletal muscle regeneration.

The recent identification of the role of p57 in the maintenance of quiescent hematopoietic (Matsumoto et al., 2011), neural (Furutachi et al., 2013) and lung (Zacharek et al., 2011) stem cells indicates that p57, along with other CDKIs, is important for stem cell function. Whether such a regulatory mechanism for CDKI expression is redeployed in other systems remains to be investigated. For example, Notch has been implicated in maintaining progenitor cell proliferation in intestinal stem cells (Riccio et al., 2008), in adult neural stem cells (Imayoshi et al., 2010) and in Rathke's pouch progenitors of the pituitary (Monahan et al., 2009) and, indeed, one proposed mechanism is the repression of CDKIs by the product of the Notch target gene *Hes1* (Monahan et al., 2009; Riccio et al., 2008). Unfortunately, these studies did not define which cells provide the ligands. Nevertheless, our data and the role of Notch and Hes1 in intestinal stem cells, neural stem cells and pituitary progenitor cells might suggest a general mechanism whereby the expansion of the progenitor cell population is regulated via modulation of CDKI genes. Such a regulatory mechanism could be used as a safeguard to prevent tumor formation by progenitor/stem cells, for instance when differentiation is impaired. It is also tempting to speculate that fine-tuning of this system could also be used for intrinsically regulating organ size.

MATERIALS AND METHODS

Mouse lines and harvest of embryos

Myf5$^{+/nlacZ}$, *Myod1*$^{+/-}$, *p21*$^{+/-}$, *p57*$^{+/-m}$ (*p57* is an imprinted gene; we indicate maternal origin of the allele by a superscript *m*), *Pax3*$^{Cre/+}$and *Rbpj*$^{flox/+}$ lines have been described previously (Deng et al., 1995; Engleka et al., 2005; Han et al., 2002; Rudnicki et al., 1992; Yan et al., 1997). For explant and ChIP experiments, C57BL/6J embryos were used (Janvier). For timed pregnancies, the morning when a vaginal plug was found was defined as embryonic day (E) 0.5. All experiments were performed on three independent embryos for each genotype.

Immunohistochemistry and X-Gal staining

Embryos and forelimbs were harvested and fixed for 2 h and for 20 min, respectively, in PBS/4% paraformaldehyde at 4°C. Cryoprotection was performed by equilibration in PBS/15% sucrose overnight at 4°C. Frozen sections were permeabilized in PBS/0.1% Triton X-100, blocked in PBS/2% bovine serum albumin for 1 h at room temperature, then immunolabeled with primary antibodies overnight at 4°C. For X-Gal staining, embryos were collected in PBS, fixed 20 min in PBS/4% paraformaldehyde at room temperature and incubated in X-Gal solution (Life Technologies) overnight at 37°C on a rotary shaker.

Development (2014) 141, 2780-2790 doi:10.1242/dev.110155

Antibodies

The following antibodies were used: mouse anti-β-galactosidase 1/500 (Promega, Z378), mouse anti-Myod1 5.8A 1/200 (DAKO, M3512), mouse anti-Myog F5D 1/200 (DSHB, F5D), mouse anti-p21 1/100 (BD Pharmingen, 556431), mouse anti-p57 1/100 (Santa Cruz, sc-56341), mouse anti-Pax7-c 1/100 (DSHB, Pax7-c), mouse anti-Pax3-c 1/100 (DSHB, Pax3-c), rabbit anti-β-galactosidase 1/1000 (Life Technologies, A-11132), rabbit anti-Myod1 M318 1/100 (Santa Cruz, sc-760), rabbit anti-Myf5 C20 1/500 (Santa Cruz, sc-302), rabbit anti-p57 H91 1/100 (Santa Cruz, sc-8298), rabbit anti-phospho-histone 3 Ser10 1/1000 (Cell Signaling, 9701), goat anti-p57 M20 1/50 (Santa Cruz, sc-1039) and goat anti-Pax3 1/100 (Santa Cruz, sc-34916). Phalloidin (649 nm) 1/500 was from Life Technologies. Secondary antibodies were coupled to Alexa Fluor 488 1/250, 594 1/1000 (Life Technologies) or 649 1/250 (Jackson ImmunoResearch).

Explant and cell culture

Forelimbs from E11.5 wild-type embryos were cultured in 12-well plates in BGJb medium (Life Technologies), without serum, with 200 µg/ml ascorbic acid (Sigma) and 100 µg/ml penicillin/streptomycin (Life Technologies). For Notch inhibition, forelimbs were immediately treated with 20 µM N-[N-(3,5-difluorophenacetyl)-L-alanyl]-S-phenylglycine t-butyl ester (DAPT; Sigma) or DMSO carrier (Sigma) for 28 h. Treated and control forelimbs originating from the same embryo were compared in each experiment. C2C12 and HEK293 cells were cultured in proliferating medium comprising DMEM with 10% fetal bovine serum and 100 µg/ml penicillin/streptomycin (Life Technologies).

Plasmid construct for transgenesis

The *p57* muscle regulatory element (*p57MRE*) (chr7: 150,587,238-150,587,924) was isolated by PCR. For cloning convenience, *Eag*I restriction sites were added to the forward and reverse primers used for amplification: forward, 5′-AAGCGGCCGCACCCAGTTTGCCCAGTGTAG-3′; reverse, 5′-AACGGCCGCCAGGTAAAGACACCCCAGA-3′. After *Eag*I digestion, the 686 bp fragment was cloned, respecting its genomic orientation, into the *Not*I site of p*tk*nlacZ(−) plasmid (Hadchouel et al., 2000) (*tk*, thymidine kinase). The *p57MRE-tk-nlacZ* fragment was released by *Sac*II/*Xho*I digestion and gel purified using the Nucleobond plasmid purification kit (Macherey-Nagel) before injection into pronuclei.

β-galactosidase assay

Hey1, *Hes1* cDNAs [gifts from S. Tajbakhsh (Pasteur Institute, Paris, France) and R. Kageyama (Institute for Virus Research, Kyoto University, Japan), respectively] and *Myod1* cDNA were cloned into the pCIG plasmid (Megason and McMahon, 2002). C2C12 cells were transfected with a total of 1.2 µg DNA using Lipofectamine LTX plus reagent (Life Technologies). Fixed concentrations of *p57MRE-tk-nlacZ* or *p57MREΔE-Boxes-tk-nlacZ* (0.6 µg), or pCIG-Myod1 (0.15 µg) were used. For pCIG-Hes1 and pCIG-Hey1, 0.15 or 0.3 µg was used. Each sample was co-transfected with 0.1 µg *tk*-Luciferase reporter for sample-to-sample normalization. Forty-eight hours after transfection, the cells were collected and the proteins were extracted and assayed for β-galactosidase activity (β-Gal assay Kit K1455-01, Life Technologies) and for luciferase activity (Luciferase assay system E1500, Promega) to normalize transfection variation. Measurements were made at least in triplicate and expressed as the mean (with s.e.m.) of the amount of β-galactosidase substrate (ONPG) hydrolyzed.

Reverse transcription and quantitative PCR (qPCR)

Total RNA from embryo forelimbs was extracted using the RNeasy mini kit (Qiagen). 1 µg RNA was used to generate cDNA using the Superscript II reverse transcriptase kit (Life Technologies). qPCR was performed using the Lightcycler 480 SYBR Green mix (Roche) and Lightcycler 480 II (Roche). RT-qPCR on FACS-isolated cells was performed using the Superscript III cell direct cDNA kit (Life Technologies). qPCR results are expressed as relative ratios of target cDNA to *Hprt*. The following oligonucleotides were used (5′-3′; forward and reverse): *Hes1*, ACACCGGACAAACCAAAGAC and AATGCCGGGAGCTATCTTTC; *Hey1*, CACCTGAAAATGCTGCACAC and ATGCTCAGATAACGGGCAAC; *Myod1*, GGCTACGACACCGCCTACTA and GAGATGCGCTCCACTATGCT; *Pax7*, AGGCCTTCGAGAGGACCCAC and CTGAACCAGACCTGGACGCG.

Chromatin immunoprecipitation (ChIP)

Myod1 ChIP-seq has been described in detail (Cao et al., 2010). For qPCR ChIP experiments, forelimbs from E11.5 embryos were frozen in liquid nitrogen and processed for ChIP according to the manufacturer's protocol (Active motif). 150 µg of chromatin was used for each experiment. 2 g of a rabbit anti-Myod1 M318 (Santa Cruz, sc-760) and 2 g of a goat anti-Hes1 (Santa Cruz, sc-13844) were used; 2 g of a rabbit anti-β-galactosidase (Life Technologies, A-11132) or 2 g of a goat anti-β-galactosidase (Santa Cruz, sc-19119) were used as the corresponding IgG negative control. The precipitated and input chromatins were analyzed by qPCR using *p57MRE* primers (forward, 5′-ATGTGCACACAG-CTCAGAGG-3′; reverse, 5′-GGAAGGATGGAGGGCTTTAC-3′) with albumin primers as negative control (forward, 5′-GGGACGAGATGGT-ACTTTGTG-3′; reverse, 5′-GATCAGTCCAAACTTCTTTCTG-3′).

For ChIP on transfected cells, HEK293 cells were transfected with a total of 7.5 µg DNA using FuGENE6 (Promega). A mutant *p57MRE* sequence, *p57MREΔE-Boxes*, was synthesized (GeneART) in which all putative E-boxes were mutated according to Iso et al. (2003). Fixed concentrations of *p57MRE-tk-nlacZ* or *p57MREΔE-Boxes-tk-nlacZ* (4 µg) were used together with either pCig-Myod1 or pCig-Hes1 (2 µg). After 48 h, chromatin was extracted and processed as above; 100 µg chromatin was used for each experiment. For ChIP, 2 µg normal mouse (Santa Cruz) and goat (Santa Cruz) IgG were used for negative controls for the Myod1 and Hes1 antibodies mentioned above. Results are expressed as fold change compared with IgG control.

Statistical test

Immunostainings were performed on at least three embryos of each genotype. Quantifications were performed using images of all muscle masses present in an embryo section (6-8 sections per slide, 2-3 frames per masse). All qPCR experiments were performed at least three times independently. Cell counting and qPCR results were analyzed by Mann–Whitney or Student's *t*-test. In Fig. 3D and Fig. 4F,G, quantifications were analyzed by ANOVA. In Fig. 5D, quantifications were analyzed by a chi-square test.

Acknowledgements

We are grateful to Drs Sonia Alonso-Martin, Edgar Gomes, Revital Rattenbach, Vanessa Ribes and David Sassoon for their assistance with this work and writing. We thank Catherine Bodin for histology. We also acknowledge the animal care facilities at UPMC and CDTA, and Catherine Blanc and Bénédicte Hoareau from the Flow Cytometry Core CyPS. We are grateful to Drs Tapscott and Fukada for sharing unpublished data, Drs Tajbakhsh and Kageyama for *Hey1* and *Hes1* cDNAs and F. Langa Vives for transgenic services.

Competing interests

The authors declare no competing financial interests.

Author contributions

A.Z. designed and performed experiments, analyzed data and wrote the paper. S.H. and F.A. designed and performed experiments, analyzed data and edited the manuscript. T.C., D.M. and P.M. designed and performed experiments, analyzed data. Z.Y. and Y.C. provided data on Myod1 ChIP-seq. D.B. provided *Rbpj* mutant embryos. C.B. analyzed data and edited the manuscript. F.R. oversaw the entire project, designed experiments, analyzed data and wrote the paper.

Funding

This work is supported by funding to F.R. from Institut National de la Santé et de la Recherche Médicale (INSERM) Avenir Program, Association Française contre les Myopathies (AFM), Association Institut de Myologie (AIM), Labex REVIVE, the European Union Seventh Framework Program in the project ENDOSTEM [grant # 241440], Ligue Nationale Contre le Cancer (LNCC), Association pour la Recherche contre le Cancer (ARC), Fondation pour la Recherche Médicale (FRM) [FDT20130928236], Institut National du Cancer

(INCa), Agence Nationale pour la Recherche (ANR) grant Epimuscle [grant # 11 BSV2 017 02] and Agence Nationale pour la Recherche Maladies Rares (MRAR) grant Pax3 in WS [grant # 06-MRAR-032]. This work was also funded by the German Research Foundation (DFG) [grant GK1631], French-German University (UFA-DFH) [grant CDFA-06-11] and the AFM as part of the MyoGrad International Research Training Group for Myology.

Supplementary material

Supplementary material available online at
http://dev.biologists.org/lookup/suppl/doi:10.1242/dev.110155/-/DC1

References

Artavanis-Tsakonas, S. and Muskavitch, M. A. T. (2010). Notch: the past, the present, and the future. *Curr. Top. Dev. Biol.* **92**, 1-29.

Ben-Yair, R. and Kalcheim, C. (2005). Lineage analysis of the avian dermomyotome sheet reveals the existence of single cells with both dermal and muscle progenitor fates. *Development* **132**, 689-701.

Besson, A., Dowdy, S. F. and Roberts, J. M. (2008). CDK inhibitors: cell cycle regulators and beyond. *Dev. Cell* **14**, 159-169.

Birchmeier, C. and Brohmann, H. (2000). Genes that control the development of migrating muscle precursor cells. *Curr. Opin. Cell Biol.* **12**, 725-730.

Bjornson, C. R. R., Cheung, T. H., Liu, L., Tripathi, P. V., Steeper, K. M. and Rando, T. A. (2012). Notch signaling is necessary to maintain quiescence in adult muscle stem cells. *Stem Cells* **30**, 232-242.

Borggrefe, T. and Liefke, R. (2012). Fine-tuning of the intracellular canonical Notch signaling pathway. *Cell Cycle* **11**, 264-276.

Bröhl, D., Vasyutina, E., Czajkowski, M. T., Griger, J., Rassek, C., Rahn, H.-P., Purfürst, B., Wende, H. and Birchmeier, C. (2012). Colonization of the satellite cell niche by skeletal muscle progenitor cells depends on Notch signals. *Dev. Cell* **23**, 469-481.

Buas, M. F. and Kadesch, T. (2010). Regulation of skeletal myogenesis by Notch. *Exp. Cell Res.* **316**, 3028-3033.

Buas, M. F., Kabak, S. and Kadesch, T. (2010). The Notch effector Hey1 associates with myogenic target genes to repress myogenesis. *J. Biol. Chem.* **285**, 1249-1258.

Buckingham, M. and Relaix, F. (2007). The role of Pax genes in the development of tissues and organs: Pax3 and Pax7 regulate muscle progenitor cell functions. *Annu. Rev. Cell Dev. Biol.* **23**, 645-673.

Cao, Y., Yao, Z., Sarkar, D., Lawrence, M., Sanchez, G. J., Parker, M. H., MacQuarrie, K. L., Davison, J., Morgan, M. T., Ruzzo, W. L. et al. (2010). Genome-wide MyoD binding in skeletal muscle cells: a potential for broad cellular reprogramming. *Dev. Cell* **18**, 662-674.

Carlson, M. E. and Conboy, I. M. (2007). Regulating the Notch pathway in embryonic, adult and old stem cells. *Curr. Opin. Pharmacol.* **7**, 303-309.

Carlson, M. E., Hsu, M. and Conboy, I. M. (2008). Imbalance between pSmad3 and Notch induces CDK inhibitors in old muscle stem cells. *Nature* **454**, 528-532.

Cherrett, C., Furutani-Seiki, M. and Bagby, S. (2012). The Hippo pathway: key interaction and catalytic domains in organ growth control, stem cell self-renewal and tissue regeneration. *Essays Biochem.* **53**, 111-127.

Cook, M. and Tyers, M. (2007). Size control goes global. *Curr. Opin. Biotechnol.* **18**, 341-350.

Delfini, M. C., Hirsinger, E., Pourquie, O. and Duprez, D. (2000). Delta 1-activated notch inhibits muscle differentiation without affecting Myf5 and Pax3 expression in chick limb myogenesis. *Development* **127**, 5213-5224.

Deng, C., Zhang, P., Harper, J. W., Elledge, S. J. and Leder, P. (1995). Mice lacking p21CIP1/WAF1 undergo normal development, but are defective in G1 checkpoint control. *Cell* **82**, 675-684.

Engleka, K. A., Gitler, A. D., Zhang, M., Zhou, D. D., High, F. A. and Epstein, J. A. (2005). Insertion of Cre into the Pax3 locus creates a new allele of Splotch and identifies unexpected Pax3 derivatives. *Dev. Biol.* **280**, 396-406.

Fortini, M. E. and Artavanis-Tsakonas, S. (1994). The suppressor of hairless protein participates in notch receptor signaling. *Cell* **79**, 273-282.

Fukada, S.-i., Uezumi, A., Ikemoto, M., Masuda, S., Segawa, M., Tanimura, N., Yamamoto, H., Miyagoe-Suzuki, Y. and Takeda, S. (2007). Molecular signature of quiescent satellite cells in adult skeletal muscle. *Stem Cells* **25**, 2448-2459.

Fukada, S.-i., Yamaguchi, M., Kokubo, H., Ogawa, R., Uezumi, A., Yoneda, T., Matev, M. M., Motohashi, N., Ito, T., Zolkiewska, A. et al. (2011). Hesr1 and Hesr3 are essential to generate undifferentiated quiescent satellite cells and to maintain satellite cell numbers. *Development* **138**, 4609-4619.

Furutachi, S., Matsumoto, A., Nakayama, K. I. and Gotoh, Y. (2013). p57 controls adult neural stem cell quiescence and modulates the pace of lifelong neurogenesis. *EMBO J.* **32**, 970-981.

Georgia, S., Soliz, R., Li, M., Zhang, P. and Bhushan, A. (2006). p57 and Hes1 coordinate cell cycle exit with self-renewal of pancreatic progenitors. *Dev. Biol.* **298**, 22-31.

Gros, J., Manceau, M., Thomé, V. and Marcelle, C. (2005). A common somitic origin for embryonic muscle progenitors and satellite cells. *Nature* **435**, 954-958.

Hadchouel, J., Tajbakhsh, S., Primig, M., Chang, T. H., Daubas, P., Rocancourt, D. and Buckingham, M. (2000). Modular long-range regulation of Myf5 reveals unexpected heterogeneity between skeletal muscles in the mouse embryo. *Development* **127**, 4455-4467.

Halevy, O., Novitch, B. G., Spicer, D. B., Skapek, S. X., Rhee, J., Hannon, G. J., Beach, D. and Lassar, A. B. (1995). Correlation of terminal cell cycle arrest of skeletal muscle with induction of p21 by MyoD. *Science* **267**, 1018-1021.

Han, H., Tanigaki, K., Yamamoto, N., Kuroda, K., Yoshimoto, M., Nakahata, T., Ikuta, K. and Honjo, T. (2002). Inducible gene knockout of transcription factor recombination signal binding protein-J reveals its essential role in T versus B lineage decision. *Int. Immunol.* **14**, 637-645.

Hawke, T. J., Meeson, A. P., Jiang, N., Graham, S., Hutcheson, K., DiMaio, J. M. and Garry, D. J. (2003). p21 is essential for normal myogenic progenitor cell function in regenerating skeletal muscle. *Am. J. Physiol. Cell Physiol.* **285**, C1019-C1027.

Hirsinger, E., Malapert, P., Dubrulle, J., Delfini, M. C., Duprez, D., Henrique, D., Ish-Horowicz, D. and Pourquie, O. (2001). Notch signalling acts in postmitotic avian myogenic cells to control MyoD activation. *Development* **128**, 107-116.

Imayoshi, I., Sakamoto, M., Yamaguchi, M., Mori, K. and Kageyama, R. (2010). Essential roles of Notch signaling in maintenance of neural stem cells in developing and adult brains. *J. Neurosci.* **30**, 3489-3498.

Iso, T., Kedes, L. and Hamamori, Y. (2003). HES and HERP families: multiple effectors of the Notch signaling pathway. *J. Cell Physiol.* **194**, 237-255.

Jarriault, S., Brou, C., Logeat, F., Schroeter, E. H., Kopan, R. and Israel, A. (1995). Signalling downstream of activated mammalian Notch. *Nature* **377**, 355-358.

John, R. M., Ainscough, J. F.-X., Barton, S. C. and Surani, M. A. (2001). Distant cis-elements regulate imprinted expression of the mouse p57(Kip2) (Cdkn1c) gene: implications for the human disorder, Beckwith–Wiedemann syndrome. *Hum. Mol. Genet.* **10**, 1601-1609.

Kablar, B., Krastel, K., Ying, C., Asakura, A., Tapscott, S. J. and Rudnicki, M. A. (1997). MyoD and Myf-5 differentially regulate the development of limb versus trunk skeletal muscle. *Development* **124**, 4729-4738.

Kablar, B., Asakura, A., Krastel, K., Ying, C., May, L. L., Goldhamer, D. J. and Rudnicki, M. A. (1998). MyoD and Myf-5 define the specification of musculature of distinct embryonic origin. *Biochem. Cell Biol.* **76**, 1079-1091.

Kassar-Duchossoy, L., Giacone, E., Gayraud-Morel, B., Jory, A., Gomès, D. and Tajbakhsh, S. (2005). Pax3/Pax7 mark a novel population of primitive myogenic cells during development. *Genes Dev.* **19**, 1426-1431.

Kitamoto, T. and Hanaoka, K. (2010). Notch3 null mutation in mice causes muscle hyperplasia by repetitive muscle regeneration. *Stem Cells* **28**, 2205-2216.

Kopan, R. and Ilagan, M. X. G. (2009). The canonical Notch signaling pathway: unfolding the activation mechanism. *Cell* **137**, 216-233.

Lagha, M., Kormish, J. D., Rocancourt, D., Manceau, M., Epstein, J. A., Zaret, K. S., Relaix, F. and Buckingham, M. E. (2008). Pax3 regulation of FGF signaling affects the progression of embryonic progenitor cells into the myogenic program. *Genes Dev.* **22**, 1828-1837.

Lepper, C. and Fan, C.-M. (2010). Inducible lineage tracing of Pax7-descendant cells reveals embryonic origin of adult satellite cells. *Genesis* **48**, 424-436.

Manceau, M., Gros, J., Savage, K., Thome, V., McPherron, A., Paterson, B. and Marcelle, C. (2008). Myostatin promotes the terminal differentiation of embryonic muscle progenitors. *Genes Dev.* **22**, 668-681.

Matsumoto, A., Takeishi, S., Kanie, T., Susaki, E., Onoyama, I., Tateishi, Y., Nakayama, K. and Nakayama, K. I. (2011). p57 is required for quiescence and maintenance of adult hematopoietic stem cells. *Cell Stem Cell* **9**, 262-271.

Megason, S. and McMahon, A. (2002). A mitogen gradient of dorsal midline Wnts organizes growth in the CNS. *Development* **129**, 2087-2098.

Monahan, P., Rybak, S. and Raetzman, L. T. (2009). The notch target gene HES1 regulates cell cycle inhibitor expression in the developing pituitary. *Endocrinology* **150**, 4386-4394.

Mourikis, P. and Tajbakhsh, S. (2014). Distinct contextual roles for Notch signalling in skeletal muscle stem cells. *BMC Dev. Biol.* **14**, 2.

Mourikis, P., Gopalakrishnan, S., Sambasivan, R. and Tajbakhsh, S. (2012a). Cell-autonomous Notch activity maintains the temporal specification potential of skeletal muscle stem cells. *Development* **139**, 4536-4548.

Mourikis, P., Sambasivan, R., Castel, D., Rocheteau, P., Bizzarro, V. and Tajbakhsh, S. (2012b). A critical requirement for notch signaling in maintenance of the quiescent skeletal muscle stem cell state. *Stem Cells* **30**, 243-252.

Murphy, M. and Kardon, G. (2011). Origin of vertebrate limb muscle: the role of progenitor and myoblast populations. *Curr. Top. Dev. Biol.* **96**, 1-32.

Osborn, D. P. S., Li, K., Hinits, Y. and Hughes, S. M. (2010). Cdkn1c drives muscle differentiation through a positive feedback loop with Myod. *Dev. Biol.* **350**, 464-475.

Picard, C. A. and Marcelle, C. (2013). Two distinct muscle progenitor populations coexist throughout amniote development. *Dev. Biol.* **373**, 141-148.

Relaix, F., Rocancourt, D., Mansouri, A. and Buckingham, M. (2005). A Pax3/Pax7-dependent population of skeletal muscle progenitor cells. *Nature* **435**, 948-953.

Development (2014) 141, 2780-2790 doi:10.1242/dev.110155

Relaix, F., Montarras, D., Zaffran, S., Gayraud-Morel, B., Rocancourt, D., Tajbakhsh, S., Mansouri, A., Cumano, A. and Buckingham, M. (2006). Pax3 and Pax7 have distinct and overlapping functions in adult muscle progenitor cells. *J. Cell Biol.* **172**, 91-102.

Reynaud, E. G., Leibovitch, M. P., Tintignac, L. A. J., Pelpel, K., Guillier, M. and Leibovitch, S. A. (2000). Stabilization of MyoD by direct binding to p57(Kip2). *J. Biol. Chem.* **275**, 18767-18776.

Riccio, O., van Gijn, M. E., Bezdek, A. C., Pellegrinet, L., van Es, J. H., Zimber-Strobl, U., Strobl, L. J., Honjo, T., Clevers, H. and Radtke, F. (2008). Loss of intestinal crypt progenitor cells owing to inactivation of both Notch1 and Notch2 is accompanied by derepression of CDK inhibitors p27Kip1 and p57Kip2. *EMBO Rep.* **9**, 377-383.

Rios, A. C., Serralbo, O., Salgado, D. and Marcelle, C. (2011). Neural crest regulates myogenesis through the transient activation of NOTCH. *Nature* **473**, 532-535.

Rudnicki, M. A., Braun, T., Hinuma, S. and Jaenisch, R. (1992). Inactivation of MyoD in mice leads to up-regulation of the myogenic HLH gene Myf-5 and results in apparently normal muscle development. *Cell* **71**, 383-390.

Rudnicki, M. A., Schnegelsberg, P. N. J., Stead, R. H., Braun, T., Arnold, H.-H. and Jaenisch, R. (1993). MyoD or Myf-5 is required for the formation of skeletal muscle. *Cell* **75**, 1351-1359.

Schienda, J., Engleka, K. A., Jun, S., Hansen, M. S., Epstein, J. A., Tabin, C. J., Kunkel, L. M. and Kardon, G. (2006). Somitic origin of limb muscle satellite and side population cells. *Proc. Natl. Acad. Sci. U.S.A.* **103**, 945-950.

Schuster-Gossler, K., Cordes, R. and Gossler, A. (2007). Premature myogenic differentiation and depletion of progenitor cells cause severe muscle hypotrophy in Delta1 mutants. *Proc. Natl. Acad. Sci. U.S.A.* **104**, 537-542.

Schweisguth, F. and Posakony, J. W. (1992). Suppressor of Hairless, the Drosophila homolog of the mouse recombination signal-binding protein gene, controls sensory organ cell fates. *Cell* **69**, 1199-1212.

Tajbakhsh, S., Rocancourt, D., Cossu, G. and Buckingham, M. (1997). Redefining the genetic hierarchies controlling skeletal myogenesis: Pax-3 and Myf-5 act upstream of MyoD. *Cell* **89**, 127-138.

Tumaneng, K., Russell, R. C. and Guan, K.-L. (2012). Organ size control by Hippo and TOR pathways. *Curr. Biol.* **22**, R368-R379.

Umbhauer, M., Boucaut, J.-C. and Shi, D.-L. (2001). Repression of XMyoD expression and myogenesis by Xhairy-1 in Xenopus early embryo. *Mech. Dev.* **109**, 61-68.

Vasyutina, E., Lenhard, D. C., Wende, H., Erdmann, B., Epstein, J. A. and Birchmeier, C. (2007). RBP-J (Rbpsuh) is essential to maintain muscle progenitor cells and to generate satellite cells. *Proc. Natl. Acad. Sci. U.S.A.* **104**, 4443-4448.

Westbury, J., Watkins, M., Ferguson-Smith, A. C. and Smith, J. (2001). Dynamic temporal and spatial regulation of the cdk inhibitor p57(kip2) during embryo morphogenesis. *Mech. Dev.* **109**, 83-89.

Wittenberger, T., Steinbach, O. C., Authaler, A., Kopan, R. and Rupp, R. A. W. (1999). MyoD stimulates delta-1 transcription and triggers notch signaling in the Xenopus gastrula. *EMBO J.* **18**, 1915-1922.

Yan, Y., Frisen, J., Lee, M. H., Massague, J. and Barbacid, M. (1997). Ablation of the CDK inhibitor p57Kip2 results in increased apoptosis and delayed differentiation during mouse development. *Genes Dev.* **11**, 973-983.

Zacharek, S. J., Fillmore, C. M., Lau, A. N., Gludish, D. W., Chou, A., Ho, J. W., Zamponi, R., Gazit, R., Bock, C., Jäger, N. et al. (2011). Lung stem cell self-renewal relies on BMI1-dependent control of expression at imprinted loci. *Cell Stem Cell* **9**, 272-281.

Zhang, P., Wong, C., Liu, D., Finegold, M., Harper, J. W. and Elledge, S. J. (1999). p21(CIP1) and p57(KIP2) control muscle differentiation at the myogenin step. *Genes Dev.* **13**, 213-224.

Zúñiga, A., Haramis, A.-P. G., McMahon, A. P. and Zeller, R. (1999). Signal relay by BMP antagonism controls the SHH/FGF4 feedback loop in vertebrate limb buds. *Nature* **401**, 598-602.

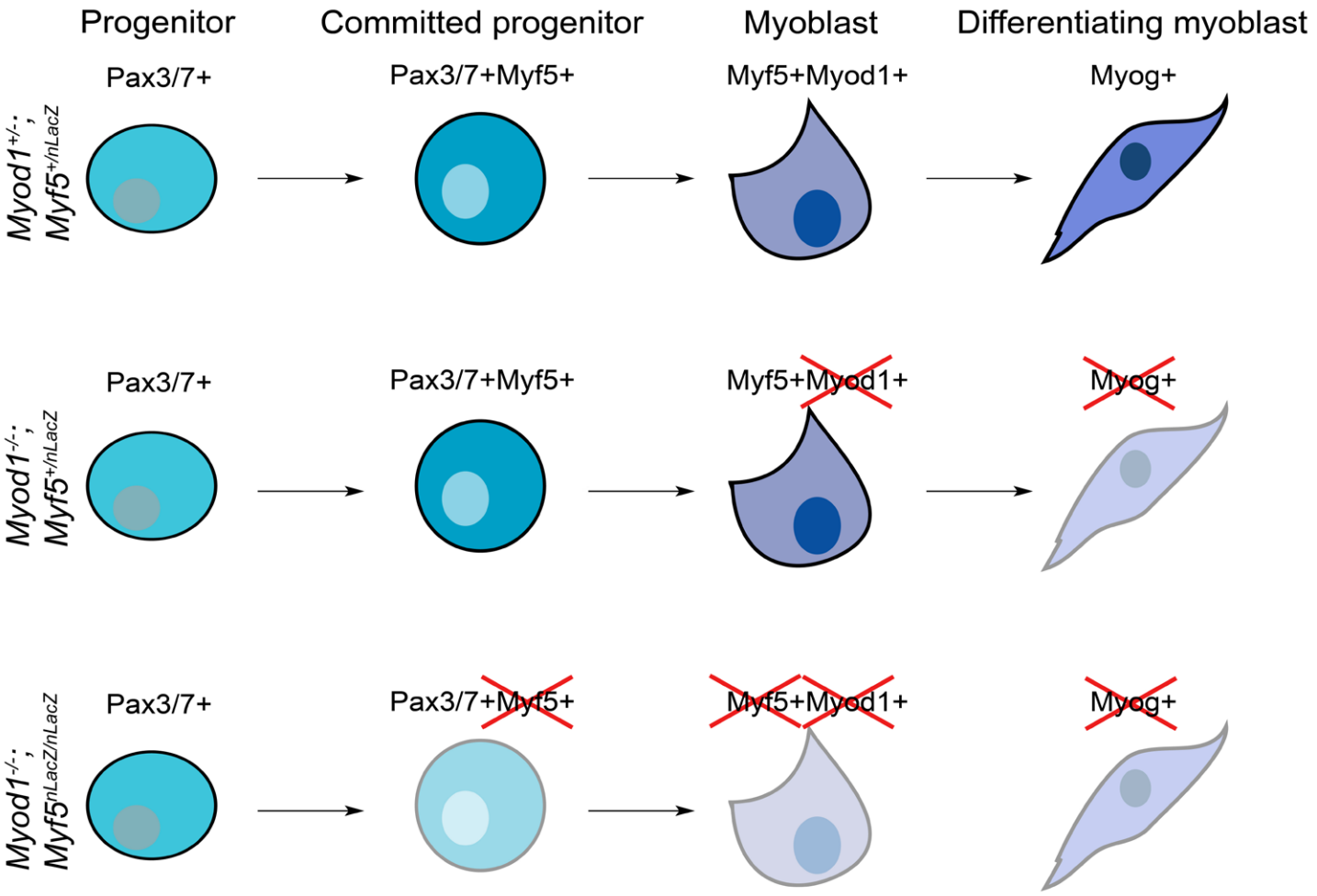

Supplementary Figure 1. Stages of myogenic differentiation impairment using the different *Myod1: Myf5* mutant compounds.

Supplementary Figure 2. Genomic sequence of p57MRE enhancer cloned in p57MRE-tk-nlacZ reporter.

Putative E-boxes are underlined with grey background. To generate *p57MREΔE-Boxes* mutant construct, every CANNTG motif has been replaced by CGNNAG.

PART II SECOND PAPER – IN REVISION

Pax3 and Pax7 play essential safeguard functions against Dioxin-induced birth defects

AUTHORS:

Antoine Zalc[1,2,3], **Revital Rattenbach**[1,2,3] **and Frédéric Relaix**[1,2,3*]

AFFILIATIONS:

1 UPMC Paris 06, U 974, F-75013, Paris, France

2 INSERM, Avenir team, Pitié-Salpétrière, F-75013, Paris, France

3 Institut de Myologie, F-75013, Paris, France

[*]Correspondence to Frédéric Relaix

Email: frelaix@gmail.com

Tel: (+33) 1 40 77 81 25

Fax: (+33) 1 53 60 08 02

SUMMARY:

Exposure to environmental teratogenic pollutant leads to severe birth defects. However, the biological events underlying these developmental abnormalities remain undefined. Here we report a molecular link between an environmental stress response pathway and key developmental genes during craniofacial development. Strikingly, mutant mice with impaired *Pax3/7* function display facial clefts analogous to those induced by 2,3,7,8-tetrachlorodibenzo-p-dioxin (TCDD) exposure. We show that these defects are associated with an up-regulation of the signaling pathway mediated by the Aryl hydrocarbon Receptor (AhR), the receptor to TCDD. Exposure of Pax3-deficient embryos to TCDD drives facial mesenchymal cells out of the cell cycle through the up-regulation of *p21* expression. Accordingly, inhibiting AhR activity rescues the cycling status of these cells and the facial closure of *Pax3/7* mutant embryos. Together, our findings demonstrate that the regulation of AhR signaling by Pax3/7 is required to protect against TCDD/AhR-mediated teratogenesis during craniofacial development.

HIGHLIGHTS:

Pax3/ Pax7; Dioxin; Teratogenesis; Craniofacial development

INTRODUCTION:

Exposure to environmental teratogenic pollutants is a major threat to the development of the embryo. In humans, 10-15% of the world population display congenital anomalies due to the exposure of pregnant women to environmental teratogenic pollutants (Gilbert-Barness, 2010). Among these developmental defects, craniofacial malformations represent a third of the defects observed (Dixon et al., 2011). It is assumed that most teratogens interfere with genetic programs regulating developmental processes (Dixon et al., 2011). For instance, exposure to TCDD, a potent teratogen (Yonemoto, 2000), during pregnancy can lead to cleft lip and/or palate as revealed after the Vietnam war and the Seveso disaster (Pratt et al., 1984; Yonemoto, 2000). However, the etiology of these TCDD-induced craniofacial defects remains unclear.

In vertebrates, the face mainly derives from the Neural Crest (NC), a transient structure that arises at the dorsal tip of the closing neural tube (Knecht and Bronner-Fraser, 2002). Cells from the neuro-epithelium undergo an epithelial-mesenchymal transition prior to migrating to various regions of the embryo. Depending on their location along the anterior-posterior axis, these cells populate different structures and give rise to a large variety of cell types (Le Douarin et al., 2004). In the most rostral part of the embryo, Cranial Neural Crest Cells (CNCC) migrate ventro-laterally to colonize facial prominences (Kulesa et al., 2004) where they participate in the formation of craniofacial bones, cartilage, connective tissue, neurons and glial cells (Dupin and Sommer, 2012; Knecht and Bronner-Fraser, 2002; Noden and Trainor, 2005). Craniofacial malformations are generally linked to anomalies in CNCC development, part of them being due to teratogen exposure. Despite the identification of gene regulatory networks underpinning CNCC development (Betancur et al., 2010), little is known about how environmental pollutants interfere with these genetic networks during craniofacial development.

Central to these gene regulatory networks are genes coding for the paralogous paired-box transcription factors Pax3 and Pax7. These transcriptional regulators play a key role in the

integration of inputs during NC induction and in controlling the specification of NC derivatives (Basch et al., 2006; Betancur et al., 2010; Minchin and Hughes, 2008; Monsoro-Burq et al., 2005; Sato et al., 2005). Although *Pax3* and *Pax7* function during early NC development is highly conserved among vertebrates (Betancur et al., 2010), their function during craniofacial formation is not understood.

Here we show that mutant mice with impaired *Pax3* and *Pax7* function display severe facial morphogenesis defects. Using a genome-wide analysis, we identified the AhR signaling pathway as specifically up-regulated during craniofacial development of *Pax3/7* deficient mice, leading to precocious growth arrest in the cranial neural crest lineage. We further show that blocking AhR signaling rescues facial growth and closure in mice with impaired *Pax3/7* function, while exposure to TCDD leads to similar defects in embryos with reduced Pax3/7 activity. Our data therefore demonstrate that important developmental genes play a key function to preserve the developing face from AhR/TCDD-mediated teratogenesis.

RESULTS:

Essential role of Pax3 and Pax7 during craniofacial development

Using mouse genetic models, we first examined the dynamics of *Pax3* and *Pax7* expression profiles during craniofacial development. As in other vertebrates (Nelms and Labosky, 2010), *Pax3* expression is detected within the anterior neural plate border prior to neural tube closure at embryonic day (E)8.5 (Figure S1A). *Pax3* expression co-localizes with the NCC marker Sox9 (Nelms and Labosky, 2010) (Figure S1B) and persists in several CNCC contributed tissues such as the frontonasal mass (FNM) and the medial and lateral nasal processes (MNP and LNP; Figure S1C). Of note, *Pax7* expression is restricted within the *Pax3* domain; first observed in the FNM and the LNP, and later maintained in the LNP at E10.5 and E11.5 (Figures S1C and S1D).

We next analyzed facial morphology in two distinct models with altered Pax3 and Pax7 functions (Figure 1A). While Pax3 is required for NC induction in the sacral, trunk and vagal regions (Li et al., 1999; Van Ho et al., 2011), cranial NC induction occurs in our genetic models. However, a strong frontonasal dysplasia phenotype with a frontal cleft was observed in both $Pax3^{GFP/GFP}$; $Pax7^{LacZ/LacZ}$ double mutant and $Pax3^{Pax3\text{-}ERD/GFP}$ mutant embryos at E13.5. In the latter, cells in the Pax3 positive lineage expressed a potent dominant negative form of Pax3 (*Pax3-ERD*) which alters both Pax3 and Pax7 function (Bajard et al., 2006) (Figure 1A and Figure S1E). This phenotype contrasted with the medial fusion of the nasal processes observed in wild-type embryos and other compound *Pax3*/*Pax7* mutants (Figure S1E), supporting the notion that both proteins are required for facial development in mice. In *Pax3; Pax7* double mutant embryos, the phenotype was more severe than in $Pax3^{Pax3\text{-}ERD/GFP}$ embryos where the medial and lateral nasal swellings were rudimentary and failed to fuse, whereas the maxillary and mandibular prominences were less affected (Figure 1A). Hence, in E13.5 $Pax3^{Pax3\text{-}ERD/GFP}$ embryos nasal processes developed correctly but did not fuse together leading to a frontonasal

cleft (Figure 1A). Skeleton staining of E17.5 *Pax3*$^{Pax3\text{-}ERD/GFP}$ fetuses showed that the premaxilla bones and the palate bones were primarily affected (Figure S2A). Histological analysis at E13.5 revealed that the nasal septum of both genetic models was severely diminished and bifurcated (Figure 1A). Together, these data demonstrate that Pax3 and Pax7 proteins are required during morphogenesis of the face.

Since CNCC reached the facial prominences and early specification is not affected in our genetic models (Figure 1B and Figures S2B-S2D), we next assessed whether craniofacial defects observed in *Pax3*$^{Pax3\text{-}ERD/GFP}$ and *Pax3; Pax7* double mutant embryos were due to increased cell death of CNCC. Strikingly, we observed an increase of the proportion of apoptotic CNCC when both *Pax3* and *Pax7* were missing (Figure 1C). Furthermore, we were unable to detect any cell co-expressing GFP (Pax3) and β-galactosidase (Pax7) at E10.5 or E11.5 (data not shown), suggesting that the Pax3^{+}/Pax7^{+} cell population is lost in double mutant embryos, precluding further analysis in this genetic model.

In contrast, no increase in cell death was observed in the CNCC of *Pax3*$^{Pax3\text{-}ERD/GFP}$ embryos (Figure 1C). In addition, expression of NC specification markers, AP2α and Sox9 (Nelms and Labosky, 2010), was not impaired in *Pax3*$^{Pax3\text{-}ERD/GFP}$ compared with *Pax3*$^{GFP/+}$ embryos at E9.5 (Figures S2B-S2D). We next tested whether the frontal cleft face phenotype in *Pax3*$^{Pax3\text{-}ERD/GFP}$ could be a consequence of tissue misspecification. We observed impaired expression of *Msx1* in the MNP and LNP (Figure 1D) associated with reduced expression of *Pax7* and *Pax9* in the LNP (Figure S2E), suggesting a proliferation defect in the nasal processes of *Pax3*$^{Pax3\text{-}ERD/GFP}$ embryos (Bhatt et al., 2013; Houzelstein et al., 1997; Nelms and Labosky, 2010). In addition, *Dlx2* expression in nasal pits was barely detectable (Figure 1D) implying patterning defects of the nasal process in *Pax3*$^{Pax3\text{-}ERD/GFP}$ embryos (McKeown et al., 2005; Thomas et al., 2000) as confirmed by skeletal staining (Figure S2A). Collectively, these data demonstrate that

Pax3 and Pax7 are essential in regulating morphogenesis, survival, patterning and specification of the frontonasal structures during facial development.

Up-regulation of AhR signaling pathway expression is associated with impaired Pax3/7 function

In order to gain insight into the molecular mechanism by which Pax3 and Pax7 regulate craniofacial development, we performed transcriptome analysis of the facial prominences from $Pax3^{Pax3\text{-}ERD/GFP}$ embryos compared with $Pax3^{GFP/+}$ embryos at E11.5 (Figure 2A). We identified 76 up-regulated (Table S1) and 44 down-regulated (Table S2) genes in cells with impaired *Pax3/7* function compared to the control (Figure 2A). Genes implicated in the AhR signaling pathway were up-regulated. Transcripts levels for *AhR* and its direct target genes, including *Aldh1a3*, a gene coding for an enzyme involved in retinoic acid production and nasal process development (Dupe et al., 2003; Hankinson, 1995) and *p21* (*Cdkn1a*, cyclin-dependent kinase inhibitor 1A), a mediator of cell cycle exit and growth arrest (Besson et al., 2008; Pang et al., 2008), were higher in $Pax3^{Pax3\text{-}ERD/GFP}$ CNCC (Figure 2B). Specific up-regulation of AhR protein was observed in the LNP using immunostaining (Figure 2C) confirming a role for Pax3 and Pax7 in regulating its expression in this tissue. *In situ* hybridization for *Aldh1a3* transcripts revealed that its expression in the nasal process was shifted to more anterior and medial positions within this tissue (Figure 2D). Thus, reinforcing the notion that AhR signaling activity domain is increased when the function of Pax3/7 is impaired. Furthermore, in the frontonasal ectoderm, *Aldh1a3* regulates *Fgf8* expression, a mediator of CNCC growth in the underlying mesenchyme (Dupe et al., 2003; Hu et al., 2003). Consistent with this, expression of *Fgf8* was lost in the nasal epithelium of $Pax3^{Pax3\text{-}ERD/GFP}$ embryos (Figure 2D), suggesting a decreased proliferation of the underlying mesenchymal CNCC that could explain the smaller nasal prominence phenotype. In addition, CNCC isolated from facial prominences exposed to TCDD, an AhR ligand (Fernandez-Salguero et al., 1996), specifically induced *Aldh1a3* and *p21*

expression (Figures 2E and 2F) demonstrating the responsiveness of AhR signaling to environmental pollutants in this tissue.

Impaired Pax3/7 function leads to CNCC growth arrest and frontal cleft face

Migration of the CNCC takes place in *Pax3*$^{Pax3\text{-}ERD/GFP}$ embryos (Figure 1B), since the number of GFP^{+} cells was essentially the same in *Pax3*$^{Pax3\text{-}ERD/GFP}$ and control embryos at E9.5 (Figure S3). However from E10.5 onwards the number of GFP^{+} cells within the frontonasal region was decreased by 30% in *Pax3*$^{Pax3\text{-}ERD/GFP}$ embryos compare to control (Figure S3). Moreover, by E11.5 the proportion of GFP^{+} FACS-sorted over the total number of cells was severely diminished, by 34%, in *Pax3*$^{Pax3\text{-}ERD/GFP}$ embryos compared to the control (Figures 3A and 3B). This decrease in the Pax3^{+}/Pax7^{+} population correlated with a decline in the number of cycling cells in this population (Figures 3C and 3E) which explains the overall reduction of nasal process size, leading to a frontal cleft face.

As we found a marked up-regulation of the growth arrest gene *p21* in *Pax3*$^{Pax3\text{-}ERD/GFP}$ embryos, we hypothesized that *p21* induction might lead to growth failure of the LNP, resulting in the frontal cleft face phenotype. Immunostaining for p21 and Pax7 demonstrated that 43% of the cells had exited the cell cycle in *Pax3*$^{Pax3\text{-}ERD/GFP}$ embryos, while only 26% of the cells normally did so at E10.5 (Figures 3D and 3F). This increased cell cycle exit was also seen at E11.5 (Figure 3F). In addition, this growth arrest was associated with a decrease in the CNCC progenitor pool, as shown by analysis of AP2α and Sox9 expression (Figures 3G and 3H). Together these results suggest that during facial prominences growth, up-regulation of AhR signaling pathway in CNCC drives these cells out of the cell cycle. Hence, this precocious cell cycle exit generates reduced craniofacial prominences unable to a fuse together, resulting in the formation of a frontal cleft face.

Pax3/7-mediated regulation of AhR signaling allows CNCC growth during craniofacial development

In order to demonstrate that up-regulation of AhR signaling leads to the morphological defects observed in $Pax3^{Pax3\text{-}ERD/GFP}$ embryos, we treated control and mutant embryos with α-naphtoflavone, an AhR antagonist (Jang et al., 2007). Treatments were performed by daily gavages administrated from E8.5 to E11.5. Strikingly, a significant proportion (12 out of 29) of treated $Pax3^{Pax3\text{-}ERD/GFP}$ embryos exhibited a rescue of the frontal cleft face at E13.5 (Figure 4A). Histological analysis of the rescued embryos revealed that the nasal septum was fused in its medial part (Figure 4A). In addition, following inhibition of AhR signaling with α-naphtoflavone, the number of cycling $Pax3^{+}/Pax7^{+}$ cells in both control and mutant embryos reached a similar level as in the DMSO-treated $Pax3^{GFP/+}$ control embryos (Figure 4B and data not shown). Hence, inhibition of AhR signaling in $Pax3^{Pax3\text{-}ERD/GFP}$ embryos was sufficient to rescue the proportion of proliferating cells in the $Pax3^{+}/Pax7^{+}$ population. To demonstrate that the rescue of the number of cycling CNCC was due to the inhibition of AhR signaling, we quantified the expression of *p21* in these embryos. As anticipated, in half of α-naphtoflavone treated $Pax3^{Pax3\text{-}ERD/GFP}$ embryos the expression level of *p21* within the facial prominences reached similar levels compared to that observed in $Pax3^{GFP/+}$ embryos (Figure 4C). This demonstrates that the specific inhibition of AhR signaling was sufficient to rescue the number of cycling CNCC in the facial prominences of these embryos.

Altogether our results demonstrate a novel function for Pax3 and Pax7 during facial morphogenesis where they act by regulating CNCC growth through the action of AhR signaling.

To further establish the link between *Pax3/7* function and AhR signaling during craniofacial development, we speculated that they act by restricting the input of AhR signaling to specific locations in the facial prominences. We therefore hypothesized that reducing Pax3/7 activity in

embryos exposed to TCDD should lead to facial defects. Accordingly, we used TCDD to stimulate AhR signaling (Fernandez-Salguero et al., 1996) in a *Pax3*-null context. To this end, we intercrossed $Pax3^{GFP/+}$ mice and treated the pregnant females with TCDD. Remarkably, while none of the TCDD-treated $Pax3^{GFP/+}$ control embryos presented any craniofacial defects, 57% of the TCDD-treated $Pax3^{GFP/GFP}$ mutant embryos displayed a frontal cleft face phenotype (Figure 4D). This phenotype is reminiscent to the one observed in $Pax3^{Pax3\text{-}ERD/GFP}$ embryos (Figure 1A). Furthermore, *p21* expression was significantly up-regulated in embryos exposed to TCDD (Figure S4A), demonstrating that up-regulation of AhR signaling was sufficient to generate craniofacial defects.

Collectively, our results reveal an unexpected safeguard function for Pax3/7 during face morphogenesis whereby they restrict AhR signaling input in order to allow the correct growth and maintenance of CNCC during craniofacial development.

DISCUSSION:

TCDD, and derived compounds such as Polychlorodibenzo-p-dioxines (PCDDs) and Polychlorodibenzofurane (PCDFs), are highly toxic persistent chemicals released into the environment as unintentional by-products of incomplete combustion of fossil fuels and wood, and during the incineration of municipal and industrial wastes. In humans, most of the exposure occurs through food, mainly meat and dairy products, fish and shellfish. The developing fetus is especially sensitive to TCDD exposure. It is therefore important to monitor the *in vivo* cellular response to TCDD during development in order to understand and prevent the molecular and cellular response following exposure to dioxins.

AhR signaling has acquired different functions during evolution, including the ability to bind TCDD in order to control pollution-induced teratogenesis. We show here that during morphogenesis of the face, Pax3 and Pax7 regulate the environmental stress response pathway mediated by AhR signaling. Restriction of AhR signaling by Pax3 and Pax7 highlights a key function for this pathway in controlling CNCC proliferation during craniofacial development. Strikingly, inhibition of AhR signaling is sufficient to rescue the frontal cleft face induced by its up-regulation in embryos with impaired Pax3/7 activity. Other aspects of *Pax3/7* mutant phenotypes are not rescued (Relaix et al., 2005), suggesting a tissue specificity of this environmental stress pathway during development. In addition, in our genetic models, despite the absence of *Pax3/7* or the impairment of their function, we observed normal NC induction and migration in the facial prominences of the embryo (Figure 1B). This suggests a divergent function for this transcription factors between trunk and craniofacial development, possibly due to the later appearance of the craniofacial component during evolution.

Importantly, TCDD-mediated activation of AhR signaling in a *Pax3* null context is sufficient to trigger craniofacial defects, arguing for a tight regulatory interaction between Pax3/7 function and AhR signaling to control growth of facial prominences. Altogether, our results

demonstrate a previously unknown function for *Pax3* and *Pax7* during facial morphogenesis and growth where they act by restricting the input of AhR signaling to prevent TCDD-induced birth defects.

EXPERIMENTAL PROCEDURES:

Mutant mice for Pax3 and Pax7 and reagents

The mutant alleles for *Pax3* (*Pax3*^{nLacZ}, *Pax3*^{GFP} and *Pax3*$^{Pax3\text{-}ERD}$) and for *Pax7* (*Pax7*^{LacZ}) have been described previously *(Bajard et al., 2006; Mansouri et al., 1996; Relaix et al., 2003; Relaix et al., 2005)*. Of note, the *Pax3*$^{Pax3\text{-}ERD}$ allele is a conditional one that drives the expression of the dominant negative form of Pax3 (Pax3-ERD) composed of the Pax3 DNA binding domain fused to the engrailed repressor domain (ERD) upon activation of a Cre recombinase. In this study, the Cre was driven by the zygote specific *PGK* enhancer *(Lallemand et al., 1998)*. α-naphtoflavone (Sigma-Aldrich) was dissolved in DMSO then diluted in 1% carboxymethylcellulose (Sigma-Aldrich). α-naphtoflavone (7.5mg/kg/day) was then administered daily, orally to pregnant female mice from E8.5 until E11.5. TCDD dissolved in toluene (Sigma-Aldrich) was diluted in Corn Oil (Sigma-Aldrich). TCDD (4µg/kg/day) was then injected intra-peritoneally, to pregnant female mice from E8.5 until E11.5.

Immunofluorescence and quantification

Mouse embryos from timed pregnant females were fixed by immersion in 4% paraformaldehyde/PBS for 45min to 2hrs at 4°C. Fixed embryos were cryoprotected by equilibration in 30% sucrose/PBS, cryosectioned and processed for immunostaining as described in (Relaix et al., 2005). The following primary antibodies were used: rabbit anti-AP2α (Santa-Cruz, 1:200), rabbit anti-Cleaved-Caspase-3 (Cell Signaling, 1:100), mouse anti-Pax7 (Developmental Studies Hybridoma Bank, 1:100), rabbit anti-Phospho-Histone-3 (Millipore, 1:500), rabbit anti-p21 (ProteinTech, 1:50), and goat anti-Sox9 (R&D Systems, 1:100). Secondary antibodies DyLight 649 donkey anti-mouse IgG (H+L), DyLight 649 donkey anti-rabbit IgG (H+L) and DyLight 649 goat anti-rabbit IgG (H+L) were purchased from

Jackson Immuno Research and Alexa 594 goat anti-mouse IgG (H+L), Alexa 594 donkey anti-goat IgG (H+L) and Alexa 594 goat anti-rabbit IgG (H+L) from LifeTechnologies. Analysis was carried out using a Leica TCS SPE confocal microscope and images processed with Adobe Photoshop CS4 software (Adobe Systems). Cells were counted using ImageJ (version 1.46; National Institutes of Health, Bethesda, Maryland, USA) and Cell Counter plugin (Kurt De Vos, University of Sheffield, Academic Neurology) and were used to calculate the percentage of one cell population against another. Mean ± standard deviation was given. The single (*), double (**) and triple (***) asterisks represent P-values $P<0.05$, $P<0.005$ and $P<0.0001$ respectively by the Mann-Whitney non-parametric statistical test. All experiments have been performed on at least 3 independent embryos for each condition.

Histology, X-Gal staining, skeletal preparation and mRNA in situ hybridization

For histology, sections of embryos prepared as for immunofluorescence were stained with Hematoxylin and Eosin (Vandenberg and Sassoon, 2009). X-Gal staining and whole mount *in situ* hybridization were performed as previously reported (Van Ho et al., 2011). Staining of bones and cartilages of whole E17.5 embryos was performed as previously described (Depew et al., 2002). For *in situ* hybridization, probes against the following mRNAs were used: *Dlx2* (Genbank Acc: BC094317), *Fgf8* (kindly provided by Martin G.), *Msx1* (Genbank Acc: BC016426), *Pax9* (Genbank Acc: BC005794). Analysis was carried out using a Leica MZ16 F stereomicroscope. Images were processed with Adobe Photoshop CS4 software (Adobe Systems). Analyses were performed on $n\geq3$ embryos.

FACS sorting, cell culture and TCDD treatment

For FACS-sorting, CNCC were isolated from faces of E11.5 embryos initially incubated in digestion buffer [DMEM (LifeTechnologies), 0.1% Trypsin and 0.1% Collagenase D (Roche)] and purified via FACS Aria II based on gating of the GFP signal.

For TCDD treatment, CNCC were isolated from faces of E10.5 embryos, incubated in digestion buffer and purified using cell strainers (100µm then 40µm, BD Falcon) to obtain a single cell preparation. CNCC were then cultured in DMEM/F12 (1:1) medium for 24h with TCDD (100nM) or carrier in a collagen-plated dish.

RNA extraction, Microarray and RT-qPCR

RNA was extracted directly from dissected facial prominences or from FACS-sorted GFP^+ cells from facial prominences using NucleoSpin RNA II Extract kit (Macherey-Nagel) and the quality assessed with a Nanodrop ND-1000 (Thermo Scientific). cDNA was synthesized using the Transcriptor First Strand cDNA Synthesis kit (Roche).

Microarrays were performed using Affimetrix GeneChip MOE130 2.0 (PartnerChip) chips containing 45000 oligonucleotide probes (25 mers) covering the totality of the 30000 genes of the mouse genome. Briefly, two-cycle cDNA synthesis was performed using 100ng of total RNA. cDNA was then hybridized to GeneChip Mouse Genome Array. Microarray analysis was performed using GeneChip Operating Software 1.4. For statistical analysis, data from three biological replicates of each genotype were averaged then normalized using the Affymetrix Mas5.0 algorithm. Statistical analysis was performed using BioConductor software (http://www.bioconductor.org/). Gene expression comparison between $Pax3^{Pax3\text{-}ERD/GFP}$ and $Pax3^{GFP/+}$ samples was performed using a statistical Student's t-test on normalized data.

RT-qPCR reactions were carried out in triplicate using the LightCycler 480 System (Roche). The expression of each gene was normalized to that of *Gapdh* transcripts. Results are given as mean ± standard deviation. The single (*), double (**) and triple (***) asterisks represent the

P-values P<0.05, P<0.005 and P<0.0001 respectively for Student's unpaired t-tests. In Fig.4C, α–naphtoflavone treated *Pax3*$^{Pax3\text{-}ERD/GFP}$ embryos can be statistically segregated into two populations using a Ki^2 test. We compared the expression value for a given gene obtained in each α–naphtoflavone treated *Pax3*$^{Pax3\text{-}ERD/GFP}$ embryo to the mean of the expression values for all the DMSO treated *Pax3*$^{GFP/+}$ embryos (control set). If there were significant differences between these two values, the embryo was classified into the population described as responsive to the α–naphtoflavone treatment, if not the embryo was associated with the non-responsive population. In Figure S4, the same analysis was performed to statistically segregate TCDD treated *Pax3*$^{GFP/GFP}$ embryos into the responsive and non-responsive populations.

The following oligonucleotides were used:

AhR: (fwd) TTCCAGGTTCTCAGGCATTC; (rev) TGGGAGCTACAGGAATCCAC

Aldh1a3: (fwd) GCAGCAGTGTTCACCAAAAA; (rev) CCTCAGGGGTTCTTCTCCTC

p21: (fwd) GTACTTCCTCTGCCCTGCTG; (rev) GGGCACTTCAGGGTTTTCTC

Gapdh: (fwd) CATGTTCCAGTATGACTCCACTC; (rev) GGCCTCACCCCATTTGATGT

AUTHOR CONTRIBUTIONS:

AZ, designed and performed experiments, analyzed data and wrote the manuscript. RR, designed and performed experiments, analyzed data. FR: oversaw the entire project, designed experiments, performed experiments, analyzed data and wrote the manuscript.

ACKNOWLEDGEMENTS:

We are grateful to Margaret Buckingham, Carmen Birchmeier, Shahragim Tajbakhsh, Robert Kelly and Sonia Alonso Martin for helpful comments. We thank Vanessa Ribes and Frédéric Auradé for their assistance with this work and writing. We thank Catherine Bodin for histology. We also wish to acknowledge the animal care facilities at UPMC and CDTA, and Catherine Blanc from Flow Cytometry Core CyPS. This work was supported by funding to FR from INSERM Avenir Program, Association Française contre les Myopathies (AFM), Association Institut de Myologie (AIM), Labex REVIVE, the European Union Sixth and Seventh Framework Program in the project MYORES and ENDOSTEM (Grant # 241440), Fondation pour la Recherche Médicale (FRM; Grant FDT20130928236), Agence Nationale pour la Recherche (ANR) grant Epimuscle and BMP-biomass, and the Agence Nationale pour la Recherche Maladies Rares (MRAR) grant Pax3 in WS. This work was also funded by the German Research Foundation (DFG; Grant GK1631), French-German University (UFA-DFH; Grant CDFA-06-11) and the AFM as part of the MyoGrad International Research Training Group for Myology. The funders had no role in study design, data collection and analysis, decision to publish, or preparation of the manuscript.

REFERENCES:

Bajard, L., Relaix, F., Lagha, M., Rocancourt, D., Daubas, P., and Buckingham, M.E. (2006). A novel genetic hierarchy functions during hypaxial myogenesis: Pax3 directly activates Myf5 in muscle progenitor cells in the limb. Genes Dev *20*, 2450-2464.

Basch, M.L., Bronner-Fraser, M., and Garcia-Castro, M.I. (2006). Specification of the neural crest occurs during gastrulation and requires Pax7. Nature *441*, 218-222.

Besson, A., Dowdy, S.F., and Roberts, J.M. (2008). CDK inhibitors: cell cycle regulators and beyond. Dev Cell *14*, 159-169.

Betancur, P., Bronner-Fraser, M., and Sauka-Spengler, T. (2010). Assembling neural crest regulatory circuits into a gene regulatory network. Annu Rev Cell Dev Biol *26*, 581-603.

Bhatt, S., Diaz, R., and Trainor, P.A. (2013). Signals and switches in Mammalian neural crest cell differentiation. Cold Spring Harbor perspectives in biology *5*.

Depew, M.J., Lufkin, T., and Rubenstein, J.L. (2002). Specification of jaw subdivisions by Dlx genes. Science *298*, 381-385.

Dixon, M.J., Marazita, M.L., Beaty, T.H., and Murray, J.C. (2011). Cleft lip and palate: understanding genetic and environmental influences. Nature reviews Genetics *12*, 167-178.

Dupe, V., Matt, N., Garnier, J.M., Chambon, P., Mark, M., and Ghyselinck, N.B. (2003). A newborn lethal defect due to inactivation of retinaldehyde dehydrogenase type 3 is prevented by maternal retinoic acid treatment. Proc Natl Acad Sci U S A *100*, 14036-14041.

Dupin, E., and Sommer, L. (2012). Neural crest progenitors and stem cells: from early development to adulthood. Dev Biol *366*, 83-95.

Fernandez-Salguero, P.M., Hilbert, D.M., Rudikoff, S., Ward, J.M., and Gonzalez, F.J. (1996). Aryl-hydrocarbon receptor-deficient mice are resistant to 2,3,7,8-tetrachlorodibenzo-p-dioxin-induced toxicity. Toxicology and applied pharmacology *140*, 173-179.

Gilbert-Barness, E. (2010). Teratogenic causes of malformations. Annals of clinical and laboratory science *40*, 99-114.

Hankinson, O. (1995). The aryl hydrocarbon receptor complex. Annual review of pharmacology and toxicology *35*, 307-340.

Houzelstein, D., Cohen, A., Buckingham, M.E., and Robert, B. (1997). Insertional mutation of the mouse Msx1 homeobox gene by an nlacZ reporter gene. Mech Dev *65*, 123-133.

Hu, D., Marcucio, R.S., and Helms, J.A. (2003). A zone of frontonasal ectoderm regulates patterning and growth in the face. Development *130*, 1749-1758.

Jang, J.Y., Shin, S., Choi, B.I., Park, D., Jeon, J.H., Hwang, S.Y., Kim, J.C., Kim, Y.B., and Nahm, S.S. (2007). Antiteratogenic effects of alpha-naphthoflavone on 2,3,7,8-tetrachlorodibenzo-p-dioxin (TCDD) exposed mice in utero. Reproductive toxicology *24*, 303-309.

Knecht, A.K., and Bronner-Fraser, M. (2002). Induction of the neural crest: a multigene process. Nature reviews Genetics *3*, 453-461.

Kulesa, P., Ellies, D.L., and Trainor, P.A. (2004). Comparative analysis of neural crest cell death, migration, and function during vertebrate embryogenesis. Dev Dyn *229*, 14-29.

Lallemand, Y., Luria, V., Haffner-Krausz, R., and Lonai, P. (1998). Maternally expressed PGK-Cre transgene as a tool for early and uniform activation of the Cre site-specific recombinase. Transgenic research *7*, 105-112.

Le Douarin, N.M., Creuzet, S., Couly, G., and Dupin, E. (2004). Neural crest cell plasticity and its limits. Development *131*, 4637-4650.

Li, J., Liu, K.C., Jin, F., Lu, M.M., and Epstein, J.A. (1999). Transgenic rescue of congenital heart disease and spina bifida in Splotch mice. Development *126*, 2495-2503.

Mansouri, A., Stoykova, A., Torres, M., and Gruss, P. (1996). Dysgenesis of cephalic neural crest derivatives in Pax7-/- mutant mice. Development *122*, 831-838.

McKeown, S.J., Newgreen, D.F., and Farlie, P.G. (2005). Dlx2 over-expression regulates cell adhesion and mesenchymal condensation in ectomesenchyme. Dev Biol *281*, 22-37.

Minchin, J.E., and Hughes, S.M. (2008). Sequential actions of Pax3 and Pax7 drive xanthophore development in zebrafish neural crest. Dev Biol *317*, 508-522.

Monsoro-Burq, A.H., Wang, E., and Harland, R. (2005). Msx1 and Pax3 cooperate to mediate FGF8 and WNT signals during Xenopus neural crest induction. Dev Cell *8*, 167-178.

Nelms, B.L., and Labosky, P.A. (2010). In Transcriptional Control of Neural Crest Development (San Rafael (CA)).

Noden, D.M., and Trainor, P.A. (2005). Relations and interactions between cranial mesoderm and neural crest populations. J Anat *207*, 575-601.

Pang, P.H., Lin, Y.H., Lee, Y.H., Hou, H.H., Hsu, S.P., and Juan, S.H. (2008). Molecular mechanisms of p21 and p27 induction by 3-methylcholanthrene, an aryl-hydrocarbon receptor agonist, involved in antiproliferation of human umbilical vascular endothelial cells. Journal of cellular physiology *215*, 161-171.

Pratt, R.M., Dencker, L., and Diewert, V.M. (1984). 2,3,7,8-Tetrachlorodibenzo-p-dioxin-induced cleft palate in the mouse: evidence for alterations in palatal shelf fusion. Teratogenesis, carcinogenesis, and mutagenesis *4*, 427-436.

Relaix, F., Polimeni, M., Rocancourt, D., Ponzetto, C., Schafer, B.W., and Buckingham, M. (2003). The transcriptional activator PAX3-FKHR rescues the defects of Pax3 mutant mice but induces a myogenic gain-of-function phenotype with ligand-independent activation of Met signaling in vivo. Genes Dev *17*, 2950-2965.

Relaix, F., Rocancourt, D., Mansouri, A., and Buckingham, M. (2005). A Pax3/Pax7-dependent population of skeletal muscle progenitor cells. Nature *435*, 948-953.

Sato, T., Sasai, N., and Sasai, Y. (2005). Neural crest determination by co-activation of Pax3 and Zic1 genes in Xenopus ectoderm. Development *132*, 2355-2363.

Thomas, B.L., Liu, J.K., Rubenstein, J.L., and Sharpe, P.T. (2000). Independent regulation of Dlx2 expression in the epithelium and mesenchyme of the first branchial arch. Development *127*, 217-224.

Van Ho, A.T., Hayashi, S., Brohl, D., Aurade, F., Rattenbach, R., and Relaix, F. (2011). Neural crest cell lineage restricts skeletal muscle progenitor cell differentiation through Neuregulin1-ErbB3 signaling. Dev Cell *21*, 273-287.

Vandenberg, A.L., and Sassoon, D.A. (2009). Non-canonical Wnt signaling regulates cell polarity in female reproductive tract development via van gogh-like 2. Development *136*, 1559-1570.

Yonemoto, J. (2000). The effects of dioxin on reproduction and development. Industrial health *38*, 259-268.

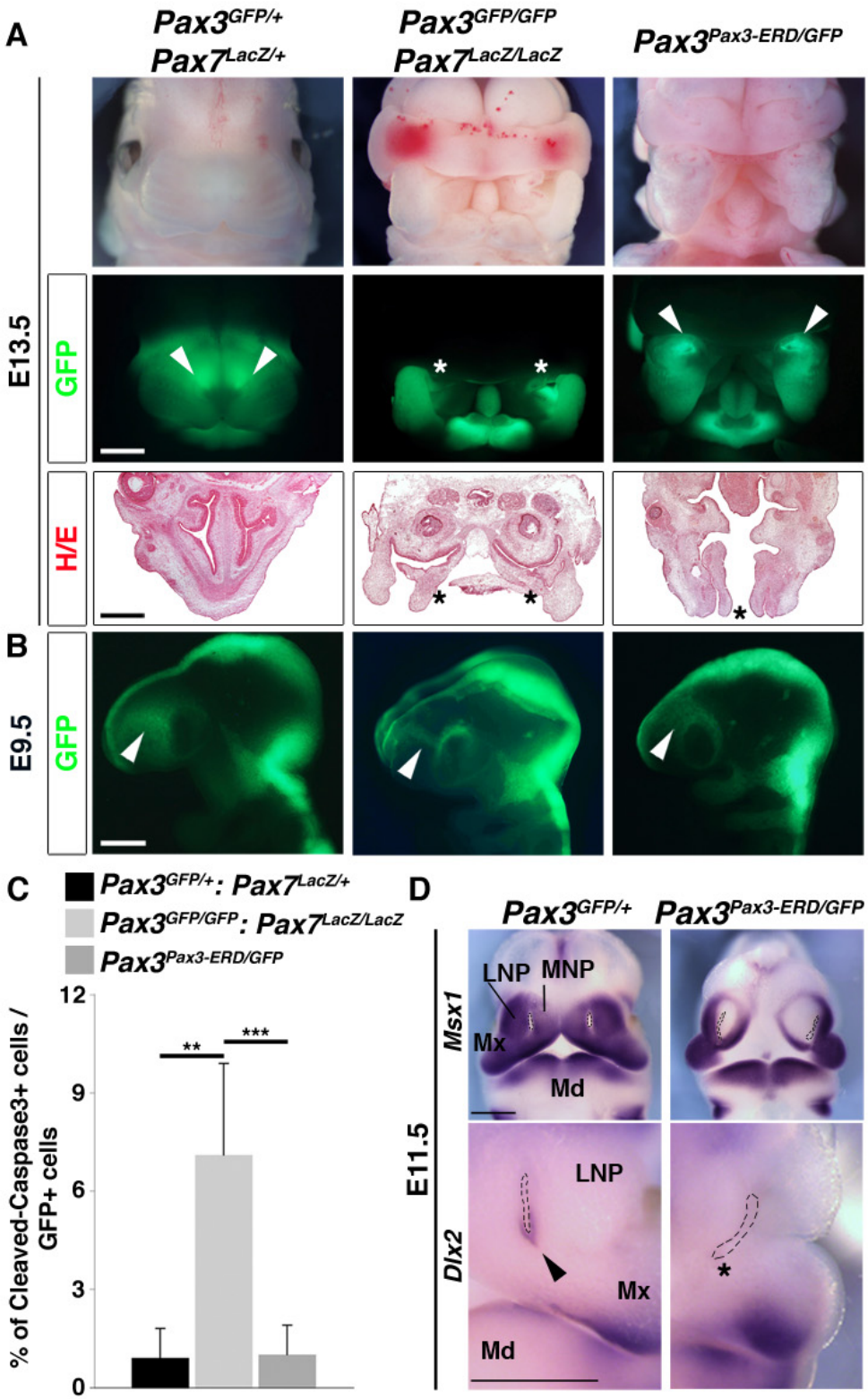
A
Pax3GFP/+
Pax7LacZ/+
Pax3GFP/GFP
Pax7LacZ/LacZ
Pax3Pax3-ERD/GFP
E13.5
GFP
H/E
B
E9.5
GFP
C
Pax3GFP/+: Pax7LacZ/+
Pax3GFP/GFP: Pax7LacZ/LacZ
Pax3Pax3-ERD/GFP
% of Cleaved-Caspase3+ cells / GFP+ cells
12
9
6
3
0
**
***
D
Pax3GFP/+
Pax3Pax3-ERD/GFP
E11.5
Msx1
LNP
MNP
Mx
Md
Dlx2
LNP
Mx
Md

Figure 1. Pax3 and Pax7 are essential for facial development.

(A) Bright field and GFP expression (top and middle panels, facial views) of E13.5 embryos of the indicated genotype. Arrowheads represent normal nasal processes. White stars indicate rudimentary nasal processes. Bottom panels show histological transverse sections through the nasal processes of these embryos. Black stars indicate divided nasal septum. Scale bars, 500μm. **(B)** GFP expression in E9.5 embryos of the indicated genotypes (lateral views, scale bar, 200μm). Arrowheads indicate the CNCC migrating into the facial prominences. **(C)** Percentage of Cleaved-Caspase3^{+} cells in the Pax3^{+} CNCC population of E11.5 embryos of the indicated genotype. (**D**) Whole mount *in situ* hybridization for *Msx1* and *Dlx2* transcripts on E11.5 embryos of the indicated genotype. Arrowhead indicates *Dlx2* expression. Star shows its absence. Scale bars, 500μm. Dotted lines indicate nasal pit location. LNP: Lateral Nasal Process, MNP: Medial Nasal Process, Mx: Maxillary process, Md: Mandibular process.

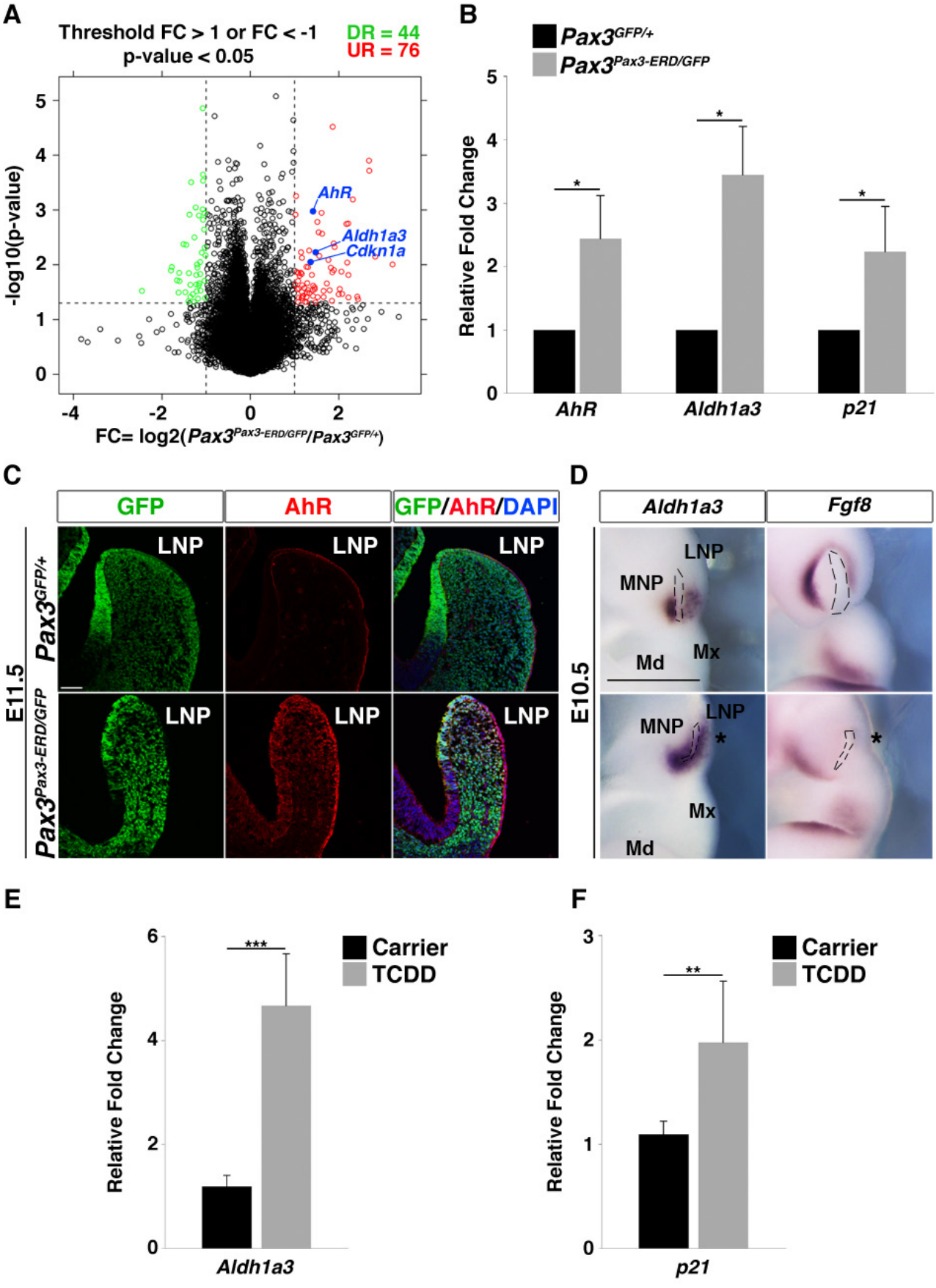
A
Threshold FC > 1 or FC < -1
p-value < 0.05
DR = 44
UR = 76
-log10(p-value)
FC= log2(Pax3Pax3-ERD/GFP/Pax3GFP/+)
AhR
Aldh1a3
Cdkn1a
B
Pax3GFP/+
Pax3Pax3-ERD/GFP
Relative Fold Change
AhR
Aldh1a3
p21
C
GFP
AhR
GFP/AhR/DAPI
E11.5
Pax3GFP/+
Pax3Pax3-ERD/GFP
LNP
D
Aldh1a3
Fgf8
E10.5
LNP
MNP
Md
Mx
E
Carrier
TCDD
Relative Fold Change
Aldh1a3
F
Carrier
TCDD
Relative Fold Change
p21

Figure 2. Impaired Pax3/7 function leads to up-regulation of AhR signaling.

(A) Volcano plot showing the 44 down-regulated genes (green) and 76 up-regulated genes (red) in GFP^{+} cells FACS-isolated from dissected facial prominences of E11.5 $Pax3^{Pax3\text{-}ERD/GFP}$ compared to $Pax3^{GFP/+}$ control embryos. Blue dots indicate the position of *AhR*, *Aldh1a3* and *p21* transcripts. **(B)** Relative expression of *AhR*, *Aldhla3* and *p21* assayed by RT-qPCR in cells FACS-sorted for GFP from E11.5 embryos of the indicated genotype. **(C)** AhR expression in red and GFP in green on transverse sections within the cranial regions of embryos with the genotypes and at the stages indicated (scale bar, 50μm). **(D)** Whole mount *in situ* hybridization for *Aldh1a3* and *Fgf8* transcripts on $Pax3^{Pax3\text{-}ERD/GFP}$ compared to $Pax3^{GFP/+}$ control embryos. Stars indicate increased area of transcripts expression for *Aldh1a3* or reduced expression for *Fgf8.* Scale bar, 500μm. **(E-F)** *Aldh1a3* and *p21* relative expression assayed by RT-qPCR in CNCC from E10.5 WT embryos, exposed to TCDD or carrier as indicated. LNP: Lateral Nasal Process, MNP: Medial Nasal Process, Mx: Maxillary process, Md: Mandibular process.

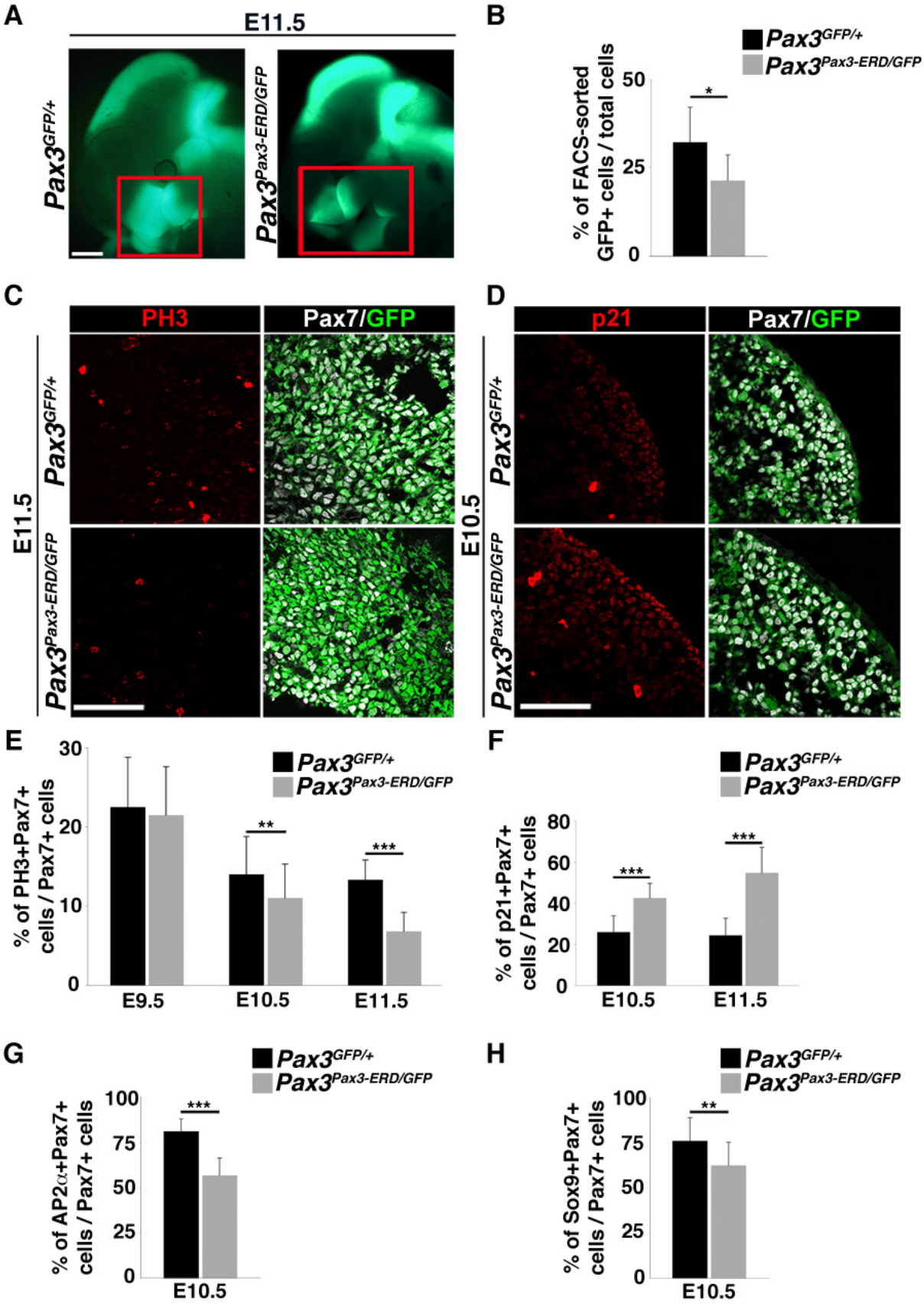
A
E11.5
Pax3GFP/+
Pax3Pax3-ERD/GFP
B
Pax3GFP/+
Pax3Pax3-ERD/GFP
% of FACS-sorted GFP+ cells / total cells
50
25
0
*
C
PH3
Pax7/GFP
E11.5
Pax3GFP/+
Pax3Pax3-ERD/GFP
D
p21
Pax7/GFP
E10.5
Pax3GFP/+
Pax3Pax3-ERD/GFP
E
Pax3GFP/+
Pax3Pax3-ERD/GFP
% of PH3+Pax7+ cells / Pax7+ cells
30
20
10
0
**
***
E9.5
E10.5
E11.5
F
Pax3GFP/+
Pax3Pax3-ERD/GFP
% of p21+Pax7+ cells / Pax7+ cells
80
60
40
20
0
***
***
E10.5
E11.5
G
Pax3GFP/+
Pax3Pax3-ERD/GFP
% of AP2α+Pax7+ cells / Pax7+ cells
100
75
50
25
0
***
E10.5
H
Pax3GFP/+
Pax3Pax3-ERD/GFP
% of Sox9+Pax7+ cells / Pax7+ cells
100
75
50
25
0
**
E10.5

Figure 3. Impairing Pax3/7 function induces cell cycle exit of CNCC.

(A) GFP expression in E11.5 embryos of the indicated genotypes (lateral views, scale bar, 500μm). Boxes delineate the facial prominences dissected to perform the FACS-sorting in B. **(B)** Percentage of FACS-sorted GFP^+ cells within the total population of cells from the dissected facial prominences of embryos of the indicated genotype. **(C-D)** Phospho-Histone H3 (PH3) and p21 expression in red, Pax7 in white and GFP in green on transverse sections within the cranial regions of embryos at indicated genotypes and stages (scale bars, 50μm). **(E, F, G, H)** Quantification of the proportion of $PH3^+$ (E), $p21^+$ (F) $AP2\alpha^+$ (G) and $Sox9^+$ (H) cells within the $Pax7^+$ population in these sections.

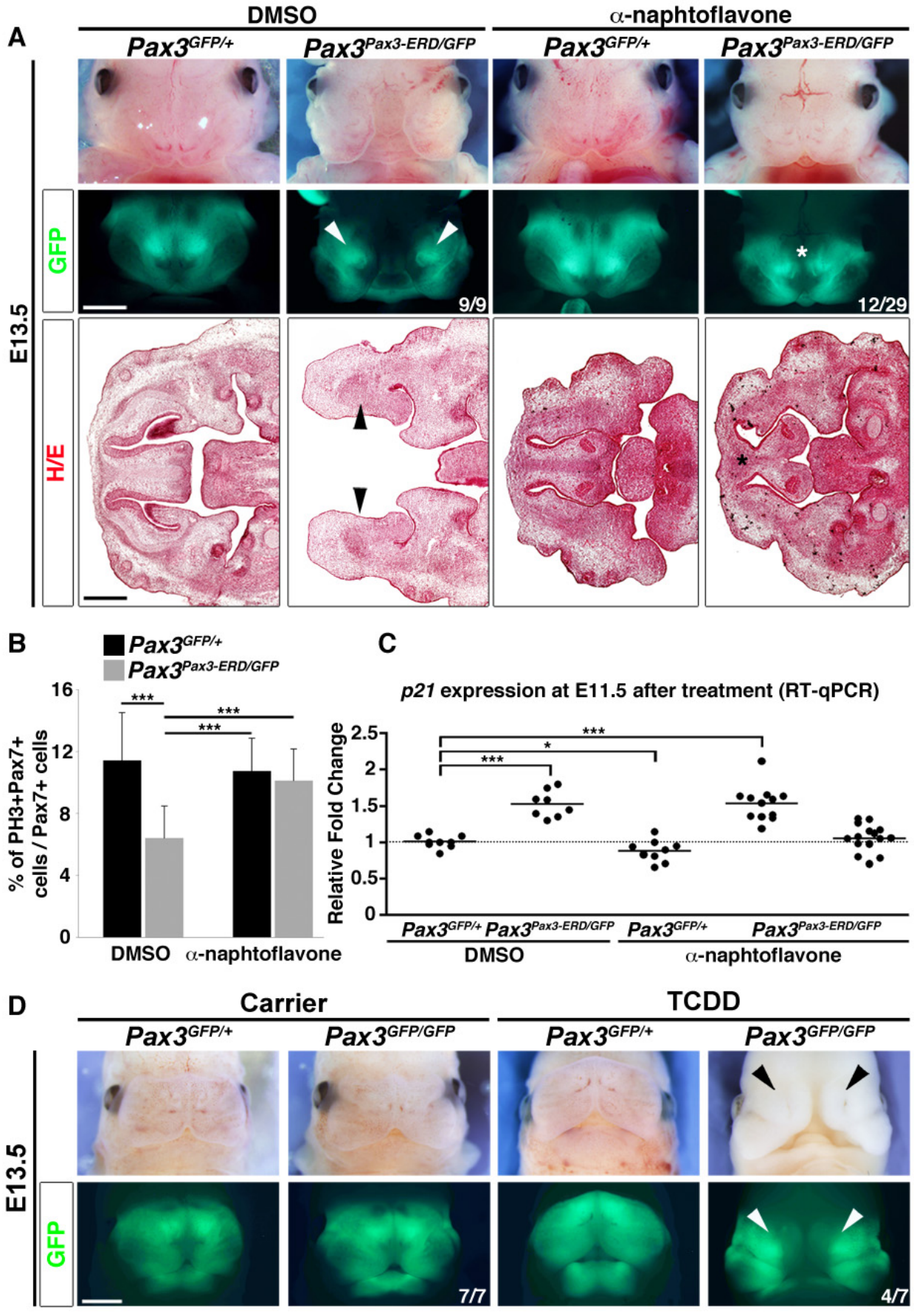
A
DMSO
α-naphtoflavone
Pax3GFP/+
Pax3Pax3-ERD/GFP
Pax3GFP/+
Pax3Pax3-ERD/GFP
E13.5
GFP
H/E
9/9
12/29
B
Pax3GFP/+
Pax3Pax3-ERD/GFP
% of PH3+Pax7+ cells / Pax7+ cells
16
12
8
4
0
***
***
***
DMSO
α-naphtoflavone
C
p21 expression at E11.5 after treatment (RT-qPCR)
Relative Fold Change
2.5
2
1.5
1
0.5
0
***
*
***
Pax3GFP/+
Pax3Pax3-ERD/GFP
Pax3GFP/+
Pax3Pax3-ERD/GFP
DMSO
α-naphtoflavone
D
Carrier
TCDD
Pax3GFP/+
Pax3GFP/GFP
Pax3GFP/+
Pax3GFP/GFP
E13.5
GFP
7/7
4/7

Figure 4. Interaction between Pax3 and AhR signaling is essential for normal craniofacial development.

(A) Bright field and GFP expression of E13.5 embryos of the indicated genotype treated with DMSO or α-naphtoflavone (facial views, top and middle panels, scale bar, 500μm). Arrowheads indicate divided nasal processes. Star marks its fusion. Bottom panels show histological transverse sections through the nasal processes of these embryos (scale bar, 500μm). Arrowheads indicate divided nasal septum. Star marks its fusion. **(B)** Percentage of $PH3^+$ cells within the $Pax7^+$ CNCC population in E11.5 embryos of the indicated genotype treated with DMSO or α-naphtoflavone. **(C)** *p21* relative expression assayed by RT-qPCR in dissected faces of independent E11.5 embryos of the indicated genotype treated with DMSO or α-naphtoflavone. Dotted line represents *p21* expression level in DMSO control embryos. **(D)** Bright field and GFP expression of E13.5 embryos of the indicated genotype treated with carrier or TCDD (facial views, scale bar, 500μm). Arrowheads indicate divided nasal processes.

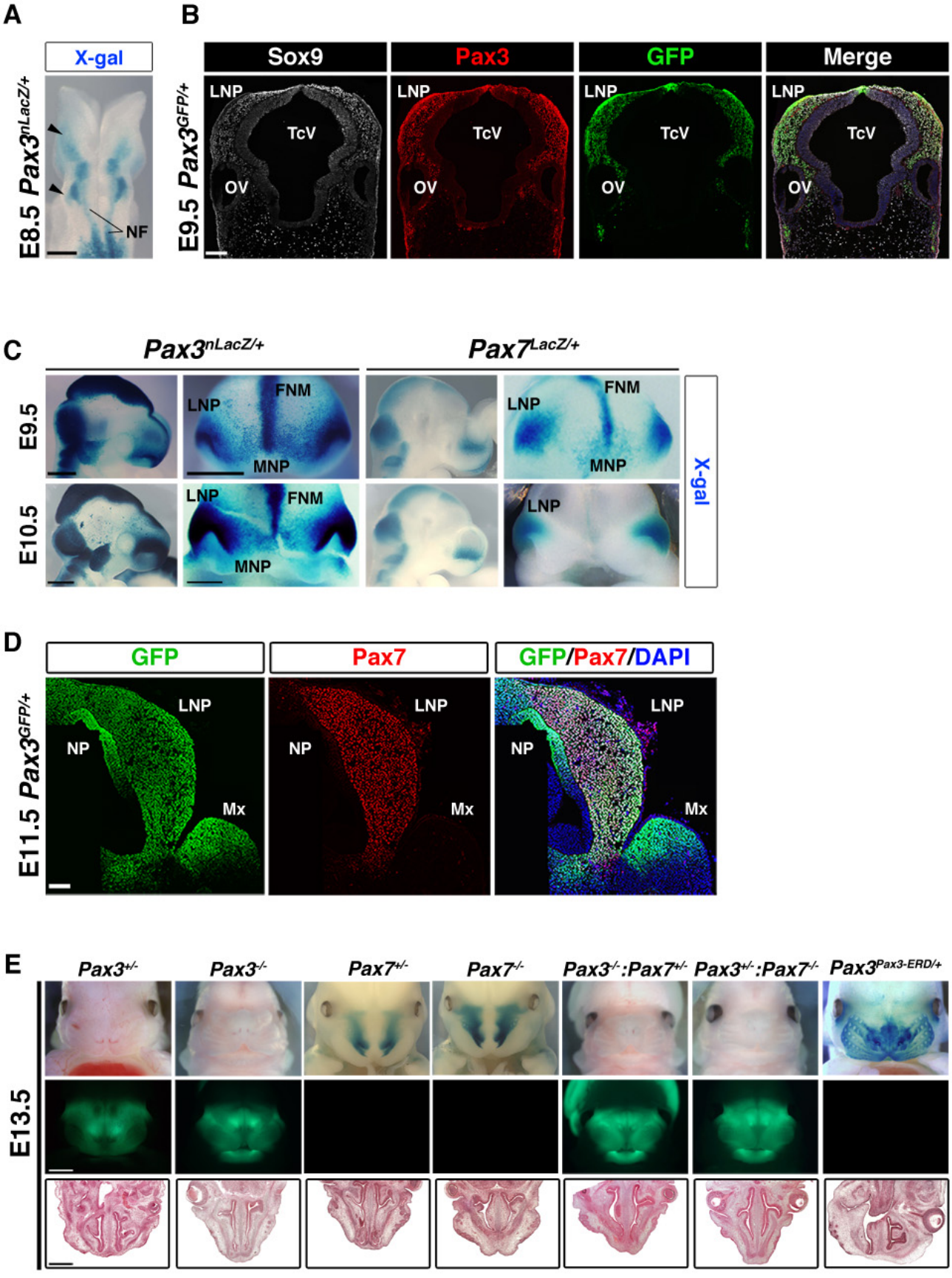
A
B
X-gal
E8.5 Pax3nLacZ/+
NF
Sox9
Pax3
GFP
Merge
E9.5 Pax3GFP/+
LNP
TcV
OV
C
Pax3nLacZ/+
Pax7LacZ/+
E9.5
E10.5
FNM
LNP
MNP
X-gal
D
GFP
Pax7
GFP/Pax7/DAPI
E11.5 Pax3GFP/+
NP
Mx
E
Pax3+/-
Pax3-/-
Pax7+/-
Pax7-/-
Pax3-/-:Pax7+/-
Pax3+/-:Pax7-/-
Pax3Pax3-ERD/+
E13.5

Figure S1. *Pax3* and *Pax7* dynamic expression and phenotypes of *Pax3/7* compound mutants.

(**A**) Whole mount X-Gal staining of a $Pax3^{nLacZ/+}$ embryo at (dorsal view, scale bar, 50μm). Arrowheads indicate *Pax3* expression in the anterior neural plate border. NF: Neural folds. **(B)** Expression of Sox9 (white), Pax3 (red) and GFP (green) proteins on transverse sections through cranial structures of on E9.5 $Pax3^{GFP/+}$ embryo. Dapi staining (blue) is also shown in the merge panel (scale bar, 100μm). Sox9 expression is found in all migrating CNCC and CNCC established in the LNP. GFP expression coincides with Pax3 expression. GFP cells are $Sox9^{+}$. LNP: Lateral Nasal Process, TcV: Telencephalic Vesicle, OV: Optic Vesicle. **(C)** Whole mount X-Gal staining of $Pax3^{nLacZ/+}$ and $Pax7^{LacZ/+}$ embryos. Left and right panels are side and facial views, respectively (scale bars, 500μm). LNP: Lateral Nasal Process, MNP: Medial Nasal Process, FNM: Fronto Nasal Mass. **(D)** Expression of GFP (green) and Pax7 (red) proteins on a transverse section through the cranial structures of an E11.5 $Pax3^{GFP/+}$embryo. Dapi staining (blue) is also shown in the merge panel (scale bar, 50μm). NP: Nasal Pit, LNP: Lateral Nasal Process, Mx: Maxillary process. **(E)** Top panels are bright field showing facial views of E13.5 $Pax3^{GFP/+}$ ($Pax3^{+/-}$), $Pax3^{GFP/GFP}$ ($Pax3^{-/-}$), $Pax7^{LacZ/+}$ ($Pax7^{+/-}$), $Pax7^{LacZ/LacZ}$ ($Pax7^{-/-}$), $Pax3^{GFP/GFP}$; $Pax7^{LacZ/+}$ ($Pax3^{-/-}$; $Pax7^{+/-}$), $Pax3^{GFP/+}$; $Pax7^{LacZ/LacZ}$ ($Pax3^{+/-}$; $Pax7^{-/-}$) and $Pax3^{Pax3\text{-}ERD/+}$ embryos. $Pax7^{+/-}$, $Pax7^{-/-}$ and $Pax3^{Pax3\text{-}ERD/+}$ show whole mount X-gal straining. Middle panels show GFP expression for $Pax3^{+/-}$, $Pax3^{-/-}$, $Pax3^{-/-}$; $Pax7^{+/-}$ and $Pax3^{+/-}$; $Pax7^{-/-}$ embryos at E13.5 (scale bar, 500μm). Bottom panels show histological transverse sections through the nasal process of these embryos (scale bar, 500μm).

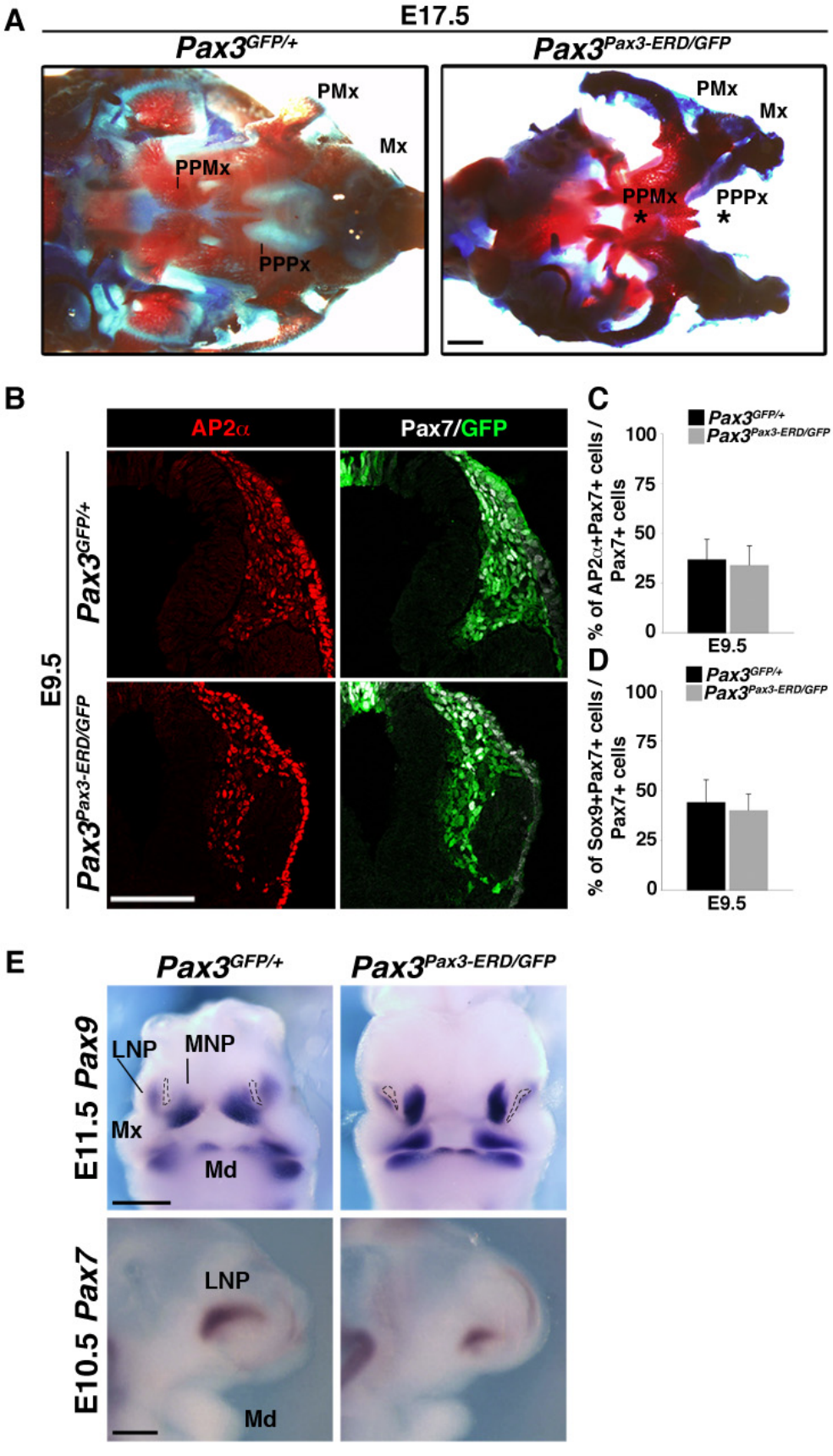
A
E17.5
Pax3GFP/+
Pax3Pax3-ERD/GFP
PMx
Mx
PPMx
PPPx
B
AP2α
Pax7/GFP
E9.5
Pax3GFP/+
Pax3Pax3-ERD/GFP
C
% of AP2α+Pax7+ cells / Pax7+ cells
100
75
50
25
0
E9.5
D
% of Sox9+Pax7+ cells / Pax7+ cells
E
E11.5 Pax9
LNP
MNP
Mx
Md
E10.5 Pax7

Figure S2. Analysis of *Pax3*$^{Pax3\text{-}ERD/GFP}$ embryos.

(A) Skeleton staining of E17.5 *Pax3*$^{GFP/+}$ control and *Pax3*$^{Pax3\text{-}ERD/GFP}$ embryo skulls. Stars show defects in primary and secondary palate in *Pax3*$^{Pax3\text{-}ERD/GFP}$ compared to *Pax3*$^{GFP/+}$ embryos (scale bar, 500μm). **(B)** Immunohistochemistry shows expression of AP2α in red, Pax7 in white and GFP in green on transverse sections within the cranial regions of *Pax3*$^{GFP/+}$ and *Pax3*$^{Pax3\text{-}ERD/GFP}$ embryos at E9.5 (scale bar, 50μm). **(C-D)** Quantification of the proportion of AP2α^{+} (C) and Sox9^{+} (D) cells within the Pax7^{+} population found on transverse sections in the cranial regions of *Pax*$^{/GFP/+}$ and *Pax3*$^{Pax3\text{-}ERD/GFP}$ embryos at the indicated stages. **(E)** Top panel shows whole mount *in situ* hybridization for *Pax9* transcripts in E11.5 *Pax3*$^{GFP/+}$ control and *Pax3*$^{Pax3\text{-}ERD/GFP}$ embryos (facial view, scale bar, 500μm). Dotted lines indicate nasal pit location. Bottom panels show whole mount *in situ* hybridization for *Pax7* transcripts in E10.5 *Pax3*$^{GFP/+}$ control and *Pax3*$^{Pax3\text{-}ERD/GFP}$ embryos (side view; scale bar, 500μm). PMx: Premaxilla, PPMx: Palatal Process of Maxilla, PPPx: Palatal Process of Premaxilla, LNP: Lateral Nasal Process, MNP: Medial Nasal Process, Mx: Maxillary process, Md: Mandibular process.

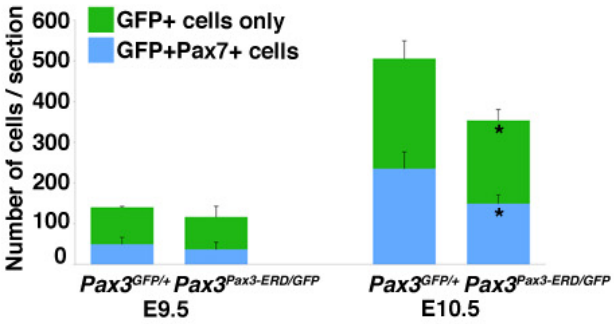
GFP+ cells only
GFP+Pax7+ cells
Number of cells / section
600
500
400
300
200
100
0
Pax3GFP/+
Pax3Pax3-ERD/GFP
E9.5
Pax3GFP/+
Pax3Pax3-ERD/GFP
E10.5
*
*

Figure S3. Quantification of CNCC in facial prominences of *Pax3*$^{GFP/+}$ and *Pax3*$^{Pax3\text{-}ERD/GFP}$ embryos.

Quantification of the number of Pax7^{+} cells within the GFP^{+} population on transverse sections of the cranial structures of E9.5 and E10.5 embryos of the indicated genotype ($n \geq 3$ embryos; mean ± s.d.; Mann-Whitney's test, *: $p<0.05$).

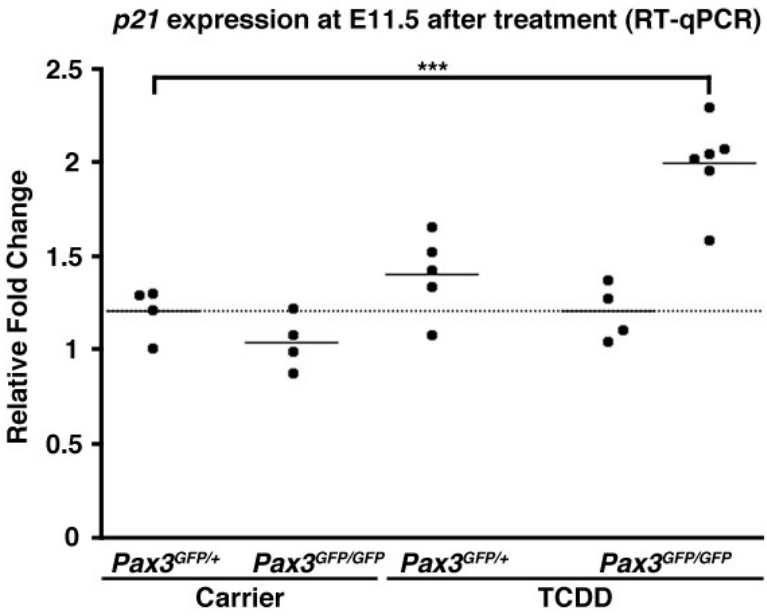
p21 expression at E11.5 after treatment (RT-qPCR)
***
Relative Fold Change
2.5
2
1.5
1
0.5
0
Pax3GFP/+
Pax3GFP/GFP
Pax3GFP/+
Pax3GFP/GFP
Carrier
TCDD

Figure S4. Up-regulation of *p21* expression upon TCDD exposure.

p21 relative expression assayed by RT-qPCR in dissected faces of independent E11.5 embryos of the indicated genotype treated with carrier or TCDD. Dotted line represents *p21* expression level in carrier treated control embryos. TCDD treated $Pax3^{GFP/GFP}$ embryos can be statistically segregated into two populations using a Ki^2 test. We compared the expression value for *p21* obtained in each TCDD treated $Pax3^{GFP/GFP}$ embryo to the mean of the expression values for all the carrier treated $Pax3^{GFP/+}$ embryos (control set). If there were significant differences between these two values, the embryo was classified into the population described as responsive to the TCDD treatment, if not the embryo was associated with the non-responsive population.

Gene Symbol	Genbank ID	Intensities (Log2)						DM vs GFP (t-test)			
		DM1	DM2	DM3	GFP1	GFP2	GFP3	logFC	DF	p-value	REG
Sparcl1	NM_010097	8,10	8,27	8,33	6,55	6,13	7,79	1,41	2,66	2,90E-02	UR
Cyp1b1	BI251808	6,35	5,13	4,64	4,01	3,83	3,91	1,45	2,74	2,79E-02	UR
Slc40a1	AF226613	8,38	7,63	9,05	6,90	6,93	7,06	1,39	2,62	1,53E-02	UR
Fmo1	BC011229	5,86	6,17	6,66	5,45	4,27	5,11	1,29	2,44	2,16E-02	UR
Bhlhb5	NM_021560	8,51	7,22	7,35	6,78	6,57	5,31	1,47	2,78	4,86E-02	UR
Lhx2	NM_010710	7,79	8,37	7,28	7,30	5,57	5,03	1,84	3,59	4,53E-02	UR
Foxg1	NM_008241	9,89	10,05	9,12	8,66	6,90	6,85	2,22	4,65	1,53E-02	UR
Lmo1	NM_057173	5,20	4,98	3,76	3,63	3,37	2,93	1,34	2,52	3,26E-02	UR
Ebf2	U71189	8,84	8,92	7,83	6,75	4,08	5,10	3,22	9,29	9,85E-03	UR
Notch1	NM_008714	10,76	10,65	10,29	9,68	9,54	9,40	1,02	2,03	1,22E-03	UR
Dll1	NM_007865	6,85	7,35	6,09	5,63	4,24	4,24	2,06	4,17	1,33E-02	UR
AW049604	BB804965	5,79	5,80	4,61	4,45	4,61	3,89	1,08	2,12	4,80E-02	UR
Colec12	NM_130449	9,06	9,09	7,86	7,85	7,29	7,02	1,29	2,44	3,23E-02	UR
Akap12	NM_031185	10,48	10,38	9,88	9,47	8,83	8,99	1,15	2,21	5,89E-03	UR
Epyc	NM_007884	4,63	3,96	3,94	2,34	3,00	3,27	1,31	2,47	1,11E-02	UR
Insm1	NM_016889	3,83	4,28	3,75	3,08	2,26	3,18	1,12	2,17	1,58E-02	UR
Ahr	BE989096	9,04	8,44	8,60	7,50	7,06	7,24	1,42	2,68	1,06E-03	UR
Neurog2	NM_009718	5,31	5,95	4,13	3,34	3,28	3,21	1,85	3,61	1,37E-02	UR
Igfbp3	AV175389	9,33	9,30	10,68	8,56	8,63	8,53	1,19	2,29	3,69E-02	UR
Nell2	AI838010	6,90	7,66	7,96	6,74	6,53	6,06	1,07	2,09	2,80E-02	UR
Lum	AK014312	12,48	12,44	12,75	11,48	11,03	10,52	1,54	2,92	2,55E-03	UR
Meox2	BC002076	5,02	4,92	3,80	3,85	3,38	3,02	1,16	2,24	4,05E-02	UR
Spon1	BC020531	4,50	5,97	4,69	3,38	2,84	3,47	1,82	3,53	1,13E-02	UR
Cdkn1a	AK007630	6,49	6,49	7,30	5,69	5,06	5,71	1,27	2,41	1,09E-02	UR
Cdh10	AF183946	10,26	9,43	10,65	9,27	8,88	8,27	1,30	2,47	2,89E-02	UR
Gpm6a	BF449735	6,72	6,88	8,14	6,14	4,60	5,62	1,79	3,47	2,91E-02	UR
---	BB398886	9,89	10,30	10,09	9,03	8,95	9,19	1,04	2,05	5,57E-04	UR
Col14a1	AJ131395	6,49	6,39	7,08	4,03	3,69	4,19	2,68	6,42	1,25E-04	UR
Car8 /// LOC676792	X61397	5,68	6,11	7,12	5,43	4,97	4,98	1,18	2,26	3,76E-02	UR
Cdh9	BQ176417	6,72	5,91	5,83	4,69	4,26	4,64	1,62	3,08	2,71E-03	UR
5830408B19Rik	BE135996	9,90	9,63	10,56	8,84	8,67	9,35	1,08	2,12	1,97E-02	UR
Tbx18	AK012980	9,99	9,90	10,17	8,95	8,10	9,01	1,33	2,51	5,49E-03	UR
Prss23	AK009847	10,57	10,36	11,44	9,47	9,26	10,15	1,17	2,24	3,12E-02	UR
Cpne8	AK004559	6,60	6,81	7,38	5,62	5,40	5,22	1,52	2,86	1,65E-03	UR
Tgm2	AW321975	7,44	6,78	8,19	6,16	5,57	6,42	1,42	2,67	2,40E-02	UR
1190002N15Rik	AV309085	9,43	9,47	10,39	8,81	8,45	8,60	1,14	2,21	1,39E-02	UR
C130076O07Rik	BB202655	6,08	5,15	5,22	4,28	3,50	3,99	1,56	2,95	6,89E-03	UR
C130071C03Rik	AV252614	6,33	6,62	4,69	3,72	2,79	2,67	2,82	7,08	7,10E-03	UR
2600009P04Rik	AV334527	7,07	6,79	6,13	6,25	4,74	5,18	1,27	2,41	4,83E-02	UR
Egfr	AV369812	6,70	6,10	6,66	5,28	4,89	6,01	1,09	2,13	2,71E-02	UR
9530028C05	BQ175154	5,99	4,56	5,55	3,53	3,40	3,87	1,76	3,40	8,15E-03	UR
---	BB284627	7,35	6,33	7,80	5,94	5,46	6,26	1,27	2,42	3,86E-02	UR
Sox21	BB046776	6,19	6,60	7,44	5,91	5,47	5,20	1,22	2,33	2,65E-02	UR
Mapk10	BB453775	7,76	7,17	6,80	6,62	5,80	5,78	1,17	2,26	2,37E-02	UR
Tgm2	BB550124	6,85	5,82	7,55	4,93	4,52	5,11	1,89	3,70	1,25E-02	UR
Prss23	BB378796	12,36	11,96	12,72	11,08	10,92	11,55	1,17	2,25	7,47E-03	UR
---	BB183456	6,81	5,31	7,01	4,63	4,57	5,35	1,52	2,88	3,89E-02	UR
Atp8b4	BM246630	4,40	5,53	5,23	4,42	3,22	2,55	1,66	3,15	3,87E-02	UR
---	BB464523	7,45	6,51	6,82	5,40	5,80	6,09	1,16	2,24	1,46E-02	UR
Abca9	AW046072	9,23	8,75	9,85	7,35	6,63	7,22	2,21	4,64	1,76E-03	UR
Lrp8	BB750940	6,36	6,61	5,22	5,08	5,13	4,25	1,24	2,36	4,80E-02	UR
C030036D22Rik	BB264612	6,30	6,64	6,27	5,76	3,47	3,93	2,02	4,06	2,76E-02	UR
Atp1a2	AV325919	6,99	6,29	5,98	4,92	3,81	5,57	1,66	3,15	2,99E-02	UR
Cspg3	BM939365	6,32	4,94	4,44	3,21	2,93	3,00	2,19	4,57	9,11E-03	UR
---	AI551516	3,92	4,16	4,71	3,60	2,95	2,98	1,09	2,13	1,42E-02	UR
Atp6v0e2	NM_133764	6,18	6,87	6,29	6,07	4,82	5,16	1,10	2,14	3,98E-02	UR
Aldh1a3	AF253409	9,02	8,34	7,94	7,12	7,05	6,67	1,48	2,80	5,99E-03	UR
Ebf2	U71189	6,18	6,32	4,56	4,57	3,53	2,73	2,08	4,22	3,40E-02	UR
Pdgfa	BB371842	7,85	7,97	7,79	6,75	6,08	5,96	1,61	3,05	1,13E-03	UR
Zfpm2	NM_011766	5,76	5,74	6,46	3,36	2,99	3,55	2,69	6,45	1,92E-04	UR
Dcn	NM_007833	9,03	8,35	11,41	7,37	6,97	7,21	2,42	5,35	3,82E-02	UR
Tbx18	NM_023814	5,17	4,99	5,18	3,29	3,03	3,43	1,86	3,64	3,03E-05	UR
Spon1	BC020531	9,56	10,21	10,00	7,92	7,09	7,80	2,32	4,99	6,42E-04	UR
---	BB224658	7,40	7,81	6,92	6,64	6,16	6,18	1,05	2,07	1,35E-02	UR
3110004L20Rik	BM234253	3,72	4,30	5,30	3,37	2,80	2,80	1,45	2,74	2,58E-02	UR
Ephb1	BQ176283	7,27	6,17	6,28	5,28	5,21	5,14	1,37	2,58	8,89E-03	UR
6430547I21Rik	BM932705	6,09	5,27	4,17	3,67	3,29	3,38	1,73	3,32	2,19E-02	UR
6430547I21Rik	BI734045	5,01	5,43	4,14	2,77	2,63	2,65	2,17	4,51	1,80E-03	UR
Insm1	BB468410	9,63	9,69	9,93	9,19	7,70	8,84	1,17	2,25	4,01E-02	UR
Lrrtm1	BB269910	4,74	4,00	6,29	3,66	2,61	2,77	2,00	3,99	3,46E-02	UR
Tgm2	BB041811	7,13	6,41	8,04	6,29	5,37	5,68	1,42	2,67	3,71E-02	UR
LOC624168	BM199323	9,79	9,88	7,64	7,53	7,07	5,41	2,44	5,41	4,25E-02	UR
LOC624168	AV322605	8,63	8,81	6,47	6,45	5,84	4,96	2,22	4,65	3,94E-02	UR
Nol4	AV323033	7,16	7,02	6,75	5,82	4,92	4,53	1,88	3,69	4,08E-03	UR
Gpm6a	BB348674	9,26	9,03	9,88	8,02	6,86	7,58	1,90	3,74	4,74E-03	UR
2310033P09Rik	BB097524	8,38	8,46	8,68	7,82	7,81	6,83	1,02	2,03	2,31E-02	UR

Table S1.

Gene expression comparison between *Pax3*$^{Pax3\text{-}ERD/GFP}$ and *Pax3*$^{GFP/+}$ embryos. Up-regulated genes (UR) were selected when the p-value < 0.05 and the log of differential factor (logFC) > 1.

Gene Symbol	Genbank ID	Intensities (Log2)						DM vs GFP (t-test)			
		DM1	DM2	DM3	GFP1	GFP2	GFP3	logFC	DF	p-value	REG
Otub1	NM_134150	4,24	4,58	5,20	6,54	5,54	6,10	-1,39	-2,62	1,42E-02	DR
Qprt	AI195046	4,47	5,04	4,28	6,43	6,03	5,69	-1,45	-2,74	4,32E-03	DR
Hpgd	AV026552	4,13	4,11	4,60	5,16	5,63	5,14	-1,03	-2,04	4,85E-03	DR
Pax3	NM_008781	9,16	9,06	10,76	10,82	10,96	11,41	-1,40	-2,64	4,66E-02	DR
Tgfa	M92420	3,09	4,09	4,79	5,65	5,69	6,01	-1,79	-3,47	1,27E-02	DR
Gstm6	NM_008184	3,30	3,44	3,72	4,64	4,70	4,35	-1,08	-2,11	9,76E-04	DR
Hyou1	BM231738	4,39	4,61	4,73	5,94	5,86	5,43	-1,16	-2,24	1,26E-03	DR
Tcfap2b	AV334599	9,72	9,47	10,29	10,77	11,04	10,97	-1,10	-2,14	5,98E-03	DR
Barx1	AI325341	4,98	5,26	6,85	7,57	7,17	7,22	-1,62	-3,08	3,20E-02	DR
Grem1	BC015293	6,38	5,83	7,12	7,35	7,33	8,19	-1,18	-2,27	4,13E-02	DR
Wif1	BC004048	10,97	10,36	11,57	11,90	12,02	12,48	-1,17	-2,24	2,36E-02	DR
Fgfr1	M65053	4,62	4,59	6,05	6,24	6,46	6,47	-1,30	-2,46	3,44E-02	DR
Prkcq	AB062122	5,13	5,17	5,94	6,28	6,50	7,13	-1,22	-2,33	1,54E-02	DR
Hrc /// Tcfap2a	BC021623	8,47	8,49	7,36	9,19	9,35	8,85	-1,02	-2,03	4,04E-02	DR
Ift122	AV319292	5,70	5,54	5,36	6,75	6,51	6,54	-1,07	-2,10	2,92E-04	DR
2810454L23Rik	BQ265914	4,81	4,69	5,43	5,78	5,95	6,86	-1,22	-2,33	2,28E-02	DR
Lsm12	BB771548	6,42	4,72	5,66	6,76	7,32	6,79	-1,36	-2,56	3,85E-02	DR
2610005L07Rik	AK012880	3,65	3,54	5,02	5,48	5,53	6,17	-1,66	-3,16	1,92E-02	DR
Pax3	AK012493	7,37	7,38	8,80	9,51	9,57	9,79	-1,78	-3,43	1,10E-02	DR
---	AK017409	5,89	5,19	5,36	6,46	6,87	6,90	-1,26	-2,40	3,16E-03	DR
AI838057	BG060788	6,70	6,45	6,48	7,67	7,11	7,88	-1,01	-2,02	6,73E-03	DR
Cox6b2	AV013496	5,77	5,32	6,23	6,41	7,00	7,00	-1,03	-2,05	1,95E-02	DR
AI464131	BG063189	7,80	7,78	7,86	8,74	8,60	9,24	-1,05	-2,06	2,27E-03	DR
Kcnd3	AW045978	5,70	5,07	5,64	7,03	6,75	6,76	-1,38	-2,60	1,21E-03	DR
Leprel1	AW553532	6,98	6,76	7,01	7,93	8,04	8,48	-1,24	-2,36	9,02E-04	DR
Dnm3	BE988832	5,31	5,27	6,37	7,18	6,79	7,81	-1,61	-3,05	1,40E-02	DR
Tacr3	BB498416	6,25	5,74	6,38	7,27	6,72	7,84	-1,15	-2,22	2,17E-02	DR
Pax3	BB759978	11,03	10,86	12,20	12,50	12,61	13,04	-1,36	-2,56	2,32E-02	DR
Pcdh19	BB732600	5,67	5,24	5,90	6,53	6,24	7,41	-1,12	-2,18	2,96E-02	DR
Eya4	AV324073	2,64	2,49	2,48	3,76	3,26	3,80	-1,07	-2,10	1,51E-03	DR
---	BG076353	4,56	3,13	3,43	4,68	6,53	7,25	-2,45	-5,46	2,99E-02	DR
Enpp2	BC003264	10,19	9,82	11,48	11,66	11,91	12,33	-1,47	-2,77	3,16E-02	DR
Pdc	NM_024458	4,22	3,60	2,83	4,90	4,97	4,42	-1,21	-2,32	3,04E-02	DR
Prcc	NM_033573	6,56	6,18	7,07	8,11	7,38	7,73	-1,13	-2,19	1,47E-02	DR
Pde1a	NM_016744	2,22	2,76	3,32	4,40	4,23	4,21	-1,51	-2,85	4,21E-03	DR
1110065P19Rik /// 2310040A07Rik	BB772205	5,00	5,04	5,16	6,14	6,07	6,22	-1,08	-2,11	1,39E-05	DR
Wdr5b	AK009247	2,70	2,82	2,55	3,71	3,64	3,93	-1,07	-2,10	2,25E-04	DR
2810047C21Rik	BB006969	6,01	5,98	5,28	7,08	6,55	7,25	-1,20	-2,30	9,87E-03	DR
Rspo2	BG067392	11,15	11,39	11,49	12,57	12,55	12,92	-1,34	-2,53	3,11E-04	DR
A530094I17Rik	AV282347	5,91	6,28	6,33	7,08	7,15	7,40	-1,04	-2,05	1,14E-03	DR
Eya4	AI646535	3,47	3,84	4,42	5,34	4,76	5,22	-1,20	-2,29	1,12E-02	DR
Tcfap2b	BB438847	7,17	5,86	7,00	7,32	8,09	8,45	-1,28	-2,42	4,77E-02	DR
8430434A19Rik	AV169955	4,57	4,57	6,08	6,58	6,61	6,83	-1,60	-3,04	1,98E-02	DR
2610305J24Rik /// BC005512 /// LOC215866 /// LOC629242 /// EG630153 /// EG630525 /// LOC631386 /// LOC637482 /// LOC641366 /// EG668904 /// LOC669019 /// LOC669231 /// LOC669436 /// LOC670270 /// LOC670719 /// LOC672061 /// LOC672196 /// LOC672939 /// LOC673876 /// LOC674912 /// LOC674927 /// LOC675168 /// LOC675410 /// LOC675706 /// LOC676247 /// LOC676718 /// LOC677506	BC002257	7,32	7,31	7,67	8,09	8,60	9,02	-1,13	-2,20	8,92E-03	DR

Table S2.

Gene expression comparison between *Pax3*$^{Pax3\text{-}ERD/GFP}$ and *Pax3*$^{GFP/+}$ embryos. Down-regulated genes (DR) were selected when the p-value < 0.05 and the log of differential factor (logFC) < -1.

DISCUSSION

Function of Notch signalling pathway during adult myogenesis

After limb muscle progenitors have entered myogenesis and differentiated into myoblasts, their final step of differentiation is to fuse together to give rise to the first multinucleated myofibres (Mintz and Baker, 1967). Among adult tissues, the skeletal muscles display impressive regenerative capacities. Even after a severe injury, complete reestablishment with newly formed myoblasts fusing with the damaged muscle fibres or forming new fibres occurs within three weeks to restore muscle function (Rosenblatt, 1992). This includes not only fibre formation, but also re-establishing connections to the nervous system and patterning of the muscle vasculature. Satellite cells have been proposed to be the cell population responsible for generating myoblasts in the adult skeletal muscle (Katz, 1961; Mauro, 1961) and also in the sporadic events of muscle hypertrophy or repair (Zammit, 2008). When postnatal muscle growth is complete, satellite cells are located in a "niche" on the surface of the muscle fibres, embedded within the basal lamina. In this location, satellite cells exit the cell cycle and enter a state of quiescence characterised by a small cellular size and a low metabolic activity.

In the context of muscle regeneration, satellite cells re-enter the cell cycle to produce myoblasts to allow formation of new muscle fibres (Reznik, 1969). As they are able to produce differentiating muscle progenitors but also to self renew in order to maintain their population (Collins et al., 2005), satellite cells are considered as the adult muscle stem cells. Interestingly, as the muscle fibres reform, satellite cells re-populate their "niche" (Church et al., 1966), exit the cell cycle and re-enter quiescence. Hence, satellite cells are able to enter then exit the cell cycle at various time points during their life. Our results demonstrated that *p57* expression is correlated with muscle differentiation and that expression of the cell cycle exit effector *p57* is tightly regulated by the antagonist actions of MRFs and Notch signalling.

Notch signalling plays an essential role in maintaining the muscle progenitor cell pool to allow its expansion during development of the limb muscles. The ligand is provided by the surrounding myoblasts (Delfini et al., 2000; Mourikis et al., 2012a) in order to tightly control the balance between progenitor pool proliferation and myoblasts differentiation.

It has been shown in mouse that satellite cells require canonical Notch signalling to be sustained in a quiescent state as they express high levels of Notch receptors and Notch signalling target genes including *Hes1*, *Hey1* and *HeyL* (Bjornson et al., 2012; Mourikis et al., 2012a). Furthermore, inducible conditional deletion of *Rbpj* induces spontaneous differentiation of the satellite cells followed by depletion of the satellite cells pool after a period of 5 to 7 weeks (Bjornson et al., 2012; Mourikis et al., 2012a). This phenotype can be rescued by mutation of *MyoD* however, even if precocious differentiation is abrogated in these rescued myoblasts, they do not adopt a satellite cell position and poorly contribute to muscle fibre growth (Brohl et al., 2012). Together, these results suggest that Notch signalling represses differentiation of satellite cells and is necessary for their entry in quiescence. According to the anatomical position of satellite cells between the muscle fibre and the basal lamina, the myofibre is most likely providing the ligand to activate Notch signalling. However, evidence coming from genetic deletion of *Dll1* and *Dll4* in the muscle fibres is still missing to clearly demonstrate this point. In addition, whether a paracrine mechanism whereby soluble factors present in the satellite cell "niche" activate Notch signalling remains to be demonstrated (Mourikis and Tajbakhsh, 2014). One can also hypothesise a similar mechanism occuring during myotome formation (Rios et al., 2011) whereby Dll-expressing cells able to form long-range protrusions that could activate Notch signalling in satellite cells. However, the existence of such a mechanism and the identity of such a kind of cell remain to be elucidated.

In addition, it was shown that when *Rbpj* and *MyoD* are lost, satellite cells do not adhere to the myofibres and the assembly of the basal lamina around them is defective. These defects are associated with a down-regulation of the expression of basal lamina components and adhesion molecules in mutant myoblasts (Brohl et al., 2012). These observations suggest a second role for Notch signalling during myogenesis where, in addition to controlling the entry in quiescence and repressing myogenic differentiation, it is involved in regulating the homing of satellite cells into their "niche", by stimulating the production of molecules required for their microenvironment and their adhesion to myofibres.

Regulation of cell cycle exit during adult myogenesis

During embryonic myogenesis, Notch promotes cell proliferation. However recent reports demonstrate that upon muscle injury, activated satellite cells display a decrease of endogenous Notch signalling while they are proliferating (Bjornson et al., 2012; Mourikis et al., 2012a). Upon disruption of the satellite cells "niche", following muscle injury for example, satellite cells systematically exit quiescence to re-entrer the cell cycle and expand the muscle progenitors pool. This disruption of the "niche" could explain how Notch signalling gets down-regulated in satellite cells during muscle regeneration as the source of Notch ligand vanishes. Moreover, data coming from *Rbpj* mutant mice strongly argue for the dispensability of Notch signalling during expansion of the muscle progenitor cells following muscle injury (Mourikis et al., 2012a). In *Rbpj* mutant mice, regeneration of injured muscles is similar compared to control animals (Bjornson et al., 2012; Mourikis et al., 2012a). Hence, Notch signalling shut down may be a pre-requisite for correct muscle regeneration. In a study, the authors have constitutively activated Notch signalling in satellite cells by inserting NICD into the Rosa26 locus and revealed that these cells are unable to exit quiescence and present a severe diminution of their proliferation (Wen et al., 2012).

Together these results support the idea that Notch signalling needs to be shut down to allow satellite cells to exit quiescence and re-enter the cell cycle. This is consistent with the observation that p38 and MyoD are among the earliest makers of activated satellite cells and that their expressions have been demonstrated to be inhibited by Notch signalling (Kondoh et al., 2007; Mourikis et al., 2012b). However, during the phase of satellite cells amplification, once cells have exited quiescence, the mechanism regulating the balance between amplification of the satellite cells pool and myoblasts differentiation remains to be elucidated. One can only speculate about the use of the same mechanism as in the embryo, whereby Notch and the MRFs act in an antagonistic manner on the regulation of *p57*.

Finally, once foetal myoblasts differentiate to give rise to the satellite cells, they exit the cell cycle. However, this exit needs to be reversible in case of muscle injury. Comparison of chromatin landscapes of fusing myoblasts that definitively exit the cell cycle and satellite cells that must retain the capacity to re-enter the cell cycle would be of great interest for the understanding of the genetic regulation of cell cycle exit.

Conservation of Pax3 and Pax7 functions

During early muscle development, expression of *Pax3* is crucial for the survival, specification and expansions of muscle progenitor cells (Buckingham and Relaix, 2007) while *Pax7* function is revealed only when Pax3 is also impaired (Figure 7C of the Introduction; Relaix et al., 2005). *Pax7*-null mutant mice do not present with any muscle phenotype at birth (Mansouri et al., 1996) but replacement of the *Pax3* gene by the *Pax7* gene in mouse ($Pax3^{Pax7/Pax7}$) demonstrated that it could substitute for *Pax3* function in most tissues where *Pax3* is expressed, including the dorsal neural tube, neural crest cells and somites but not in limb muscles development (Relaix et al., 2004). Formation of limb muscles requires delamination, migration, and proliferation of

muscle progenitor cells. However, in *Pax3*$^{Pax7/Pax7}$embryos, *c-Met* expression is not properly activated in the hypaxial somite (Relaix et al., 2004). This suggests that activation of migration in muscle progenitor cells is a function exclusive to *Pax3* that was acquired after *Pax3* and *Pax7* have diverged during evolution. Strikingly, after birth, *Pax7*-null mutant mice present with severe growth retardation, with most of them being lost within two weeks (Seale et al., 2000) demonstrating that postnatally, *Pax7* is essential for muscle growth (Kuang et al., 2006; Oustanina et al., 2004; Relaix et al., 2006). This is correlated with a rapid depletion of the number of satellite cells in the absence of *Pax7*, demonstrating the essential function of *Pax7* in the maintenance of satellite cells. Consistently, loss of *Pax7* results in impaired skeletal muscle regeneration capacities due to the depletion of the satellite cells population (Oustanina et al., 2004; Relaix et al., 2006).

In order to get insight into the molecular mechanisms associated with *Pax3* and *Pax7* functions during myogenesis, ChIP-seq analyses were performed on adult myoblasts cultured *in vitro*. These analyses revealed that Pax3 only binds a small subset of Pax7 targets (Soleimani et al., 2012) and demonstrated that Pax3 and Pax7 do bind to identical DNA motifs but that Pax7 preferentially uses the homeodomain. Even if they identified a significant overlap between Pax3 and Pax7 transcriptional network, they also show that Pax7 could be acting as a pioneer transcription factor (Budry et al., 2012; Soleimani et al., 2012).

ChIP-seq analyses on craniofacial tissues remain a challenging issue, as there is no *in vitro* model recapitulating late CNCC development. Nevertheless, identification of Pax3 and Pax7 direct target genes in different tissues would be of great interest for the in-depth understanding of their functions during development.

Pax3 and *Pax7* have been described as essential factors for the formation of the neural crest (Basch et al., 2006; Betancur et al., 2010). However, our mouse mutants for *Pax3* and *Pax7* revealed that one copy of either of these two genes is sufficient to allow a correct craniofacial development (see figure S1E in Second Paper). This can be surprising when looking at *Pax3* and *Pax7* expression profiles in facial prominences. While *Pax3* is expressed in all prominences, *Pax7* expression is strictly restricted to the LNP. It is easy to understand how *Pax3* can compensate for *Pax7* loss during formation of the face in *Pax7* mutant. However, it remains puzzling to understand how *Pax7* compensates for *Pax3* loss in *Pax3* mutant as its expression domain remains unchanged (Relaix et al., 2004). While our work reveals the function of *Pax3* and *Pax7* in maintaining the growth of CNCC, their functions during early mouse neural crest development remains unclear. Interestingly, in $Pax3^{Pax7/Pax7}$embryos, migration of CNCC is not affected and the craniofacial complex develops normally (Relaix et al., 2004). This can suggest that *Pax3* and *Pax7* functions are more redundant in the CNCC development or, alternatively it can also reflect that GRNs controlling formation of the face are more robust than the ones controlling muscle development. The latter hypothesis seems more plausible when looking at the complexity of the GRNs controlling each different steps of CNCC development (Betancur et al., 2010), with several transcription factors being described to be binding to the same target gene to ensure its correct expression during the different processes of craniofacial development.

<u>*Pax3* and *Pax7* function during neural crest evolution</u>

In the tunicate *Ciona intestinalis*, forced expression of the neural crest specifier *Twist* is sufficient to reprogram cells from the cephalic melanocyte lineage into migrating neural crest-like cells (Abitua et al., 2012). These results suggest that the GRNs controlling neural crest development were in place before the apparition of vertebrates and that neural crest

evolution relied on the novel expression of transcription factors into neural plate border (Abitua et al., 2012), possibly via the reorganization of the embryonic layers and signalling pathways during evolution (Hall and Gillis, 2013).

Amphioxus are cephalochordates regarded as the closest living species related to the vertebrates (Hall and Gillis, 2013). Amphioxus contain only one *Pax3/7* gene called *Amphi-Pax3/7* (Holland et al., 1999), suggesting that *Pax3* and *Pax7* genes have arisen by gene duplication at the onset of vertebrate evolution (Holland et al., 1999). *Amphi-Pax3/7* expression suggests that a population of cells similar to the vertebrate premigratory neural crest cells may have been present in the common ancestor of all extant chordates (Holland et al., 1999). However, Amphioxus do not possess any migratory CNCC.

In order to evaluate *Pax3* and *Pax7* activity during evolution, we have performed evo-devo studies of *Pax3* and *Pax7* function. In $Pax3^{Amphi\text{-}Pax3/7/Amphi\text{-}Pax3/7}$; $Pax7^{LacZ/LacZ}$ mutant mouse embryos, the ancestral *Pax3/7* gene (*Amphi-Pax3/7*) replaces *Pax3* and *Pax7* is absent. Interestingly, despite the absence of both mouse *Pax3* and *Pax7* genes, these embryos present a normal craniofacial complex demonstrating that the ancestral *Amphi-Pax3/7* is able to replace *Pax3* and *Pax7* function during formation of the face (Hayashi et *al.*, unpublished). The fact that the ancestral *Amphi-Pax3/7* is able to activate the mouse GRNs controlling CNCC development argues against the idea that genomic landscapes necessary for formation of the vertebrate craniofacial complex were already present in pre-vertebrate species as it should then possess migratory CNCC. Presumably, apparition of the neural crest relied on the evolution of regulatory elements such as enhancers across the genome, allowing new expression of transcription factors in different locations.

Pax3 and *Pax7* tissue-specificity

Interestingly, inhibition of AhR signalling only rescues the craniofacial phenotype of $Pax3^{Pax3\text{-}ERD/GFP}$ mutant embryos. Severe defects in PNS and muscle development are maintained in the trunk of these embryos. This suggests that fundamental divergences exist between the GRNs controlling cranial and trunk neural crest development. Moreover, it points out that the regulation of AhR signalling by Pax3 may be a feature unique to the cranial neural crest. In the trunk, Pax3 has been shown to control migration and early specification of NCC generating the PNS (Van Ho et al., 2011; Tremblay et al., 1995). Plus, in $Pax3^{Pax3\text{-}ERD/GFP}$ mutant embryos trunk NCC do not migrate away from the neural tube suggesting an essential function of *Pax3* in early trunk NCC development (Relaix et *al.,* unpublished). In the head, our data demonstrate that *Pax3* is mainly involved in regulating the cell cycle progression of CNCC via the regulation of AhR signalling. Most probably, this reflects the wider range of derivatives that CNCC give rise to compare to trunk NCC. Our study has been focusing on mesenchymal cells generally. Analysis of the development of cranial PNS in $Pax3^{Pax3\text{-}ERD/GFP}$ mutant embryos would further confirm or refute the divergence between trunk and cranial GRNs governing NCC development.

A missing link between Pax3 and AhR

The analysis of $Pax3^{GFP/GFP}$; $Pax7^{LacZ/LacZ}$ and $Pax3^{Pax3\text{-}ERD/GFP}$ mutant embryos revealed the essential role of *Pax3* and *Pax7* in regulating cell cycle progression of mesenchymal cranial neural crest-derived cells via the restriction of AhR signalling expression and activity to specific locations in the facial prominences. However, our microarray screen clearly pointed out that *AhR* is not a direct target of Pax3 or Pax7 as it is up-regulated in dominant negative embryos. Among genes potentially linking Pax3 and AhR, *AP-2α* appears as a serious candidate. Mouse mutants for *AP-2α* display severe craniofacial malformations with defects of facial closure (Schorle et al., 1996) reminiscent of the phenotypes observed in our mutants.

In addition to *AP-2α* being strongly down-regulated in our screen, analysis of an intronic enhancer revealed the presence of two putative binding sites for Pax3 (Feng et al., 2008). Furthermore, whole genome analysis of AP-2α binding in human neural crest cells uncovered that AP-2α binds to *AhR* regulatory elements (Rada-Iglesias et al., 2012).

In our microarray screen, *AP-2α* expression is down-regulated while *AhR* is up regulated. An analysis of *AhR* expression in *AP-2α* mutant embryo would truly demonstrate this potential direct regulation of *AhR* by AP-2α and possibly elucidate the mechanism by which Pax3 regulates *AhR* expression during craniofacial development.

Function of AhR during development

Persistent activation of AhR due to TCDD exposition has been shown to result in a plethora of developmental and physiological defects including cognitive and locomotor abnormalities, teratogenesis, chloracne, endocrine and reproductive toxicity, cardiovascular diseases and an higher risk to develop certain cancers (Bock and Köhle, 2006). Once in a cell, TCDD is an almost non-metabolizable compound. Hence, TCDD-mediated activation of AhR may not reflect AhR inner function as it is activated 'too long and too hard' (Bock and Köhle, 2006).

AhR signalling activation can also be beneficial, especially when activated by transient ligands under physiological conditions. For instance, dietary plant constituents, especially cruciferous vegetables, which are metabolised in tryptophan derivatives, have been shown to enhance proliferation of the gut immune system (Kiss et al., 2011; Li et al., 2011). Moreover, other studies demonstrate that *in vitro* AhR binds directly in the first intron of *p21* (Barnes-Ellerbe et al., 2004; Dere et al., 2011; Lo and Matthews, 2012) and that it also regulates *p27* expression (Pang et al., 2008). While being performed in a different system than ours, these studies confirm that one of AhR's core functions during development and homeostasis is linked to the control of cell cycle progression.

The ability of AhR to bind TCDD has made it a crucial regulator of pollution-induced teratogenesis. However, it is believed that the AhR protein evolved about 450 million years ago, prior to the divergence of bony and cartilaginous fishes (Hankinson, 1995). At the time, natural fires were the only production source of dioxins. Hence, AhR signalling's primitive and major function during evolution must have been different than its now famous environmental stress response capacity. Consistently, our data show that during craniofacial development, Pax3 and Pax7 regulate AhR signalling expression and activity. Restriction of AhR signalling by Pax3 and Pax7 highlights a previously unknown key function for this pathway in controlling CNCC proliferation during craniofacial development.

REFERENCES

Abbott, B.D., Birnbaum, L.S., and Perdew, G.H. (1995). Developmental expression of two members of a new class of transcription factors: I. Expression of aryl hydrocarbon receptor in the C57BL/6N mouse embryo. Dev. Dyn. *204*, 133–143.

Abitua, P.B., Wagner, E., Navarrete, I.A., and Levine, M. (2012). Identification of a rudimentary neural crest in a non-vertebrate chordate. Nature *492*, 104–107.

Akiyama, H., Kim, J.-E.E., Nakashima, K., Balmes, G., Iwai, N., Deng, J.M., Zhang, Z., Martin, J.F., Behringer, R.R., Nakamura, T., et al. (2005). Osteo-chondroprogenitor cells are derived from Sox9 expressing precursors. Proc. Natl. Acad. Sci. U. S. A. *102*, 14665–14670.

Albini, S., and Puri, P.L. (2010). SWI/SNF complexes, chromatin remodeling and skeletal myogenesis: it's time to exchange! Exp. Cell Res. *316*, 3073–3080.

Alvares, E., Schubert, F.R., Thorpe, C., Mootoosamy, R.C., Cheng, L., Parkyn, G., Lumsden, A., Dietrich, S., and London, C. (2003). Intrinsic , Hox -Dependent Cues Determine. *5*, 379–390.

Amthor, H., Christ, B., and Patel, K. (1999). A molecular mechanism enabling continuous embryonic muscle growth - a balance between proliferation and differentiation. Development *126*, 1041–1053.

Armand, A.-S., Bourajjaj, M., Martínez-Martínez, S., el Azzouzi, H., da Costa Martins, P.A., Hatzis, P., Seidler, T., Redondo, J.M., and De Windt, L.J. (2008). Cooperative synergy between NFAT and MyoD regulates myogenin expression and myogenesis. J. Biol. Chem. *283*, 29004–29010.

Armand, O., Boutineau, A.M., Mauger, A., Pautou, M.P., and Kieny, M. (1983). Origin of satellite cells in avian skeletal muscles. Arch. Anat. Microsc. Morphol. Exp. *72*, 163–181.

Aulehla, A., Wiegraebe, W., Baubet, V., Wahl, M.B., Deng, C., Taketo, M., Lewandoski, M., and Pourquié, O. (2008). A beta-catenin gradient links the clock and wavefront systems in mouse embryo segmentation. Nat. Cell Biol. *10*, 186–193.

Bajard, L., Relaix, F., Lagha, M., Rocancourt, D., Daubas, P., and Buckingham, M.E. (2006). A novel genetic hierarchy functions during hypaxial myogenesis: Pax3 directly activates Myf5 in muscle progenitor cells in the limb. Genes Dev *20*, 2450–2464.

Barnes-Ellerbe, S., Knudsen, K.E., and Puga, A. (2004). 2,3,7,8-Tetrachlorodibenzo-p-dioxin blocks androgen-dependent cell proliferation of LNCaP cells through modulation of pRB phosphorylation. Mol. Pharmacol. *66*, 502–511.

Del Barrio, M.G., and Nieto, M.A. (2002). Overexpression of Snail family members highlights their ability to promote chick neural crest formation. Development *129*, 1583–1593.

Barrios, A., Poole, R.J., Durbin, L., Brennan, C., Holder, N., and Wilson, S.W. (2003). Eph/Ephrin Signaling Regulates the Mesenchymal-to-Epithelial Transition of the Paraxial Mesoderm during Somite Morphogenesis. Curr. Biol. *13*, 1571–1582.

Basch, M.L., Bronner-Fraser, M., and Garcia-Castro, M.I. (2006). Specification of the neural crest occurs during gastrulation and requires Pax7. Nature *441*, 218–222.

Batlle, E., Sancho, E., Francí, C., Domínguez, D., Monfar, M., Baulida, J., and García De Herreros, A. (2000). The transcription factor snail is a repressor of E-cadherin gene expression in epithelial tumour cells. Nat. Cell Biol. *2*, 84–89.

Beckers, J., Clark, A., Wünsch, K., Hrabé De Angelis, M., and Gossler, A. (1999). Expression of the mouse Delta1 gene during organogenesis and fetal development. Mech. Dev. *84*, 165–168.

Beischlag, T. V, Luis Morales, J., Hollingshead, B.D., and Perdew, G.H. (2008). The aryl hydrocarbon receptor complex and the control of gene expression. Crit. Rev. Eukaryot. Gene Expr. *18*, 207–250.

Ben-Yair, R., and Kalcheim, C. (2005). Lineage analysis of the avian dermomyotome sheet reveals the existence of single cells with both dermal and muscle progenitor fates. Development *132*, 689–701.

Bénazéraf, B., and Pourquié, O. (2013). Formation and segmentation of the vertebrate body axis. Annu. Rev. Cell Dev. Biol. *29*, 1–26.

Besson, A., Dowdy, S.F., and Roberts, J.M. (2008). CDK inhibitors: cell cycle regulators and beyond. Dev Cell *14*, 159–169.

Betancur, P., Bronner-Fraser, M., and Sauka-Spengler, T. (2010). Assembling neural crest regulatory circuits into a gene regulatory network. Annu Rev Cell Dev Biol *26*, 581–603.

Bhatt, S., Diaz, R., and Trainor, P.A. (2013). Signals and switches in Mammalian neural crest cell differentiation. Cold Spring Harb Perspect Biol *5*.

Birchmeier, C., and Brohmann, H. (2000). Genes that control the development of migrating muscle precursor cells. Curr Opin Cell Biol *12*, 725–730.

Bismuth, K., and Relaix, F. (2010). Genetic regulation of skeletal muscle development. Exp. Cell Res. *316*, 3081–3086.

Bjornson, C.R., Cheung, T.H., Liu, L., Tripathi, P. V, Steeper, K.M., and Rando, T.A. (2012). Notch signaling is necessary to maintain quiescence in adult muscle stem cells. Stem Cells *30*, 232–242.

Bladt, F., Riethmacher, D., Isenmann, S., Aguzzi, A., and Birchmeier, C. (1995). Essential role for the c-met receptor in the migration of myogenic precursor cells into the limb bud. Nature *376*, 768–771.

Blake, J.A., and Ziman, M.R. (2014). Pax genes: regulators of lineage specification and progenitor cell maintenance. Development *141*, 737–751.

Bock, K.W., and Köhle, C. (2006). Ah receptor: dioxin-mediated toxic responses as hints to deregulated physiologic functions. Biochem. Pharmacol. *72*, 393–404.

Borycki, A.G., Li, J., Jin, F., Emerson, C.P., and Epstein, J.A. (1999). Pax3 functions in cell survival and in pax7 regulation. Development *126*, 1665–1674.

Braun, T., Buschhausen-Denker, G., Bober, E., Tannich, E., and Arnold, H.H. (1989). A novel human muscle factor related to but distinct from MyoD1 induces myogenic conversion in 10T1/2 fibroblasts. EMBO J. *8*, 701–709.

Braun, T., Bober, E., Rudnicki, M.A., Jaenisch, R., and Arnold, H.H. (1994). MyoD expression marks the onset of skeletal myogenesis in Myf-5 mutant mice. Development *120*, 3083–3092.

Brohl, D., Vasyutina, E., Czajkowski, M.T., Griger, J., Rassek, C., Rahn, H.P., Purfurst, B., Wende, H., and Birchmeier, C. (2012). Colonization of the satellite cell niche by skeletal muscle progenitor cells depends on Notch signals. Dev Cell *23*, 469–481.

Bronner-Fraser, M., and Fraser, S.E. (1988). Cell lineage analysis reveals multipotency of some avian neural crest cells. Nature *335*, 161–164.

Buas, M.F., and Kadesch, T. (2010). Regulation of skeletal myogenesis by Notch. Exp Cell Res *316*, 3028–3033.

Buckingham, M., and Relaix, F. (2007). The role of Pax genes in the development of tissues and organs: Pax3 and Pax7 regulate muscle progenitor cell functions. Annu Rev Cell Dev Biol *23*, 645–673.

Buckingham, M., and Rigby, P.W. (2014). Gene Regulatory Networks and Transcriptional Mechanisms that Control Myogenesis. Dev. Cell *28*, 225–238.

Budry, L., Balsalobre, A., Gauthier, Y., Khetchoumian, K., L'honoré, A., Vallette, S., Brue, T., Figarella-Branger, D., Meij, B., and Drouin, J. (2012). The selector gene Pax7 dictates alternate pituitary cell fates through its pioneer action on chromatin remodeling. Genes Dev. *26*, 2299–2310.

Burstyn-Cohen, T., Stanleigh, J., Sela-Donenfeld, D., and Kalcheim, C. (2004). Canonical Wnt activity regulates trunk neural crest delamination linking BMP/noggin signaling with G1/S transition. Development *131*, 5327–5339.

Bush, J.O., and Jiang, R. (2012). Palatogenesis: morphogenetic and molecular mechanisms of secondary palate development. Development *139*, 231–243.

Cai, D.H., Vollberg, T.M., Hahn-Dantona, E., Quigley, J.P., and Brauer, P.R. (2000). MMP-2 expression during early avian cardiac and neural crest morphogenesis. Anat. Rec. *259*, 168–179.

Cano, A., Pérez-Moreno, M.A., Rodrigo, I., Locascio, A., Blanco, M.J., del Barrio, M.G., Portillo, F., and Nieto, M.A. (2000). The transcription factor snail controls epithelial-mesenchymal transitions by repressing E-cadherin expression. Nat. Cell Biol. *2*, 76–83.

Cao, Y., Yao, Z., Sarkar, D., Lawrence, M., Sanchez, G.J., Parker, M.H., MacQuarrie, K.L., Davison, J., Morgan, M.T., Ruzzo, W.L., et al. (2010). Genome-wide MyoD binding in skeletal muscle cells: a potential for broad cellular reprogramming. Dev Cell *18*, 662–674.

Carlson, M.E., and Conboy, I.M. (2007). Regulating the Notch pathway in embryonic, adult and old stem cells. Curr Opin Pharmacol *7*, 303–309.

Carlson, M.E., Hsu, M., and Conboy, I.M. (2008). Imbalance between pSmad3 and Notch induces CDK inhibitors in old muscle stem cells. Nature *454*, 528–532.

Carmona-Fontaine, C., Matthews, H.K., Kuriyama, S., Moreno, M., Dunn, G.A., Parsons, M., Stern, C.D., and Mayor, R. (2008). Contact inhibition of locomotion in vivo controls neural crest directional migration. Nature *456*, 957–961.

Cebra-Thomas, J.A., Betters, E., Yin, M., Plafkin, C., McDow, K., and Gilbert, S.F. (2007). Evidence that a late-emerging population of trunk neural crest cells forms the plastron bones in the turtle Trachemys scripta. Evol. Dev. *9*, 267–277.

Cebra-Thomas, J.A., Terrell, A., Branyan, K., Shah, S., Rice, R., Gyi, L., Yin, M., Hu, Y., Mangat, G., Simonet, J., et al. (2013). Late-emigrating trunk neural crest cells in turtle embryos generate an osteogenic ectomesenchyme in the plastron. Dev. Dyn. *242*, 1223–1235.

Cheng, M., Olivier, P., Diehl, J.A., Fero, M., Roussel, M.F., Roberts, J.M., and Sherr, C.J. (1999). The p21(Cip1) and p27(Kip1) CDK "inhibitors" are essential activators of cyclin D-dependent kinases in murine fibroblasts. EMBO J. *18*, 1571–1583.

Cheung, M., and Briscoe, J. (2003). Neural crest development is regulated by the transcription factor Sox9. Development *130*, 5681–5693.

Cheung, M., Chaboissier, M.-C., Mynett, A., Hirst, E., Schedl, A., and Briscoe, J. (2005). The transcriptional control of trunk neural crest induction, survival, and delamination. Dev. Cell *8*, 179–192.

Chi, N., and Epstein, J.A. (2002). Getting your Pax straight: Pax proteins in development and disease. Trends Genet. *18*, 41–47.

Chiang, C., Litingtung, Y., Lee, E., Young, K.E., Corden, J.L., Westphal, H., and Beachy, P.A. (1996). Cyclopia and defective axial patterning in mice lacking Sonic hedgehog gene function. Nature *383*, 407–413.

Christ, B., Huang, R., and Scaal, M. (2007). Amniote somite derivatives. Dev. Dyn. *236*, 2382–2396.

Church, J.C.T., Noronha, R.F.X., and Allbrook, D.B. (1966). Satellite cells and skeletal muscle regeneration. Br. J. Surg. *53*, 638–642.

Clouthier, D.E., Hosoda, K., Richardson, J.A., Williams, S.C., Yanagisawa, H., Kuwaki, T., Kumada, M., Hammer, R.E., and Yanagisawa, M. (1998). Cranial and cardiac neural crest defects in endothelin-A receptor-deficient mice. Development *125*, 813–824.

Collins, C.A., Olsen, I., Zammit, P.S., Heslop, L., Petrie, A., Partridge, T.A., and Morgan, J.E. (2005). Stem cell function, self-renewal, and behavioral heterogeneity of cells from the adult muscle satellite cell niche. Cell *122*, 289–301.

Conway, S.J., Henderson, D.J., and Copp, A.J. (1997a). Pax3 is required for cardiac neural crest migration in the mouse: evidence from the splotch (Sp2H) mutant. Development *124*, 505–514.

Conway, S.J., Henderson, D.J., Kirby, M.L., Anderson, R.H., and Copp, A.J. (1997b). Development of a lethal congenital heart defect in the splotch (Pax3) mutant mouse. Cardiovasc. Res. *36*, 163–173.

Conway, S.J., Godt, R.E., Hatcher, C.J., Leatherbury, L., Zolotouchnikov, V. V, Brotto, M.A., Copp, A.J., Kirby, M.L., and Creazzo, T.L. (1997c). Neural crest is involved in development of abnormal myocardial function. J. Mol. Cell. Cardiol. *29*, 2675–2685.

Conway, S.J., Bundy, J., Chen, J., Dickman, E., Rogers, R., and Will, B.M. (2000). Decreased neural crest stem cell expansion is responsible for the conotruncal heart defects within the splotch (Sp(2H))/Pax3 mouse mutant. Cardiovasc. Res. *47*, 314–328.

Cook, M., and Tyers, M. (2007). Size control goes global. Curr Opin Biotechnol *18*, 341–350.

Del Corral, R.D., Olivera-Martinez, I., Goriely, A., Gale, E., Maden, M., and Storey, K. (2003). Opposing FGF and retinoid pathways control ventral neural pattern, neuronal differentiation, and segmentation during body axis extension. Neuron *40*, 65–79.

Couly, G., Grapin-Botton, A., Coltey, P., Ruhin, B., and Le Douarin, N.M. (1998). Determination of the identity of the derivatives of the cephalic neural crest: incompatibility between Hox gene expression and lower jaw development. Development *125*, 3445–3459.

Couly, G.F., Coltey, P.M., and Le Douarin, N.M. (1993). The triple origin of skull in higher vertebrates: a study in quail-chick chimeras. Development *117*, 409–429.

Courtney, K.D., and Moore, J.A. (1971). Teratology studies with 2,4,5-trichlorophenoxyacetic acid and 2,3,7,8-tetrachlorodibenzo-p-dioxin. Toxicol. Appl. Pharmacol. *20*, 396–403.

Crane, J.F., and Trainor, P.A. (2006). Neural crest stem and progenitor cells. Annu. Rev. Cell Dev. Biol. *22*, 267–286.

Creuzet, S., Couly, G., Vincent, C., and Le Douarin, N.M. (2002). Negative effect of Hox gene expression on the development of the neural crest-derived facial skeleton. Development *129*, 4301–4313.

Creuzet, S., Couly, G., and Le Douarin, N.M. (2005). Patterning the neural crest derivatives during development of the vertebrate head: insights from avian studies. J Anat *207*, 447–459.

Cusella-De Angelis, M.G., Molinari, S., Le Donne, A., Coletta, M., Vivarelli, E., Bouche, M., Molinaro, M., Ferrari, S., and Cossu, G. (1994). Differential response of embryonic and fetal myoblasts to TGF beta: a possible regulatory mechanism of skeletal muscle histogenesis. Development *120*, 925–933.

Daston, G., Lamar, E., Olivier, M., and Goulding, M. (1996). Pax-3 is necessary for migration but not differentiation of limb muscle precursors in the mouse. Development *122*, 1017–1027.

Davidson, E.H. (2010). Emerging properties of animal gene regulatory networks. Nature *468*, 911–920.

Delfini, M.-C., Dubrulle, J., Malapert, P., Chal, J., and Pourquié, O. (2005). Control of the segmentation process by graded MAPK/ERK activation in the chick embryo. Proc. Natl. Acad. Sci. U. S. A. *102*, 11343–11348.

Delfini, M.C., Hirsinger, E., Pourquie, O., Duprez, D., and Pourquié, O. (2000). Delta 1-activated notch inhibits muscle differentiation without affecting Myf5 and Pax3 expression in chick limb myogenesis. Development *127*, 5213–5224.

Depew, M.J., Lufkin, T., and Rubenstein, J.L.R. (2002). Specification of jaw subdivisions by Dlx genes. Science (80-.). *298*, 381–385.

Dequéant, M.-L., and Pourquié, O. (2008). Segmental patterning of the vertebrate embryonic axis. Nat. Rev. Genet. *9*, 370–382.

Dere, E., Lo, R., Celius, T., Matthews, J., and Zacharewski, T.R. (2011). Integration of genome-wide computation DRE search, AhR ChIP-chip and gene expression analyses of TCDD-elicited responses in the mouse liver. BMC Genomics *12*, 365.

Dias, A.S., de Almeida, I., Belmonte, J.M., Glazier, J. a, and Stern, C.D. (2014). Somites without a clock. Science *343*, 791–795.

Dietrich, S., Schubert, F.R., Healy, C., Sharpe, P.T., and Lumsden, a (1998). Specification of the hypaxial musculature. Development *125*, 2235–2249.

Dietrich, S., Abou-Rebyeh, F., Brohmann, H., Bladt, F., Sonnenberg-Riethmacher, E., Yamaai, T., Lumsden, A., Brand-Saberi, B., and Birchmeier, C. (1999). The role of SF/HGF and c-Met in the development of skeletal muscle. Development *126*, 1621–1629.

Dilworth, F.J., Seaver, K.J., Fishburn, A.L., Htet, S.L., and Tapscott, S.J. (2004). In vitro transcription system delineates the distinct roles of the coactivators pCAF and p300 during MyoD/E47-dependent transactivation. Proc. Natl. Acad. Sci. U. S. A. *101*, 11593–11598.

Dixon, M.J., Marazita, M.L., Beaty, T.H., and Murray, J.C. (2011). Cleft lip and palate: understanding genetic and environmental influences. Nat Rev Genet *12*, 167–178.

Le Douarin, N. (1973). A biological cell labeling technique and its use in expermental embryology. Dev. Biol. *30*, 217–222.

Le Douarin, N.M. (2004). The avian embryo as a model to study the development of the neural crest: a long and still ongoing story. Mech Dev *121*, 1089–1102.

Le Douarin, N., and Kalcheim, C. (1999). The Neural Crest (Cambridge University Press).

Le Douarin, N.M., and Dupin, E. (2012). The neural crest in vertebrate evolution. Curr. Opin. Genet. Dev. *22*, 381–389.

Le Douarin, N.M., Creuzet, S., Couly, G., and Dupin, E. (2004). Neural crest cell plasticity and its limits. Development *131*, 4637–4650.

Dubrulle, J., McGrew, M.J., and Pourqui??, O. (2001). FGF signaling controls somite boundary position and regulates segmentation clock control of spatiotemporal Hox gene activation. Cell *106*, 219–232.

Dupin, E., Calloni, G.W., and Le Douarin, N.M. (2010). The cephalic neural crest of amniote vertebrates is composed of a large majority of precursors endowed with neural, melanocytic, chondrogenic and osteogenic potentialities. Cell Cycle *9*, 238–249.

Endo, Y., Osumi, N., and Wakamatsu, Y. (2002). Bimodal functions of Notch-mediated signaling are involved in neural crest formation during avian ectoderm development. Development *129*, 863–873.

Engleka, K.A., Gitler, A.D., Zhang, M., Zhou, D.D., High, F.A., and Epstein, J.A. (2005). Insertion of Cre into the Pax3 locus creates a new allele of Splotch and identifies unexpected Pax3 derivatives. Dev Biol *280*, 396–406.

Epstein, D.J., Vekemans, M., and Gros, P. (1991). splotch (Sp2H), a mutation affecting development of the mouse neural tube, shows a deletion within the paired homeodomain of Pax-3. Cell *67*, 767–774.

Epstein, J.A., Shapiro, D.N., Cheng, J., Lam, P.Y., and Maas, R.L. (1996). Pax3 modulates expression of the c-Met receptor during limb muscle development. Proc. Natl. Acad. Sci. U. S. A. *93*, 4213–4218.

Epstein, J.A., Li, J., Lang, D., Chen, F., Brown, C.B., Jin, F., Lu, M.M., Thomas, M., Liu, E., Wessels, A., et al. (2000). Migration of cardiac neural crest cells in Splotch embryos. Development *127*, 1869–1878.

Escot, S., Blavet, C., Härtle, S., Duband, J.-L., and Fournier-Thibault, C. (2013). Misregulation of SDF1-CXCR4 signaling impairs early cardiac neural crest cell migration leading to conotruncal defects. Circ. Res. *113*, 505–516.

Feng, W., Huang, J., Zhang, J., and Williams, T. (2008). Identification and analysis of a conserved Tcfap2a intronic enhancer element required for expression in facial and limb bud mesenchyme. Mol. Cell. Biol. *28*, 315–325.

Ferguson, C.A., Tucker, A.S., and Sharpe, P.T. (2000). Temporospatial cell interactions regulating mandibular and maxillary arch patterning. Development *127*, 403–412.

Fernandez-Salguero, P., Pineau, T., Hilbert, D.M., McPhail, T., Lee, S.S., Kimura, S., Nebert, D.W., Rudikoff, S., Ward, J.M., and Gonzalez, F.J. (1995). Immune system impairment and hepatic fibrosis in mice lacking the dioxin-binding Ah receptor. Sci. (New York, NY) *268*, 722–726.

Floss, T., Arnold, H.H., and Braun, T. (1996). Myf-5(m1)/Myf-6(m1) compound heterozygous mouse mutants down-regulate Myf-5 expression and exert rib defects: evidence for long-range cis effects on Myf-5 transcription. Dev. Biol. *174*, 140–147.

Franz, T. (1992). Neural tube defects without neural crest defects in splotch mice. Teratology *46*, 599–604.

Franz, T., and Kothary, R. (1993). Characterization of the neural crest defect in Splotch (Sp1H) mutant mice using a lacZ transgene. Brain Res Dev Brain Res *72*, 99–105.

Fukada, S., Yamaguchi, M., Kokubo, H., Ogawa, R., Uezumi, A., Yoneda, T., Matev, M.M., Motohashi, N., Ito, T., Zolkiewska, A., et al. (2011). Hesr1 and Hesr3 are essential to generate undifferentiated quiescent satellite cells and to maintain satellite cell numbers. Development *138*, 4609–4619.

Furness, S.G., Lees, M.J., and Whitelaw, M.L. (2007). The dioxin (aryl hydrocarbon) receptor as a model for adaptive responses of bHLH/PAS transcription factors. FEBS Lett *581*, 3616–3625.

Gammill, L.S., Gonzalez, C., and Bronner-Fraser, M. (2007). Neuropilin 2/semaphorin 3F signaling is essential for cranial neural crest migration and trigeminal ganglion condensation. Dev. Neurobiol. *67*, 47–56.

Gans, C., and Northcutt, R.G. (1983). Neural crest and the origin of vertebrates: a new head. Sci. (New York, NY) *220*, 268–273.

García-Castro, M.I., Marcelle, C., and Bronner-Fraser, M. (2002). Ectodermal Wnt function as a neural crest inducer. Science *297*, 848–851.

Gensch, N., Borchardt, T., Schneider, A., Riethmacher, D., and Braun, T. (2008). Different autonomous myogenic cell populations revealed by ablation of Myf5-expressing cells during mouse embryogenesis. Development *135*, 1597–1604.

Gerber, A.N., Klesert, T.R., Bergstrom, D.A., and Tapscott, S.J. (1997). Two domains of MyoD mediate transcriptional activation of genes in repressive chromatin: a mechanism for lineage determination in myogenesis. Genes Dev. *11*, 436–450.

Gierthy, J.F., and Crane, D. (1984). Reversible inhibition of in vitro epithelial cell proliferation by 2,3,7,8-tetrachlorodibenzo-p-dioxin. Toxicol. Appl. Pharmacol. *74*, 91–98.

Gilbert, S.F. (2013). Developmental Biology 10th edition.

Gilbert-Barness, E. (2010). Teratogenic causes of malformations. Ann. Clin. Lab. Sci. *40*, 99–114.

Giordani, J., Bajard, L., Demignon, J., Daubas, P., Buckingham, M., and Maire, P. (2007). Six proteins regulate the activation of Myf5 expression in embryonic mouse limbs. Proc. Natl. Acad. Sci. U. S. A. *104*, 11310–11315.

Glazier, J.A., Zhang, Y., Swat, M., Zaitlen, B., and Schnell, S. (2008). Coordinated action of N-CAM, N-cadherin, EphA4, and ephrinB2 translates genetic prepatterns into structure during somitogenesis in chick. Curr. Top. Dev. Biol. *81*, 205–247.

Golding, J.P., Trainor, P., Krumlauf, R., and Gassmann, M. (2000). Defects in pathfinding by cranial neural crest cells in mice lacking the neuregulin receptor ErbB4. Nat. Cell Biol. *2*, 103–109.

Golding, J.P., Sobieszczuk, D., Dixon, M., Coles, E., Christiansen, J., Wilkinson, D., and Gassmann, M. (2004). Roles of erbB4, rhombomere-specific, and rhombomere-independent cues in maintaining neural crest-free zones in the embryonic head. Dev. Biol. *266*, 361–372.

Gonzalez, F.J., and Fernandez-Salguero, P. (1998). The aryl hydrocarbon receptor: studies using the AHR-null mice. Drug Metab Dispos *26*, 1194–1198.

Goulding, M.D., Chalepakis, G., Deutsch, U., Erselius, J.R., and Gruss, P. (1991). Pax-3, a novel murine DNA binding protein expressed during early neurogenesis. EMBO J *10*, 1135–1147.

Grammatopoulos, G.A., Bell, E., Toole, L., Lumsden, A., and Tucker, A.S. (2000). Homeotic transformation of branchial arch identity after Hoxa2 overexpression. Development *127*, 5355–5365.

Grifone, R., Demignon, J., Houbron, C., Souil, E., Niro, C., Seller, M.J., Hamard, G., and Maire, P. (2005). Six1 and Six4 homeoproteins are required for Pax3 and Mrf expression during myogenesis in the mouse embryo. Development *132*, 2235–2249.

Grifone, R., Demignon, J., Giordani, J., Niro, C., Souil, E., Bertin, F., Laclef, C., Xu, P.-X., and Maire, P. (2007). Eya1 and Eya2 proteins are required for hypaxial somitic myogenesis in the mouse embryo. Dev. Biol. *302*, 602–616.

Gros, J., Manceau, M., Thome, V., and Marcelle, C. (2005). A common somitic origin for embryonic muscle progenitors and satellite cells. Nature *435*, 954–958.

Haldar, M., Karan, G., Tvrdik, P., and Capecchi, M.R. (2008). Two cell lineages, myf5 and myf5-independent, participate in mouse skeletal myogenesis. Dev. Cell *14*, 437–445.

Halevy, O., Novitch, B.G., Spicer, D.B., Skapek, S.X., Rhee, J., Hannon, G.J., Beach, D., and Lassar, A.B. (1995). Correlation of terminal cell cycle arrest of skeletal muscle with induction of p21 by MyoD. Science (80-.). *267*, 1018–1021.

Hall, B.K. (2000). The neural crest as a fourth germ layer and vertebrates as quadroblastic not triploblastic. Evol. Dev. *2*, 3–5.

Hall, B.K. (2008). The neural crest and neural crest cells: discovery and significance for theories of embryonic organization. J. Biosci. *33*, 781–793.

Hall, B.K., and Gillis, J.A. (2013). Incremental evolution of the neural crest, neural crest cells and neural crest-derived skeletal tissues. J. Anat. *222*, 19–31.

Han, J., Ishii, M., Bringas, P., Maas, R.L., Maxson, R.E., and Chai, Y. (2007). Concerted action of Msx1 and Msx2 in regulating cranial neural crest cell differentiation during frontal bone development. Mech. Dev. *124*, 729–745.

Hankinson, O. (1995). The aryl hydrocarbon receptor complex. Annu Rev Pharmacol Toxicol *35*, 307–340.

Hankinson, O. (2005). Role of coactivators in transcriptional activation by the aryl hydrocarbon receptor. Arch. Biochem. Biophys. *433*, 379–386.

Hasty, P., Bradley, A., Morris, J.H., Edmondson, D.G., Venuti, J.M., Olson, E.N., and Klein, W.H. (1993). Muscle deficiency and neonatal death in mice with a targeted mutation in the myogenin gene. Nature *364*, 501–506.

Helms, J.A., and Schneider, R.A. (2003). Cranial skeletal biology. Nature *423*, 326–331.

Helms, J.A., Cordero, D., and Tapadia, M.D. (2005). New insights into craniofacial morphogenesis. Development *132*, 851–861.

Henderson, D.J., Ybot-Gonzalez, P., and Copp, A.J. (1997). Over-expression of the chondroitin sulphate proteoglycan versican is associated with defective neural crest migration in the Pax3 mutant mouse (splotch). Mech. Dev. *69*, 39–51.

Hirsinger, E., Malapert, P., Dubrulle, J., Delfini, M.C., Duprez, D., Henrique, D., Ish-Horowicz, D., and Pourquie, O. (2001). Notch signalling acts in postmitotic avian myogenic cells to control MyoD activation. Development *128*, 107–116.

Van Ho, A.T., Hayashi, S., Brohl, D., Aurade, F., Rattenbach, R., and Relaix, F. (2011). Neural crest cell lineage restricts skeletal muscle progenitor cell differentiation through Neuregulin1-ErbB3 signaling. Dev Cell *21*, 273–287.

Holland, L.Z., Schubert, M., Kozmik, Z., and Holland, N.D. (1999). AmphiPax3/7, an amphioxus paired box gene: insights into chordate myogenesis, neurogenesis, and the possible evolutionary precursor of definitive vertebrate neural crest. Evol. Dev. *1*, 153–165.

Holleville, N., Matéos, S., Bontoux, M., Bollerot, K., and Monsoro-Burq, A.-H. (2007). Dlx5 drives Runx2 expression and osteogenic differentiation in developing cranial suture mesenchyme. Dev. Biol. *304*, 860–874.

Hong, C.-S.S., and Saint-Jeannet, J.-P.P. (2007). The activity of Pax3 and Zic1 regulates three distinct cell fates at the neural plate border. Mol. Biol. Cell *18*, 2192–2202.

Houzelstein, D., Cohen, A., Buckingham, M.E., and Robert, B. (1997). Insertional mutation of the mouse Msx1 homeobox gene by an nlacZ reporter gene. Mech Dev *65*, 123–133.

Houzelstein, D., Auda-Boucher, G., Chéraud, Y., Rouaud, T., Blanc, I., Tajbakhsh, S., Buckingham, M.E., Fontaine-Pérus, J., and Robert, B. (1999). The homeobox gene Msx1 is expressed in a subset of somites, and in muscle progenitor cells migrating into the forelimb. Development *126*, 2689–2701.

Hu, D., and Marcucio, R.S. (2012). Neural crest cells pattern the surface cephalic ectoderm during FEZ formation. Dev. Dyn. *241*, 732–740.

Hu, D., Marcucio, R.S., and Helms, J.A. (2003). A zone of frontonasal ectoderm regulates patterning and growth in the face. Development *130*, 1749–1758.

Hunter, M.P., and Prince, V.E. (2002). Zebrafish hox paralogue group 2 genes function redundantly as selector genes to pattern the second pharyngeal arch. Dev. Biol. *247*, 367–389.

Hutcheson, D.A., Zhao, J., Merrell, A., Haldar, M., and Kardon, G. (2009). Embryonic and fetal limb myogenic cells are derived from developmentally distinct progenitors and have different requirements for beta-catenin. Genes Dev. *23*, 997–1013.

Ido, A., and Ito, K. (2006). Expression of chondrogenic potential of mouse trunk neural crest cells by FGF2 treatment. Dev. Dyn. *235*, 361–367.

Ikeya, M., and Takada, S. (1998). Wnt signaling from the dorsal neural tube is required for the formation of the medial dermomyotome. Development *125*, 4969–4976.

Ishii, M., Han, J., Yen, H.-Y., Sucov, H.M., Chai, Y., and Maxson, R.E. (2005). Combined deficiencies of Msx1 and Msx2 cause impaired patterning and survival of the cranial neural crest. Development *132*, 4937–4950.

Jain, S., Maltepe, E., Lu, M.M., Simon, C., and Bradfield, C.A. (1998). Expression of ARNT, ARNT2, HIF1 alpha, HIF2 alpha and Ah receptor mRNAs in the developing mouse. Mech. Dev. *73*, 117–123.

Jarriault, S., Le Bail, O., Hirsinger, E., Pourquié, O., Logeat, F., Strong, C.F., Brou, C., Seidah, N.G., and Isra l, A. (1998). Delta-1 activation of notch-1 signaling results in HES-1 transactivation. Mol. Cell. Biol. *18*, 7423–7431.

Jiang, X., Iseki, S., Maxson, R.E., Sucov, H.M., and Morriss-Kay, G.M. (2002). Tissue origins and interactions in the mammalian skull vault. Dev. Biol. *241*, 106–116.

Jin, D.Q., Jung, J.W., Lee, Y.S., and Kim, J.A. (2004). 2,3,7,8-Tetrachlorodibenzo-p-dioxin inhibits cell proliferation through arylhydrocarbon receptor-mediated G1 arrest in SK-N-SH human neuronal cells. Neurosci. Lett. *363*, 69–72.

Johnson, R.L., Laufer, E., Riddle, R.D., and Tabin, C. (1994). Ectopic expression of Sonic hedgehog alters dorsal-ventral patterning of somites. Cell *79*, 1165–1173.

Kablar, B., Krastel, K., Ying, C., Asakura, A., Tapscott, S.J., and Rudnicki, M.A. (1997). MyoD and Myf-5 differentially regulate the development of limb versus trunk skeletal muscle. Development *124*, 4729–4738.

Kassar-Duchossoy, L., Gayraud-Morel, B., Gomès, D., Rocancourt, D., Buckingham, M., Shinin, V., and Tajbakhsh, S. (2004). Mrf4 determines skeletal muscle identity in Myf5:Myod double-mutant mice. Nature *431*, 466–471.

Kassar-Duchossoy, L., Giacone, E., Gayraud-Morel, B., Jory, A., Gomes, D., and Tajbakhsh, S. (2005). Pax3/Pax7 mark a novel population of primitive myogenic cells during development. Genes Dev *19*, 1426–1431.

Katz, B. (1961). The Terminations of the Afferent Nerve Fibre in the Muscle Spindle of the Frog. Philos. Trans. R. Soc. B Biol. Sci. *243*, 221–240.

Kiecker, C., and Lumsden, A. (2005). Compartments and their boundaries in vertebrate brain development. Nat. Rev. Neurosci. *6*, 553–564.

King-Heiden, T.C., Mehta, V., Xiong, K.M., Lanham, K.A., Antkiewicz, D.S., Ganser, A., Heideman, W., and Peterson, R.E. (2012). Reproductive and developmental toxicity of dioxin in fish. Mol Cell Endocrinol *354*, 121–138.

Kiss, E.A., Vonarbourg, C., Kopfmann, S., Hobeika, E., Finke, D., Esser, C., and Diefenbach, A. (2011). Natural aryl hydrocarbon receptor ligands control organogenesis of intestinal lymphoid follicles. Science (80-.). *334*, 1561–1565.

Kist, R., Greally, E., and Peters, H. (2007). Derivation of a mouse model for conditional inactivation of Pax9. Genesis *45*, 460–464.

Kitamoto, T., and Hanaoka, K. (2010). Notch3 null mutation in mice causes muscle hyperplasia by repetitive muscle regeneration. Stem Cells *28*, 2205–2216.

Knecht, A.K., and Bronner-Fraser, M. (2002). Induction of the neural crest: a multigene process. Nat Rev Genet *3*, 453–461.

Kondoh, K., Sunadome, K., and Nishida, E. (2007). Notch signaling suppresses p38 MAPK activity via induction of MKP-1 in myogenesis. J. Biol. Chem. *282*, 3058–3065.

Kopan, R., Nye, J.S., and Weintraub, H. (1994). The intracellular domain of mouse Notch: a constitutively activated repressor of myogenesis directed at the basic helix-loop-helix region of MyoD. Development *120*, 2385–2396.

Kransler, K.M., McGarrigle, B.P., and Olson, J.R. (2007). Comparative developmental toxicity of 2,3,7,8-tetrachlorodibenzo-p-dioxin in the hamster, rat and guinea pig. Toxicology *229*, 214–225.

Kuang, S., Chargé, S.B., Seale, P., Huh, M., and Rudnicki, M.A. (2006). Distinct roles for Pax7 and Pax3 in adult regenerative myogenesis. J. Cell Biol. *172*, 103–113.

Kulesa, P.M., Bailey, C.M., Kasemeier-Kulesa, J.C., and McLennan, R. (2010). Cranial neural crest migration: new rules for an old road. Dev. Biol. *344*, 543–554.

De la Serna, I.L., Carlson, K.A., and Imbalzano, A.N. (2001). Mammalian SWI/SNF complexes promote MyoD-mediated muscle differentiation. Nat. Genet. *27*, 187–190.

De la Serna, I.L., Ohkawa, Y., Berkes, C.A., Bergstrom, D.A., Dacwag, C.S., Tapscott, S.J., and Imbalzano, A.N. (2005). MyoD targets chromatin remodeling complexes to the myogenin locus prior to forming a stable DNA-bound complex. Mol. Cell. Biol. *25*, 3997–4009.

LaBonne, C., and Bronner-Fraser, M. (1998). Neural crest induction in Xenopus: evidence for a two-signal model. Development *125*, 2403–2414.

Landacre, F.L. (1921). The fate of the neural crest in the head of the urodeles. J. Comp. Neurol. *33*, 1–43.

Lang, D., Chen, F., Milewski, R., Li, J., Lu, M.M., and Epstein, J.A. (2000). Pax3 is required for enteric ganglia formation and functions with Sox10 to modulate expression of c-ret. J. Clin. Invest. *106*, 963–971.

Lee, Y.-H., and Saint-Jeannet, J.-P. (2011). Sox9 function in craniofacial development and disease. Genesis *49*, 200–208.

Lepper, C., and Fan, C.M. (2010). Inducible lineage tracing of Pax7-descendant cells reveals embryonic origin of adult satellite cells. Genesis *48*, 424–436.

Li, Y., Innocentin, S., Withers, D.R., Roberts, N.A., Gallagher, A.R., Grigorieva, E.F., Wilhelm, C., and Veldhoen, M. (2011). Exogenous stimuli maintain intraepithelial lymphocytes via aryl hydrocarbon receptor activation. Cell *147*, 629–640.

Lo, R., and Matthews, J. (2012). High-Resolution Genome-wide Mapping of AHR and ARNT Binding Sites by ChIP-Seq. Toxicol. Sci. *130*, 349–361.

Lumsden, A., and Guthrie, S. (1991). Alternating patterns of cell surface properties and neural crest cell migration during segmentation of the chick hindbrain. Development *Suppl 2*, 9–15.

Luo, T., Lee, Y.-H., Saint-Jeannet, J.-P., and Sargent, T.D. (2003). Induction of neural crest in Xenopus by transcription factor AP2alpha. Proc. Natl. Acad. Sci. U. S. A. *100*, 532–537.

Manceau, M., Gros, J., Savage, K., Thome, V., McPherron, A., Paterson, B., and Marcelle, C. (2008). Myostatin promotes the terminal differentiation of embryonic muscle progenitors. Genes Dev *22*, 668–681.

Mankoo, B.S., Collins, N.S., Ashby, P., Grigorieva, E., Pevny, L.H., Candia, A., Wright, C. V, Rigby, P.W., and Pachnis, V. (1999). Mox2 is a component of the genetic hierarchy controlling limb muscle development. Nature *400*, 69–73.

Mansouri, A., Stoykova, A., Torres, M., and Gruss, P. (1996). Dysgenesis of cephalic neural crest derivatives in Pax7-/- mutant mice. Development *122*, 831–838.

Marchant, L., Linker, C., Ruiz, P., Guerrero, N., and Mayor, R. (1998). The inductive properties of mesoderm suggest that the neural crest cells are specified by a BMP gradient. Dev. Biol. *198*, 319–329.

Marlowe, J., and Puga, A. (2005). Aryl hydrocarbon receptor, cell cycle regulation, toxicity, and tumorigenesis. J. Cell. Biochem. *96*, 1174–1184.

Maroto, M., Bone, R.A., and Dale, J.K. (2012). Somitogenesis. Development *139*, 2453–2456.

Martinsen, B.J., and Bronner-Fraser, M. (1998). Neural crest specification regulated by the helix-loop-helix repressor Id2. Science *281*, 988–991.

Mauro, A. (1961). Satellite cell of skeletal muscle fibers. J. Biophys. Biochem. Cytol. *9*, 493–495.

Mayeuf, A., and Relaix, F. (2011). [Notch pathway: from development to regeneration of skeletal muscle]. Med. Sci. (Paris). *27*, 521–526.

Mayor, R., and Carmona-Fontaine, C. (2010). Keeping in touch with contact inhibition of locomotion. Trends Cell Biol. *20*, 319–328.

Mayor, R., Guerrero, N., and Martínez, C. (1997). Role of FGF and noggin in neural crest induction. Dev. Biol. *189*, 1–12.

McKeown, S.J., Lee, V.M., Bronner-Fraser, M., Newgreen, D.F., and Farlie, P.G. (2005). Sox10 overexpression induces neural crest-like cells from all dorsoventral levels of the neural tube but inhibits differentiation. Dev. Dyn. *233*, 430–444.

McLennan, R., Teddy, J.M., Kasemeier-Kulesa, J.C., Romine, M.H., and Kulesa, P.M. (2010). Vascular endothelial growth factor (VEGF) regulates cranial neural crest migration in vivo. Dev. Biol. *339*, 114–125.

Merlo, G.R., Zerega, B., Paleari, L., Trombino, S., Mantero, S., and Levi, G. (2000). Multiple functions of Dlx genes. Int. J. Dev. Biol. *44*, 619–626.

Milet, C., Maczkowiak, F., Roche, D.D., and Monsoro-Burq, A.H. (2013). Pax3 and Zic1 drive induction and differentiation of multipotent, migratory, and functional neural crest in Xenopus embryos. Proc Natl Acad Sci U S A *110*, 5528–5533.

Mimura, J., and Fujii-Kuriyama, Y. (2003). Functional role of AhR in the expression of toxic effects by TCDD. Biochim. Biophys. Acta *1619*, 263–268.

Mimura, J., Yamashita, K., Nakamura, K., Morita, M., Takagi, T.N., Nakao, K., Ema, M., Sogawa, K., Yasuda, M., Katsuki, M., et al. (1997). Loss of teratogenic response to 2,3,7,8-tetrachlorodibenzo-p-dioxin (TCDD) in mice lacking the Ah (dioxin) receptor. Genes Cells *2*, 645–654.

Minchin, J.E., and Hughes, S.M. (2008). Sequential actions of Pax3 and Pax7 drive xanthophore development in zebrafish neural crest. Dev Biol *317*, 508–522.

Minoux, M., and Rijli, F.M. (2010). Molecular mechanisms of cranial neural crest cell migration and patterning in craniofacial development. Development *137*, 2605–2621.

Mintz, B., and Baker, W.W. (1967). Normal mammalian muscle differentiation and gene control of isocitrate dehydrogenase synthesis. Proc. Natl. Acad. Sci. U. S. A. *58*, 592–598.

Mitchell, P.J., Timmons, P.M., Hébert, J.M., Rigby, P.W., and Tjian, R. (1991). Transcription factor AP-2 is expressed in neural crest cell lineages during mouse embryogenesis. Genes Dev. *5*, 105–119.

Mok, G.F., and Sweetman, D. (2011). Many routes to the same destination: lessons from skeletal muscle development. Reproduction *141*, 301–312.

Molkentin, J.D., Black, B.L., Martin, J.F., and Olson, E.N. (1995). Cooperative activation of muscle gene expression by MEF2 and myogenic bHLH proteins. Cell *83*, 1125–1136.

Moncaut, N., Rigby, P.W.J., and Carvajal, J.J. (2013). Dial M(RF) for myogenesis. FEBS J. *280*, 3980–3990.

Monsoro-Burq, A.-H., Fletcher, R.B., and Harland, R.M. (2003). Neural crest induction by paraxial mesoderm in Xenopus embryos requires FGF signals. Development *130*, 3111–3124.

Monsoro-Burq, A.H., Wang, E., and Harland, R. (2005). Msx1 and Pax3 cooperate to mediate FGF8 and WNT signals during Xenopus neural crest induction. Dev Cell *8*, 167–178.

Moore, J.A., Gupta, B.N., Zinkl, J.G., and Vos, J.G. (1973). Postnatal effects of maternal exposure to 2,3,7,8-tetrachlorodibenzo-p-dioxin (TCDD). Environ. Health Perspect. *5*, 81–85.

Mori-Akiyama, Y., Akiyama, H., Rowitch, D.H., and de Crombrugghe, B. (2003). Sox9 is required for determination of the chondrogenic cell lineage in the cranial neural crest. Proc. Natl. Acad. Sci. U. S. A. *100*, 9360–9365.

Morriss-Kay, G.M. (1996). Craniofacial defects in AP-2 null mutant mice. Bioessays *18*, 785–788.

Mourikis, P., and Tajbakhsh, S. (2014). Distinct contextual roles for Notch signalling in skeletal muscle stem cells. BMC Dev Biol *14*, 2.

Mourikis, P., Sambasivan, R., Castel, D., Rocheteau, P., Bizzarro, V., and Tajbakhsh, S. (2012a). A critical requirement for notch signaling in maintenance of the quiescent skeletal muscle stem cell state. Stem Cells *30*, 243–252.

Mourikis, P., Gopalakrishnan, S., Sambasivan, R., and Tajbakhsh, S. (2012b). Cell-autonomous Notch activity maintains the temporal specification potential of skeletal muscle stem cells. Development *139*, 4536–4548.

Murphy, M., and Kardon, G. (2011). Origin of vertebrate limb muscle: the role of progenitor and myoblast populations. Curr Top Dev Biol *96*, 1–32.

Nabeshima, Y., Hanaoka, K., Hayasaka, M., Esumi, E., Li, S., and Nonaka, I. (1993). Myogenin gene disruption results in perinatal lethality because of severe muscle defect. Nature *364*, 532–535.

Nakatomi, M., Wang, X., Key, D., Lund, J.J., Turbe-Doan, A., Kist, R., Aw, A., Chen, Y., Maas, R.L., and Peters, H. (2010). Genetic interactions between Pax9 and Msx1 regulate lip development and several stages of tooth morphogenesis. Dev. Biol. *340*, 438–449.

Nelms, B., and Labosky, P. (2011). Transcriptional Control of Neural Crest Development.

Noden, D.M. (1983). The role of the neural crest in patterning of avian cranial skeletal, connective, and muscle tissues. Dev. Biol. *96*, 144–165.

Noden, D.M., and Trainor, P.A. (2005). Relations and interactions between cranial mesoderm and neural crest populations. J Anat *207*, 575–601.

Ontell, M., and Kozeka, K. (1984). The organogenesis of murine striated muscle: a cytoarchitectural study. Am. J. Anat. *171*, 133–148.

Opitz, C.A., Litzenburger, U.M., Sahm, F., Ott, M., Tritschler, I., Trump, S., Schumacher, T., Jestaedt, L., Schrenk, D., Weller, M., et al. (2011). An endogenous tumour-promoting ligand of the human aryl hydrocarbon receptor. Nature *478*, 197–203.

Osborn, D.P.S., Li, K., Hinits, Y., and Hughes, S.M. (2011). Cdkn1c drives muscle differentiation through a positive feedback loop with Myod. Dev. Biol. *350*, 464–475.

Oustanina, S., Hause, G., and Braun, T. (2004). Pax7 directs postnatal renewal and propagation of myogenic satellite cells but not their specification. EMBO J. *23*, 3430–3439.

Palmeirim, I., Henrique, D., Ish-Horowicz, D., and Pourquié, O. (1997). Avian hairy gene expression identifies a molecular clock linked to vertebrate segmentation and somitogenesis. Cell *91*, 639–648.

Palmeirim, I., Dubrulle, J., Henrique, D., Ish-Horowicz, D., and Pourquié, O. (1998). Uncoupling segmentation and somitogenesis in the chick presomitic mesoderm. Dev. Genet. *23*, 77–85.

Pang, P.H., Lin, Y.H., Lee, Y.H., Hou, H.H., Hsu, S.P., and Juan, S.H. (2008). Molecular mechanisms of p21 and p27 induction by 3-methylcholanthrene, an aryl-hydrocarbon receptor agonist, involved in antiproliferation of human umbilical vascular endothelial cells. J Cell Physiol *215*, 161–171.

Parker, M.H., von Maltzahn, J., Bakkar, N., Al-Joubori, B., Ishibashi, J., Guttridge, D., and Rudnicki, M.A. (2012). MyoD-dependent regulation of NF- κ B activity couples cell-cycle withdrawal to myogenic differentiation. Skelet. Muscle *2*, 6.

Pasqualetti, M., Ori, M., Nardi, I., and Rijli, F.M. (2000). Ectopic Hoxa2 induction after neural crest migration results in homeosis of jaw elements in Xenopus. Development *127*, 5367–5378.

Perez-Alcala, S., Nieto, M.A., and Barbas, J.A. (2004). LSox5 regulates RhoB expression in the neural tube and promotes generation of the neural crest. Development *131*, 4455–4465.

Peters, H., Neubüser, A., Kratochwil, K., and Balling, R. (1998). Pax9-deficient mice lack pharyngeal pouch derivatives and teeth and exhibit craniofacial and limb abnormalities. Genes Dev. *12*, 2735–2747.

Pfisterer, P., Ehlermann, J., Hegen, M., and Schorle, H. (2002). A subtractive gene expression screen suggests a role of transcription factor AP-2 alpha in control of proliferation and differentiation. J. Biol. Chem. *277*, 6637–6644.

Picard, C.A., and Marcelle, C. (2013). Two distinct muscle progenitor populations coexist throughout amniote development. Dev. Biol. *373*, 141–148.

Platt, J. (1893). Ectodermic origin of the cartilages of the head. Anat. Anz.

Potthoff, M.J., and Olson, E.N. (2007). MEF2: a central regulator of diverse developmental programs. Development *134*, 4131–4140.

Pourquié, O. (2011). Vertebrate segmentation: from cyclic gene networks to scoliosis. Cell *145*, 650–663.

Pourquié, O., Fan, C.-M.M., Coltey, M., Hirsinger, E., Watanabe, Y., Bréant, C., Francis-West, P., Brickell, P., Tessier-Lavigne, M., Le Douarin, N.M., et al. (1996). Lateral and axial signals involved in avian somite patterning: a role for BMP4. Cell *84*, 461–471.

Pratt, R.M., Dencker, L., and Diewert, V.M. (1984). 2,3,7,8-Tetrachlorodibenzo-p-dioxin-induced cleft palate in the mouse: evidence for alterations in palatal shelf fusion. Teratog Carcinog Mutagen *4*, 427–436.

Puga, A., Ma, C., and Marlowe, J. (2009). The aryl hydrocarbon receptor cross-talks with multiple signal transduction pathways. Biochem. Pharmacol. *77*, 713–722.

Puri, P.L., Sartorelli, V., Yang, X.J., Hamamori, Y., Ogryzko, V. V, Howard, B.H., Kedes, L., Wang, J.Y., Graessmann, A., Nakatani, Y., et al. (1997a). Differential roles of p300 and PCAF acetyltransferases in muscle differentiation. Mol. Cell *1*, 35–45.

Puri, P.L., Avantaggiati, M.L., Balsano, C., Sang, N., Graessmann, A., Giordano, A., and Levrero, M. (1997b). p300 is required for MyoD-dependent cell cycle arrest and muscle-specific gene transcription. EMBO J. *16*, 369–383.

Qiu, M., Bulfone, A., Martinez, S., Meneses, J.J., Shimamura, K., Pedersen, R.A., and Rubenstein, J.L. (1995). Null mutation of Dlx-2 results in abnormal morphogenesis of proximal first and second branchial arch derivatives and abnormal differentiation in the forebrain. Genes Dev. *9*, 2523–2538.

Qiu, M., Bulfone, A., Ghattas, I., Meneses, J.J., Christensen, L., Sharpe, P.T., Presley, R., Pedersen, R.A., and Rubenstein, J.L. (1997). Role of the Dlx homeobox genes in proximodistal patterning of the branchial arches: mutations of Dlx-1, Dlx-2, and Dlx-1 and -2 alter morphogenesis of proximal skeletal and soft tissue structures derived from the first and second arches. Dev. Biol. *185*, 165–184.

Rada-Iglesias, A., Bajpai, R., Prescott, S., Brugmann, S.A., Swigut, T., and Wysocka, J. (2012). Epigenomic Annotation of Enhancers Predicts Transcriptional Regulators of Human Neural Crest. Cell Stem Cell.

Rawls, A., Morris, J.H., Rudnicki, M., Braun, T., Arnold, H.H., Klein, W.H., and Olson, E.N. (1995). Myogenin's functions do not overlap with those of MyoD or Myf-5 during mouse embryogenesis. Dev. Biol. *172*, 37–50.

Relaix, F., and Zammit, P.S. (2012). Satellite cells are essential for skeletal muscle regeneration: the cell on the edge returns centre stage. Development *139*, 2845–2856.

Relaix, F., Polimeni, M., Rocancourt, D., Ponzetto, C., Schafer, B.W., and Buckingham, M. (2003). The transcriptional activator PAX3-FKHR rescues the defects of Pax3 mutant mice but induces a myogenic gain-of-function phenotype with ligand-independent activation of Met signaling in vivo. Genes Dev *17*, 2950–2965.

Relaix, F., Rocancourt, D., Mansouri, A., and Buckingham, M. (2004). Divergent functions of murine Pax3 and Pax7 in limb muscle development. Genes Dev *18*, 1088–1105.

Relaix, F., Rocancourt, D., Mansouri, A., and Buckingham, M. (2005). A Pax3/Pax7-dependent population of skeletal muscle progenitor cells. Nature *435*, 948–953.

Relaix, F., Montarras, D., Zaffran, S., Gayraud-Morel, B., Rocancourt, D., Tajbakhsh, S., Mansouri, A., Cumano, A., and Buckingham, M. (2006). Pax3 and Pax7 have distinct and overlapping functions in adult muscle progenitor cells. J Cell Biol *172*, 91–102.

Relaix, F., Demignon, J., Laclef, C., Pujol, J., Santolini, M., Niro, C., Lagha, M., Rocancourt, D., Buckingham, M., and Maire, P. (2013). Six homeoproteins directly activate Myod expression in the gene regulatory networks that control early myogenesis. PLoS Genet. *9*, e1003425.

Reynaud, E.G., Leibovitch, M.P., Tintignac, L.A., Pelpel, K., Guillier, M., and Leibovitch, S.A. (2000). Stabilization of MyoD by direct binding to p57(Kip2). J Biol Chem *275*, 18767–18776.

Reznik, M. (1969). Thymidine-3H uptake by satellite cells of regenerating skeletal muscle. J. Cell Biol. *40*, 568–571.

Rhodes, S.J., and Konieczny, S.F. (1989). Identification of MRF4: a new member of the muscle regulatory factor gene family. Genes Dev. *3*, 2050–2061.

Rijli, F.M., Mark, M., Lakkaraju, S., Dierich, A., Dollé, P., and Chambon, P. (1993). A homeotic transformation is generated in the rostral branchial region of the head by disruption of Hoxa-2, which acts as a selector gene. Cell *75*, 1333–1349.

Rios, A.C., Serralbo, O., Salgado, D., and Marcelle, C. (2011). Neural crest regulates myogenesis through the transient activation of NOTCH. Nature *473*, 532–535.

Rosenblatt, J.D. (1992). A time course study of the isometric contractile properties of rat extensor digitorum longus muscle injected with bupivacaine. Comp. Biochem. Physiol. Comp. Physiol. *101*, 361–367.

Sacks, O. (2010). FACE-BLIND. Why are some of us terrible at recognizing faces? New Yorker p36.

Sahar, D.E., Longaker, M.T., and Quarto, N. (2005). Sox9 neural crest determinant gene controls patterning and closure of the posterior frontal cranial suture. Dev. Biol. *280*, 344–361.

Sakai, D., Suzuki, T., Osumi, N., and Wakamatsu, Y. (2006). Cooperative action of Sox9, Snail2 and PKA signaling in early neural crest development. Development *133*, 1323–1333.

Santagati, F., and Rijli, F. (2003). Cranial neural crest and the building of the vertebrate head. Nat. Rev. Neurosci. *4*, 806–818.

Sartorelli, V., Huang, J., Hamamori, Y., and Kedes, L. (1997). Molecular mechanisms of myogenic coactivation by p300: direct interaction with the activation domain of MyoD and with the MADS box of MEF2C. Mol. Cell. Biol. *17*, 1010–1026.

Sartorelli, V., Puri, P.L., Hamamori, Y., Ogryzko, V., Chung, G., Nakatani, Y., Wang, J.Y., and Kedes, L. (1999). Acetylation of MyoD directed by PCAF is necessary for the execution of the muscle program. Mol. Cell *4*, 725–734.

Sato, T., Sasai, N., and Sasai, Y. (2005). Neural crest determination by co-activation of Pax3 and Zic1 genes in Xenopus ectoderm. Development *132*, 2355–2363.

Sato, T., Kurihara, Y., Asai, R., Kawamura, Y., Tonami, K., Uchijima, Y., Heude, E., Ekker, M., Levi, G., and Kurihara, H. (2008). An endothelin-1 switch specifies maxillomandibular identity. Proc. Natl. Acad. Sci. U. S. A. *105*, 18806–18811.

Satokata, I., and Maas, R. (1994). Msx1 deficient mice exhibit cleft palate and abnormalities of craniofacial and tooth development. Nat. Genet. *6*, 348–356.

Satokata, I., Ma, L., Ohshima, H., Bei, M., Woo, I., Nishizawa, K., Maeda, T., Takano, Y., Uchiyama, M., Heaney, S., et al. (2000). Msx2 deficiency in mice causes pleiotropic defects in bone growth and ectodermal organ formation. Nat Genet *24*, 391–395.

Sauka-Spengler, T., and Bronner, M. (2010). Snapshot: neural crest. Cell *143*, 486–486.e1.

Sauka-Spengler, T., and Bronner-Fraser, M. (2008). A gene regulatory network orchestrates neural crest formation. Nat Rev Mol Cell Biol *9*, 557–568.

Scaal, M., Bonafede, A., Dathe, V., Sachs, M., Cann, G., Christ, B., and Brand-Saberi, B. (1999). SF/HGF is a mediator between limb patterning and muscle development. Development *126*, 4885–4893.

Schienda, J., Engleka, K.A., Jun, S., Hansen, M.S., Epstein, J.A., Tabin, C.J., Kunkel, L.M., and Kardon, G. (2006). Somitic origin of limb muscle satellite and side population cells. Proc Natl Acad Sci U S A *103*, 945–950.

Schneider, R.A., and Helms, J.A. (2003). The cellular and molecular origins of beak morphology. Science (80-.). *299*, 565–568.

Schorle, H., Meier, P., Buchert, M., Jaenisch, R., and Mitchell, P.J. (1996). Transcription factor AP-2 essential for cranial closure and craniofacial development. Nature *381*, 235–238.

Schuster-Gossler, K., Cordes, R., and Gossler, A. (2007). Premature myogenic differentiation and depletion of progenitor cells cause severe muscle hypotrophy in Delta1 mutants. Proc Natl Acad Sci U S A *104*, 537–542.

Seale, P., Sabourin, L.A., Girgis-Gabardo, A., Mansouri, A., Gruss, P., and Rudnicki, M.A. (2000). Pax7 is required for the specification of myogenic satellite cells. Cell *102*, 777–786.

Sela-Donenfeld, D., and Kalcheim, C. (2002). Localized BMP4-noggin interactions generate the dynamic patterning of noggin expression in somites. Dev. Biol. *246*, 311–328.

Serbedzija, G.N., and McMahon, A.P. (1997). Analysis of neural crest cell migration in Splotch mice using a neural crest-specific LacZ reporter. Dev. Biol. *185*, 139–147.

Sherr, C.J., and Roberts, J.M. (1999). CDK inhibitors: positive and negative regulators of G1-phase progression. Genes Dev. *13*, 1501–1512.

Sherr, C.J., and Roberts, J.M. (2004). Living with or without cyclins and cyclin-dependent kinases. Genes Dev. *18*, 2699–2711.

Shimeld, S.M., McKay, I.J., and Sharpe, P.T. (1996). The murine homeobox gene Msx-3 shows highly restricted expression in the developing neural tube. Mech. Dev. *55*, 201–210.

Smith, A., Robinson, V., Patel, K., and Wilkinson, D.G. (1997). The EphA4 and EphB1 receptor tyrosine kinases and ephrin-B2 ligand regulate targeted migration of branchial neural crest cells. Curr. Biol. *7*, 561–570.

Soleimani, V.D., Punch, V.G., Kawabe, Y., Jones, A.E., Palidwor, G.A., Porter, C.J., Cross, J.W., Carvajal, J.J., Kockx, C.E., van Ijcken, W.F., et al. (2012). Transcriptional Dominance of Pax7 in Adult Myogenesis Is Due to High-Affinity Recognition of Homeodomain Motifs. Dev. Cell.

Spitz, F., and Furlong, E.E.M. (2012). Transcription factors: from enhancer binding to developmental control. Nat. Rev. Genet.

Spokony, R.F., Aoki, Y., Saint-Germain, N., Magner-Fink, E., and Saint-Jeannet, J.-P. (2002). The transcription factor Sox9 is required for cranial neural crest development in Xenopus. Development *129*, 421–432.

Szabo-Rogers, H.L., Smithers, L.E., Yakob, W., and Liu, K.J. (2010). New directions in craniofacial morphogenesis. Dev Biol *341*, 84–94.

Tajbakhsh, S., Rocancourt, D., and Buckingham, M. (1996). Muscle progenitor cells failing to respond to positional cues adopt non-myogenic fates in myf-5 null mice. Nature *384*, 266–270.

Tajbakhsh, S., Rocancourt, D., Cossu, G., and Buckingham, M. (1997). Redefining the genetic hierarchies controlling skeletal myogenesis: Pax-3 and Myf-5 act upstream of MyoD. Cell *89*, 127–138.

Taneyhill, L.A., and Bronner-Fraser, M. (2005). Dynamic alterations in gene expression after Wnt-mediated induction of avian neural crest. Mol Biol Cell *16*, 5283–5293.

Taneyhill, L.A., Coles, E.G., and Bronner-Fraser, M. (2007). Snail2 directly represses cadherin6B during epithelial-to-mesenchymal transitions of the neural crest. Development *134*, 1481–1490.

Tapscott, S.J. (2005). The circuitry of a master switch: Myod and the regulation of skeletal muscle gene transcription. Development *132*, 2685–2695.

Tapscott, S.J., Davis, R.L., Thayer, M.J., Cheng, P.F., Weintraub, H., and Lassar, A.B. (1988). MyoD1: a nuclear phosphoprotein requiring a Myc homology region to convert fibroblasts to myoblasts. Science *242*, 405–411.

Theveneau, E., and Mayor, R. (2012). Neural crest delamination and migration: From epithelium-to-mesenchyme transition to collective cell migration. Dev. Biol. *366*, 34–54.

Theveneau, E., Marchant, L., Kuriyama, S., Gull, M., Moepps, B., Parsons, M., and Mayor, R. (2010). Collective chemotaxis requires contact-dependent cell polarity. Dev. Cell *19*, 39–53.

Théveneau, E., Duband, J.-L., and Altabef, M. (2007). Ets-1 confers cranial features on neural crest delamination. PLoS One *2*, e1142.

Thiery, J.P., and Sleeman, J.P. (2006). Complex networks orchestrate epithelial-mesenchymal transitions. Nat. Rev. Mol. Cell Biol. *7*, 131–142.

Thomas, B.L., Tucker, A.S., Qui, M., Ferguson, C.A., Hardcastle, Z., Rubenstein, J.L., and Sharpe, P.T. (1997). Role of Dlx-1 and Dlx-2 genes in patterning of the murine dentition. Development *124*, 4811–4818.

Todeschini, A.-L., Georges, A., and Veitia, R.A. (2014). Transcription factors: specific DNA binding and specific gene regulation. Trends Genet. *30*, 211–219.

Trainor, P.A., and Krumlauf, R. (2000). Patterning the cranial neural crest: hindbrain segmentation and Hox gene plasticity. Nat. Rev. Neurosci. *1*, 116–124.

Trainor, P.A., and Krumlauf, R. (2001). Hox genes, neural crest cells and branchial arch patterning. Curr. Opin. Cell Biol. *13*, 698–705.

Tremblay, P., Kessel, M., and Gruss, P. (1995). A transgenic neuroanatomical marker identifies cranial neural crest deficiencies associated with the Pax3 mutant Splotch. Dev. Biol. *171*, 317–329.

Tremblay, P., Dietrich, S., Mericskay, M., Schubert, F.R., Li, Z., and Paulin, D. (1998). A crucial role for Pax3 in the development of the hypaxial musculature and the long-range migration of muscle precursors. Dev. Biol. *203*, 49–61.

Trokovic, N., Trokovic, R., and Partanen, J. (2005). Fibroblast growth factor signalling and regional specification of the pharyngeal ectoderm. Int. J. Dev. Biol. *49*, 797–805.

Tucker, A.S., and Lumsden, A. (2004). Neural crest cells provide species-specific patterning information in the developing branchial skeleton. Evol. Dev. *6*, 32–40.

Vasyutina, E., and Birchmeier, C. (2006). The development of migrating muscle precursor cells. Anat. Embryol. (Berl). *211 Suppl* , 37–41.

Vasyutina, E., Stebler, J., Brand-Saberi, B., Schulz, S., Raz, E., and Birchmeier, C. (2005). CXCR4 and Gab1 cooperate to control the development of migrating muscle progenitor cells. Genes Dev. *19*, 2187–2198.

Vasyutina, E., Lenhard, D.C., Wende, H., Erdmann, B., Epstein, J.A., and Birchmeier, C. (2007). RBP-J (Rbpsuh) is essential to maintain muscle progenitor cells and to generate satellite cells. Proc Natl Acad Sci U S A *104*, 4443–4448.

Villanueva, S., Glavic, A., Ruiz, P., and Mayor, R. (2002). Posteriorization by FGF, Wnt, and retinoic acid is required for neural crest induction. Dev. Biol. *241*, 289–301.

Wang, W., Chen, X., Xu, H., and Lufkin, T. (1996). Msx3: a novel murine homologue of the Drosophila msh homeobox gene restricted to the dorsal embryonic central nervous system. Mech. Dev. *58*, 203–215.

Weintraub, H., Tapscott, S.J., Davis, R.L., Thayer, M.J., Adam, M.A., Lassar, A.B., and Miller, A.D. (1989). Activation of muscle-specific genes in pigment, nerve, fat, liver, and fibroblast cell lines by forced expression of MyoD. *86*, 5434–5438.

Wen, Y., Bi, P., Liu, W., Asakura, A., Keller, C., and Kuang, S. (2012). Constitutive Notch activation upregulates Pax7 and promotes the self-renewal of skeletal muscle satellite cells. Mol. Cell. Biol. *32*, 2300–2311.

White, S.S., and Birnbaum, L.S. (2009). An overview of the effects of dioxins and dioxin-like compounds on vertebrates, as documented in human and ecological epidemiology. J. Environ. Sci. Heal. Part C, Environ. Carcinog. Ecotoxicol. Rev. *27*, 197–211.

Wilkie, A.O., and Morriss-Kay, G.M. (2001). Genetics of craniofacial development and malformation. Nat Rev Genet *2*, 458–468.

Wright, W.E., Sassoon, D. a, and Lin, V.K. (1989). Myogenin, a factor regulating myogenesis, has a domain homologous to MyoD. Cell *56*, 607–617.

Wu, M., Li, J., Engleka, K.A., Zhou, B., Lu, M.M., Plotkin, J.B., and Epstein, J.A. (2008). Persistent expression of Pax3 in the neural crest causes cleft palate and defective osteogenesis in mice. J Clin Invest *118*, 2076–2087.

Wu, P., Jiang, T.-X., Shen, J.-Y., Widelitz, R.B., and Chuong, C.-M. (2006). Morphoregulation of avian beaks: comparative mapping of growth zone activities and morphological evolution. Dev. Dyn. *235*, 1400–1412.

Yang, L., Zhang, H., Hu, G., Wang, H., Abate-Shen, C., and Shen, M.M. (1998). An early phase of embryonic Dlx5 expression defines the rostral boundary of the neural plate. J. Neurosci. *18*, 8322–8330.

Yee, S.P., and Rigby, P.W. (1993). The regulation of myogenin gene expression during the embryonic development of the mouse. Genes Dev. *7*, 1277–1289.

Yin, H., Price, F., and Rudnicki, M.A. (2013). Satellite cells and the muscle stem cell niche. Physiol. Rev. *93*, 23–67.

Yonemoto, J. (2000). The effects of dioxin on reproduction and development. Ind Heal. *38*, 259–268.

York, G., and Hayley, M. (2008). "Last ghost" of the Vietnam War - The Globe and Mail.

Yoshida, T., Vivatbutsiri, P., Morriss-Kay, G., Saga, Y., and Iseki, S. (2008). Cell lineage in mammalian craniofacial mesenchyme. Mech. Dev. *125*, 797–808.

Zalc, B., and Colman, D.R. (2000). Origins of vertebrate success. Science *288*, 271–272.

Zalc, B., Goujet, D., and Colman, D. (2008). The origin of the myelination program in vertebrates. Curr. Biol. *18*, R511–2.

Zammit, P.S. (2008). All muscle satellite cells are equal, but are some more equal than others? J. Cell Sci. *121*, 2975–2982.

Abstract

This thesis aims to decipher how the paralogous paired-box transcription factors Pax3 and Pax7 control cell cycle progression and the fates of progenitor cells in different tissues, and is composed of two main parts.

- **Uncoupling cell cycle from cell differentiation; cell fate decision of Pax3^{+} myogenic progenitor cells during limb skeletal muscle development.**

It has been previously shown that muscle formation relies on a proliferating population of progenitor cells that express and require the activity of both *Pax3* and *Pax7*. In addition, key molecular pathways have been identified that regulate the differentiation and the growth arrest of these progenitors. Hence, skeletal muscle represents a good model to study the cross talk between these distinct regulators that coordinate cell cycle exit with muscle progenitor cell differentiation. In a close collaboration with other members of the team, I have shown that cell cycle exit mediated by the cyclin-dependent kinases inhibitors (CDKIs, p21^{cip1} and p57^{kip2}) and myogenic differentiation controlled by the myogenic regulatory factors (MRFs, Myf5 and MyoD) can be genetically uncoupled during muscle development. We have identified a functional interplay between Notch signalling and both the MRFs and CDKIs activities. Importantly, we demonstrated that cell-cell signalling between progenitors and differentiated muscle cells (myoblasts) is required to maintain the cycling status of the progenitors population. The analysis of several mouse models and *ex vivo* experimental approaches indicates that when either the progenitor-myoblast interaction or Notch signalling is impaired, progenitor cells activate p57 and leave the cell cycle. Moreover, we identified a muscle-specific regulatory element of *p57* directly activated by the MRFs in the myoblasts but repressed by the Notch effectors Hes1 and Hey1 in progenitor cells. Therefore, we demonstrate that the integration at the level of a single key cell cycle enhancer regulating both Notch and MRFs activities is a strong means by which the equilibrium between amplification of the progenitor pool and the establishment of definitive functions of skeletal muscle is ensured.

- **Unexpected requirement of an environmental stress response pathway in the control of Pax3^{+} neural crest derivatives growth and maintenance during craniofacial development.**

Exposure to environmental teratogenic pollutants is a major threat to the development of the embryo. For instance, exposure to dioxin, a violent teratogen, during pregnancy can lead to severe developmental defects as revealed after the Vietnam War and the Seveso disaster. Most teratogens have been shown to interfere with genetic programs regulating developmental processes. However, the molecular and cellular events underlying these developmental defects remain undefined. Here we report a molecular link between an environmental stress response pathway and *Pax3* and *Pax7*, two key developmental genes. Previous studies have shown that *Pax3* and *Pax7* play pivotal role for the integration of various inputs during neural crest induction and for controlling the specification of neural crest derivatives. Although *Pax3* and *Pax7* function during early neural crest development is highly conserved among vertebrates, their function during craniofacial formation is unknown. Using mutant mice with impaired *Pax3/7* function that display facial clefts, we showed these defects are associated with an up-regulation of the signalling pathway mediated by the Aryl hydrocarbon Receptor (AhR), the receptor to dioxin. In *Pax3/7* mutants, increased AhR activity drives facial mesenchymal cells out of the cell cycle through the up-regulation of the expression of the cyclin-dependent kinase inhibitor *p21*. Accordingly, inhibiting AhR activity rescues the cycling status of these cells and the facial closure of *Pax3/7* mutant embryos. Together, our results demonstrate the necessity of the interaction between this environmental stress response pathway with *Pax3* and *Pax7* downstream gene regulatory network during normal craniofacial development.

Résumé

Mon travail de thèse a porté sur l'étude des mécanismes contrôlant la progression du cycle cellulaire et le devenir des cellules progénitrices dans différents tissus. Il a comporté deux parties différentes, l'une centrée sur le développement du muscle squelettique, l'autre sur celui des dérivés de la crête neurale. Ces deux études ont en commun l'analyse de la population des cellules progénitrices exprimant les facteurs de transcription à domaine Paired, Pax3 et Pax7.

- **L'étude du découplage entre sortie du cycle cellulaire et différenciation cellulaire dans la formation du muscle squelettique du membre.**

La formation des muscles dépend d'une population cellulaire hautement proliférative exprimant *Pax3* et *Pax7*. Cette population peut être analysée à l'aide de lignées murines transgéniques dédiées. Les voies de signalisation régulant la différenciation et l'arrêt de la croissance cellulaire de ces progéniteurs ont déjà été identifiées. Le muscle squelettique représente ainsi un bon modèle pour l'étude des interactions entre les différents régulateurs de la sortie du cycle cellulaire et de la différentiation des cellules progénitrices. En collaboration avec d'autres membres de l'équipe, nous avons montré que la sortie du cycle cellulaire, régulée par l'activité des inhibiteurs de kinases cycline-dépendantes (CDKIs, $p21^{cip1}$ et $p57^{kip2}$) et la différentiation musculaire, contrôlée par les facteurs régulant la myogenèse (MRFs, Myf5 and MyoD), peuvent être découplées génétiquement pendant la formation du muscle ; démontrant par la même occasion que ces deux mécanismes peuvent fonctionner indépendamment pendant le développement. Nous avons identifié des interactions entre la voie de signalisation Notch, impliquée dans le contrôle de la différenciation cellulaire dans différents tissus, et les MRFs et les CDKIs. Nous avons également montré qu'une communication entre progéniteurs musculaires et cellules musculaires différenciées (myoblastes) est nécessaire pour maintenir la prolifération des progéniteurs. L'analyse de plusieurs modèles murins associée à des approches *ex vivo* démontre en effet que le blocage de l'interaction entre progéniteurs et myoblastes, ou le blocage de la voie Notch dans les progéniteurs conduisent à l'activation de l'expression de p57 et à la sortie du cycle cellulaire. Nous avons en outre identifié une séquence régulatrice de l'expression de *p57*, spécifique au muscle, qui est directement activée par les MRFs dans les myoblastes mais réprimée par la voie Notch dans les progéniteurs. Ainsi nous avons démontré qu'au niveau d'une séquence régulatrice unique de *p57*, l'intégration de l'activité de la voie Notch et des MRFs permet de contrôler la balance entre l'amplification de la population de

progéniteurs et l'établissement de la population de myoblastes nécessaire a la formation du muscle squelettique.

- **L'étude d'une voie de signalisation impliquée dans la réponse au stress environnemental dans le contrôle de la croissance des dérivés de crête neurale.**

L'exposition à des polluants environnementaux aux effets tératogènes est une menace majeure pour le développement de l'embryon. Ainsi, l'exposition à la dioxine, pendant la gestation engendre la formation d'anomalies majeures du développement, comme l'ont illustré la guerre du Vietnam et plus récemment l'accident industriel de Seveso. Si l'on sait que la plupart des tératogènes interfèrent avec les voies génétiques contrôlant les processus de développement, les évènements moléculaires et cellulaires engendrant ces défauts restent inconnus. Nous avons mis en évidence l'existence d'un lien moléculaire entre une voie de signalisation impliquée dans la réponse au stress environnemental et deux gènes essentiels au développement, *Pax3* et *Pax7*. Des études précédentes avaient montré le rôle majeur de ces deux facteurs dans l'intégration de différents signaux, lors de l'induction de la crête neurale et de la spécification de ses dérivés. Bien que la fonction de *Pax3* et *Pax7* pendant le développement précoce de la crête neurale soit hautement conservée chez les vertébrés, leurs fonctions durant le développement craniofacial restent inconnues. Des mutants murins chez lesquels la fonction de *Pax3/7* est perturbée présentent des fentes oro-faciales. En utilisant ces mutants, nous avons montré que ces défauts sont associés à la surexpression de la voie de signalisation régulée par le récepteur Aryl hydrocarbon (AhR), qui est le récepteur à la dioxine. Chez les mutants *Pax3/7*, l'augmentation de l'activité d'AhR « pousse » les cellules mésenchymateuses de la face hors du cycle cellulaire via la surexpression de l'inhibiteur de kinases cycline-dépendantes *p21*. En outre, nous avons montré, *in vitro et in vivo*, que l'inhibition de l'activité d'AhR restaure la prolifération de ces cellules, permettant ainsi la fermeture de la face des mutants *Pax3/7*. Nos résultats démontrent qu'une interaction entre une voie de signalisation impliquée dans la réponse au stress environnemental et les voies moléculaires contrôlées par *Pax3* et *Pax7* est nécessaire pour un développement craniofacial normal.

Abstrakt

Waehrend meiner Dissertation habe ich mich mit der Entschluesselung der Zellzykluskontrolle und der Bestimmung des Zellschicksals von Vorlaeuferzellen verschiedener Gewebetypen durch die paralogen paired-box Transkriptionsfaktoren Pax 3 und Pax7 beschaeftigt. Daher laesst sich meine Arbeit in zwei Hauptteile unterteilen.

- **Die Entkoppelung von Zellzyklus und Zelldifferenzierung - das Zellschicksal von Pax3-positiven myogenen Vorlaeuferzellen waehrend der Skeletmuskelentwicklung**

Skeletmuskelentwicklung ist abhaengig von einer proliferierenden Population von Vorlaeuferzellen, die Pax3 und Pax 7 exprimieren und gleichzeitig auf die Aktivitaet beider Transkriptionsfaktoren angewiesen sind. Signalwege, die Differenzierung und Wachstumsstillstand dieser Vorlaeuferzellen regulieren, sind bereits entschluesselt worden. Daher ist der Skeletmuskel ein geeignetes Model, um Ueberschneidungen in Signalwegen dieser Regulatoren, die Zellzyklus und Zelldifferenzierung der Muskelvorlaeuferzellen koordinieren, zu untersuchen. In Zusammenarbeit mit einem PostDoc konnte ich zeigen, dass Zellzyklusaustritt, vermittelt durch die Zyklin-abhaengigen Kinaseinhibitoren $p21^{cip1}$ und $p57^{kip2}$ und myogene Differenzierung, kontrolliert durch die Muskelregulationsfaktoren (MRF) Myf5 und MyoD, waehrend der Muskelentwicklung genetisch voneinander entkoppelt werden koennen. Im Gegensatz dazu konnten wir ein Zusammenspiel des Notch-Signalweges mit MRFs sowie mit Zyklin-abhaengigen Kinaseinhibitoren identifizieren. Besonders hervorzuheben ist, dass wir zeigen konnten, dass Zell-Zell-Kommunikation zwischen Vorlaeuferzellen und determinierten Muskelzellen (Myoblasten) notwendig ist fuer die Zellzyklusaktivitaet der Vorlaeuferzellen. Die Analyse verschiedener Mausmodelle und von *ex vivo* Experimenten gibt Hinweis darauf, dass eine Stoerung der Zell-Zell-Kommunikation zwischen Vorlaeuferzellen und Myoblasten oder des Notch-Signalweges zur Aktivierung von p57 in Vorlaeuferzellen und zum Zellzyklysaustritt fuehren. Daruber hinaus, haben wir ein Muskel-spezifisches Regulatorelement von p57 identifiziert, das in Myoblasten durch die MRFs aktiviert und von den Notch Effektoren Hes1 und Hey1 in Vorlaeuferzellen inhibiert wird. So konnten wir zeigen, dass die Regulation eines der Hauptregulatoren des Zellzyklus (i.e. p57) durch einen einzelnen Signalverstaerker, der Notch und MRF Aktivitaet vermittelt,

als Traeger des Equilibriums zwischen Vorlaeuferzellpool und Etablierung definitiver Skeletmuskelfunktion, stattfindet.

- **Unerwartete Notwendigkeit eines umgebungsbedingten Stressantwort-Signalwegs in der Kontrolle von Wachstum und Erhaltung Pax3-positiver Neuralleistenderivate**

Eine Hauptgefaehrdung der Embryonalentwicklung sind umgebungsbedingte teratogene Schadstoffe. Der Kontakt mit Dioxin, einem starken Teratogen waehrend der Schwangerschaft kann zur Bildung einer Lippen- und/oder Gaumenspalte fuehren, wie in Folge des Vietnamkrieges und des Sevesoungluecke erkannt wurde. Die meisten Teratogene greifen in die genetische Regulation von Entwicklungsprozessen ein. Allerdings sind die molekularen und zellulaeren Vorgaenge dieser Entwicklungsstoerungen noch nicht definiert.
Wir zeigen hier eine Verbindung auf molekularer Ebene zwischen umgebungsbedingtem Stressantwort-Signalweg und den Schluesselentwicklungsgenen Pax3 und Pax7. Fruehere Studien haben gezeigt, dass Pax3 und Pax7 eine entscheidende Rolle fuer die Vernetzung verschiedener Signale waehrend der Neuralleistenindukion und der Spezifizierung von Neuralleistenderivaten sind. Obwohl die Funktion von Pax3 und Pax7 waehrend der Neurralleistenentwicklung in Vertebraten hochkonserviert ist, ist ihre Funktion in der kraniofazialen Entwicklung nicht bekannt. In Mausmodellen mit eingeschreankter Pax3/7 Funktion, die Gesichtsspalten analog zu Dioxin-induzierten Fehlbildungen aufweisen, konnten wir zeigen, dass diese Defekte mit einer Hochregulierung des Dioxin-Rezeptor Aryl-Hydrocarbon-Rezeptor (AhR) vermittelten Signalwegs einhergehen. Im Pax3/7 mutanten Mausmodel werden faziale mesenchymale Zellen aufgrund erhoehter AhR Aktivitaet durch erhoehte Expression des Zyklin-abhaengigen Kinase Inhibitors p21 aus dem Zellzyklus entlassen. Dementsprechend fuehrt die Inhibierung von AhR Aktivitaet zur Aufrechterhaltung der Zellzyklusaktivitaet dieser Zellen und zum Schliessen der Gesichtspalte in Pax3/7 mutanten Embryonen. Dies zeigt die Notwendigkeit der Interaktion zwischen dem umgebungsbedingten Stressantwort-Signalweg und der nachgeschalteten Pax3 und Pax7 kontrollierten Genregulation in der normalen kraniofazialen Gesichtsentwicklung.

Travaillez, prenez de la peine :

C'est le fonds qui manque le moins.

Un riche Laboureur, sentant sa mort prochaine,

Fit venir ses enfants, leur parla sans témoins.

Gardez-vous, leur dit-il, de vendre l'héritage

Que nous ont laissé nos parents.

Un trésor est caché dedans.

Je ne sais pas l'endroit ; mais un peu de courage

Vous le fera trouver, vous en viendrez à bout.

Remuez votre champ dès qu'on aura fait l'Oût.

Creusez, fouiller, bêchez ; ne laissez nulle place

Où la main ne passe et repasse.

Le père mort, les fils vous retournent le champ

Deçà, delà, partout ; si bien qu'au bout de l'an

Il en rapporta davantage.

D'argent, point de caché. Mais le père fut sage

De leur montrer avant sa mort

Que le travail est un trésor.

Catherine Lubetzki, quoting "*Le laboureur et ses enfants*" from Jean de la Fontaine since 2004…